ENGINEERING SOLUBLE, HIGH AFFINITY T CELL RECEPTOR DOMAINS FOR DETECTION OF STAPHYLOCOCCAL AND STREPTOCOCCAL EXOTOXINS

BY

PREETI SHARMA

DISSERTATION

Submitted in partial fulfillment of the requirements
for the degree of Doctor of Philosophy in Biochemistry
in the Graduate College of the
University of Illinois at Urbana-Champaign, 2015

Urbana, Illinois

Doctoral Committee:

Professor David M. Kranz, Chair
Professor Susan A. Martinis
Professor James H. Morrissey
Professor Wilfred A. van der Donk

ABSTRACT

Staphylococcus aureus and group A *Streptococcus* express a family of exotoxins including staphylococcal enterotoxins A, B, C (SEA, SEB, SEC), toxic shock syndrome toxin-1 (TSST-1) and streptococcal pyrogenic exotoxins (SpeA, SpeC) that possess superantigenic properties, by virtue of which they stimulate a large fraction of an individual's T cells, leading to hyperinflammation and in some cases, organ failure and death. The molecular mechanism behind hyperinflammation has been attributed to the binding of superantigen (SAg) to both a T cell receptor (TCR) on a T cell, and a class II product of the major histocompatibility complex (MHC) on an antigen presenting cell, which leads to cross-linking of cells and excessive cytokine release from both cell types. Although SAgs bind with low affinity to the variable region of the beta chain (Vβ) of the TCR, they are very potent toxins. These toxins have been incriminated in food poisoning, sepsis, toxic shock syndrome (TSS), infective endocarditis, and skin conditions like atopic dermatitis. For purposes of neutralizing or detecting SAg, soluble versions of several Vβ domains against various SAgs have been engineered in the Kranz laboratory. Yeast display and directed evolution have allowed development of soluble, high-affinity Vβ proteins some of which have also been successfully used in animal models of *S. aureus* infections. In this work, a high-affinity Vβ receptor for Staphylococcal enterotoxin A (SEA) was generated, and the use of this and other engineered, high-affinity Vβ proteins as specific and sensitive detecting agents was explored.

SEA is one among the collection of enterotoxins secreted by *Staphylococcus aureus*, which acts as a superantigen. It is also the most common enterotoxin recovered from food poisoning outbreaks in the United States. It is estimated that in most cases, the dose of SEA that causes the disease is of the order of a few micrograms per individual. In this study, I engineered a soluble form of a Vβ that had high affinity toward SEA, for purposes of understanding its molecular interaction with SEA and also to develop specific, sensitive assays for detection of SEA.

In chapter 2, the process of engineering of human Vβ22 protein for improving its affinity towards SEA is described. In this chapter, yeast display coupled with random mutagenesis and fluorescence-activated cell sorting (FACS) was used to select for stably expressing Vβ22 mutants on yeast cell surface. Because the affinity of stabilized Vβ22 mutants for SEA was low, these were then subjected to directed mutagenesis to select for mutants with enhanced affinity towards SEA. Incorporation of additional mutations by site-directed mutagenesis, yielded the high affinity mutant called "FL". Selected Vβ22 mutants were expressed in *E.coli* and refolded *in vitro*, for assessing their binding properties. In collaboration with Dr. Eric Sundberg, the binding constants for interaction of *wt* Vβ22 and high affinity "FL" protein with SEA were determined by surface plasmon resonance. FL protein was shown to bind SEA with a K_D value of 4nM, which was a 25,000-fold improvement in affinity compared to the wild-type protein, which binds SEA with low affinity (K_D ~100μM). The SEA:Vβ interface was centered around residues within the complementarity determining region 2 (CDR2) loop of the Vβ. The engineered, high-affinity Vβ22 protein was specific for SEA, in that it did not bind to two other closely related enterotoxins SEE or SED, providing information on the SEA residues possibly involved in the interaction. Finally, the high-affinity Vβ22 mutant protein was used for development of a capture-ELISA based platform for specific detection of SEA.

In Chapter 3, a bead-based, two-color flow cytometry approach was used to develop a multiplex assay for simultaneous detection of staphylococcal (SEA, SEB and TSST-1) and streptococcal (SpeA and SpeC) toxins in a single sample. Vβ domains that were engineered for for binding with high-affinity to these toxins were used together with commercial, polyclonal, anti-toxin reagents to enable specific and sensitive detection with SD_{50} values of 400 pg/ml (SEA), 3 pg/ml (SEB), 25 pg/ml (TSST-1), 6 ng/ml (SpeA), and 100 pg/ml (SpeC) in singleplex assays. These sensitivities were in the range of 4- to 80-fold higher than achieved with standard ELISAs using the same reagents. The singleplex assays were combined to yield a multiplex assay that

allowed reliable detection of the toxins in a single sample. In multiplex format, the sensitivity of detecting individual toxin was reduced due to higher noise associated with the use of multiple polyclonal agents, but the sensitivities were still well within the range necessary for detection in food sources or for rapid detection of toxins in culture supernatants. For example, the assay specifically detected SEA, SEB and TSST-1 in supernatants derived from cultures of various strains of *Staphylococcus aureus*. Thus, these reagents and the flow cytometry-based platform can be used for simultaneous detection of the toxins in food sources or culture supernatants of potential pathogenic strains of *Staphylococcus aureus* and *Streptococcus pyogenes*, or directly in clinical samples.

ACKNOWLEDGEMENTS

First and foremost, I would like to thank my advisor Dr. David M. Kranz for accepting me as a graduate student in his laboratory. I feel extremely fortunate that I had the opportunity of working under his guidance. He is an excellent mentor and I have learnt an enormous amount from him over the years. Every interaction with him has been fruitful. He has always encouraged me to learn from my mistakes and to become a smarter scientist, who anticipates possible errors as well as results in an experiment. In addition to providing research advice, he has also guided me immensely in improving my scientific writing. I am very excited to venture into a post-doctoral career with him in cancer immunology, and that I will have the continuous opportunity of learning more from him. I also had the opportunity to work with him as his teaching assistant for immunology, which was not only an enriching experience intellectually, but also had a positive impact on my personality resulting in boosting my confidence and realizing my potential. I am extremely thankful to him for providing me with the opportunities to serve in this challenging role.

I also had the pleasure of working with excellent collaborators whose skill-set complemented my studies. I would like to thank Dr. Sandra Postel and Dr. Eric Sundberg (University of Maryland) for their help in measuring the dissociation constants for interaction of staphylococcal enterotoxin A (SEA) with its wild-type and affinity-matured receptor. I would also like to thank Dr. Jefferey DeGrasse for mass spectrometry experiments, and Dr. Sandra Tallent (FDA) for her initial studies with a flow cytometry based approach for toxin detection. I would like to thank Dr. Barbara Pilas and Ben Montez (Flow Cytometry Facility, University of Illinois) for providing technical assistance in sorting libraries of the SEA receptor, and Core DNA sequencing facility (University of Illinois) for their timely assistance in sequencing.

I would like to thank past and present members of the Kranz laboratory in not only providing me with their help and advice in the laboratory, but also for being a great group of people to be friends with. Being an introvert, international student, I want to thank all of them from the

bottom of my heart, for being so warm and friendly. I would specially like to thank Dr. Natalie Bowerman and Dr. Adam Chervin for training me in flow cytometry and cell culture techniques, when I joined the lab. I would like to thank Dr. Ningyan Wang and Daiva Mattis for being my “superantigen” buddies. I am grateful for their intellectual support in both my projects. I would also like to thank Dr. Lionel Low for providing technical advice on the multiplex toxin detection project, not only when he was in the Kranz lab but also over emails after he moved to Singapore. I would like to thank Dr. Jennifer Stone for being a wonderful co-worker, who constantly provided advice and suggestions whenever I ran into problems. I would specially like to thank her for her insightful contributions during my experiments in chapter 3. Dr. Jennifer Stone, and also Dr. Samanthi Narayanan have been great friends to me, and I would like to thank them for providing a listening ear whenever I needed them. I will always cherish their help and support during my PhD career. I would also like to thank Dr. David Aggen, Elizabeth Marshall, Dr. Sheena Smith and members of Dr. Ed Roy’s lab for being wonderful colleagues. I would like to thank current members of the Kranz lab, Daniel Harris and Dr. Qi Cai, for their continuous support and encouragement. I am delighted that I will continue to work with these excellent scientists.

I would also like to thank all my friends at Urbana-Champaign for providing a heathy environment to relax. I have enjoyed the trips, the midnight birthday parties, potluck dinners and celebrating Indian festivals with them. I would like to thank Somashekar Viswanath (Som), Sravanthi Puligilla and Rimpa Ghosh for providing emotional support during my personal hardships. I would specially like to thank Sravanthi for being a great roommate, as well as a great friend. I have no words to explain the support and encouragement Som has provided me with, during these years.

Last but not the least, I would like to thank my family members who have been understanding and supportive all these years. I would specially like to thank my grandparents for keeping faith in me, and believing in me. My parents, although miles away, have been very loving

and supportive of my career and it means a lot to me. I am thankful to my brother Pravesh, sister-in-law Swati, sister Poonam, and brother-in-law Rajeev for their love and encouragement.

TABLE OF CONTENTS

LIST OF TABLES

LIST OF FIGURES

LIST OF ABBREVIATIONS

BSA – Bovine serum albumin
CDR – Complementarity determining region
ELFA – Enzyme-linked fluorescence assay
ELISA – Enzyme-linked immunosorbent assay
Fab – Fragment antigen binding
FACS – Fluorescence-activated cell sorting
FR – Framework region
HA – Hemagglutinin
HPLC – High-performance liquid chromatography
HRP – Horse radish peroxidase
HV – Hypervariable (region)
hVβ2.1 – human Vβ2.1
hVβ22 – human Vβ22
IFN-γ – Interferon-γ
IL-2 – Interleukin-2
MFU – Median fluorescence units
MHC – Major histocompatibility complex
mVβ8.2 – murine Vβ8.2
PBS – Phosphate-buffered saline
PCR – Polymerase chain reaction
SAv – Streptavidin
SAg – Superantigen
SE – Staphylocccal enterotoxin
SEA – Staphylococcal enterotoxin A
SEB – Staphylococcal enterotoxin B
SEC – Staphylococcal enterotoxin C
SED – Staphylococcal enterotoxin D
SEE – Staphylococcal enterotoxin E
SEH – Staphylococcal enterotoxin H
SEK – Staphylococcal enterotoxin K
SEQ – Staphylococcal enterotoxin Q
SMEZ – Streptococcal mitogenic exotoxin Z
SpeA – Streptococcal pyrogenic exotoxin A
SpeC – Streptococcal pyrogenic exotoxin C
SPR – Surface plasmon resonance
SSA – Streptococcal superantigen A
TCR – T cell receptor
TMB –3, 3', 5, 5'–Tetramethylbenzidine
TNF-α – Tumor necrosis factor-α
TSS – Toxic shock syndrome
TSST-1– Toxic shock syndrome toxin-1
Vα – Variable domain of α chain of TCR
Vβ – Variable domain of β chain of TCR

CHAPTER ONE

ENGINEERING SOLUBLE T CELL RECEPTOR DOMAINS FOR HIGH-AFFINITY BINDING TO STAPHYLOCOCCAL AND STREPTOCOCCAL SUPERANTIGENS[1]

Staphylococcal and streptococcal superantigens

Over the past 30 years, the family of exotoxins expressed by *Staphylococcus aureus* and group A *Streptococcus* known as "superantigens" (SAgs) [1] has been studied extensively at the molecular and structural levels. These toxins are referred as superantigens because they stimulate a large fraction of an individual's T cells. One consequence of this hyperactivity is massive cytokine release leading to severe tissue inflammation and, in some cases, systemic organ failure and death. The molecular basis of action of SAg involves its binding to both the variable region of the beta chain (Vβ) of a T cell receptor (TCR) on a T cell and a class II product of the major histocompatibility complex (MHC) on an antigen presenting cell. This cross-linking leads to aggregation of the TCR complex that initiates downstream signaling resulting in massive release of inflammatory cytokines, including tumor necrosis factor-α (TNF-α), interferon-γ (IFN-γ), and interleukin (IL-2), into the circulation or tissues. A common feature of SAgs is that they bind with relatively low affinity to the variable region of the beta chain (Vβ) of the TCR. Despite this low affinity binding, SAgs are very potent, as each T cell requires only a small fraction of their receptors to be bound in order to trigger cytokine release.

There are 24 SAgs known to be expressed by *S. aureus* and 11 SAgs known to be expressed by group A *Streptococcus* [2-5]. Despite their sequence diversity, these toxins exhibit a canonical structural motif that consists of two domains, a smaller N-terminal domain with two β-sheets and a larger C-terminal domain with a central α-helix and a five-stranded β-sheet [5-8].

[1] This chapter is adapted from a review article published in *Toxins* journal as: Sharma P., Wang N., and Kranz D.M. (2014) "Soluble T cell receptor Vβ domains engineered for high-affinity binding to staphylococcal or streptococcal superantigens.", *Toxins* (Basel), 6(2):556-74.

This canonical structure has presumably allowed SAgs to maintain their ability to interact with a T cell receptor Vβ domain on one side of the molecule and a class II product of the MHC on another side [6]. This dual binding is required for activation of T cells and subsequent cytokine release, as monovalent binding of a ligand to the TCR is not sufficient for signaling. SAg-mediated crosslinking with MHC allows multiple MHC-bound SAg molecules to form a multivalent TCR complex, thereby initiating signaling [6, 9, 10].

The pathogenic function of SAgs is not clear, although it is likely related to their ability to dysregulate an immune response, or perhaps to generate a cytokine milieu that is favorable for survival of the organism. While the precise functional or evolutionary advantage of expressing a large family of SAgs with extensive sequence diversity is unclear, one clinical consequence has been that antibodies generated against one of the SAgs are not likely to cross-react with most of the other SAgs, thereby limiting the ability of an individual to neutralize multiple toxins [11]. Understanding the clinical correlates of SAg expression are further complicated because of the varied prevalence of individual SAg genes among different bacterial isolates, especially of *S. aureus* [12, 13]. Most of the SAgs, including staphylococcal enterotoxin A (SEA), SEB, SEC, and toxic shock syndrome toxin-1 (TSST-1), are encoded on variable genetic elements [14-17]. Thus, some strains express one or more SAgs while other strains can express a different pattern of SAgs. Finally, there is additional complexity because there is variation in SAg protein expression levels, with some evidence that SAgs SEB, SEC and TSST-1 may be expressed at higher levels than the other SAgs, due to transcriptional regulation [18].

Despite this variability in prevalence and expression levels, it is clear that the potency of SAgs is a direct cause of disease or at the least exacerbates a host of diseases. These include toxic shock syndrome (TSS), pneumonia, purpura fulminans, severe atopic dermatitis, and endocarditis [19-25]. While TSS is the disease most often associated with SAgs, especially TSST-1, the frequency of staphylococcal or streptococcal infections in specific tissues (e.g. lung, skin,

soft tissue) results in SAg-mediated, hyper-inflammatory reactions at these sites [26, 27]. Specific inhibition of such severe tissue inflammation could be a useful adjunct to treatment of these diseases.

Given the considerable structural information about SAgs and their interaction with Vβ domains, research in the Kranz laboratory has been directed toward engineering soluble versions of the Vβ domains against various SAgs for the purpose of developing potent neutralizing agents that could suppress the hyper-inflammatory properties of SAgs [28]. A similar receptor-based strategy has worked for neutralizing the effects of TNF-α with the soluble TNF-α receptor/immunoglobulin fusion Etanercept (trade name Enbrel) [29, 30]. Because of the low affinity of SAgs for their Vβ receptors, the reasoning has been that effective neutralization would require the generation of higher affinity variants of the Vβ, which would outcompete toxin engagement by cell-bound TCRs bearing any Vβ region since the same binding epitope on the SAg is used regardless of the Vβ region expressed by the T cell. To achieve this affinity maturation, directed evolution process and yeast display [31, 32] have been used, an approach that has yielded, to date, high-affinity Vβ proteins against the six SAgs: SEA (this work, Chapter 2), SEB, SEC3, TSST-1, SpeA, and SpeC [28, 33-37]. Several of these have also been used successfully in animal models of *S. aureus* infections involving (TSS), pneumonia, skin disease, and endocarditis [20, 33, 35, 36, 38]. The engineered, high-affinity Vβ receptors also have dual use as specific and sensitive detecting agents, as described in Chapter 3.

Structural features of the superantigens

SAgs are structurally homologous, even though the primary sequences of the proteins are diverse [1, 5]. These proteins are globular and range between 20 and 30 kilodaltons [5]. Staphylococcal and streptococcal SAgs have been classified into five groups based on differences in their amino acid sequences [5]. Sequence alignments of specific members of these

groups (TSST-1 from Group I; SEB, SEC3 and SpeA from Group II; SEA from Group III and SpeC from Group IV), that have been the targets high-affinity Vβ regions engineered by yeast display (see below) are shown in Figure 1.1. These six SAgs have 10 to 65% sequence identity among each other. SEB, SEC3 and SpeA are 50 to 65% identical, and perhaps it is not surprising that all three stimulate T cells with the same Vβ, mouse Vβ8.2 [5]. Although SpeC belongs to a different group than SEB, SEC3 and SpeA, it exhibits significant sequence homology with these proteins in specific regions, despite having overall low sequence identity (21% identity with SEB and SEC3, and 24% identity with SpeA). Overall, TSST-1 is the most distant and contains the lowest level of sequence homology (and 7 to 20% identity) to these SAgs.

Examination of the aligned sequences shows that there are several linear stretches of amino acids that are more similar among the six SAgs. However, examination of their co-crystal structures with the variable regions of beta chain (Vβ) of TCRs or with class II MHC ligands suggest that the regions interacting with these ligands are among the least homologous (Fig.1.1). These include residues at the N-terminus centered near position 20 which is part of the epitope for binding the Vβ region of the TCR [39-42]. Other Vβ binding regions are found between residues 90 to 95, and near the C-terminus of the protein sequences (positions 215-220), which also appear to lack the same degree of homology as flanking regions which are involved the structural framework for the SAgs. Thus, the residues in these regions, and also their atomic interactions with the cognate Vβ, most often differ and thereby account for the specificity of the interactions between SAg and the TCR. Nevertheless, SAgs that employ a zinc-dependent binding site for interaction with class II MHC ligands use conserved residues for coordinating zinc ion (Fig.1.1).

SEA, SEB, SEC3 and SpeA also contain a conserved region (residues 45 to 55 in Fig.1.1) that serves as a binding site for class II MHC [43-47]. These same four SAgs, but not SpeC and TSST-1, possess a characteristic cystine loop of 9 to 19 residues [48, 49], which has been

implicated in emetic activity of SAgs. Toxins such as SpeC and TSST-1 that lack the cystine loop have been shown to exhibit reduced or no emetic activity [50].

Although many of the staphylococcal and streptococcal SAgs possess overall low sequence identity, their structures possess striking similarity. The canonical structure consists of a N-terminal, β-barrel containing domain and a C-terminal domain containing a β-grasp motif and an α-helix which spans the center of the structure, connecting the two domains [5] (Fig.1.2). In the past two decades, a number of crystal structures of SAg have been solved some of which are listed in Table 1.1. Co-crystal structures with the Vβ region of TCR or class II MHC, have provided the basis for understanding SAg interactions with receptors on T cells and antigen presenting cells. The different modes of interaction of each SAg with these receptors reveal the diversity in mechanisms of binding to Vβ and class II MHC, which is particularly intriguing considering they possess highly conserved three-dimensional folds.

Four different modes of interaction of SAgs with class II MHC have been described: (1) SEB, SEC, SpeA bind to class II MHC alpha chain with a single, low affinity binding site that is located in the N-terminal domain of the protein. This binding is independent of the peptide located in the groove of the MHC-II molecule. (2) TSST-1 on the other hand uses a peptide-dependent binding mechanism to interact with low affinity to the class II MHC alpha chain through the TSST-1 N-terminal binding domain. (3) SpeC binds to the beta chain of class II MHC with high affinity, in a zinc-dependent manner through the C-terminal domain of SpeC. (4) SEA contains both a low affinity binding site and a high affinity, zinc-dependent site which could possibly involve cross-linking of MHC molecules [43-45, 47, 51, 52].

Process of engineering high-affinity T cell receptor Vβ domains against superantigens SEA, SEB, SEC3, TSST-1, SpeA, and SpeC

Except for staphylococcal enterotoxin H (SEH), which has been shown to interact primarily with the variable region of the alpha chain (Vα) of the TCR [53, 54], SAgs are known to specifically interact with variable regions of TCR beta chain (Vβ). The hallmark feature of SAgs is that they stimulate T-cells that bear a specific subset of variable regions in their beta chains (Vβ) [55, 56]. Interestingly, despite their potent activity, SAgs are known to bind to their cognate Vβ receptors with low affinity (K_D values in the micromolar range) (Table 1.2 and [57-59]). Several soluble, high-affinity TCR Vβ mutants have been engineered for purposes of developing antagonists that can effectively neutralize their toxic effects *in vivo*, or for detecting them in food sources, or culture supernatants of potential pathogenic strains of *Staphylococcus aureus* and *Streptococcus pyogenes* [28, 33-37]. These Vβ mutants bind to one of six key staphylococcal and streptococcal SAgs (SEA, SEB, SEC3, TSST1, SpeA, and SpeC), at the same epitope as the wild type receptors but with much higher affinity, in the picomolar to nanomolar range. These represent 1,000 to 3,000,000-fold increases in affinity, compared to wild-type (Table 1.2). Unlike antibodies, which could bind to any epitope of the SAg, engineering of the Vβ ensures that the neutralizing agent binds the identical SAg epitope as the wild-type receptor, thereby ensuring that direct competition and corresponding neutralization occurs.

The process of engineering high-affinity T cell receptor Vβ domains against SAgs SEA, SEB, SEC3, TSST-1, SpeA, and SpeC is described below. All high-affinity Vβ mutants were engineered using yeast display technology (Fig.1.3) [31, 32] and directed evolution. The process involved use of a wild type Vβ from TCRs known to be stimulated by the SAg of interest. This Vβ gene was cloned into the yeast display vector (pCT302) in frame with the yeast mating protein, Aga2 to be displayed on the yeast surface. The Vβ gene was flanked by hemagglutinin (HA) and c-myc tags, which served as probes of the protein expression. Unlike many antibody variable

domains, wild type Vβ domains typically require that one or more key mutations be engineered into the protein in order to be expressed on the yeast cell surface [60, 61]. To accomplish this, the Vβ gene was subjected to error-prone PCR to introduce random mutations, and the library was selected by fluorescence-activated cell sorting (FACS) with a conformation-specific anti-Vβ antibody (these are typically available commercially against most of the human Vβ regions). Anti-Vβ antibody is used, rather than fluorophore-labeled SAg at this stage, as the affinity of the SAgs with wild type Vβ are so low that detection by flow cytometry is not possible. The mutated Vβ region that allows it to be expressed on the surface of yeast is often called a "stabilized Vβ" as it has been shown that such mutations yield stabilized, soluble domains [62] (Fig.1.4).

Stabilized Vβ region genes serve as templates for either additional random mutagenesis or for site-directed mutagenesis to generate libraries (Fig.1.4) with mutations in the putative SAg-binding sites. Typically, selection of the sites for mutagenesis was guided by the crystal structure of Vβ:SAg complexes. If structural information was not available, such as with the engineering of Vβ against SEA (Chapter 2), [37], residues in CDR2 were chosen to generate the first generation site-directed mutagenesis libraries because of its central role in the interaction of other Vβ regions with SAgs, as observed in Vβ:SAg crystal structures [39-42]. To construct the site-directed mutagenesis libraries, amino acid positions were encoded by randomized codons (NNS) in primers, and cloned by PCR using overlapping primers. PCR products were transformed into yeast cells by homologous recombination, yielding library sizes of 10^6-10^8 transformants.

Pre-selected degenerate libraries typically exhibit no detectable binding with SAg by flow cytometry due to their low affinity, or loss of binding, by the great majority of mutants. To select for the rare Vβ mutants that exhibit higher affinity binding, libraries were subjected to several rounds of selection with a decreasing concentration of biotinylated-SAg, followed by staining with fluorescently-labeled streptavidin, and fluorescence-activated cell sorting (FACS). In each round of selection, a small fraction of cells that exhibited the top 1% fluorescence upon selection with

SAg of interest, were collected and expanded for subsequent rounds of screening. When a distinct yeast population with positive SAg-staining emerged after 3~4 rounds of selection, yeast cells were plated and higher affinity clones were isolated, characterized and sequenced. In the engineering of Vβ22 against SEA, mutations isolated from the CDR2 library alone were capable of increasing the SEA affinity by 25,000-fold (Chapter 2), [37]. Even more strikingly, with the engineering of mouse Vβ8.2 against SEB, mutations from one CDR2 library accounted for a 220,000-fold increase of Vβ affinity with SEB (from 144 μM wild-type affinity to 650 pM for G2-5) [33]. These results have further validated the essential role of CDR2 loop in Vβ:SAg interactions (see below).

Following the initial selection, additional mutagenized libraries were often constructed in regions (CDR1, HV4 and FR3) that flank CDR2 in the tertiary structure, using one or a combination of the first generation lead mutants as templates. After further affinity- or off-rate-based selections, mutants exhibited a more modest 10 to ~100 fold further increase in affinity. The specific region(s) where higher affinity mutations were successfully isolated for each pair of Vβ/SAg reflected, in part, the diverse binding modes of the SAgs with their cognate Vβs. Ultimately, mutations isolated from multiple libraries could be combined to generate the highest affinity mutants that yielded 1,000 to 3,000,000-fold increases in affinity with targeted SAgs compared to the wild type Vβ.

Topology of Vβ:superantigen interactions

Crystal structures of five out of six SAgs discussed in this review have been solved in complex with their cognate Vβ receptor ligand (Fig.1.5 B-F) [39-42]. In general, the Vβ receptor docks in the cleft between the two domains of the SAg and uses its hypervariable loops (CDRs), or specific framework (FR) regions for engagement (Fig.1.5). Co-crystal structures of different SAg with their cognate Vβ ligands indicate that Vβ domains interact with the SAgs with

considerable diversity in positioning and in interaction chemistries. However, the CDR2 loop of Vβ appears to be central to each SAg-TCR interaction [63, 64] (Fig.1.5). Other regions of the Vβ appear to play important, but supporting roles, in the binding energy and specificity for the SAg [34, 63, 65].

SEB, SEC3 and SpeA (Group II SAg) are more structurally similar and each has been co-crystallized with murine Vβ8.2 (mVβ8.2) [39-41]. As indicated, these three SAgs possess 50-65% sequence identity and they engage with the mVβ8.2 region of the TCR using similar residues (Fig.1.1), thereby determining their specificity for mVβ8.2. Accordingly, SEB, SEC3 and SpeA interact with mVβ8.2 with similar topologies (Fig.1.5), and they engage in intermolecular contacts primarily with CDR2 (accounting for 50%, 63% and 33% of total contacts respectively), HV4 and to some extent framework (FR) regions.

The mechanisms by which these three SAgs interact with mVβ8.2 are largely dependent on the common conformation of CDR2 and HV4, although SpeA forms a distinct contact via its E94 residue, by forming hydrogen bonds with N28 of CDR1 loop of mVβ8.2 [41]. Since SEB and SEC3 depend primarily on interactions with main chain atoms of Vβ-CDR2, their Vβ binding specificity is considerably reduced. However, SpeA:Vβ8.2 interaction specificity appears to be enhanced because the interface involves H-bonds between side chain atoms from both SpeA and the Vβ molecule.

In contrast, SpeC interacts with human Vβ2.1 (hVβ2.1) with more extensive use of the Vβ region, engaging all of the hypervariable loops. The specificity of the SpeC:hVβ2.1 interaction is increased by numerous H-bonds and van der Waals interactions with both main chain and side chain atoms of hVβ2.1. Non-canonical amino acid insertions in CDR1 and CDR2, and the presence of an extended CDR3 loop (at least in some β-chains), also increase the specificity of hVβ2.1 for SpeC [41].

Human Vβ2.1 is also the highly restricted target of TSST-1. Thus, both SpeC and TSST-1 interact with hVβ2.1 and both engage residues in CDR2 to make contacts with Vβ. Although the two toxins engage a few common residues in CDR2, each also uses other distinct, non-overlapping regions for binding and for achieving specificity. TSST-1 uniquely binds FR3 while SpeC engages with Vβ in a distinct mode by making extensive contacts involving residues from CDR1, HV4, FR2, FR3 and CDR3 in Vβ [41, 42]. The specificity of TSST-1 for hVβ2.1 has been attributed to the involvement of hVβ2.1 FR3 residues E61 and K62. It has been speculated that TSST-1 does not activate T-cells bearing other Vβ domains because 75% of all other human TCR Vβ regions possess a proline at position 61, resulting in reduced conformational flexibility; this reduced flexibility could prevent the specific conformation required for interaction with TSST-1. In addition, the absence of a residue at position 62 in 50% of human TCR Vβ domains also contributes to the high specificity of TSST-1 for hVβ2.1 [42]. Finally, the residues that TSST-1 uses to interact with Vβ2.1 share little homology with residues that other SAgs (including SpeC) interact with their cognate Vβ ligand (Fig.1.1), which further enhances TSST-1 specificity towards hVβ2.1. The molecular basis of the extreme Vβ specificity of TSST-1 has recently been determined to be the combination of both the non-canonical conformation adopted by CDR2 region of the Vβ along with residues Y56 and K62 on FR3 region [64].

Structural basis of high-affinity and specificity of the Vβ:SAg interactions

Although CDR2 regions have served as the predominant site for improving the affinities of Vβ domains for binding to their SAgs, it is clear that other regions can also serve to enhance affinity through structural changes in each Vβ:SAg interface. The involvement of regions other than CDR2, also can contribute to the high level of specificity in Vβ:SAg interactions exhibited by the high-affinity Vβ mutants. Several structures have been solved of SAgs in complex with engineered, high affinity Vβ domains, thereby providing an understanding of the interactions that

confer both higher affinity and specificity [42, 66, 67]. Not surprisingly, multiple factors, including increases in van der Waals interactions, hydrogen bonds, hydrophobic interactions, cooperativity, and conformational flexibility have all been shown to be involved. The generation and structural basis of high affinity for select Vβ domains is discussed below.

In order to generate a high affinity Vβ mutant for binding SEC3, mVβ8.2 was displayed on the surface of yeast and mutations were introduced by error-prone PCR, followed by site directed mutagenesis to combine mutations. One resulting mutant, called L2CM (K_D = 7 nM) (also called mL2.1/A52V, a first generation variant of L3, Table 1.2) exhibited ~450 fold increase in affinity compared to the wild type [28]. The structural basis of the SEC3:Vβ interaction has been studied extensively by alanine scan mutagenesis [68], and the high-affinity interaction with L2CM has been examined for binding energetics [69] and crystallization of various L2CM variants [66]. Although L2CM contained nine mutations, only four (A52V, S54N, K66E, Q72H) were energetically significant [69]. Structural analysis [66] indicated that the A52V mutation in CDR2, allowed an increase in hydrophobic contact area and also induced conformational changes in Q72 of the Vβ. The S54N mutation in CDR2 participated in affinity maturation by allowing recruitment of water molecules to SEC3:Vβ interface hence mediating contacts between $N26^{Vβ}$ and $N24^{Vβ}$ with D204, K205 and F206 in SEC3. Residue K66 appeared to be conformationally restrained in the SEC3:wtVβ8.2 structure, but it adopted a more extended conformation when mutated to glutamate. This also resulted in loss of van der Waals interactions with SEC3 and unfavorable change in enthalpy of binding but a highly favorable entropic change, resulting in a higher affinity complex [69]. Mutations Q72H and A52V were shown to be involved in inducing subtle conformational changes in hypervariable loops, thereby affecting how CDR1 residues, and CDR2 residue 52, interacted with SEC3. Although the A52V mutation had a dominant effect in affinity maturation by mediating restructuring events of the hypervariable loops, Q72H had a minor but significant contribution to affinity maturation [66]. Recently, L2CM was further engineered by

incorporating additional mutations in CDR1, HV4 and framework regions to obtain mutant L3 (K_D = 3 nM) (Table 1.2 and [36]).

mVβ8.2 was engineered for binding to SEB with a remarkable 3-million fold increase in affinity relative to wild-type mVβ8.2 (Table 1.2 and [33]). The engineered protein (G5-8) was crystallized in complex with SEB [67]. The structural details of this complex indicated that lengthening CDR1 loop by incorporation of a serine residue at CDR1 residue 27a, and incorporation of additional mutations N28Y and H29F, resulted in a distinct conformation of CDR1 loop. These mutations resulted in an increase in intermolecular contacts with SEB. Y28 in G5-8 was involved in pi stacking interaction with R110 in SEB and in H-bond interaction with N60. Additionally, two mutations (A52I and G53R) acquired in CDR2, resulted in replacement of residues with smaller side chains to relatively larger side chains which resulted in an increase in van der Waals contacts and H-bond formation with N31, N60 and N88 in SEB. Overall, it was concluded that an increase in the number of intermolecular contacts between G5-8 and SEB resulted in the significant increase in binding affinity [67].

mVβ8.2 was also engineered for high affinity (K_D = 270 pM) for SpeA, using yeast display [35]. Key mutations which were responsible for affinity maturation were acquired in CDR2 (G53K, S54H), CDR1 (N30K) and in HV4 (Q72R). The resulting mutant, KKR showed a 22,000 fold affinity improvement compared to wt Vβ8.2 (K_D= 6 μM) [41]. Although there is no crystal structure of SpeA with the high affinity Vβ, revertant mutants and energy minimized computer modeling of the mutated Vβ-SpeA complex allowed predictions of the basis of the affinity increase. The analysis revealed that the side chain of arginine acquired at position 53 in mutant KKR could be accommodated in a binding pocket in SpeA and promoted favorable interactions with side chain oxygen of Y90 and E88 of SpeA. Not only could this account for the affinity maturation, it could contribute to reduced cross-reactivity with SEC3, yet the ability of mutant KKR to not only retain cross-reactivity with SEB but to do so with high-affinity.

The mutant of hVβ2.1 called D10 was engineered for high affinity (K_D = 180 pM) against TSST-1, using yeast display (Table 1.2 and [34]). D10 contained 14 mutations relative to stabilized wt Vβ2.1 (EP-8). Of these 14 mutations, four were found to be energetically significant: three mutations in CDR2 (at residues 51, 52a and 53) and one mutation in FR3 (at residue 61). Surprisingly, positive cooperativity was observed between the distant mutations in CDR2 and FR3 [65]. Crystal structure analysis indicated that changes in intermolecular contacts, buried surface and/or shape complementarity were not the primary driving factor in affinity maturation of hVβ2.1 to TSST-1. Instead, altered conformational flexibility of D10 was proposed to have resulted in affinity increase by linking CDR2 and FR3 at the Vβ:SAg interface [42]. Using a similar approach, the hVβ2.1 region gene has also been engineered for high-affinity binding to SpeC [Wang & Kranz, Unpublished].

In Chapter 2, the hVβ22 region was engineered for high affinity binding (K_D = 4 nM) to SEA using yeast display [37]. The engineered mutant called FL contained ten mutations, of which five were located in CDR2. In the absence of a crystal structure of SEA with cognate Vβ, it was proposed that the structural basis of high affinity was probably due to improved electrostatic interactions (due to mutations N52E and E53D in CDR2), and pi stacking interactions involving N51Y in CDR2 with Y94 and Y205 in SEA's putative TCR binding site.

High-affinity Vβ domains as neutralizing agents

The first study to validate the use of soluble, high-affinity Vβ domains in the neutralization of SAg activity was performed with the Vβ L2CM against the SAg SEC3. This work showed that soluble L2CM, but not soluble wild-type Vβ8, was able to completely inhibit SEC3-mediated T cell cytolysis at nanomolar concentrations [28]. This same high-affinity Vβ was fused to a class II MHC molecule in an attempt to increase the avidity of the interaction with SEC3 [70]. Although the

fusion was shown to inhibit SEC3 activity *in vitro*, this study did not show whether the fusion had greater activity than the high-affinity Vβ alone.

Subsequent studies showed that the high-affinity Vβ against SEB, G5-8, but not the wild-type Vβ8.2, was able to inhibit both *in vitro* and *in vivo* activities of SEB [33]. In this study, the *in vitro* activity was shown to be progressively improved in comparing different generations of mutants, with K_D values from 100 μM to 50 pM. For example, the 50 pM G5-8 protein was more effective at inhibition (i.e. had a lower IC_{50}) than the 650 pM G2-5 protein. Furthermore, the G5-8 protein was administered to rabbits intravenously at the same time or after SEB administration, in an LPS-enhancement model of lethality. The protein was able to prevent death even at concentrations close to stoichiometric with the SEB. In the same study, G5-8 administered daily to rabbits implanted with pumps containing SEB was able to prevent temperature increases and lethality due to the SAg. In a rabbit model of skin disease, G5-8 was able to inhibit the hypersensitivity reactions caused by SEB [38].

An in-frame fusion of the high-affinity G5-8 against SEB and the high-affinity D10 against TSST-1 (yielding a single 30kDa protein, expressed in *E. coli*) was able to completely inhibit the *in vitro* activity of both SEB and TSST-1 [71], raising the possibility that multiple SAgs might be neutralized with a single therapeutic. An alternative approach is to identify a high-affinity Vβ domain that cross-reacts with multiple SAgs. While this has not been possible for structurally distinct SAgs (e.g. SEB and TSST-1), it has been shown that Vβ domains against SEB (e.g. G5-8) cross-reacted with high-affinity against SpeA, and that Vβ domains were capable of inhibiting both SEB and SpeA in the LPS enhancement models [35]. More recent findings showed that it is possible to engineer a cross-reactive neutralizing Vβ (L3) against both SEC3 and SEB [36].

The greatest clinical potential of soluble, high-affinity Vβ domains, aside from possible applications in biodefense, would be in serious diseases caused by *S. aureus*. The first study to show that high-affinity Vβ proteins were effective in diseases caused by *S. aureus* (i.e. rather than

the purified toxins), involved a rabbit model of pneumonia [20]. Rabbits receiving an intrabronchial inoculation (2 x 10^9 cells) of *S. aureus* USA400 strain CA-MRSA c99–529 (SEB^+) were protected from death when treated with 100 µg of G5-8, administered intravenously on a daily basis. Subsequent studies have shown that the high-affinity Vβ L3 against SEC3 also protected rabbits exposed to an SEC-positive strain of MRSA (USA400 MW2) in the pneumonia model [36]. Interestingly, the same L3 protein was capable of significantly reducing the bacterial burden of the MRSA (USA400 MW2) strain in an infective endocarditis model [36]. These pre-clinical studies suggest that these small Vβ proteins could be used intravenously, with antibiotics, to manage staphylococcal diseases that involve SAgs. The diversity of SAgs among different strains of *S. aureus* will likely require that diagnostics be developed for detection of the specific SAgs in patients, or that a multi-targeted therapeutic that can neutralize many of the SAgs be developed.

High-affinity Vβ domains as detecting agents

In Chapter 3, my efforts were directed toward using high-affinity Vβ domains for detecting SAgs. Capture ELISAs as well as flow-cytometry based methods were developed for detection of each SAg. Multiplex assays using the flow-cytometry platform were also developed to detect several SAgs in the same sample. This approach allowed specific detection and also quantitative determination of staphylococcal SAgs SEA, SEB and TSST-1 in supernatants derived from cultures of 18 strains of *Staphylococcus aureus* (Chapter 3).

FIGURES

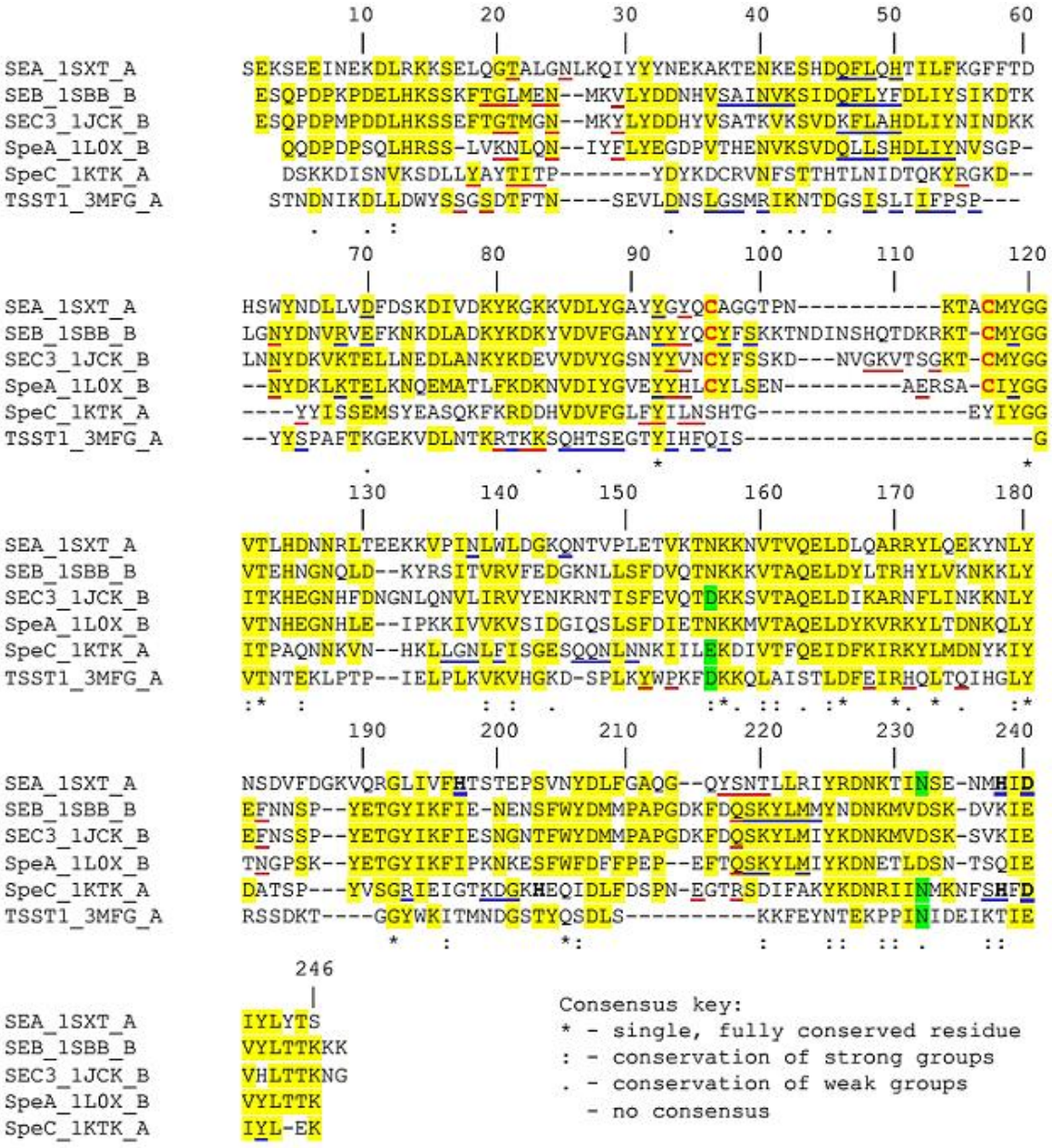

Fig. 1.1. Multiple sequence alignment of various Superantigen sequences
The sequence of each superantigen (SAg) was obtained from the PDB file corresponding to its crystal structure. Multiple sequence alignment (CLUSTAL W (1.81)) was performed using “Biology WorkBench” online tool. Positions with homologous amino acids in three or more SAg sequences are highlighted in yellow or green. Residues in red are involved in forming the characteristic disulfide loop in certain SAg. Residues underlined in red and in blue are involved in binding to Vβ and class II MHC, respectively. Residues in bold are involved in binding zinc.

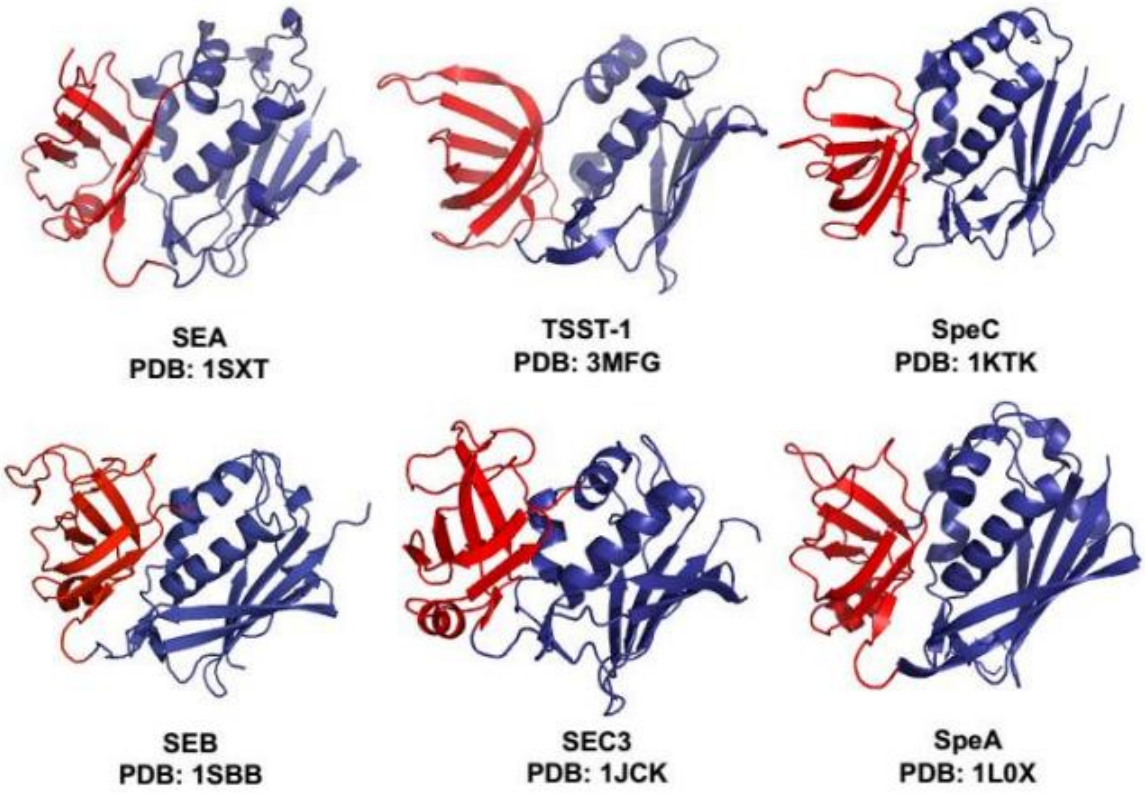

Fig. 1.2. Two-domain architecture of Superantigens
The canonical structure of SAg consists of two domains. The N-terminal domain (red) consists of a β barrel motif and C-terminal domain (blue) consists of a β-grasp motif and an α-helix which spans the center of the structure.

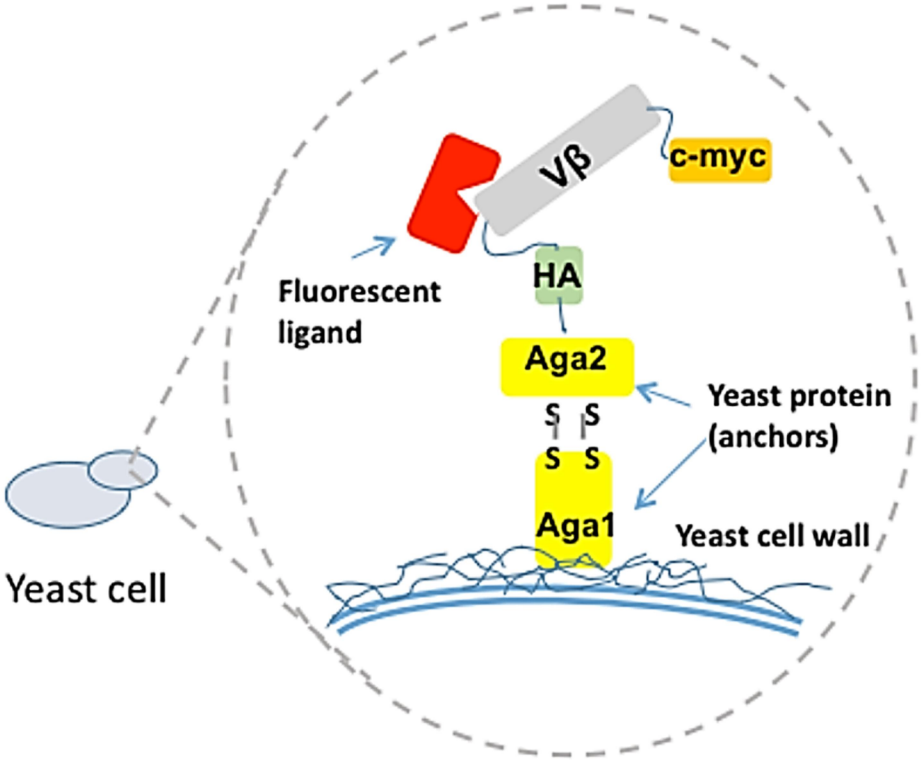

Fig. 1.3. Schematic of yeast display system for engineering high-affinity Vβ domains against Superantigens
The Vβ libraries with various mutations are fused to the C terminus of the yeast mating protein Aga-2 to be displayed on the yeast cell surface. HA and c-myc tags are included in the fusion gene to probe and quantify the Vβ protein expression level. Fluorescent ligands include either a monoclonal antibody to the Vβ region or the SAg.

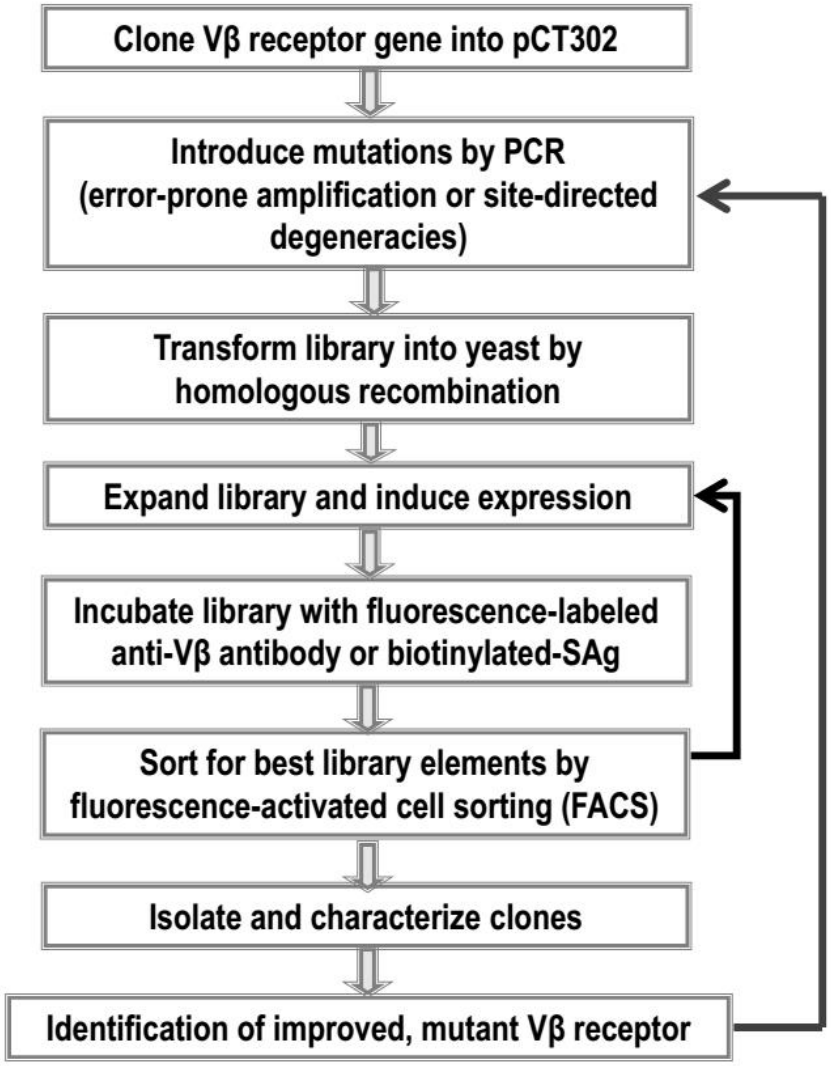

Fig. 1.4. General flow chart for the cloning, display and engineering of high-affinity Vβ domains by yeast display

A Vβ clone that is specific for the SAg of interest is cloned into the yeast display vector, pCT302 (Figure 3) and used to generate libraries of mutants. The libraries are selected with fluorescently-labeled ligands, (e.g. conformation-specific anti-Vβ antibodies or the SAg of interest). Multiple rounds of selections are conducted to enrich the Vβ mutants with desired properties, which serve as templates for subsequent library design and screening to achieve desirable stability or affinity of Vβ with SAg.

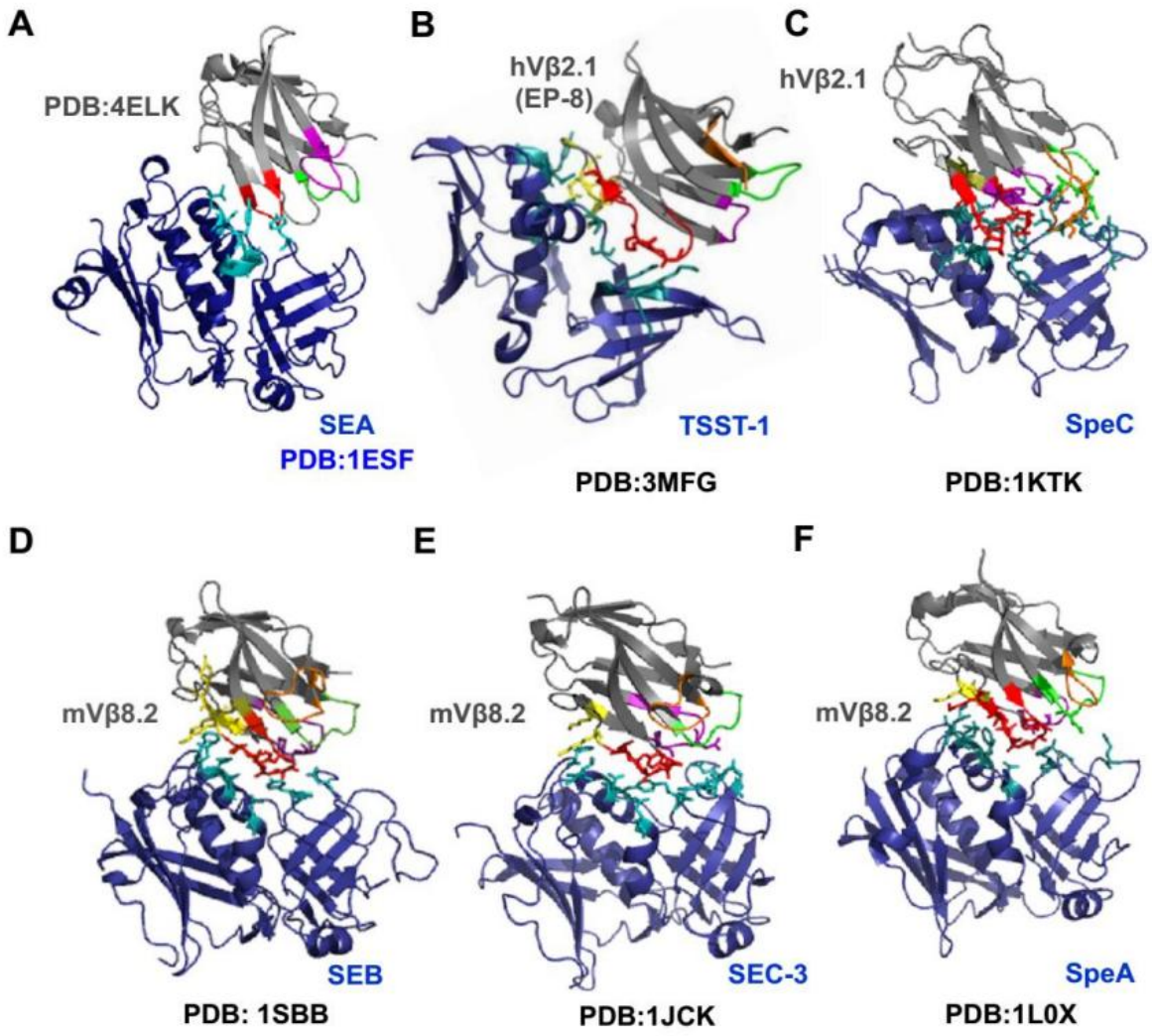

Fig. 1.5. Co-crystal structures of six superantigens with cognate Vβ domain of the T cell receptor

Except for SEA, the co-crystal structures of SAg (blue) with their cognate Vβ ligand (gray) are available in PDB (Table 1). In Panel A, the SEA crystal structure was manually docked with mouse Vβ16 crystal structure (PDB: 4ELK), that is 66% identical to human Vβ22 protein sequence. Residues of SAg interacting with Vβ are indicated in teal. Various regions of Vβ are colored as follows: CDR1 (green); CDR2 (Red); CDR3 (orange); HV4 (purple); FR2 (olive) and FR3 (yellow). Interacting residues of Vβ and SAg are displayed in stick configurations.

TABLES

Table 1.1. Crystal structures of staphylococcal and streptococcal superantigens and their complexes with Vβ domains

Organism	SAg	Crystal Structure (PDB code, ligand)	Year	Reference
S. aureus	SEA	1ESF (co-crystallized with Cd^{2+})	1995	[72]
S. aureus		1SXT (co-crystallized with Zn^{2+})	1996	[73]
S. aureus	SEB	3SEB	1998	[74]
S. aureus		1SBB (co-crystallized with mVβ8.2)	1998	[39]
S. aureus		3R8B(co-crystallized with affinity matured mVβ8.2 mutant G5-8)	2011	[67]
S. aureus	SEC3	1CK1 (co-crystallized with Zn^{2+})	2002	[75]
S. aureus		1JCK (co-crystallized with mVβ8.2)	1996	[40]
S. aureus		2AQ3 (co-crystallized with affinity matured mVβ8.2 mutant L2CM)	2005	[66]
S. aureus	TSST-1	2QIL	1996	[76]
S. aureus		2IJ0 (co-crystallized with affinity matured hVβ2.1 mutant D10)	2007	[42]
S. aureus		3MFG (co-crystallized with hVβ2.1 stabilized wild-type EP-8)	2011	[67]
S. pyogenes	SpeA	1FNU (co-crystallized with Cd^{2+}) 1FNV (co-crystallized with Cd^{2+}) 1FNW (co-crystallized with Cd^{2+})	2000	[77]
S. pyogenes		1L0X(co-crystallized with mVβ8.2) 1L0Y(co-crystallized with mVβ8.2 and Zn^{2+})	2002	[41]
S. pyogenes	SpeC	1AN8	1997	[78]
S. pyogenes		1KTK (co-crystallized with hVβ2.1)	2002	[41]

Table 1.2. High-affinity Vβ domains that bind to various superantigens

Organism	SAg	Wild-type Vβ		High-affinity Vβ		Improvement in affinity (fold)	References
		Name	Affinity (μM)	Name	Affinity (pM)		
S. aureus	SEA	Human Vβ22	100	FL	4000	25,000	[37] (this work, Chapter 2)
S. aureus	SEB	Mouse Vβ8.2	144	G5-8	50	2,880,000	[33, 57]
S. aureus	SEC3	Mouse Vβ8.2	3	L3	3000	1,000	[36, 57]
S. aureus	TSST-1	Human Vβ2.1	2.3	D10	180	13,000	[34]
S. pyogenes	SpeA	Mouse Vβ8.2	6	KKR	270	22,000	[35, 57]
S. pyogenes	SpeC	Human Vβ2.1	20	HG_FI	500	40,000	[41], Wang & Kranz, Unpublished

CHAPTER TWO

ENGINEERING A Vβ DOMAIN OF THE T CELL RECEPTOR FOR BINDING WITH HIGH AFFINITY TO STAPHYLOCOCCAL ENTEROTOXIN A (SEA)[2]

Introduction

Staphylococcus aureus is a ubiquitous microorganism that causes a wide range of conditions including food poisoning, skin rashes, pneumonia, endocarditis, and toxic shock syndrome. CDC estimated that for foodborne illnesses in the United States in 2011, *S. aureus* was among the top five pathogens. Other reports have suggested that *S. aureus* mediates approximately 240,000 food-borne illnesses per year in the United States [79]. It is known that *S. aureus* secretes a collection of enterotoxins that are heat resistant, 20-30 kDa proteins [3, 5, 80], which upon ingestion with food cause symptoms that include abdominal cramps, nausea, emesis and diarrhea.

More than twenty staphylococcal enterotoxins (SEs) and SE-like proteins have been described, of which approximately half possess emetic properties [5, 81]. These enterotoxins, along with other toxins from *Staphylococcus aureus* and *Streptococcus pyogenes,* have been classified into five distinct homology groups. SEA, SED, and SEE are in Group III. SEA and SEE are 83% identical in sequence, while SEA and SED are 48% identical in sequence (SED and SEE are 50% identical in sequence). The structures of enterotoxins among the different groups have been shown to be remarkably similar, despite low sequence identity among many of the members. The canonical structure consists of an N-terminal, beta barrel containing domain and a C-terminal

[2] Sections of this chapter were published in Protein Engineering, Design and Selection (PEDS) journal as a research article: Sharma P., Postel S., Sundberg E.J., Kranz D.M. (2013) "Characterization of the Staphylococcal enterotoxin A: Vβ receptor interaction using human receptor fragments engineered for high affinity", *Protein Engineering Design and Selection*, 26(12):781-9

domain that consists of a beta-grasp motif and an alpha helix which spans the center of the structure [39, 40, 43, 73, 82].

Characterization of various food poisoning outbreaks throughout the world has indicated that the presence of SEA in food, either alone or with other enterotoxins such as SED, SEE and SEH, was most often associated with the illness [83-88]. It has been estimated that the dose of SEA that is capable of causing the disease was a few hundred nanograms per individual [84, 89].

Other than its role in inducing gastrointestinal problems, SEA is also known to act as a superantigen, inducing hyper-inflammatory reactions in conditions such as endocarditis and toxic shock [90, 91]. As discussed in the introductory chapter, superantigens mediate hyper-inflammatory reactions because of their ability to stimulate a very large fraction of the body's T cells, as compared to conventional peptide-major histocompatibility complex (MHC) antigens, resulting in massive release of inflammatory cytokines, including tumor necrosis factor-α (TNF-α), interferon-γ (IFN-γ), and interleukin (IL-2), into the circulation or tissues [9, 80]. The mechanisms of these hyper-inflammatory reactions involve the binding of the superantigen to the Vβ region of the T cell receptor [39, 40, 42, 92] and also to a class II MHC product on an antigen presenting cell. This trimolecular interaction leads to the stimulation of a large fraction (e.g. 20%) of T cells because of the limited number of Vβ genes in human T-cell repertoire. This process differs from recognition of conventional peptide-MHC antigens which interact with the hypervariable regions (complementarity determining regions, CDRs) of both TCR chains (αβ), and typically stimulates only a small fraction (e.g. <0.1%) of T cells [93]. More recently, the involvement of a co-stimulatory molecule (CD28) on T cells has been proposed to be involved in the hyper-immune response against superantigens [94]. It is thought that the superantigen also binds to CD28 that interacts with B7 molecule on antigen presenting cells, hence providing the second co-stimulatory signal which is required to activate the T cells. The involvement of CD28

is proposed to be involved in formation of a potentially more stable complex at the immunological synapse, hence playing a role in T-cell activation [94].

For most superantigens, it is known that they interact with their cognate Vβ receptors with low affinity (K_D in micromolar range) [57-59]. Although SEA was the first *S. aureus* enterotoxin discovered from a strain isolated from a food poisoning outbreak [95, 96], the details of its interaction with its cognate Vβ receptor are largely unknown. As far as its interaction with class II MHC is concerned, investigators have established that SEA contains two separate binding sites for class II MHC molecule: a low-affinity binding site, and a high-affinity, zinc-dependent site, which possibly results in cross-linking of MHC molecules, hence activating antigen presenting cells, in addition to T cells [43, 52, 97].

Several recent studies involving yeast surface display coupled with mutagenesis and superantigen-binding selections have been conducted to isolate mutants of various Vβ proteins (mouse Vβ8, human Vβ2), that were stabilized for expression as soluble proteins, and that had enhanced affinity for superantigens, SEB, SEC, or TSST-1 [28, 33-36]. These engineered Vβ proteins have enabled the structural characterization of their interactions with the cognate toxin [42], as well as studies on the molecular basis of affinity improvement [67]. Following an analogous process, I engineered soluble forms of both the wild-type receptor and a high-affinity Vβ receptor of SEA, for purposes of understanding its molecular interactions with SEA. Because of its high affinity, the engineered Vβ receptor developed in this study was also useful in developing specific, sensitive assays for detection of SEA.

Based on earlier studies showing that human T cells expressing the Vβ22 region were selectively expanded when stimulated by SEA [98], I chose human Vβ22 as a target for engineering for improving its affinity towards SEA. As with other Vβ22 domains, the wild-type Vβ22 was not expressed well on the surface of yeast. However, I selected for increased surface expression among random Vβ22 mutants, and identified several framework mutations in Vβ22

gene that enabled surface expression, and soluble expression of the mutant proteins. Like other superantigen:Vβ interactions, the Vβ22:SEA interaction had low affinity (K_D = 100 μM). Affinity engineering by selection from a collection of directed Vβ22 libraries revealed the importance of the CDR2 region of Vβ22 in its interaction with SEA. Mutations in CDR2 alone were capable of increasing the SEA affinity by 25,000-fold. The highest affinity mutant bound to SEA with a K_D value of 4 nM, and exhibited a high level of specificity for SEA. The results provided insights into the mode of interaction of Vβ22 with SEA, and the affinity-engineered Vβ22 was also employed for development of sensitive assays for detection of SEA (2.5 ng/ml by capture ELISA, 0.4 ng/ml by bead-based, flow cytometry assay) and as a component of multiplex detection system for staphylococcal and streptococcal toxins, as discussed in chapter 3.

Materials and Methods

Cloning and expression of human Vβ22 on yeast cell surface

The gene encoding human Vβ22 (referred to as hVβ22, hereafter) (Accession number: M64351), synthesized and codon optimized for expression in both *E. coli* and *Saccharomyces cerevisiae* (Genscript USA Inc.), was subcloned as an Aga-2 fusion (under the control of GAL1 promoter) into yeast display vector pCT302 that contains an N-terminal hemagluttinin (HA) and a C-terminal myc (c-myc) tag (Fig. 2.1 A). HA and c-myc tags served as internal controls for protein expression. AGA-2 is a yeast mating agglutinin protein and allows the expression of the protein of interest on the yeast cell surface as a fusion protein [32].

S. cerivisiae EBY100 strain was transformed with hVβ22-pCT302 construct, followed by plating on selective media (SD-CAA (Trp^-) agar plates). Single colony was cultured in SD-CAA (Trp^-) media at 30°C for 48 hours, followed by induction in galactose containing, SG-CAA (Trp^-) media at 20°C for 48 hours. For analyzing expression of HA, Vβ22 and c-myc on the surface, induced yeast cells were incubated with anti-HA antibody (1:50 dilution) (mouse IgG1, clone

HA.11, Covance), anti-Vβ22 antibody (1:10 dilution) (mouse IgG1, clone: IMMU546, Beckman Coulter), or anti-c-myc antibody (1:100 dilution) (chicken IgY, Life Technologies), followed by washing and incubation with Alexa Fluor 488-conjugated secondary antibody (1:100 dilution) (goat anti-mouse or goat anti-chicken, Life Technologies). After washing, cells were analyzed by flow cytometry. 1X PBS (containing 0.5% BSA) was used for diluting all reagents and washing the cells.

Construction of random mutagenesis (error-prone) library and selection of stabilized Vβ22 mutants

Error-prone PCR was used to generate a library of random mutants of hVβ22 gene [99, 100]. The hVβ22 gene was amplified from the pCT302 plasmid using the flanking, splice 4L and T7 promoter primers. PCR products with random mutations were then electroporated into the *S. cerivisiae* EBY100 strain, along with NheI and XhoI digested pCT302 vector. The library in yeast was generated by homologous recombination, followed by expansion in SD-CAA (Trp^-) media at 30°C for 48 hours to allow the growth of yeast cells that were transformed with pCT302 vector. Based on counting the number of colonies obtained after plating different dilutions of error-prone library on selective media (SD-CAA (Trp^-) agar plates), approximate library size was calculated.

The expanded error-prone library was cultured in galactose containing, SG-CAA (Trp^-) media at 20°C for 48 hours to induce protein expression. After induction, the yeast library was incubated with 1:10 dilution of anti-Vβ22 antibody (mouse IgG1, clone: IMMU546, Beckman Coulter) for one hour on ice. Cells were then washed with 1X PBS (containing 0.5% BSA), followed by incubation with goat anti-mouse IgG F(ab')2 conjugated with Alexa Fluor 488 or 647 secondary antibody (Life Technologies) for one hour on ice. After washing, the yeast library was subjected to several rounds of selection using a FACS Aria cell sorter (BD Bioscience). After each sort, the most fluorescent cells from the library were collected and cultured in SD-CAA (Trp^-) media, and then induced in SG-CAA (Trp^-) media for next sorting procedure. After five sorts,

individual yeast clones were obtained by plating the sorted cells on selective media (SD-CAA (Trp^-) agar plates) and their sequences were analyzed.

Flow cytometric analysis of mutants isolated from error-prone library

Individual yeast clones isolated from error-prone library, were cultured in SD-CAA (Trp^-) media at 30°C for 48 hours, followed by induction in SG-CAA (Trp^-) media at 20°C for 48 hours. Expression of HA, Vβ22 and c-myc was examined by incubating the cells with anti-HA antibody (1:50 dilution) (mouse IgG1, clone HA.11, Covance), anti-Vβ22 antibody (1:10 dilution) (mouse IgG1, clone: IMMU546, Beckman Coulter), or anti-c-myc antibody (1:100 dilution) (chicken IgY, Life Technologies), followed by washing and incubation with Alexa Fluor 488-conjugated secondary antibody (1:100 dilution) (goat anti-mouse or goat anti-chicken, Life Technologies). After washing, cells were analyzed by flow cytometry.

For assessing binding of *wt* Vβ22 or Vβ22 mutants to SEA (Toxin Technology, Inc.), induced yeast cells were incubated with various concentrations of non-recombinant, biotinylated-SEA, followed by washing and incubation with streptavidin-Alexa Fluor 488 conjugate (Life Technologies) at 1:200 dilution. After washing, yeast cells were analyzed by flow cytometry.

Thermostability analysis of selected mutants isolated from error-prone library

Selected mutants of Vβ22 from the error-prone library were subjected to thermostability analysis by incubating induced yeast cells at higher temperatures (up to 80ºC for 30 minutes) before incubation with anti-Vβ22 antibody. After incubating with anti-Vβ22 antibody (1:10 dilution) for an hour, the cells were washed and incubated with Alexa Fluor 488-conjugated secondary antibody (1:100 dilution) (Life Technologies). After washing, yeast cells were analyzed by flow cytometry.

Construction of directed mutagenesis (affinity) libraries and selection of high-affinity, SEA-binding Vβ22 mutants

Thermostable Vβ22 mutants obtained from the error-prone library were used as templates for making directed mutagenesis libraries. Degenerate primers were used to introduce diversity in CDR2 region (residues 49 to 54) of Vβ22. Three overlapping, 4-codon libraries were generated, randomizing 4 residues at a time. PCR products were electroporated into *S. cerivisiae* EBY100 strain, along with NheI, XhoI digested pCT302 vector for generation of directed mutagenesis libraries by homologous recombination. Libraries were mixed in equal proportion and subjected to several rounds of sorting for selecting Vβ22 mutant proteins that could bind to SEA with higher affinity. With each round of sorting, a lower concentration of SEA (biotinylated, non-recombinant) (Toxin Technology, Inc.) was used (1μM to 10nM), in order to obtain high-affinity mutants. Binding was assessed by staining with streptavidin-Alexa Fluor 488 or 647 conjugate (Invitrogen) at 1:200 dilution. Individual yeast clones were isolated after sorting the library seven times, and analyzed by flow cytometry for protein expression on cell surface and binding to SEA. Distinct clones were identified by DNA sequencing.

Off-rate analysis of various Vβ22 mutants

Induced yeast cells expressing various mutants of Vβ22 were incubated with 10 nM biotinylated-SEA (non-recombinant) at 4°C. Cells were washed to remove unbound ligand, and then incubated with 100 nM recombinant SEA (unlabeled) at 37ºC for 24 hours. Aliquots of yeast cells were removed at regular intervals to monitor the dissociation of biotinylated SEA molecules. Each aliquot of cells was saved at 4°C until the end of time course, after which they were incubated with streptavidin-Alexa Fluor 647 conjugate (1:200 dilution) for 30 minutes. After washing, the cells were analyzed by flow cytometry.

Effect of site-directed mutations at residues 30 in CDR1, and 49-54 in CDR2 in Vβ22 mutants

Site-directed mutations were generated at residues 30, 49, 50, 51, 52, 53 and 54 in different Vβ22 mutants isolated from CDR2 libraries, using Quikchange Lightning Kit (Stratagene) as described by the manufacturer. After transformation into *S. cerivisiae* EBY100 strain, protein expression on yeast cell surface and binding to SEA by each mutant, was analyzed by flow cytometry.

Biotinylation of recombinant SEA

Recombinant SEA (Toxin Technology, Inc.) was biotinylated at primary amines using EZ-Link™ Sulfo-NHS-LC-Biotin (Pierce). After removing excess biotin, biotinylation of SEA was assessed by incubating with streptavidin (SAv) and analyzing change in mobility ("gel-shift") on 4-20% polyacrylamide gel. Biotinylated SEA was quantified by BCA Protein Assay kit (Thermo Fisher Scientific Inc).

Experiments to determine unknown component in non-recombinant SEA preparation that bound to PS7-2 mutant with high affinity

Soluble PS7-2 was immobilized on Dynabeads® M-270 Epoxy beads (Life Technologies) which possess surface epoxy groups, hence allowing direct covalent binding of proteins via primary amino or sulfhydryl groups. Immobilization of soluble PS7-2 on the surface of beads was performed at 4°C or 37°C. To assess the time required for immobilization, the reaction was allowed to proceed to different time points (4, 8, 12, 24 hours). After washing any unbound protein, the PS7-2 coated beads were incubated with 1 mg/ml biotinylated, non-recombinant SEA. After one hour, the beads were washed and then incubated with streptavidin-Alexa Fluor 647 conjugate (Life Technologies) at 1:200 dilution. After washing, the beads were analyzed by flow cytometry.

For determining the unknown component in non-recombinant SEA preparation that bound to PS7-2 mutant with high affinity, PS7-2 was incubated with Dynabeads for four hours at 4°C. After washing any unbound protein, the beads were incubated with 1 mg/ml biotinylated, non-

recombinant SEA. After one hour, PS7-2 coated beads were washed and shipped to Dr. Jeffrey A. DeGrasse at FDA for mass spectrometric analysis, who digested the proteins bound to the beads and analyzed the resultant peptides by LC-MS.

Sorting directed mutagenesis (affinity) libraries with recombinant, biotinylated-SEA and selection of true, high-affinity, SEA-binding Vβ22 mutants

Three directed mutagenesis libraries in CDR2 region (residues 49 to 54) of Vβ22 were mixed in equal proportion and subjected to several rounds of sorting for selecting Vβ22 mutant proteins that could bind to recombinant SEA with higher affinity. With each round of sorting, a lower concentration of SEA (biotinylated, recombinant) (Toxin Technology, Inc.) was used (1μM to 10nM), in order to obtain high-affinity mutants. Binding to biotinylated-SEA (recombinant) was assessed by staining with streptavidin-Alexa Fluor 647 conjugate (Invitrogen) at 1:200 dilution. Individual yeast clones were isolated after sorting the library six times, and analyzed by flow cytometry for protein expression on cell surface and binding to SEA. Distinct clones were identified by DNA sequencing.

Expression and purification of soluble Vβ22 mutant proteins

Specific Vβ22 mutants were subcloned into a pET28a expression vector (Novagen) for protein expression in *E. coli* BL21 (DE3) cells as inclusion bodies. Proteins were refolded (by slow dilution) from denatured inclusion bodies, followed by affinity purification with Ni agarose resin (Qiagen) and HPLC (Biocad Sprint) using a Superdex 200 (GE Healthcare) size exclusion column as described previously [33]. Secondary structure of refolded FL mutant was analyzed by circular dichroism experiments conducted in collaboration with Irisbel Guzman Sanchez (graduate student in Gruebele Lab, Department of Chemistry, University of Illinois).

Binding of soluble Vβ22 mutants to SEA

Binding of soluble Vβ22 mutant proteins to SEA was examined by ELISA and surface plasmon resonance (SPR). For ELISA, soluble Vβ22 mutant proteins (5 μg/ml) were coated on

the wells of an ELISA plate. Unbound proteins were washed away with 1X PBS + 0.1% Tween-20, and any unoccupied sites on the wells were blocked with blocking buffer (1X PBS + 0.5% milk). This was followed by incubation with varying concentrations of recombinant, biotinylated-SEA, followed by washing the wells and incubating with 1:2000 dilution of streptavidin-conjugated horse radish peroxidase (HRP) enzyme. After washing the wells twice, TMB substrate (KPL, Inc.) was added and the colorimetric reaction catalyzed by HRP was allowed to proceed for ~ 2 minutes, after which it was stopped by addition of 1N H_2SO_4 to yield a yellow colored product whose absorbance was measured at 450 nm using a plate reader (Biorad).

Affinity constants and kinetic parameters for Vβ22:SEA binding were determined by SPR using a Biacore T100 instrument (GE Healthcare) by Dr. Sandra Postel in Dr. Eric Sundberg's laboratory, University of Maryland. 500 RU (Response units) of recombinant SEA was immobilized on a CM5 sensor chip. Various concentrations of soluble Vβ22 proteins were injected over the sensor surface and response was recorded. Global kinetic fits of the data were performed using the BiaEvaluation 4.1 software.

Capture ELISA for detection of SEA

To measure binding of recombinant-SEA (not biotinylated), an SEA detection assay was used in a "capture ELISA" format. For this assay, soluble Vβ22 mutant proteins (PS5-1 or FL) were coated on the wells of ELISA plates at 5μg/ml. Unbound proteins were washed away with 1X PBS + 0.1% Tween-20, and any unoccupied sites on the wells were blocked with blocking buffer (1X PBS + 0.5% milk). Vβ22 mutant protein molecules immobilized on the wells were used to "capture" various concentrations of recombinant-SEA. After washing, 50 μl of 1:1000 dilution of rabbit anti-SEA (whole antiserum, Sigma-Aldrich) was added to the wells, followed by washing and incubation with 1:2000 dilution of goat-anti rabbit IgG(H+L) labelled with HRP (Sigma-Aldrich). After washing the wells twice, TMB substrate (KPL, Inc.) was added and the colorimetric reaction catalyzed by HRP was allowed to proceed for ~ 2 minutes, after which it was stopped by

addition of 1N H_2SO_4 to yield a yellow colored product whose absorbance was measured at 450 nm using a plate reader (Biorad).

Cross-reactivity of engineered Vβ22 protein with other superantigens

For cross-reactivity studies, induced yeast cells expressing PS7-1 F49M L30S (FL mutant) protein on the surface were incubated with a mixture of 100nM recombinant biotinylated-SEA and various concentrations of non-biotinylated SEA, SED and SEE (Toxin Technology, Inc.) for 1 hour on ice. The amount of biotinylated-SEA bound to FL protein, was detected using streptavidin-Alexa Fluor 647 conjugate by flow cytometry.

Results

Cloning and expression of human Vβ22 on yeast cell surface

The human Vβ22 gene was cloned in frame with the yeast cell wall protein Aga-2, with flanking HA an c-myc epitope tags, in the yeast display vector pCT302 (Fig. 2.1A). The yeast display construct was transformed into yeast cells, which were then cultured in D-CAA, followed by induction in SG-CAA media. Induced yeast cells were analyzed for surface expression of HA, Vβ22 and c-myc using anti-HA antibody, anti-Vβ22 antibody and anti-c-myc antibody respectively. Although yeast cells containing the wild-type Vβ22 (*wt* Vβ22) construct showed detectable levels of the HA and c-myc tags, an antibody to the Vβ22 region did not detect the fusion on the surface of yeast cells (Fig.2.1B). These results suggested that the Vβ22 protein was not folded properly, as has been observed with several other Vβ domains [34, 101, 102].

Expression of stable, human Vβ22 on the yeast cell surface

In order to determine if a stable Vβ22 protein could be isolated, the *wt* Vβ22 gene was subjected to random mutagenesis by error-prone PCR. PCR products along with NheI and XhoI digested pCT302 vector, were transformed into yeast to generate error-prone library by

homologous recombination. The resulting library size was 2 x 10^6 transformants with an average of approximately 1 mutation per gene.

The expanded error-prone library was induced in galactose-containing media, following which it was subjected to several rounds of sorting (FACS) with a saturating concentration of anti-Vβ22 antibody. After five sorts, a population of most fluorescent cells was collected (Fig. 2.2B), from which ten yeast clones were isolated and analyzed by flow cytometry and DNA sequencing (Fig.2.3A). Nine out of ten Vβ22 mutants (except PS5-6) were detected on yeast cell surface with anti-Vβ22 antibody. Sequence analysis indicated that the PS5-6 clone did not acquire any stabilizing mutations, which explained the lack of anti-Vβ22 staining. This clone also did not express HA and c-myc on the cell surface, which probably happened due to an upstream mutation leading to inefficient export of fusion protein to the cell surface. T13A mutation in framework region (FR1) was acquired by eight out of the nine mutants indicating its importance in stabilizing Vβ22. Overall, four different classes of mutants were obtained (Fig. 2.4, Table 2.1). PS5-7 clone only acquired one mutation (D63G). Upon transforming PS5-7 plasmid DNA into yeast, Vβ22 expression was not observed indicating that the clone probably contained multiple plasmids, and D63G mutation had no role in stabilizing Vβ22. Hence, representative mutants from the remaining three classes (PS5-1, PS5-2 and PS5-4) were carried forward for further experimentation and analysis. Flow cytometry experiments indicated that yeast cells expressing these stabilized, hVβ22 mutants (PS5-1, PS5-2 and PS5-4) also expressed higher levels of HA and anti-c-myc (Fig. 2.3B) indicating a greater number of the fusions were expressed and exported to the cell surface when the Vβ22 domain was stabilized.

To further compare the stability of these three stabilized Vβ22 mutants, each was subjected to an irreversible thermal denaturation assay in which yeast cells expressing PS5-1, PS5-2 or PS5-4 were incubated at various temperatures, followed by flow cytometry with the anti-Vβ22 antibody (Fig.2.5) [103]. The 50% melting temperatures of the proteins ranged from 40°C

(PS5-1) to 60°C (PS5-2, PS5-4). The PS5-2 and PS5-4 Vβ22 mutants exhibited the highest level of stability (Fig. 2.5B).

As mentioned earlier, PS5-1, PS5-2 and PS5-4 acquired identical framework mutation, T13A, suggesting that this mutation was important in stabilization of the Vβ22 domain on the yeast cell surface. Another framework mutation, T82A, was acquired by PS5-1 and PS5-2 mutants indicating this mutation might also have a role in stabilizing Vβ22 (Fig. 2.4, Table 2.1). Since PS5-4 lacked T82A mutation, this suggested that Q11L (framework) and L30S (CDR1) mutations might have contributed to its stability, in addition to T13A mutation. Higher stability of PS5-2 and PS5-4 appear to be due to Q11L (framework), L30S (CDR1) and/or L97Q (CDR3). Interestingly, mutations in the framework regions resulted in substitution of polar amino acids (Thr, Gln and Met) with hydrophobic amino acids (Ala, Leu and Val). In contrast, mutations in CDRs resulted in substitution of a hydrophobic amino acid (Leu) with polar amino acids (Ser and Gln). Protein modeling indicated that the mutations in framework regions were located on the face opposite the antigen binding face of the Vβ (CDRs) (Fig. 2.6).

Since the affinity of SEA for binding to *wt* Vβ22 was unknown, micromolar concentrations of SEA were chosen for assessing binding to stabilized Vβ22 mutants based on the observation that most superantigens have affinities for their Vβ ligands in the micromolar range [57, 58, 104]. Despite being stable and folded on the surface of yeast, none of the mutants showed detectable binding to biotinylated SEA (non-recombinant) at concentrations as high as 2.5μM, by flow cytometry (Fig. 2.7)

Selection of high-affinity, SEA-binding Vβ22 mutants

In order to engineer Vβ22 mutants for binding with higher affinity to SEA, stabilized Vβ22 mutants PS5-1, PS5-2 and PS5-4 were used as templates for constructing various directed mutagenesis libraries (affinity libraries). In the absence of a crystal structure of the SEA:Vβ complex, I elected to start by generating libraries in the CDR2, which is known to be central in the

binding of other superantigens to their cognate Vβ receptors [39, 42, 64, 92, 105]. The CDR2 region in Vβ22 consists of six residues. Three overlapping libraries were generated, each in a contiguous stretch of four amino acids in the CDR2 region (Fig. 2.8A). The three libraries, consisting of ~2 x 10^7 independent clones each, were combined and subjected to consecutive rounds of sorting with decreasing concentrations of biotinylated-SEA (non-recombinant) (1μM to 10nM). As expected, incubation of the pre-sorted CDR2 libraries with 1μM SEA did not yield detectable staining (Fig. 2.8B, left). However, after four consecutive rounds of sorting with 1μM SEA, a distinct population of cells that bound to SEA was obtained (Fig. 2.8B, middle). After seventh sort, Vβ22 mutants that bound to 10 nM biotinylated SEA were obtained, of which twelve clones were isolated (Fig. 2.8B, right). Upon sequencing, four different mutants, designated PS7-1, PS7-2, PS7-4 and PS7-6, were identified with highly conserved features among them (Fig. 2.9). All the mutants (PS7-1, PS7-2, PS7-4 and PS7-6) retained the conserved T13A and T82A stabilizing mutations. The PS7-1 mutant was derived from the 50-53 CDR2 library, whereas PS7-2, PS7-4 and PS7-6 were all derived from the 49-52 CDR2 library (Fig. 2.8, 2.9). The latter three mutants also retained the L30S mutation in CDR1 mutation.

These mutants were verified to have improved binding to 10 nM biotinylated-SEA (non-recombinant), compared with the stabilized mutant, PS5-1 (Fig. 2.10A). Binding titrations with biotinylated-SEA (non-recombinant) indicated that the approximate dissociation constants of PS7-1 was 30 nM, while that of the remaining three mutants ranged from 60-80 nM (Fig. 2.10B). In addition to SEA titrations, the Vβ22 mutants were examined to determine dissociation rates and half-lives of the Vβ22:SEA complexes. Three of the four mutants (PS7-2, PS7-4 and PS7-6) were able to bind SEA (non-recombinant) with long half-lives (e.g. ~40-50% of the SEA remained bound after 24 hours at 37°C) (Fig. 2.11). Both binding experiments and off-rate experiments indicated that the mutants derived from the 49-52 CDR2 library (PS7-2, PS7-4 and PS7-6) bound to SEA (non-recombinant) better than the mutant derived from the 50-53 library

(PS7-1). However it is important to note that in the dissociation experiment, recombinant SEA was used as a competing agent against bound, non-recombinant biotinylated SEA. In future experiments, it was realized that the non-recombinant SEA preparation from Toxin Technology Inc. was contaminated with an unidentified substance (along with SEB), to which mutants PS7-2, PS7-4 and PS7-6 were binding with high affinity (see below).

Role of specific amino acids at positions 30, 49 and 52 in Vβ22 mutants isolated from CDR2 library

Conservation in the mutations (F49M, Y50S/A, N51Y, N52E/G and E53D) in the mutants isolated from CDR2 library suggested that they were important in high-affinity binding to SEA. In order to study the role of several of these mutations in binding, further mutagenesis studies were conducted.

Since the PS7-1 mutant lacked the F49M mutation that was present in PS7-2, PS7-4 and PS7-6, I reasoned that its incorporation into PS7-1 might increase its SEA-binding affinity. Similarly, PS7-2, PS7-4 and PS7-6 contained L30S mutation that was absent in PS7-1. In order to study the effect of F49M and L30S mutations, I introduced these mutations in PS7-1. The mutants generated (PS7-1 F49M and PS7-1 L30S) were transformed into yeast cells and analyzed by flow cytometry for surface expression and binding to SEA (non-recombinant). The introduction of F49M mutation in PS7-1 resulted in moderate increase in binding to SEA, although the surface levels of PS7-1 and PS7-1-F49M were similar (Fig. 2.12, panels C and D). Introduction of L30S mutation in PS7-1 also resulted in moderate increase in binding to SEA, although this mutation resulted in increase in surface expression (Fig. 2.12, panels C and D). In order to assess if these mutations would act synergistically, F49M and L30S mutations were inserted into PS7-1 to generate PS7-1 F49M L30S mutant (or, FL mutant). Yeast cells transformed with FL mutant exhibited higher median fluorescence units (MFU) for expression on cell surface, and also for SEA binding, compared with PS7-1 (Fig. 2.12, panels C and D).

The PS7-1 mutant contained the N52E mutation, whereas the PS7-2, PS 7-4, PS 7-6 mutants contained the N52G mutation. To examine the role of position 52 in the high-affinity state, I generated an E52G mutation in PS7-1, and the G52E mutation in PS7-2, PS 7-4, PS 7-6 mutants. These four mutants were examined by flow cytometry with 10 nM SEA (non-recombinant) and each of the reciprocal mutations showed a loss of SEA binding, to background levels (Fig. 2.13A). Thus, the glutamate at position 52 in PS7-1 and the glycine at the same position in PS7-2, PS7-4 and PS7-6 were important residues for SEA binding, but within the context of the surrounding mutations in these mutants. Staining with anti-Vβ22 antibody indicated that glycine was preferred residue at position 52 than glutamate, as far as surface expression was concerned (Fig. 2.13B).

Difference in binding of PS7-2 mutant to non-recombinant SEA versus recombinant SEA preparation due to possible contamination of non-recombinant SEA with SEB

During the course of experimentation, a selected mutant from CDR2 library was analyzed for binding to recombinant and non-recombinant SEA. For this purpose, recombinant SEA was biotinylated at primary amines using EZ-Link™ Sulfo-NHS-LC-Biotin (Pierce). Extent of biotinylation was analyzed by gel-shift assay (Fig. 2.14A). A change in the mobility of biotinylated, SEA (recombinant) was observed in the absence or presence of streptavidin. The streptavidin-biotinylated SEA complexes were high molecular weight (perhaps larger than 250 kDa) and hence did not migrate from the wells, while the biotinylated SEA was seen as an expected ~25 kDa band on the polyacrylamide gel (Fig. 2.14A).

Flow cytometry experiments for binding of PS7-2 mutant to recombinant or non-recombinant SEA indicated that the mutant bound poorly to recombinant SEA than to non-recombinant SEA (Fig. 2.14B). This hinted that the PS7-2 mutant was possibly binding to an unknown component (possibly, another superantigen which co-purified with SEA) in the non-recombinant SEA preparation from Toxin Technology, Inc. The company provided with the

information that the non-recombinant SEA was purified from the FRI722 strain of *Staphylococcus aureus*. Review of existing literature and also consultation with Dr. Patrick Schlievert (University of Iowa) confirmed that FRI722 is known to secrete SEB, SEK and SEQ, in addition to SEA [106].

In order to assess if the contaminant in the non-recombinant SEA preparation, was a known superantigen, different concentrations of SEB, SEC and TSST-1 were added to yeast cells expressing PS7-2, and binding was analyzed. Binding of PS7-2 to SEB, SEC or TSST-1 was not detected even when the superantigen was at a high concentration (1μM) (Fig. 2.14C). In a parallel experiment, high-affinity Vβ mutant proteins, G5-8, L3 and D10 (engineered against SEB, SEC and TSST-1 respectively) [33, 34, 36], were analyzed for binding with non-recombinant and recombinant SEA. While G5-8 did not show detectable binding to recombinant SEA, binding to non-recombinant SEA was seen. Similarly, L3 did not show detectable binding to recombinant SEA, but bound to non-recombinant SEA. Since L3 protein also has affinity towards SEB (K_D = 4nM) [36], these observations pointed toward possible contamination of non-recombinant SEA prep with SEB. Binding of D10 to recombinant or non-recombinant SEA was not detected, indicating the non-recombinant SEA preparation did not contain TSST-1 as a contaminant.

In order to identify the unknown component in the SEA (non-recombinant) preparation that bound with high affinity to PS7-2 mutant, the protein was expressed in *E.coli* as inclusion bodies and refolded (Fig. 2.15A, B). Refolded PS7-2 protein was coated on Dynabeads for different time intervals, at either 37°C or 4°C. Coating of the PS7-2 protein on the surface of the beads was confirmed by assessing binding to non-recombinant SEA preparation, by flow cytometry. Results indicated that the coating reaction was complete within 4 hours, and more efficient at 4°C than at 37°C. Such PS7-2 coated Dynabeads were washed and then incubated with 1 mg/ml biotinylated, non-recombinant SEA. Washed beads were shipped to Dr. Jeffrey A. DeGrasse at FDA, who performed tryptic-digestion on the proteins bound to the beads and analyzed the resultant

peptides by LC-MS. However, no other peptides other than those derived from SEA or Vβ22 mutants were retrieved.

Identification of true, high-affinity, SEA-binding Vβ22 mutants

Since it was found that the PS7-2 mutant isolated from CDR2 libraries did not bind recombinant SEA well, yeast cells expressing CDR2 libraries were now subjected to consecutive rounds of sorting with decreasing concentrations of biotinylated-SEA (recombinant) (1μM to 10nM). After six sorts, Vβ22 mutants that bound to 10 nM biotinylated SEA were obtained, of which several clones (prefixed as PS6 mutants) were isolated and analyzed for binding to 10 nM biotinylated SEA (recombinant) by flow cytometry (Fig. 2.16A). Upon sequencing, it was noted that the mutants that bound to 10 nM recombinant SEA had highly conserved features among them, and were derived from 50-53 CDR2 library, like the PS7-1 mutant that was isolated when the same libraries were sorted with non-recombinant SEA (Fig. 2.17). Because of these conserved mutations in PS7-1 and PS6 mutants, I hypothesized that the PS7-1 mutant (although isolated from CDR2 libraries by sorting with non-recombinant SEA), was a true recombinant-SEA binder.

To assess how a selected mutant, PS6-A10 (isolated from CDR2 libraries sorted with recombinant SEA) would compare with PS7-1 (and its mutant, PS7-1 F49M L30S or FL mutant) and PS7-2, a binding titration with biotinylated-SEA (recombinant) was performed. The mutants derived from 50-53 CDR2 library (PS7-1, PS6-A10) and FL mutant bound to SEA (recombinant) at concentrations as low as 3 nM (Fig. 2.18 panels A and B). Comparatively, PS7-2 mutant (derived from 49-52 library) did not bind as well to 10 nM SEA (recombinant). Of all the mutants analyzed, FL mutant exhibited highest maximum median fluorescence units (MFU) for recombinant SEA binding. The higher MFU for SEA binding by FL mutant (PS7-1 F49M L30S) positively correlated with higher expression on yeast cell surface (Fig. 2.18C).

To understand the contribution of F49M and L30S mutations, yeast cells expressing PS7-1, and single and double mutants of PS7-1 (PS7-1 F49M, PS7-1 L30S and FL) were subjected to binding titration with biotinylated-SEA (recombinant). All the Vβ22 mutants analyzed, could bind to SEA at concentrations as low as 0.3 nM (Fig. 2.19A). Although the maximum surface levels of PS7-1 and PS7-1 F49M were similar (Fig. 2.19C), and below that of L30S mutant, the F49M mutation, resulted in a modest increase in affinity, from 30 to 10 nM, for PS7-1 and PS7-1-F49M, respectively (Fig. 2.19B, left). As indicated, the introduction of the stabilizing mutation L30S into PS7-1 increased its surface expression significantly (Fig. 2.19C, left) and also had an effect on affinity (from 30 to 20 nM, for PS7-1 and PS7-1-L30S, respectively). Combining F49M and L30S mutations resulted in higher surface levels and higher affinity compared with PS7-1, with an estimated apparent K_D of 15 nM (Fig. 2.19, panels B and C). Mutants PS7-2, PS7-4 and PS7-6 were also compared with PS7-1 and its mutants. As shown, these mutants bound to ~3-10 nM recombinant SEA, but exhibited very low MFU although their surface expression was high (Fig. 2.19, panels B and C, right). Following these experiments, FL mutant was identified as the best mutant which bound to recombinant SEA with high-affinity. In future experiments, FL mutant was expressed in soluble form for further analyzing its binding properties.

Analysis of revertant mutants of Vβ22 mutant, "FL"

For understanding the role of each amino acid in CDR2 of FL in contributing toward binding with high affinity to SEA (recombinant), single-site revertant mutants (to *wt* residues) of FL were generated. The mutants were transformed into yeast cells, and analyzed for SEA-binding and surface expression (anti-Vβ22 staining). The sequence of M49F mutant of FL was same as PS7-1 L30S mutant that has already been discussed above. It was noted in mutants isolated from CDR2 libraries (with recombinant or non-recombinant SEA), that a non-aromatic residue (alanine) was often selected at position 50 in place of tyrosine (aromatic), and that an aromatic residue (tyrosine or phenylalanine) was often acquired at position 51 (Fig. 2.9, 2.17 and 2.20A). Hence, it

was my hypothesis that these mutations (Y50A and N51Y/F) were fulfilling a structural (space) requirement for binding with SEA. That is, to accommodate the conserved N51Y/F mutation at the SEA binding surface, the aromatic residue at position 50 was mutated to alanine that requires much less space. To test this hypothesis, I generated the FL A50Y mutant that possesses aromatic residues at position 50 as well as 51 (Fig. 2.20A). It was noted that the binding of this mutant to SEA was substantially inhibited (Fig. 2.20B). This suggested that the inhibition in binding possibly happened due to the molecular crowding caused by two adjacent aromatic residues at the SEA binding interface. The requirement of at least one aromatic residue at the SEA-binding interface was proved by the inhibition of binding by FL Y51 mutant (Fig. 2.20B). Similarly, the importance of acidic residues at position 52 and 53 was highlighted by decrease in SEA-binding by FL E52N, FL D53E and D53A mutants (Fig. 2.20A). Specifically, aspartate was essential at positon 53 for binding of FL mutant to SEA (Fig. 2.20A). Mutations in CDR2 did not greatly affect surface expression of the Vβ, except for the I54A mutation (Fig. 2.20C). It was interesting to note that mutations at this position were not selected when the CDR2 libraries were sorted for binding with SEA, probably because isoleucine at position 54 contributed to the stability of Vβ22 protein. Loss of stabilization of FL I54A mutant, may have resulted in its inability to bind SEA (Fig. 2.20B).

Expression of soluble human Vβ22 mutant proteins and analysis of their binding to SEA

Previous studies have indicated that mutants expressed at higher levels on the surface of yeast are also expressed at higher levels in secretion or refolding systems [62, 102, 107]. In order to study the SEA-binding properties of Vβ22, several of the Vβ mutants (PS5-1, PS7-1, PS7-2 and FL) were expressed as inclusion bodies in *E.coli*, solubilized, refolded and subjected to gel filtration. The Vβ22 mutants had a tendency to multimerize, and hence only a small fraction was purified as monomers (Fig. 2.21A). The secondary structure of refolded, FL mutant was verified to consist of beta sheets by circular dichroism by the characteristic dip in molar ellipticity at ~ 217

nm (Fig. 2.21B). Circular dichroism experiments were conducted in collaboration with graduate student, Irisbel Guzman Sanchez (Gruebele Lab, Department of Chemistry, University of Illinois).

Binding of refolded, soluble Vβ22 mutant proteins to SEA was examined by ELISA and surface plasmon resonance (SPR). The format of the ELISA titrations do not allow an accurate K_D determination due to several washing steps, but a minimum K_D value for proteins that have adequate dissociation kinetics can be estimated. As shown, the soluble, monomeric PS5-1 protein (equivalent to the wild-type SEA-binding domain, with the stabilizing mutations for expression) did not bind detectably (Fig. 2.22). In contrast, the soluble, monomeric mutants PS7-1, PS7-2 and FL bound to SEA with minimum estimated K_D values of 55 ± 20, 135 ± 70 and 30 ± 5 nM, respectively (Fig. 2.22). The SEA-binding of PS5-1 and FL mutants were also analyzed by SPR. Based on SPR equilibrium measurements, the K_D value of the PS5-1 protein was ~100 μM (Fig. 2.23A), similar to the low affinities of other superantigens for their Vβ regions [57, 58, 104]. The SPR-based measurement of the K_D value for the FL mutant was ~4 nM, a 25,000-fold improvement in affinity (Fig. 2.23B).

Capture ELISA for detection of SEA

The high affinity of the FL protein allows one to use it as a probe for detection of SEA in samples. Accordingly, I developed a capture ELISA assay for detection of SEA, in which immobilized high-affinity FL mutant was used to capture SEA. Polyclonal anti-SEA was then added to detect the bound SEA. Without any optimization, this assay detected SEA at a concentration of 1-10 nM (~100 ng/ml) (Fig. 2.24). In chapter 3, it was determined that the sensitivity of SEA detection by this method was ~2.5-10 ng/ml.

Specificity of superantigen binding by engineered Vβ22 mutant FL

Since the SEE and SED toxins are in the same group as SEA, and exhibit 83 and 48% sequence identity with SEA, respectively, I assessed cross-reactivity of the Vβ22 FL mutant with these related enterotoxins. For this purpose, I used a competition assay with yeast cells that

expressed the FL mutant. In this assay, biotinylated-SEA (recombinant) was incubated with various concentrations of unlabeled recombinant SEA, SED or SEE and the mixture was added to the yeast cells expressing FL protein on their surface. Bound biotinylated-SEA was detected with streptavidin-PE by flow cytometry. SEA was able to completely inhibit the binding at higher concentrations, and detectable inhibition was observed at concentrations as low as 5 nM. In contrast, binding (competition) of SED and SEE by the FL mutant was not detected even at the highest concentration, 500 nM (Fig.2.25). This result suggested that the FL mutant exhibited a high level of specificity for SEA.

Discussion

Among the various exotoxins secreted by *S. aureus*, enterotoxin A has been most often associated with food poisoning outbreaks involving *S. aureus* [83, 84, 86-88]. For this reason, there has been interest in developing rapid, sensitive assays for food safety testing. However, SEA is also known to act as a superantigen, inducing hyper-inflammatory reactions in conditions such as endocarditis and toxic shock [90, 91]. The goal of this study was to understand more about the molecular interactions involved in the superantigen activities, but the engineered, high-affinity receptors developed in this effort also have dual use as specific, sensitive detecting agents.

Like other superantigens, the mechanism by which SEA exerts hyper-inflammatory effects involves the simultaneous binding of the enterotoxin to class II MHC molecules on antigen presenting cells and to the Vβ domain of the T-cell receptor present on T cells. Co-crystallization of other *S. aureus* superantigens with Vβ receptors has revealed different topologies of binding [39, 40, 42, 92], but in each case the center of the interface has involved CDR2 [64]. Thus, in my efforts with the cognate receptor for SEA (Vβ22), I focused on creating initial libraries in the CDR2 loop. If I had not isolated higher affinity variants within these libraries, I might have concluded that

the Vβ22:SEA interaction differs substantially from other superantigens (e.g. SEB, SEC, TSST-1, and SpeA, for which higher affinity variants were isolated from CDR2 libraries [28, 33-36]). However, I was able to isolate CDR2 mutants with up to a 25,000-fold improvement in affinity, supporting the notion that the CDR2 loop of Vβ22 also resides at the interface of its interaction with SEA.

Unlike many V_H domains, Vβ domains are typically unable to be expressed in soluble form, or on the surface of yeast [34, 60]. One of the key reasons for this is that Vβ residues that are normally buried at the interface with the constant region domain of the β-chain, are destabilized when exposed in the isolated Vβ domain. Similarly, the Vβ22 domain shown here was more stable on the surface of yeast when several key mutations were made in the region opposite the CDR (Fig. 2.6), where the β chain constant region would normally be located. Somewhat surprisingly, these stabilizing mutations in the framework of Vβ22 were substitutions to hydrophobic residues. One might have predicted for a region that is normally buried (e.g. at the Vβ:Cβ interface) the residues would prefer to be more hydrophilic when exposed. Interestingly though, some other Vβ regions do normally contain similar or identical same amino acid residues identified here in the mutated Vβ22 domains (Fig. 2.26). The yeast surface levels of the Vβ22 domain were also increased, irrespective of SEA binding, by two CDR loop mutations, L30S and L97Q. L30S was shown especially to have a significant effect on the total surface levels of Vβ22 protein. These changes may act by increasing the hydrophilicity of these exposed loops. It has been shown previously that CDR1 mutations also have a significant effect on stabilization of a Vα:Vβ single-chain TCR [102] , and other Vα or Vβ domains have also been stabilized through CDR mutations [61] .

The low affinity of SEA for the stabilized Vβ22 domain (K_D value of 100 μM) is similar to that measured for other superantigen interactions such as SEB:Vβ8.2 [33, 57]. Despite this low affinity, superantigens are capable of potent activity in part because only a small fraction of the

surface TCRs on a T cell needs to be bound in order to trigger activity [108]. In addition, ternary interactions with Vβ and class II MHC can further stabilize the active complex [109]. Thus, SEA appears to follow the same principles of low-affinity interactions with the TCR as with other superantigens.

The structural basis of how high-affinity Vβ22 mutants bind to SEA remains to be determined, but it was interesting that the two adjacent aromatic residues at positions 49 and 50 in the wild type V region, were both mutated to other residues (Met and Ala, respectively), whereas the adjacent residue at 51 was mutated to an aromatic residue (Tyr). These substitutions may allow optimal positioning of the Tyr51 side chain for stacking interactions with SEA. Additional mutations at 52 and 53 in the FL mutant yielded two adjacent negative charged residues (N52E and E52D), which could play a role in enhanced electrostatic interactions with SEA.

The putative TCR binding site on SEA has been proposed to include T21, N25, Y94, Y205, N207, and T208 [110-113]. These residues are closely located in the tertiary structure of SEA (Fig. 2.26A), and could form the binding site for Vβ. The aromatic residue (Y51) in the CDR2 region of FL could potentially be involved in pi-stacking interactions with Y94 or Y205 from SEA. The only positions within or near these six SEA residues that differ between SEA and both SED and SEE are positions 206 and 207 (Fig. 2.27). Interestingly, both SED and SEE have negatively charged residues at position 207, which could pose an electrostatic repulsion with negative charges (residues 52 and 53) in the Vβ22 FL mutant's binding site.

Finally, the Vβ22 protein FL, with a 25,000-fold increase in affinity for SEA compared to the wild-type Vβ, was capable of being expressed, purified, and immobilized as a detection agent for SEA. This engineered, high-affinity Vβ22 mutant protein was used for development of a capture-ELISA (this chapter) and a flow-cytometry based platform (chapter 3) for specific detection of SEA. The engineered protein was also used as a component of a multiplex system for simultaneous detection of staphylococcal and streptococcal toxins (chapter 3), that was

successfully used for detection of SEA, SEB and TSST-1 in supernatants derived from cultures of *S. aureus*. The same approach can possibly be used to detect toxins in food.

FIGURES

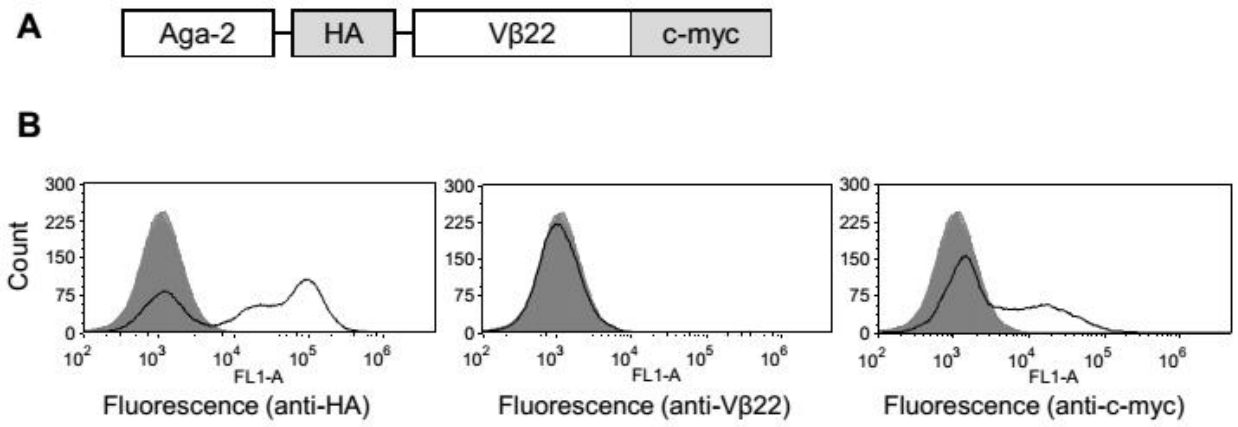

Fig. 2.1. Cloning and expression of human *wt* Vβ22 on yeast cell surface
(A) Schematic of yeast display construct containing human Vβ22 gene. (B) Flow cytometric analysis of induced yeast cells transformed with hVβ22-yeast display construct shown in panel A. Yeast cells were incubated with anti-HA, anti-Vβ22 or anti-c-myc (black), followed by a secondary antibody conjugated to a fluorophore (Alexa-488). The fluorescence exhibited by the cells incubated with secondary antibody only is represented by the gray peak.

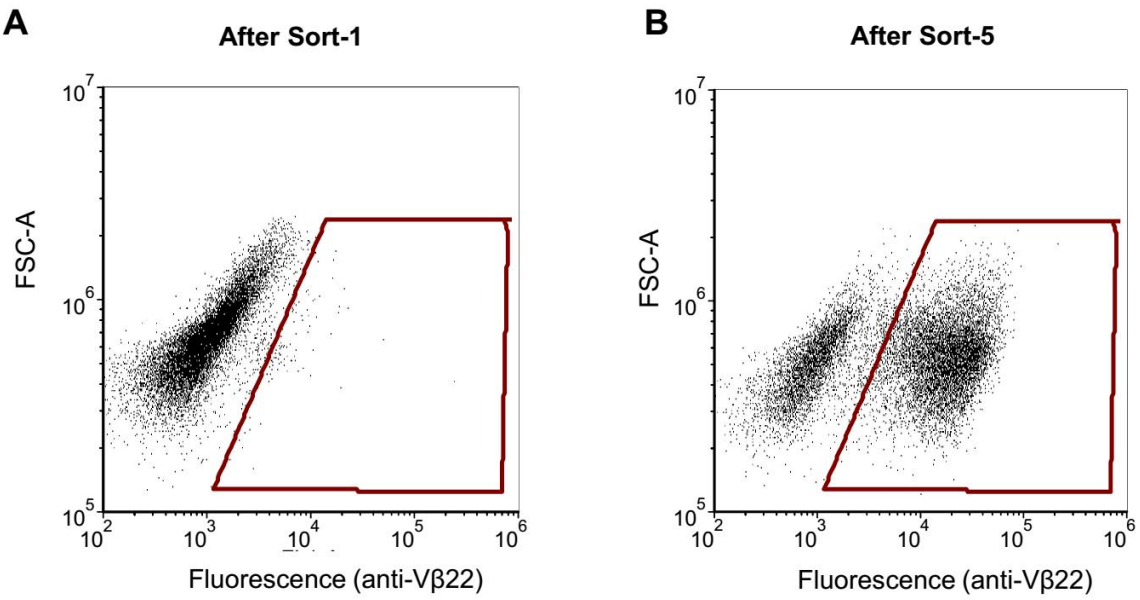

Fig. 2.2. Scatter plots indicating sub-populations of yeast cells at different stages of sorting the error-prone library

Yeast cells transformed with error-prone library of human Vβ22 were sorted several times for binding with anti-Vβ22 antibody. Scatter plots indicating sub-populations of yeast cells in the sorted library after sort-1 (panel A) and sort-5 (panel B), are shown. The most fluorescent cells (shown in the polygon, maroon) after sort-5 were collected, from which distinct, stabilized Vβ22 mutants were isolated in future experiments.

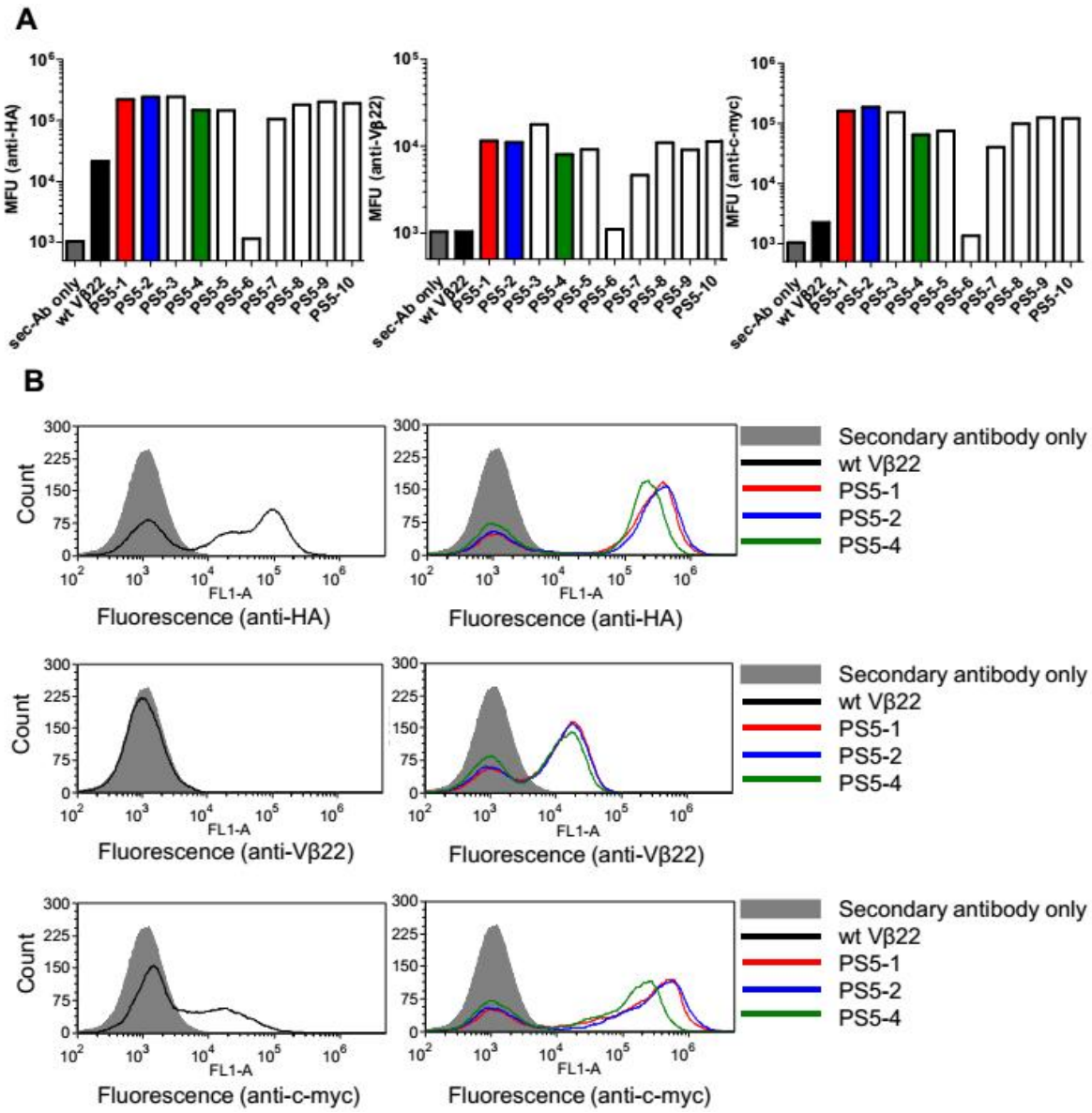

Fig. 2.3. Yeast surface display of human Vβ22

(A) Ten yeast colonies obtained after plating sorted error-prone library were cultured and induced, followed by analysis of surface expression of HA, Vβ22 and c-myc by flow cytometry. Median fluorescence units obtained from histograms were used to generate bar graphs shown. Fluorescence in the presence of secondary antibody only is represented by gray bar. (B) Histograms representing flow cytometric analysis of induced yeast cells expressing either wt Vb22 or mutant proteins (PS5-1, PS5-2 and PS5-4) isolated from error-prone library. The fluorescence exhibited by the cells incubated with secondary antibody only is represented by the gray peak.

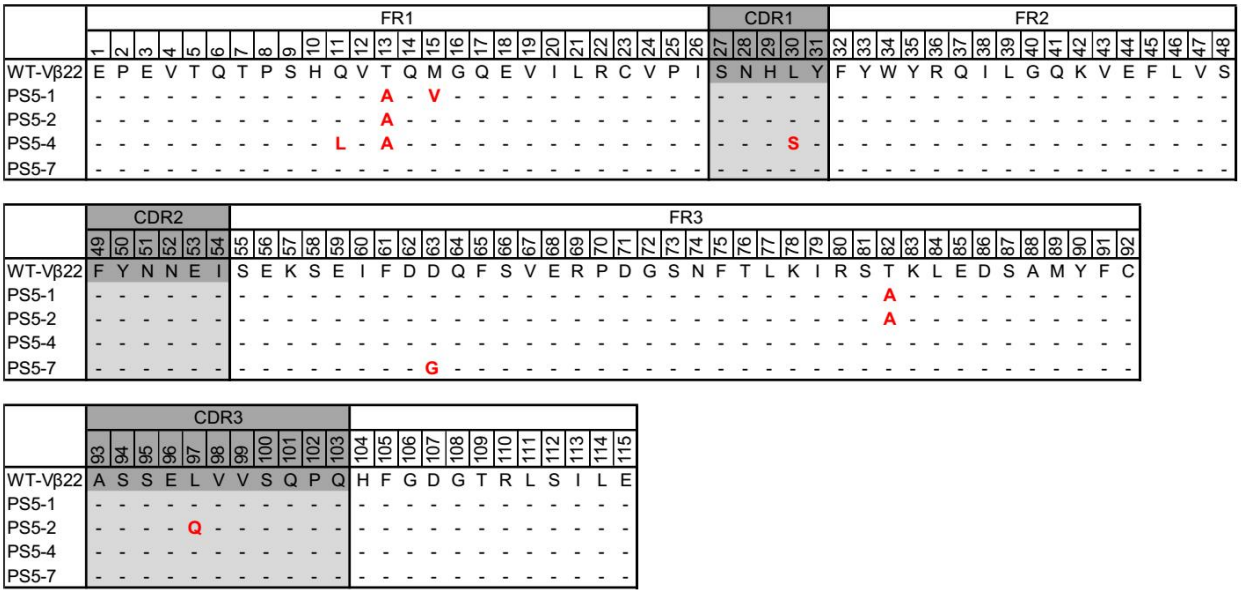

Fig. 2.4. Amino acid sequences of distinct mutants obtained from error-prone library
Four different mutants (PS5-1, PS5-2, PS5-4 and PS5-7) were isolated from Vβ22 error-prone library, after sorting it five times. Mutated residues are in bold (red); CDR regions are highlighted in gray.

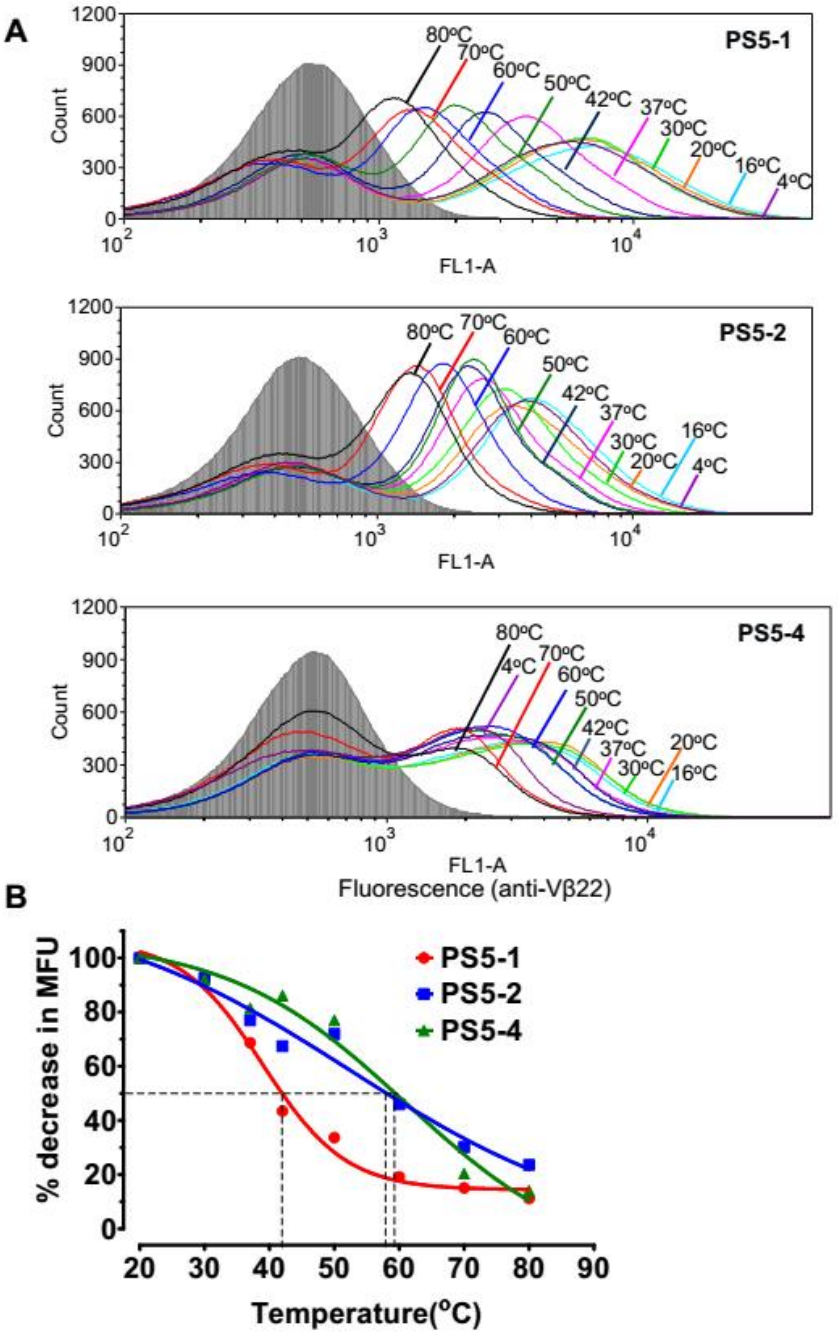

Fig. 2.5. Thermostability analysis of stabilized Vβ22 mutants obtained from error-prone library

(A) Induced yeast cells expressing stabilized Vβ22 mutant proteins (PS5-1, PS5-2 and PS5-4) were incubated at temperatures up to 80ºC for 30 minutes, before incubation with anti-Vβ22 antibody. After washing, cells were incubated with secondary antibody conjugated to Alexa Fluor 488. After washing, the cells were analyzed by flow cytometry. Fluorescence emitted by the cells in the presence of secondary antibody only is represented by the gray peak. (B) Median fluorescence units (MFU) obtained from histograms were used to generate melting curves shown. The point of 50% melting temperatures of individual mutants are indicated.

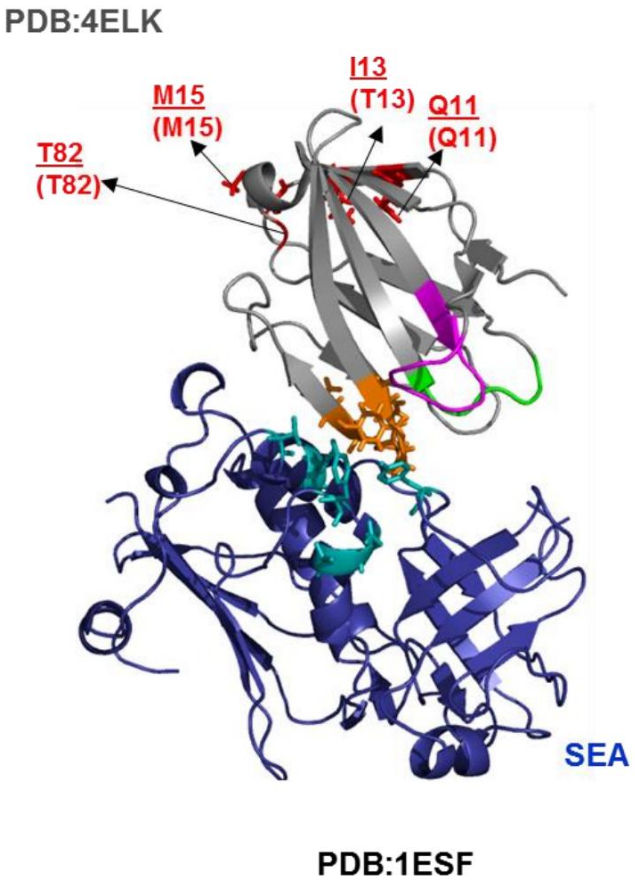

Fig. 2.6. Structural analysis of mutations in the framework region of human Vβ22
The SEA crystal structure (blue) (PDB: 1ESF) was manually docked with mouse Vβ16 crystal structure (gray) (PDB: 4ELK), that is 66% identical to human Vβ22 protein sequence. mVβ16 residues in the structure are underlined, while the corresponding residues in wt hVβ22 are indicated in parenthesis. The residues indicated in (red) correspond to the framework residues in Vβ22, which were mutated for protein stabilization. As indicated, the stabilizing mutations were located on the face opposite CDRs. CDR1 is shown in green, CDR2 in orange and CDR3 in pink. Putative TCR-binding residues of SEA are indicated in teal.

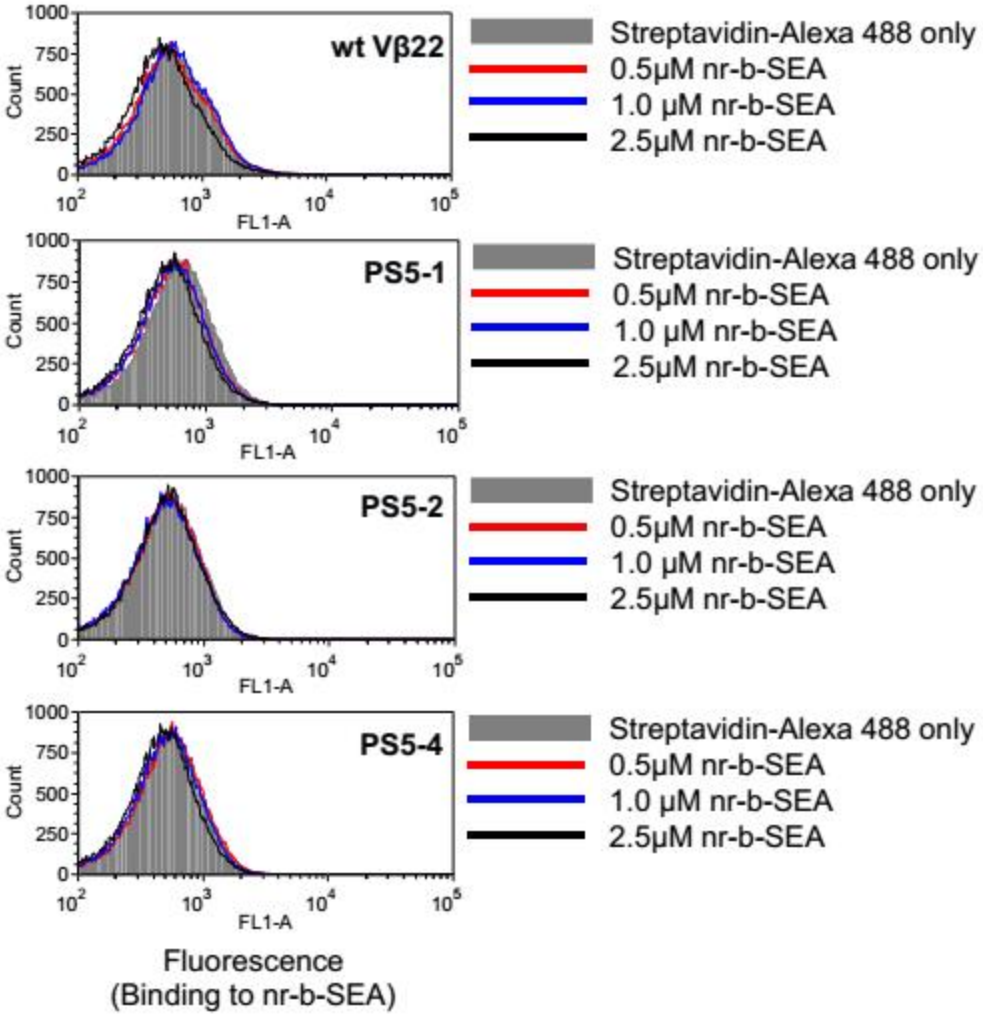

Fig. 2.7. Flow cytometry histograms for analyzing binding of *wt* Vβ22 and stabilized Vβ22 mutants to various concentrations of SEA

Induced yeast cells expressing either *wt* Vβ22 or stabilized mutant proteins (PS5-1, PS5-2 and PS5-4), were incubated with various concentrations of non-recombinant, biotinylated-SEA (nr-b-SEA), followed by a streptavidin-Alexa Fluor 488 conjugate. The fluorescence exhibited by the cells incubated with streptavidin-Alexa-488 only is represented by the gray peak.

A

	CDR2					
	49	50	51	52	53	54
WT-Vβ22	F	Y	N	N	E	I
Library 1	*	*	*	*	E	I
Library 2	F	*	*	*	*	I
Library 3	F	Y	*	*	*	*

* = Degenerate codons

B

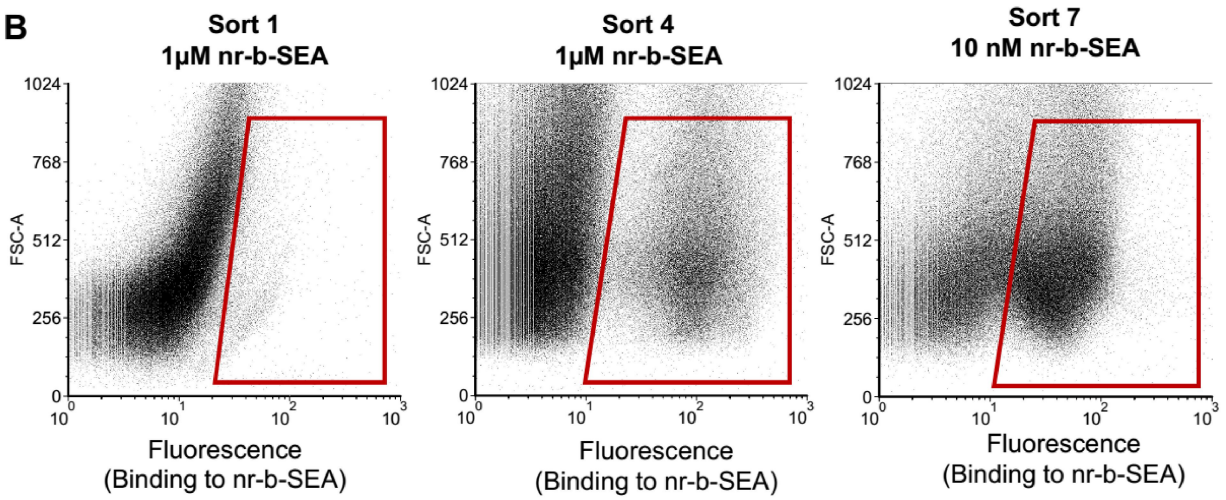

Fig. 2.8. Design and sorting of CDR2 libraries of Vβ22
(A) Residue positions in Vβ22 sequence that were the target of three directed mutagenesis (CDR2) libraries are shown. Diversity was introduced at residue positions indicated with asterisk (*) using degenerate primers. (B) Yeast cells transformed with a mixture of three CDR2 libraries, were sorted several times with decreasing concentrations of non-recombinant, biotinylated-SEA (nr-b-SEA). Scatter plots representing different stages of sorting are shown. The cells indicated in the polygon (maroon) after sort-7 were collected, from which distinct Vβ22 mutants were isolated in future experiments.

	FR1																										CDR1					FR2																
	1	2	3	4	5	6	7	8	9	10	11	12	13	14	15	16	17	18	19	20	21	22	23	24	25	26	27	28	29	30	31	32	33	34	35	36	37	38	39	40	41	42	43	44	45	46	47	48
WT-Vβ22	E	P	E	V	T	Q	T	P	S	H	Q	V	T	Q	M	G	Q	E	V	I	L	R	C	V	P	I	S	N	H	L	Y	F	Y	W	Y	R	Q	I	L	G	Q	K	V	E	F	L	V	S
PS5-1	-	-	-	-	-	-	-	-	-	-	-	-	**A**	-	**V**	-	-	-	-	-	-	-	-	-	-	-	-	-	-	-	-	-	-	-	-	-	-	-	-	-	-	-	-	-	-	-	-	-
PS5-2	-	-	-	-	-	-	-	-	-	-	-	-	**A**	-	-	-	-	-	-	-	-	-	-	-	-	-	-	-	-	-	-	-	-	-	-	-	-	-	-	-	-	-	-	-	-	-	-	-
PS5-4	-	-	-	-	-	-	-	-	-	-	**L**	-	**A**	-	-	-	-	-	-	-	-	-	-	-	-	-	-	-	-	**S**	-	-	-	-	-	-	-	-	-	-	-	-	-	-	-	-	-	-
PS7-1	-	-	-	-	-	-	-	-	-	-	-	-	**A**	-	**V**	-	-	-	-	-	-	-	-	-	-	-	-	-	-	-	-	-	-	-	-	-	-	-	-	-	-	-	-	-	-	-	-	-
PS7-2	-	-	-	-	-	-	-	-	-	-	**L**	-	**A**	-	-	-	-	-	-	-	-	-	-	-	-	-	-	-	-	**S**	-	-	-	-	-	-	-	-	-	-	-	-	-	-	-	-	-	-
PS7-4	-	-	-	-	-	-	-	-	-	-	-	-	**A**	-	**V**	-	-	-	-	-	-	-	-	-	-	-	-	-	-	**S**	-	-	-	-	-	-	-	-	-	-	-	-	-	-	-	-	-	-
PS7-6	-	-	-	-	-	-	-	-	-	-	-	-	**A**	-	-	-	-	-	-	-	-	-	-	-	-	-	-	-	-	**S**	-	-	-	-	-	-	-	-	-	-	-	-	-	-	-	-	-	-
FL	-	-	-	-	-	-	-	-	-	-	-	-	**A**	-	**V**	-	-	-	-	-	-	-	-	-	-	-	-	-	-	**S**	-	-	-	-	-	-	-	-	-	-	-	-	-	-	-	-	-	-

	CDR2						FR3																																					
	49	50	51	52	53	54	55	56	57	58	59	60	61	62	63	64	65	66	67	68	69	70	71	72	73	74	75	76	77	78	79	80	81	82	83	84	85	86	87	88	89	90	91	92
WT-Vβ22	F	Y	N	N	E	I	S	E	K	S	E	I	F	D	D	Q	F	S	V	E	R	P	D	G	S	N	F	T	L	K	I	R	S	T	K	L	E	D	S	A	M	Y	F	C
PS5-1	-	-	-	-	-	-	-	-	-	-	-	-	-	-	-	-	-	-	-	-	-	-	-	-	-	-	-	-	-	-	-	-	-	**A**	-	-	-	-	-	-	-	-	-	-
PS5-2	-	-	-	-	-	-	-	-	-	-	-	-	-	-	-	-	-	-	-	-	-	-	-	-	-	-	-	-	-	-	-	-	-	**A**	-	-	-	-	-	-	-	-	-	-
PS5-4	-	-	-	-	-	-	-	-	-	-	-	-	-	-	-	-	-	-	-	-	-	-	-	-	-	-	-	-	-	-	-	-	-	-	-	-	-	-	-	-	-	-	-	-
PS7-1	-	**A**	**Y**	**E**	**D**	-	-	-	-	-	-	-	-	-	-	-	-	-	-	-	-	-	-	-	-	-	-	-	-	-	-	-	-	**A**	-	-	-	-	-	-	-	-	-	-
PS7-2	**M**	**A**	**Y**	**G**	-	-	-	-	-	-	-	-	-	-	-	-	-	-	-	-	-	-	-	-	-	-	-	-	-	-	-	-	-	**A**	-	-	-	-	-	-	-	-	-	-
PS7-4	**M**	**S**	**Y**	**G**	-	-	-	-	-	-	-	-	-	-	-	-	-	-	-	-	-	-	-	-	-	-	-	-	-	-	-	-	-	**A**	-	-	-	-	-	-	-	-	-	-
PS7-6	**M**	**A**	**Y**	**G**	-	-	-	-	-	-	-	-	-	-	-	-	-	-	-	-	-	-	-	-	-	-	-	-	-	-	-	-	-	**A**	-	-	-	-	-	-	-	-	-	-
FL	**M**	**A**	**Y**	**E**	**D**	-	-	-	-	-	-	-	-	-	-	-	-	-	-	-	-	-	-	-	-	-	-	-	-	-	-	-	-	**A**	-	-	-	-	-	-	-	-	-	-

	CDR3																						
	93	94	95	96	97	98	99	100	101	102	103	104	105	106	107	108	109	110	111	112	113	114	115
WT-Vβ22	A	S	S	E	L	V	V	S	Q	P	Q	H	F	G	D	G	T	R	L	S	I	L	E
PS5-1	-	-	-	-	-	-	-	-	-	-	-	-	-	-	-	-	-	-	-	-	-	-	-
PS5-2	-	-	-	-	**Q**	-	-	-	-	-	-	-	-	-	-	-	-	-	-	-	-	-	-
PS5-4	-	-	-	-	-	-	-	-	-	-	-	-	-	-	-	-	-	-	-	-	-	-	-
PS7-1	-	-	-	-	**Q**	-	-	-	-	-	-	-	-	-	-	-	-	-	-	-	-	-	-
PS7-2	-	-	-	-	-	-	-	-	-	-	-	-	-	-	-	-	-	-	-	-	-	-	-
PS7-4	-	-	-	-	**Q**	-	-	-	-	-	-	-	-	-	-	-	-	-	-	-	-	-	-
PS7-6	-	-	-	-	-	-	-	-	-	-	-	-	-	-	-	-	-	-	-	-	-	-	-
FL	-	-	-	-	**Q**	-	-	-	-	-	-	-	-	-	-	-	-	-	-	-	-	-	-

Fig. 2.9. Amino acid sequences of distinct mutants isolated from CDR2 library
Four different mutants (PS7-1, PS7-2, PS7-4 and PS7-6) were isolated from CDR2 libraries, after sorting multiple rounds with non-recombinant, biotinylated-SEA. Their sequences are compared with wt-Vβ22 and stabilized Vβ22 mutants (PS5-1, PS5-2, PS5-4) isolated from error-prone library. Two mutations (F49M and L30S) were introduced into PS7-1 to yield the mutant designated FL. Mutated residues are in bold (red); CDR regions are highlighted in gray.

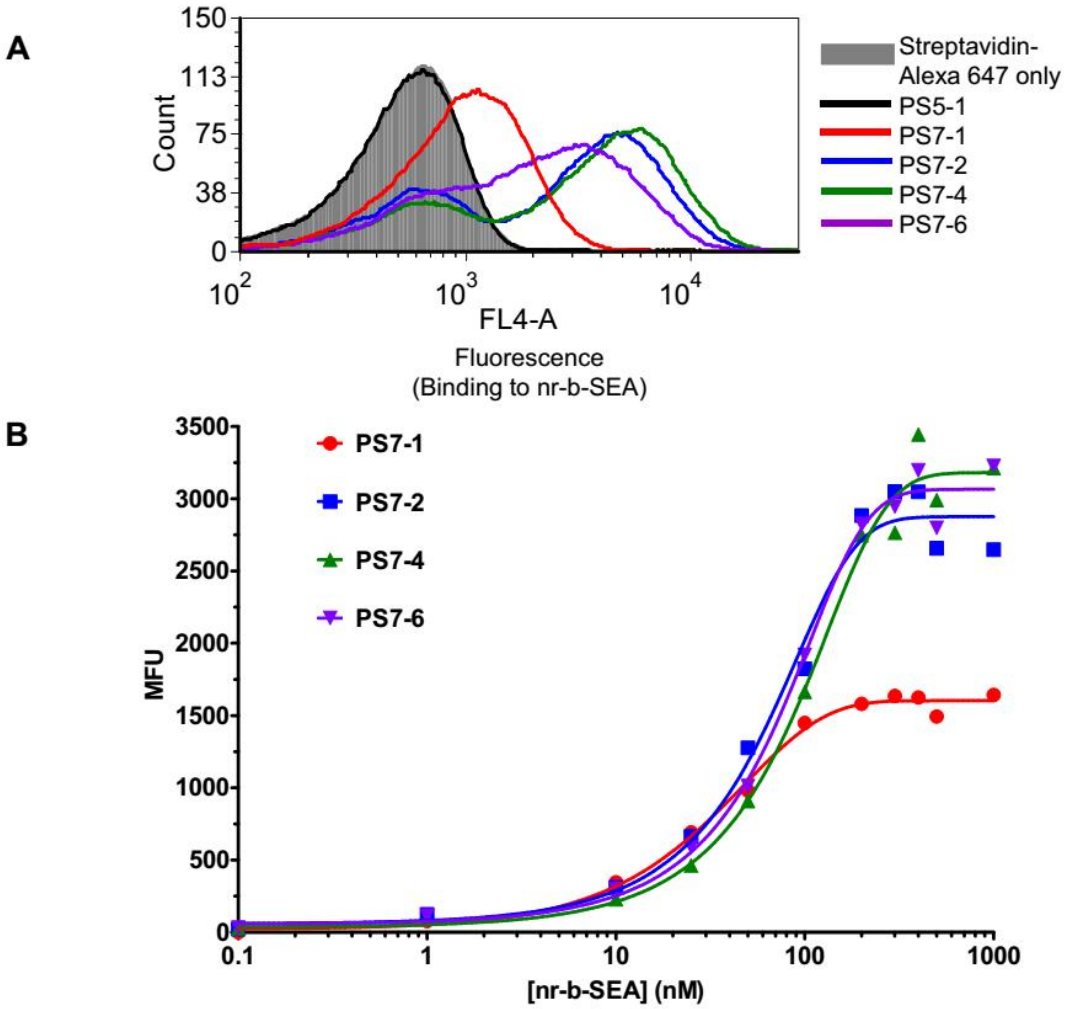

Fig. 2.10. Binding analysis of distinct Vβ22 mutants isolated from CDR2 library
(A) Histograms representing binding of Vβ22 mutants to SEA are shown. Induced yeast cells expressing four different Vβ22 mutants (PS7-1, PS7-2, PS7-4 and PS7-6) isolated from CDR2 libraries, were incubated with 10 nM non-recombinant, biotinylated-SEA (nr-b-SEA), followed by a streptavidin conjugated with a fluorophore (Alexa Fluor 647). The fluorescence exhibited by yeast cells incubated with streptavidin-Alexa Fluor 647 conjugate only, is represented by the gray peak. (B) SEA-binding titration of Vβ22 mutants isolated from CDR2 libraries. Median fluorescence units (MFU) obtained from the histograms were used to generate binding curves shown.

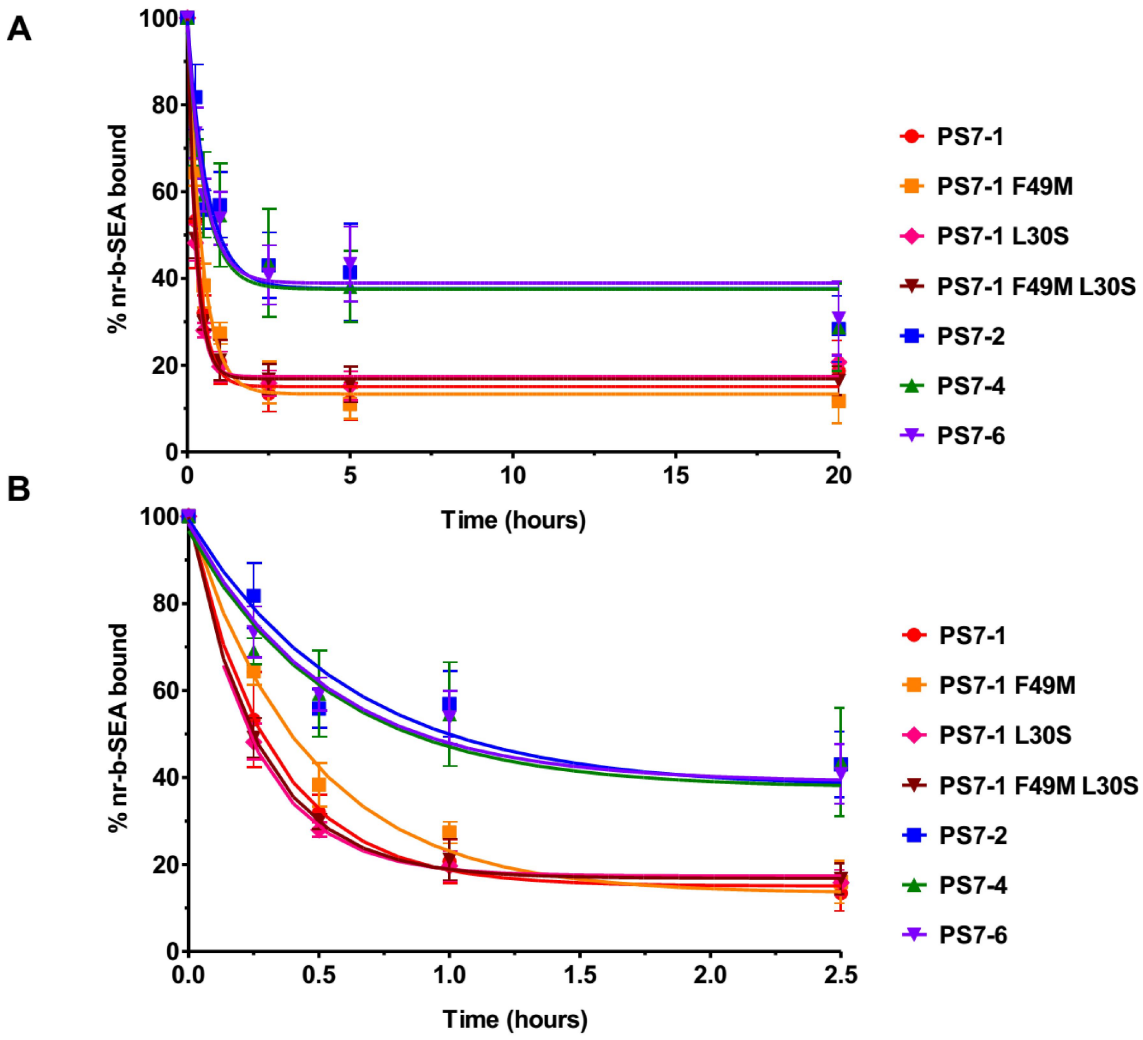

Fig. 2.11. Off-rate analysis of various Vβ22 mutants
Induced yeast cells expressing Vβ22 mutants (PS7-1, PS7-2, PS7-4 and PS7-6) isolated from CDR2 libraries or site-directed mutants of PS7-1, were incubated with biotinylated-SEA (nr-b-SEA). After washing, dissociation of biotinylated-SEA was monitored by addition of a competing reagent (unlabeled SEA, recombinant, in this case). Aliquots of cells were removed at different time points, and stained with streptavidin conjugated with a fluorophore. Median fluorescence units (MFU) at each time point was recorded. % biotinylated SEA bound at each time point was calculated as $100*(MFU_{(time\ point)} - MFU_{(negative\ control)})/(MFU_{(positive\ control)} - MFU_{(negative\ control)})$. In panel A, dissociation of bound, biotinylated SEA from 0 to ~20 hours is shown. In panel B, dissociation of bound, biotinylated SEA from 0 to 2.5 hours is shown.

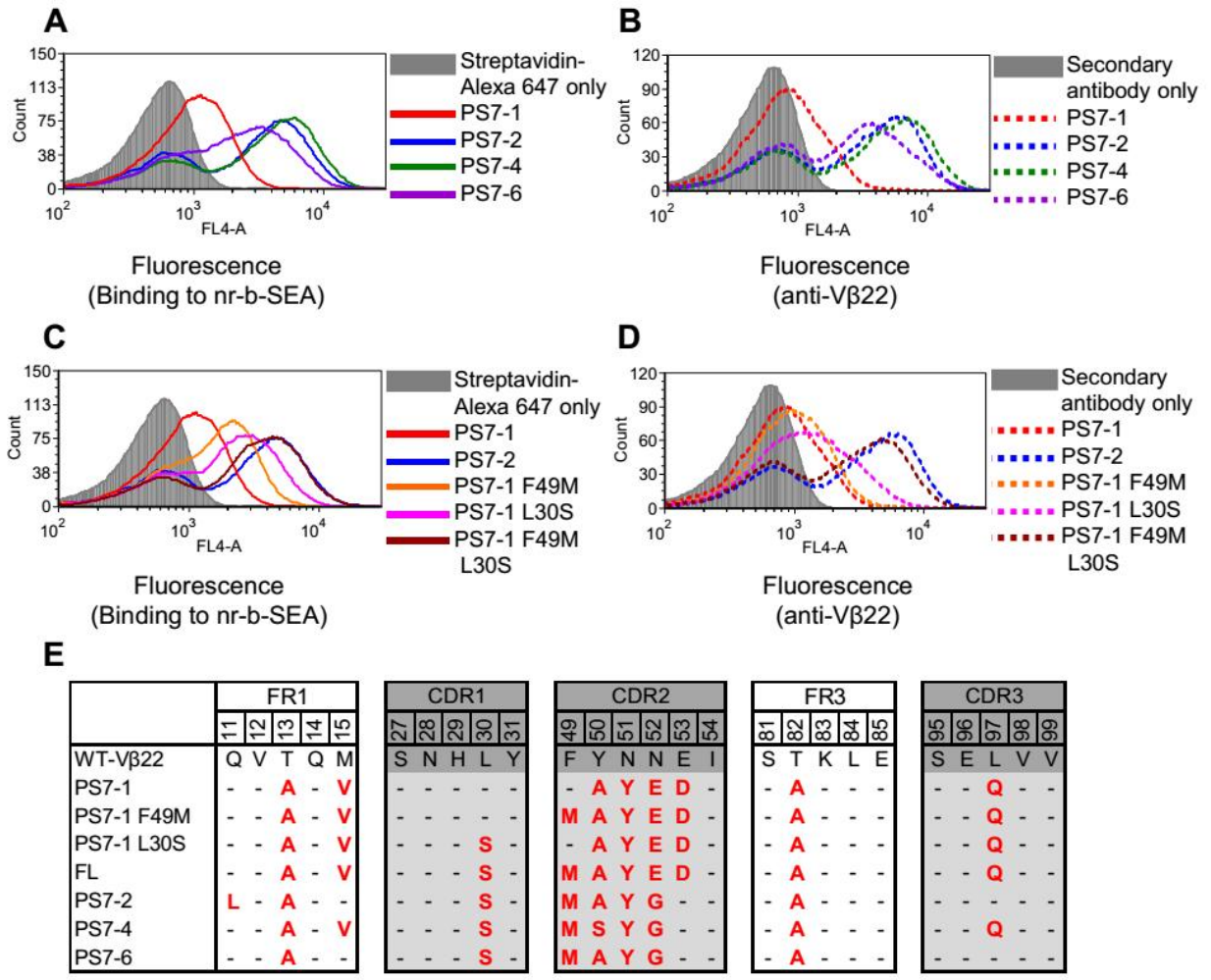

E

	FR1					CDR1					CDR2						FR3					CDR3				
	11	12	13	14	15	27	28	29	30	31	49	50	51	52	53	54	81	82	83	84	85	95	96	97	98	99
WT-Vβ22	Q	V	T	Q	M	S	N	H	L	Y	F	Y	N	N	E	I	S	T	K	L	E	S	E	L	V	V
PS7-1	-	-	A	-	V	-	-	-	-	-	-	A	Y	E	D	-	-	A	-	-	-	-	-	Q	-	-
PS7-1 F49M	-	-	A	-	V	-	-	-	-	-	M	A	Y	E	D	-	-	A	-	-	-	-	-	Q	-	-
PS7-1 L30S	-	-	A	-	V	-	-	-	S	-	-	A	Y	E	D	-	-	A	-	-	-	-	-	Q	-	-
FL	-	-	A	-	V	-	-	-	S	-	M	A	Y	E	D	-	-	A	-	-	-	-	-	Q	-	-
PS7-2	L	-	A	-	-	-	-	-	S	-	M	A	Y	G	-	-	-	A	-	-	-	-	-	-	-	-
PS7-4	-	-	A	-	V	-	-	-	S	-	M	S	Y	G	-	-	-	A	-	-	-	-	-	Q	-	-
PS7-6	-	-	A	-	-	-	-	-	S	-	M	A	Y	G	-	-	-	A	-	-	-	-	-	-	-	-

Fig. 2.12. Effect of mutations at residues 30 and 49 in PS7-1 mutant
Flow cytometry histograms indicating effect of introducing F49M and/or L30S mutations in PS7-1 mutant are shown. Binding to 10 nM non-recombinant, biotinylated-SEA (nr-b-SEA) (panels A and C) and surface expression of Vβ22 protein (anti-Vβ22 staining in panels B and D) by yeast cells expressing various Vβ22 mutants were analyzed. The fluorescence exhibited by yeast cells incubated with streptavidin-Alexa Fluor 647 conjugate only (panels A and C) or secondary antibody only (Alexa Fluor 647-conjugated goat anti-mouse IgG in panels B and D) is represented by the gray peak. Stretches of Vβ22 sequence where mutations are located are shown in panel E.

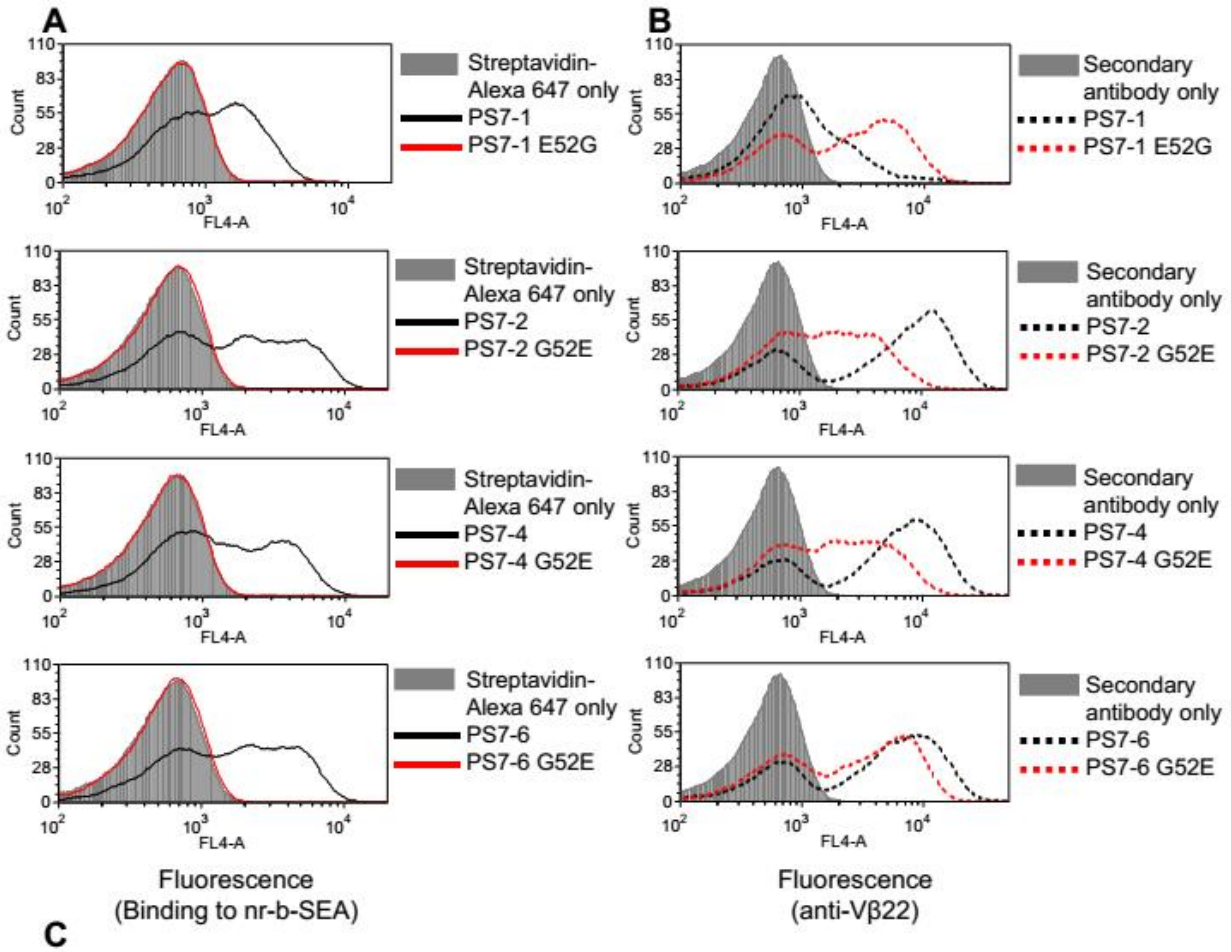

C

	FR1					CDR1					CDR2						FR3					CDR3				
	11	12	13	14	15	27	28	29	30	31	49	50	51	52	53	54	81	82	83	84	85	95	96	97	98	99
WT-Vβ22	Q	V	T	Q	M	S	N	H	L	Y	F	Y	N	N	E	I	S	T	K	L	E	S	E	L	V	V
PS7-1	-	-	A	-	V	-	-	-	-	-	-	A	Y	E	D	-	-	A	-	-	-	-	-	Q	-	-
PS7-2	L	-	A	-	-	-	-	-	S	-	M	A	Y	G	-	-	-	A	-	-	-	-	-	-	-	-
PS7-4	-	-	A	-	V	-	-	-	S	-	M	S	Y	G	-	-	-	A	-	-	-	-	-	Q	-	-
PS7-6	-	-	A	-	-	-	-	-	S	-	M	A	Y	G	-	-	-	A	-	-	-	-	-	-	-	-
PS7-1 E52G	-	-	A	-	V	-	-	-	-	-	-	A	Y	G	D	-	-	A	-	-	-	-	-	Q	-	-
PS7-2 G52E	L	-	A	-	-	-	-	-	S	-	M	A	Y	E	-	-	-	A	-	-	-	-	-	-	-	-
PS7-4 G52E	-	-	A	-	V	-	-	-	S	-	M	S	Y	E	-	-	-	A	-	-	-	-	-	Q	-	-
PS7-6 G52E	-	-	A	-	-	-	-	-	S	-	M	A	Y	E	-	-	-	A	-	-	-	-	-	-	-	-

Fig. 2.13. Importance of specific residues at position 52 isolated in Vβ22 mutants for binding to SEA

To understand the role of specific amino acids at position 52, glycine was introduced in PS7-1 while glutamate was introduced in PS7-2, PS7-4 and PS7-6. Binding to 10 nM non-recombinant, biotinylated-SEA (nr-b-SEA) (panel A) and surface expression of Vβ22 (panel B) by yeast cells expressing different Vβ22 mutants were analyzed. The fluorescence exhibited by cells incubated with streptavidin-Alexa Fluor 647 conjugate only (panel A) or secondary antibody only (Alexa Fluor 647-conjugated goat anti-mouse IgG in panel B), is represented by the gray peak. Stretches of Vβ22 sequence where mutations are located are shown in panel C.

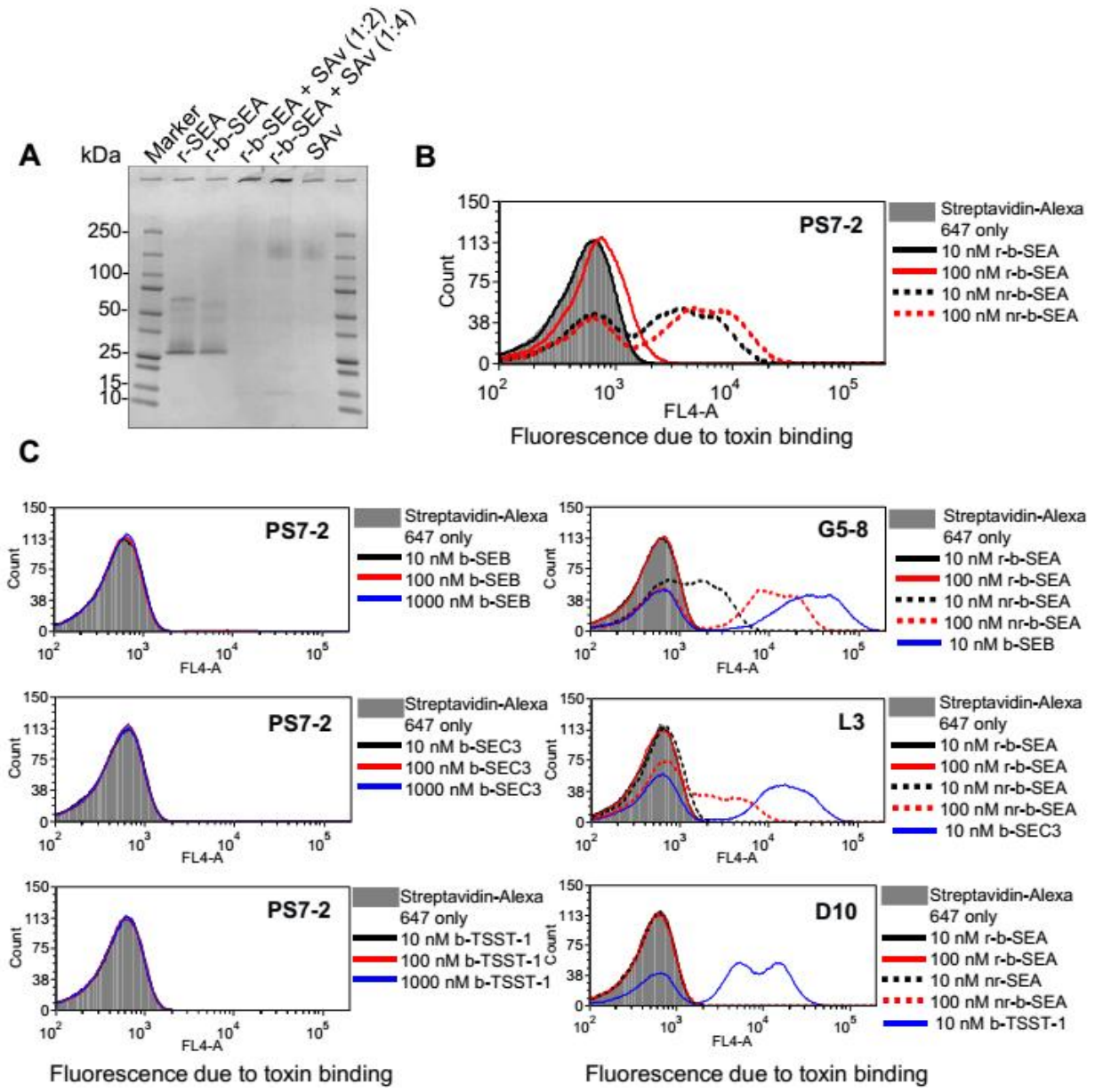

Fig. 2.14. Difference in binding of PS7-2 mutant to non-recombinant SEA versus recombinant SEA preparation due to possible contamination of non-recombinant SEA with SEB

(A) Gel-shift assay showing biotinylation of recombinant SEA. (B) Induced yeast cells expressing PS7-2 protein were incubated with 10 or 100 nM recombinant or non-recombinant, biotinylated SEA (r-b-SEA or nr-b-SEA), followed by incubation with streptavidin-Alexa Fluor 647 conjugate. Binding to SEA was assessed as an increase in fluorescence, compared to the fluorescence exhibited by the cells when no toxin was added (gray peak). (C) Induced yeast cells expressing PS7-2, G5-8, L3 or D10 protein on their surface, were incubated with 10 or 100 nM of the biotinylated toxins indicated, followed by incubation with a streptavidin-Alexa Fluor 647 conjugate. Binding to each toxin was assessed as an increase in fluorescence, compared to the fluorescence exhibited by the cells when no toxin was added (gray peak).

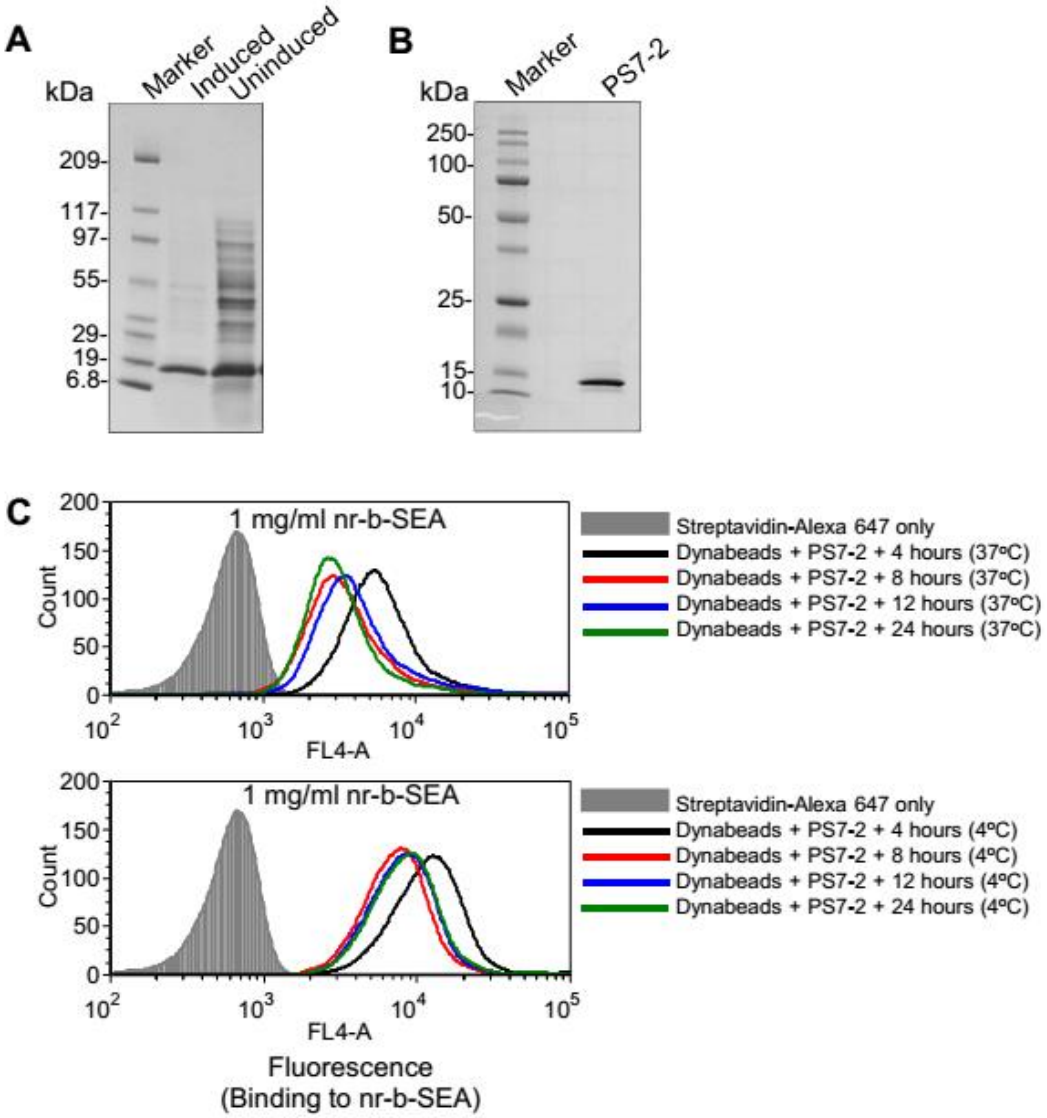

Fig. 2.15. Binding of soluble PS7-2 protein coated on Dynabeads to SEA
(A) Test induction indicating expression of PS7-2 protein in transformed *E.coli* BL21 (DE3) cells upon induction with IPTG. Lysates of induced and uninduced cultures were loaded on 4-20% SDS-PAGE gels for assessing protein expression. (B) Purified PS7-2 protein loaded on 4-20% SDS-PAGE gel, after refolding inclusion bodies harvested from *E.coli*. (C) Soluble PS7-2 was coated on Dynabeads for 4, 8, 12, 24 hours at 4ºC or 37ºC. Coated beads were washed and incubated with non-recombinant, biotinylated-SEA (nr-b-SEA) followed by incubation with streptavidin-Alexa Fluor 647 conjugate. Binding to SEA was assessed as an increase in fluorescence, compared to the fluorescence emitted by the beads when no toxin was added (gray peak).

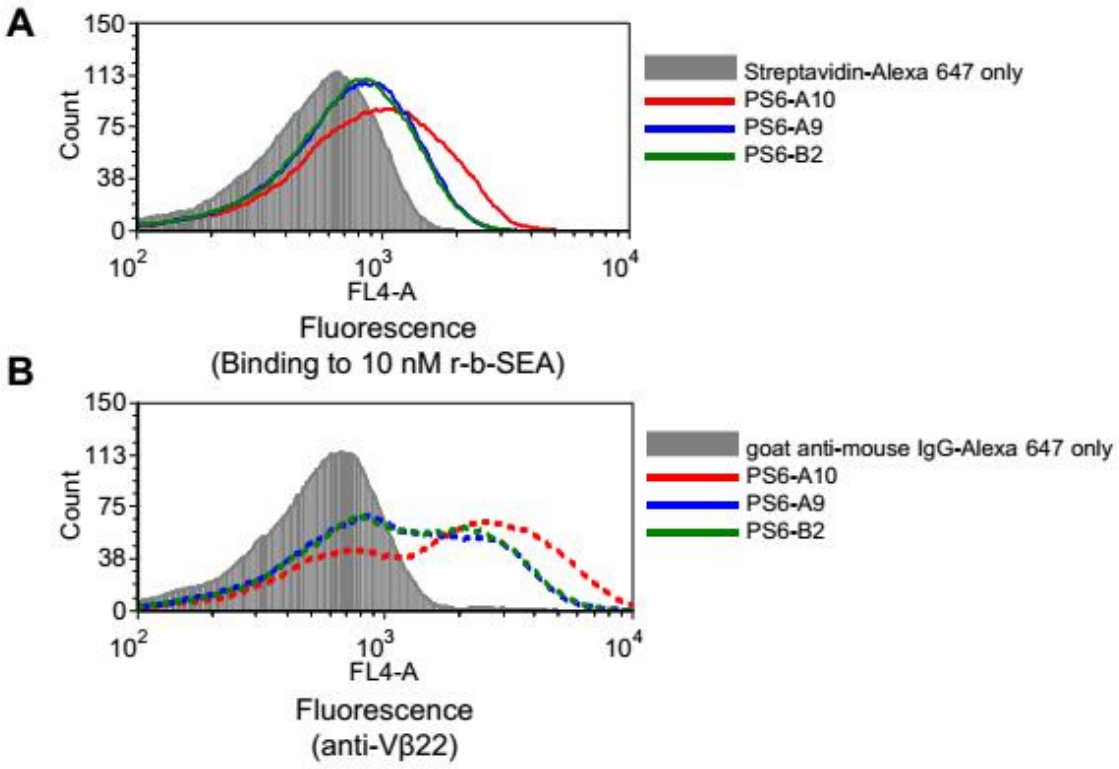

Fig. 2.16. Binding analysis of selected Vβ22 mutants isolated from CDR2 library after sorting with recombinant-biotinylated-SEA

(A) Histogram representing binding of Vβ22 mutants to recombinant-SEA is shown. Induced yeast cells expressing three different Vβ22 mutants (PS6-A9, PS6-A10 and PS6-B2) isolated from CDR2 libraries, were incubated with 10 nM recombinant, biotinylated-SEA (r-b-SEA), followed by streptavidin-Alexa Fluor 647 conjugate. The fluorescence exhibited by yeast cells incubated with streptavidin-Alexa Fluor 647 conjugate only, is represented by the gray peak. (B) Histogram representing surface expression of Vβ22 on yeast cells expressing various Vβ22 mutants.

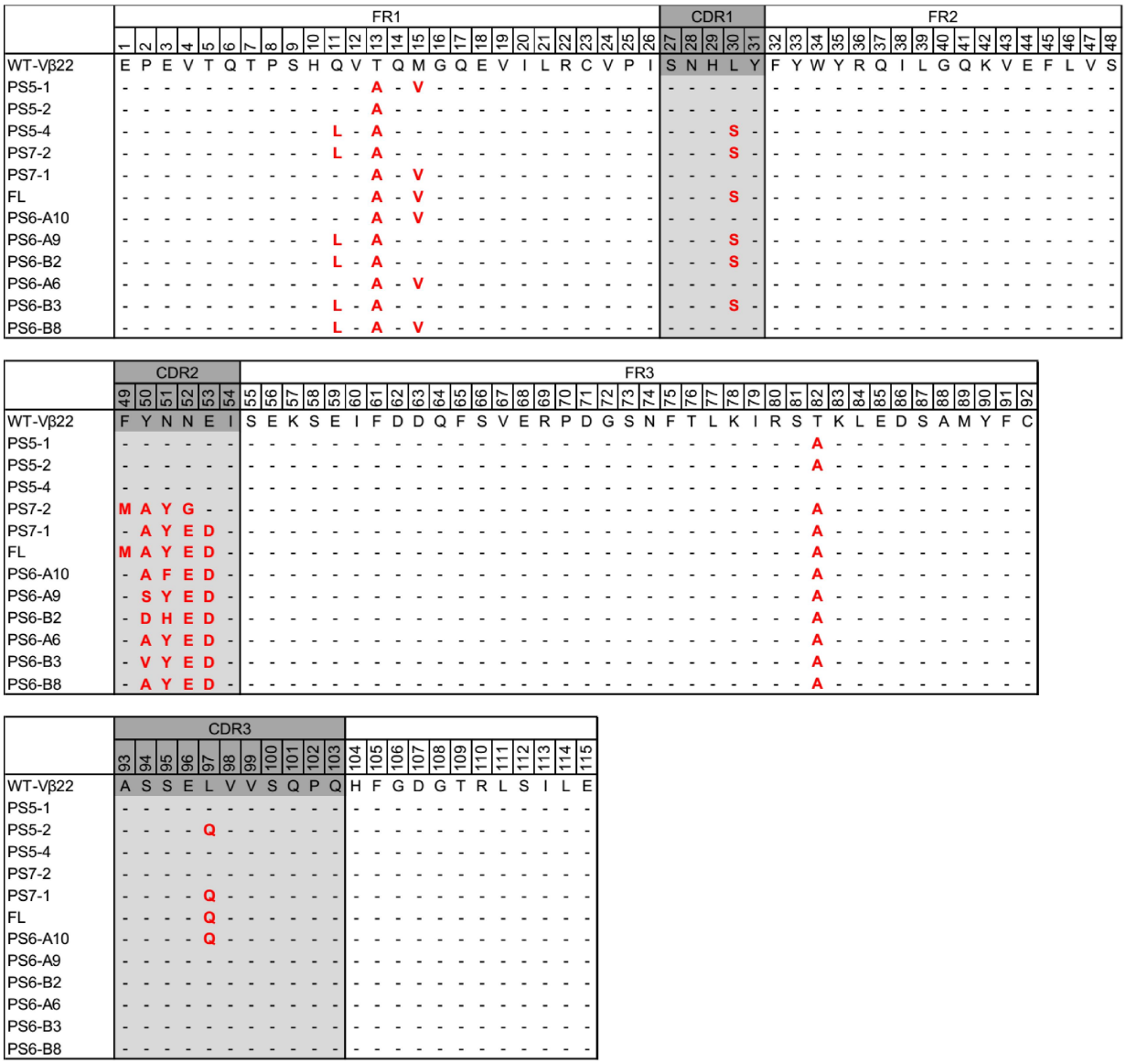

Fig. 2.17. Amino acid sequences of distinct mutants isolated from CDR2 library after sorting with recombinant-biotinylated-SEA

Distinct Vβ22 mutants (prefixed with PS6 in the sequence analysis shown above) were isolated from CDR2 libraries, after sorting multiple rounds with recombinant, biotinylated-SEA. Their sequences are compared with *wt*-Vβ22, stabilized Vβ22 mutants (PS5-1, PS5-2, and PS5-4) isolated from error-prone library, and mutants isolated from CDR2 libraries (PS7-1, PS7-2) after sorting with non-recombinant, biotinylated SEA. Two mutations (F49M and L30S) were introduced into PS7-1 to yield the mutant designated FL. Mutated residues are in bold (red); CDR regions are highlighted in gray.

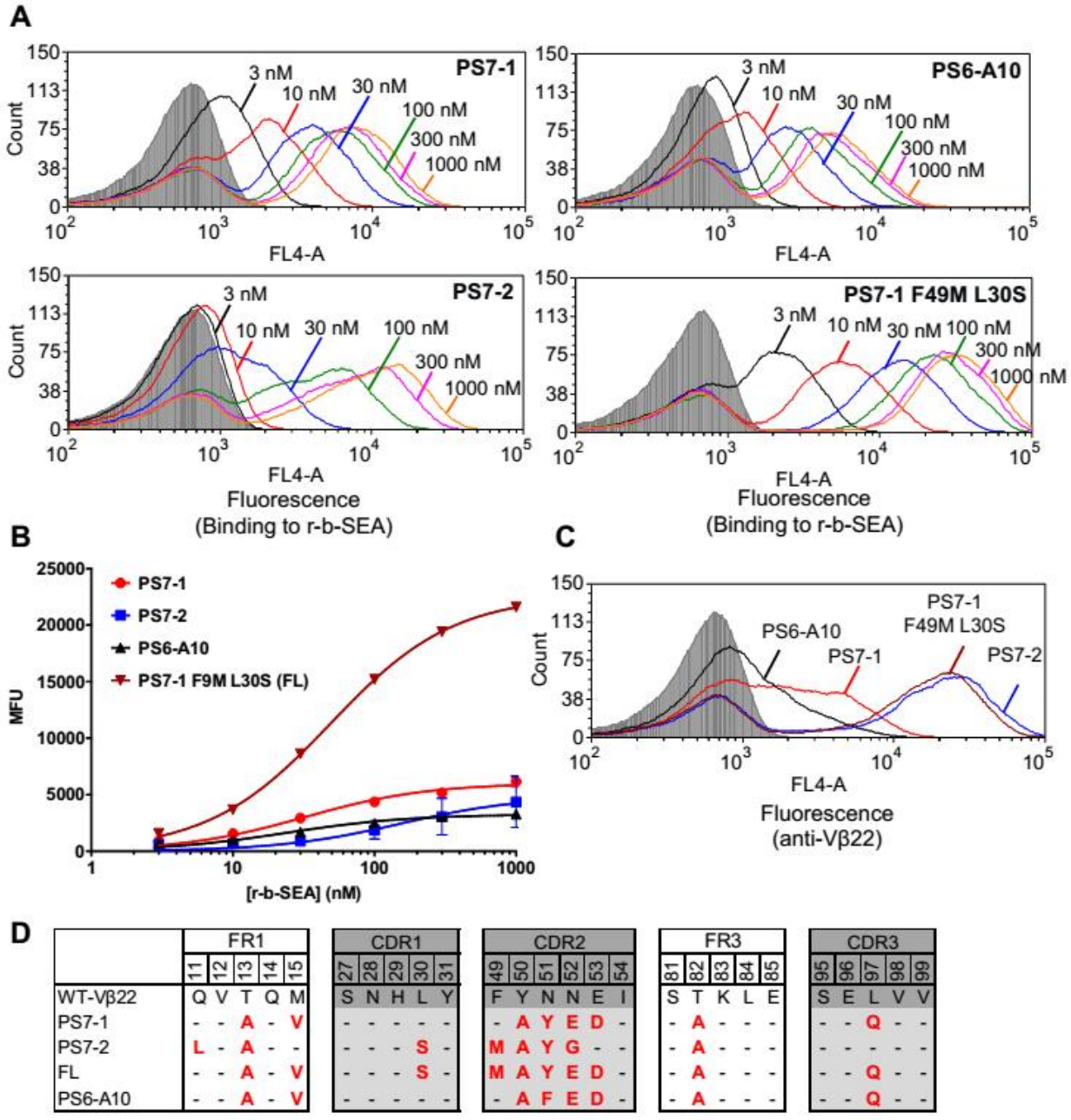

Fig. 2.18. Binding analysis of key Vβ22 mutants to recombinant SEA
(A) Flow cytometry histograms for binding of PS7-1, PS7-2, PS6-A10 and PS7-1 F49M L30S (FL mutant) to various concentrations of recombinant, biotinylated-SEA (r-b-SEA). Fluorescence in the absence of SEA is represented by gray (filled) peak. Concentrations of SEA used are indicated in the histograms. (B) Median fluorescence units (MFU) obtained from histograms shown in panel A were used to generate binding curves shown. (C) Analysis of levels of surface expression of Vβ22 by various Vβ22 mutants is shown. (D) Stretches of Vβ22 sequence where mutations are located in the Vβ22 mutants being analyzed, are shown.

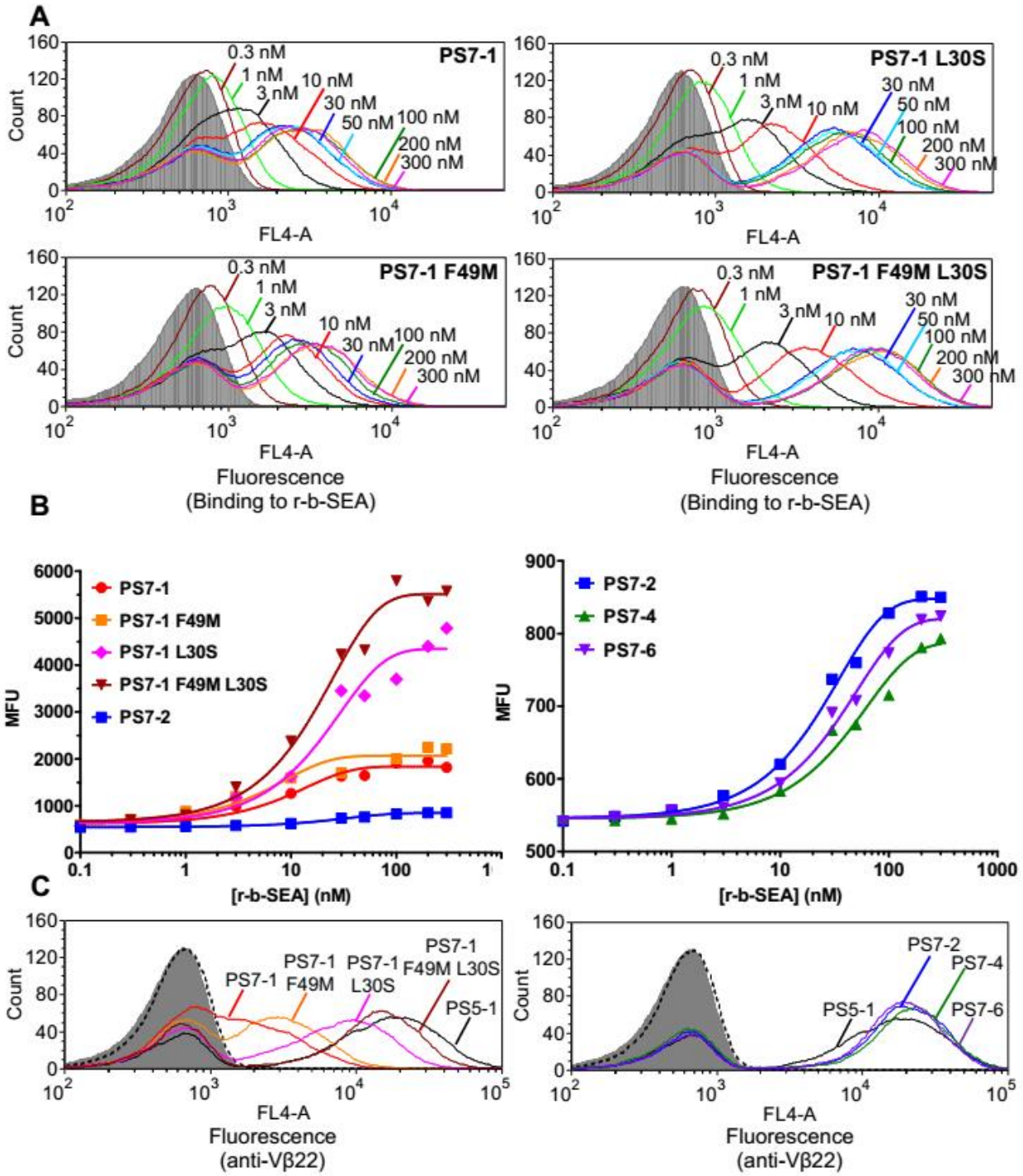

Fig. 2.19. Effect of mutations at residues 30 and 49 in PS7-1 mutant
(A) Flow cytometry histograms for binding of PS7-1, PS7-1 F49M, PS7-1 L30S and PS7-1 F49M L30S (FL mutant) with various concentrations of recombinant, biotinylated-SEA (r-b-SEA). Fluorescence in the absence of SEA is represented by gray (filled) peak. Concentrations of SEA used are indicated in the histograms. (B) Median fluorescence units (MFU) obtained from histograms shown in panel A were used to generate binding curves shown. (C) Flow-cytometric analysis of levels of surface expression by various Vβ22 mutants is shown.

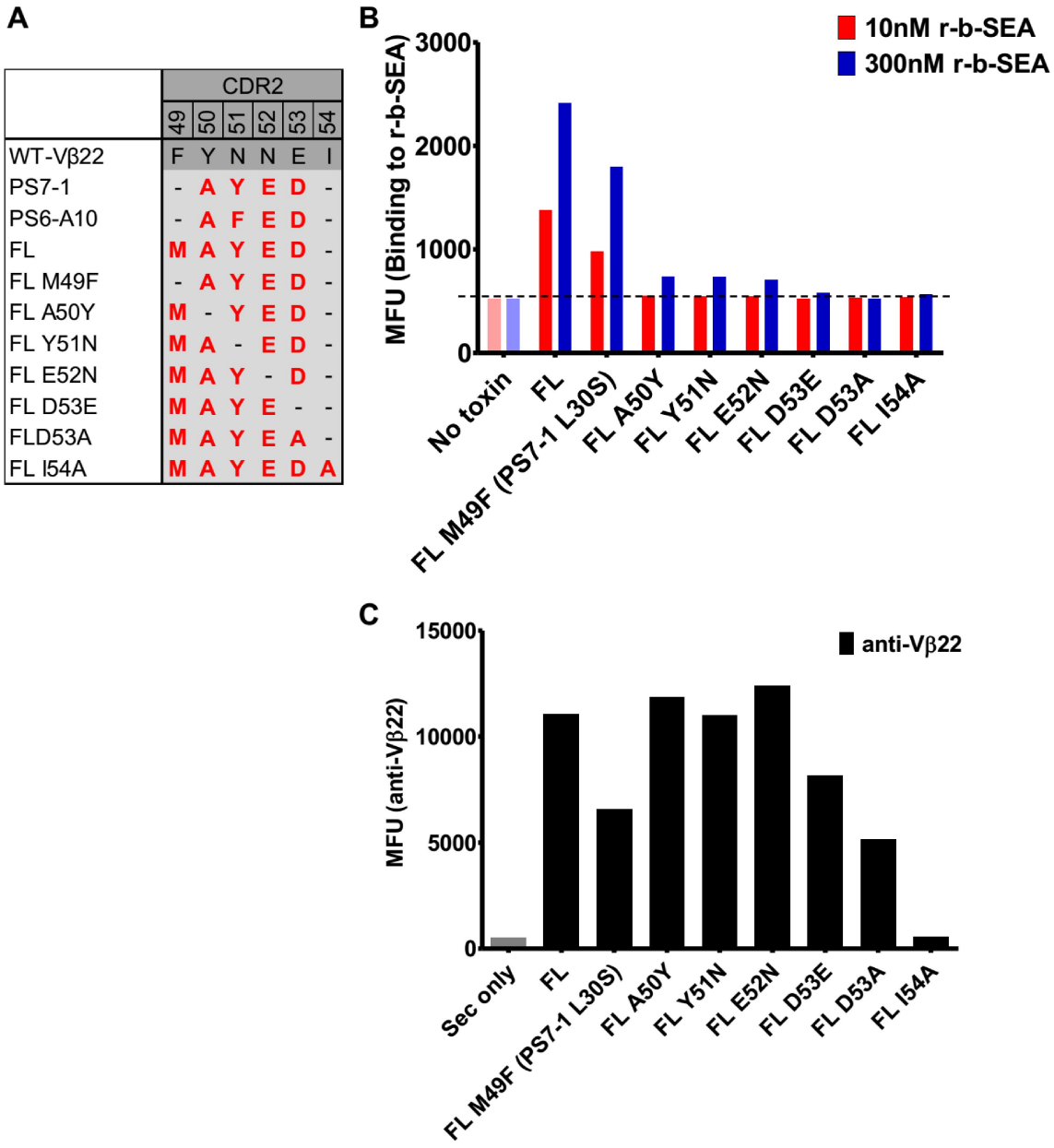

Fig. 2.20. Analysis of revertant mutants of high affinity Vβ22 mutant, "FL"
Sequences of *wt* Vβ22, mutants isolated from CDR2 libraries (PS7-1, PS6-A10), FL and its revertant mutants are shown in panel A. Effect of single-site revertant mutations on binding to SEA (panel B), and surface expression (panel C) was analyzed. The revertant mutants were transformed into yeast and analyzed for binding with different concentrations of recombinant-biotinylated SEA (r-b-SEA) (panel B) or anti-Vβ22 (panel C). Median fluorescence units from flow cytometry histograms were used to generate the bar graphs shown.

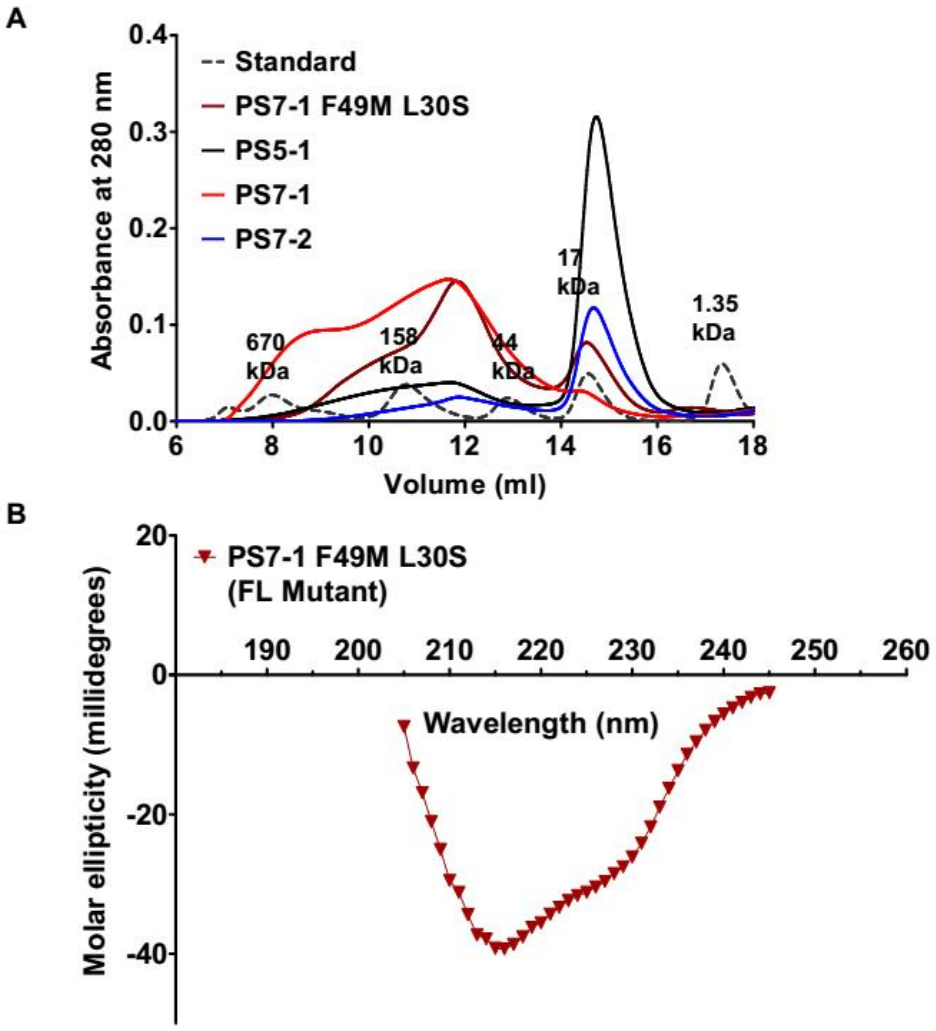

Fig. 2.21. Purification of refolded Vβ22 mutant proteins
(A) Purification of monomeric fractions of refolded, high-affinity Vβ22 mutants by size-exclusion chromatography. Dashed line indicates the molecular weight standards. (B) Circular dichroism spectrum of refolded FL protein.

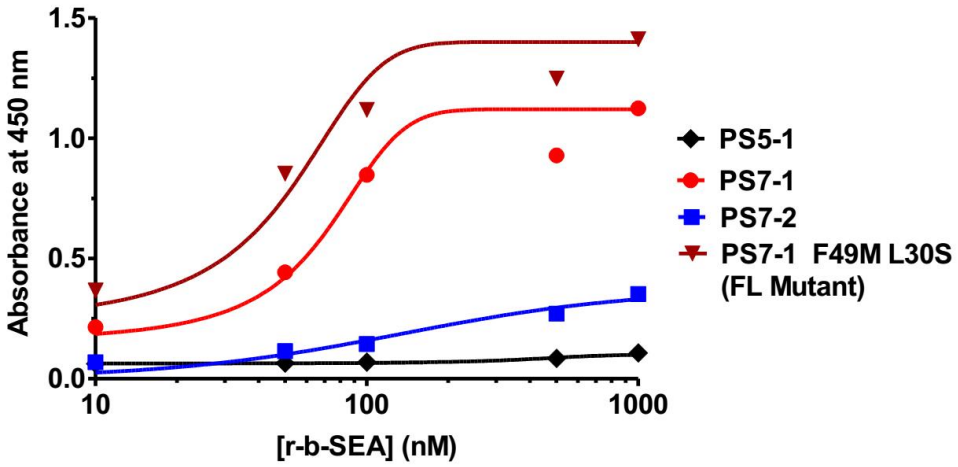

Fig. 2.22. ELISA-based titration for binding of soluble Vβ22 mutant proteins to recombinant, biotinylated SEA.

Purified Vβ22 mutant proteins were coated on wells of an ELISA plate at 5μg/ml, followed by incubation with various concentrations of recombinant-biotinylated-SEA (r-b-SEA), followed by streptavidin-conjugated HRP. Bound SEA was detected by measuring absorbance of colorimetric product formed at 450nm, upon addition of TMB substrate.

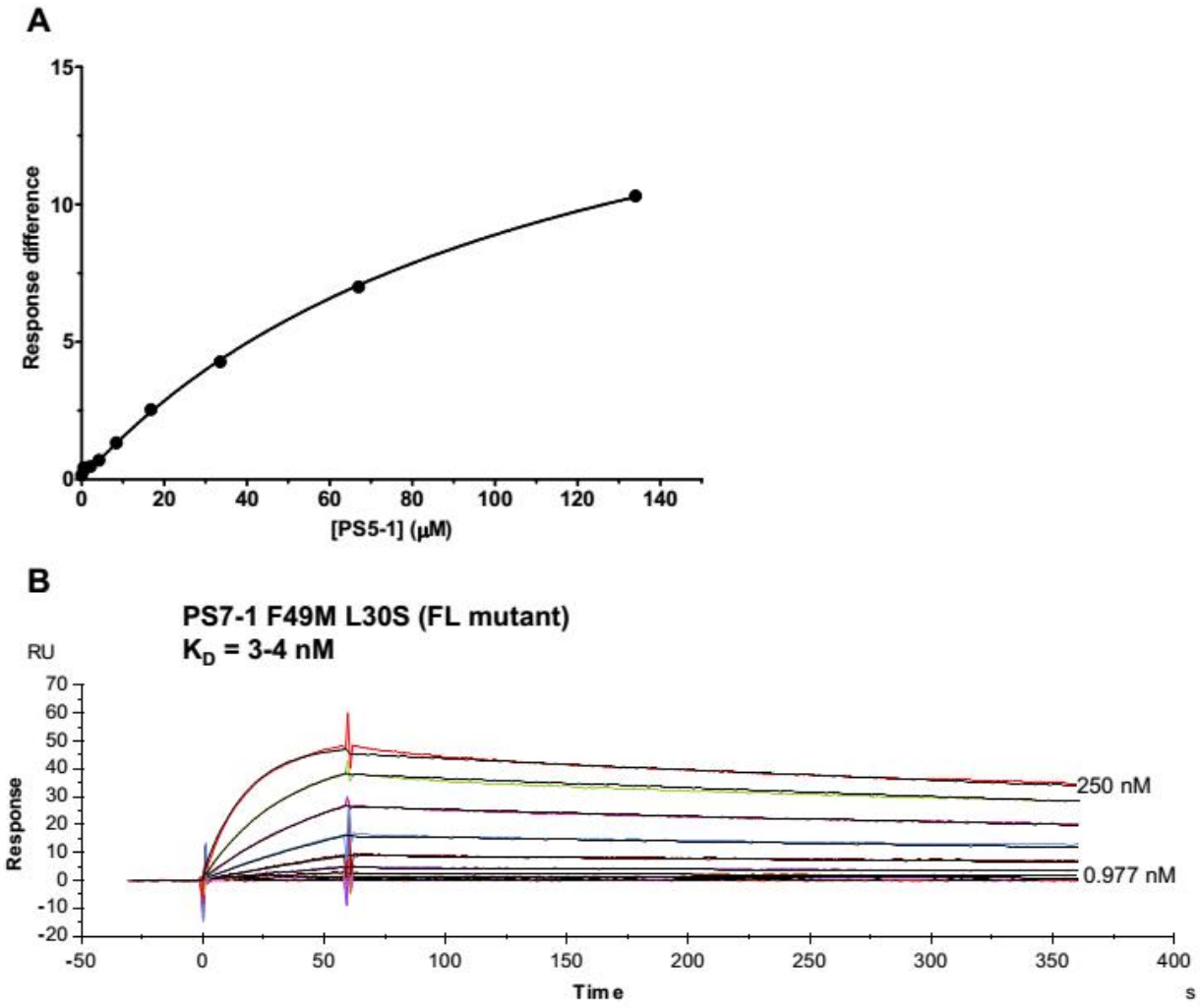

k_{on} (M^{-1} s^{-1})	k_{off} (s^{-1})	$K_D = k_{off} / k_{on}$ (nM)
2.73×10^5	9.04×10^{-4}	3.3
2.69×10^5	8.60×10^{-4}	3.19
2.52×10^5	9.55×10^{-4}	3.78
2.35×10^5	8.73×10^{-4}	3.71

Fig. 2.23. Binding analysis of selected Vβ22 mutants by surface plasmon resonance
(A) SPR-based binding analysis for the interaction between immobilized recombinant, SEA and PS5-1 soluble protein. Non-linear regression analysis of maximal response versus concentration is depicted. Binding affinity constant for the interaction is indicated. (B) SPR sensorgram for the interaction between immobilized recombinant, SEA and affinity-matured Vβ22 mutant, FL. On-rates (k_{on}) and off-rates (k_{off}) of the interaction were used to calculate the binding affinity constant for the interaction, as shown.

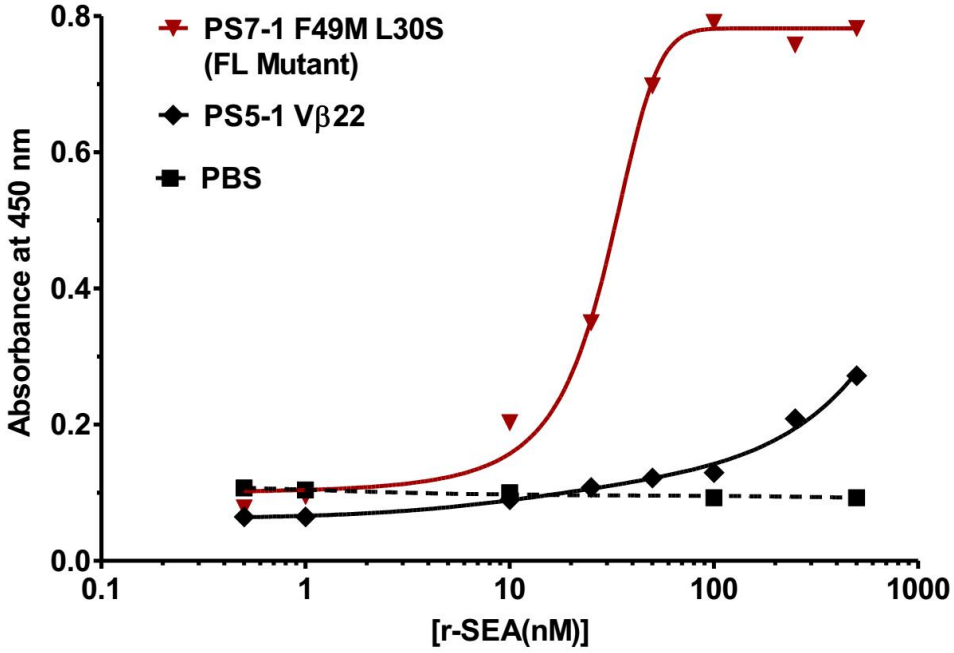

Fig. 2.24. Capture ELISA for detection of SEA
Soluble Vβ22 mutant proteins (PS5-1 or FL) were coated on the wells of ELISA plates at 5μg/ml. These were used to capture various concentrations of recombinant SEA (r-SEA). Bound SEA was detected with anti-SEA antibody (whole antiserum, rabbit), followed by goat anti-rabbit IgG-HRP.

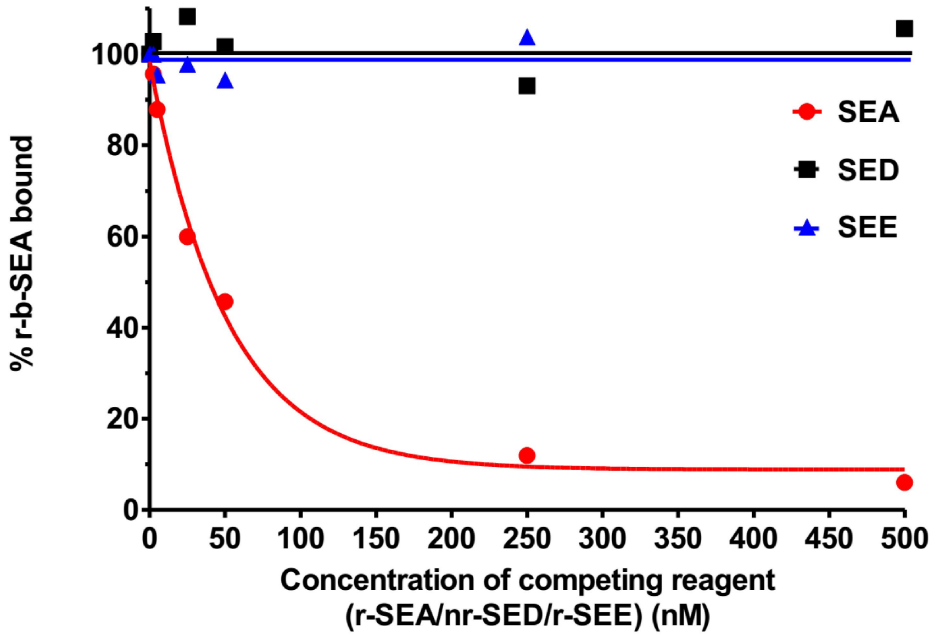

Fig. 2.25. High-affinity Vβ22 mutant FL does not cross-react with related toxins SED and SEE

Induced yeast cells expressing FL protein on the surface were incubated in a mixture of 100 nM recombinant, biotinylated-SEA (r-b-SEA) and various concentrations of non-biotinylated SEA, SED and SEE. Bound, biotinylated SEA was detected using streptavidin-Alexa Fluor 647 conjugate. Median florescence units (MFU) were recorded. % biotinylated-SEA bound was calculated as $100*(MFU_{(experiment)} - MFU_{(negative\ control)})/(MFU_{(positive\ control)} - MFU_{(negative\ control)})$, and plotted against concentration of competing reagent to generate the curve shown.

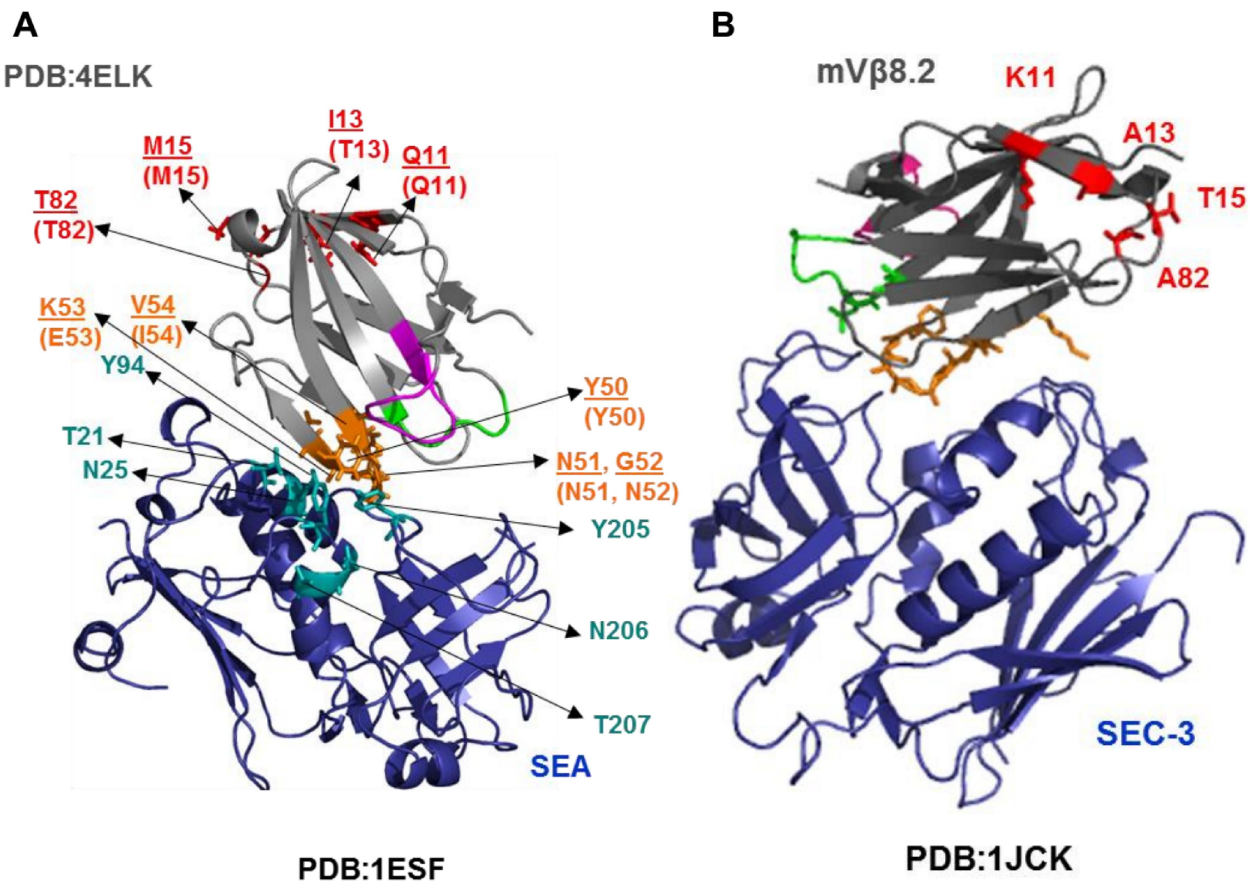

Fig. 2.26. Structural analysis of specific residues in superantigen:Vβ interactions
In panel A, the SEA crystal structure (blue) was manually docked with mouse Vβ16 crystal structure (gray) (PDB: 4ELK), that is 66% identical to human Vβ22 protein sequence. mVβ16 residues in the structure are underlined, while the corresponding residues in *wt* hVβ22 are indicated in parenthesis. The residues indicated in (red) correspond to the framework residues in Vβ22, which were mutated for protein stabilization. Wild type residues at the same location in other Vβ proteins (gray) which have been crystallized in complex with other superantigens (blue), are indicated in red in panels B, C and D. Putative TCR-binding residues of SEA are indicated in teal in panel A; these are proposed to contact residues in CDR2 (orange) of Vβ22, in the current study. For all superantigens, CDR1 is shown in green, CDR2 in orange and CDR3 in pink.

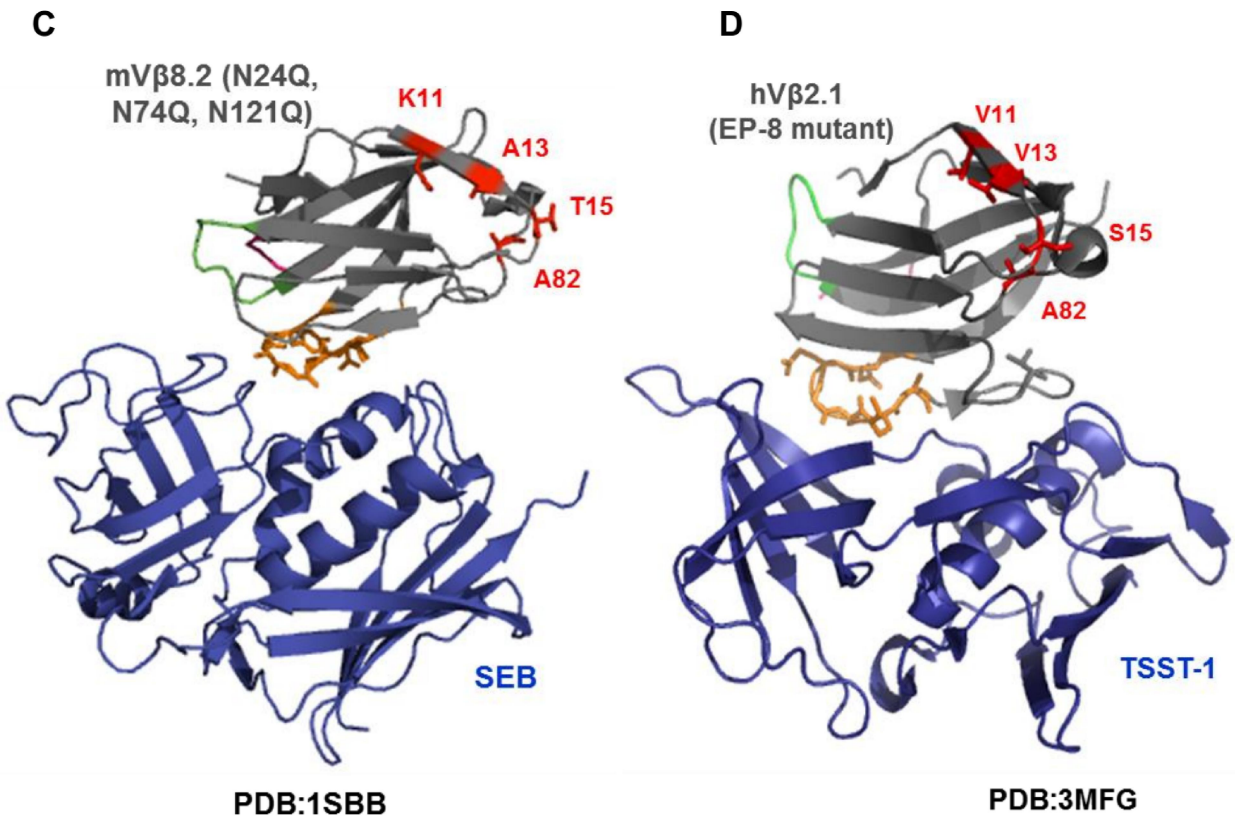

Fig. 2.26 (cont.). Structural analysis of specific residues in superantigen:Vβ interactions In panel A, the SEA crystal structure (blue) was manually docked with mouse Vβ16 crystal structure (gray) (PDB: 4ELK), that is 66% identical to human Vβ22 protein sequence. mVβ16 residues in the structure are underlined, while the corresponding residues in *wt* hVβ22 are indicated in parenthesis. The residues indicated in (red) correspond to the framework residues in Vβ22, which were mutated for protein stabilization. Wild type residues at the same location in other Vβ proteins (gray) which have been crystallized in complex with other superantigens (blue), are indicated in red in panels B, C and D. Putative TCR-binding residues of SEA are indicated in teal in panel A; these are proposed to contact residues in CDR2 (orange) of Vβ22, in the current study. For all superantigens, CDR1 is shown in green, CDR2 in orange and CDR3 in pink.

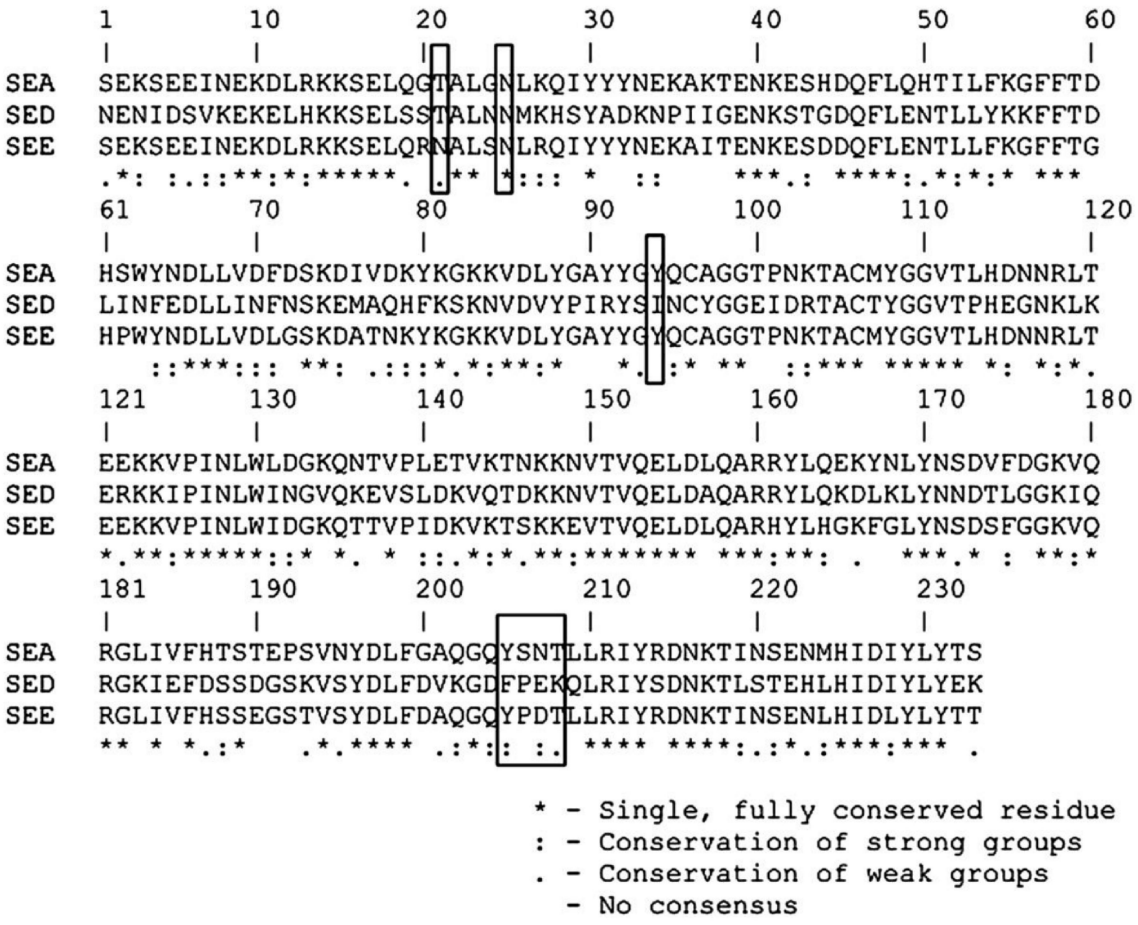

Fig. 2.27. Sequence alignment of SEA, SED and SEE
Multiple sequence alignment between sequences of SEA, SED and SEE toxins. Putative TCR binding residues of SEA are boxed.

TABLES

Table 2.1 . Classes of mutants obtained from Vβ22 error-prone library
Nine Vβ22 mutants were isolated from the error-prone library after sorting it five times. Four classes of mutants were established based on the mutations they contained. Representative mutants from each class which were analyzed in this work are underlined.

Class	Mutants	Location of mutations			
		FR1	CDR1	FR3	CDR3
1	PS5-1 PS5-3 PS5-5 PS5-8 PS5-9 PS5-10	T13A M15V		T82A	
2	PS5-2	T13A		T82A	L97Q
3	PS5-4	Q11L T13A	L30S		
4	PS5-7			D63G	

CHAPTER THREE

DEVELOPMENT OF A MULTIPLEX ASSAY FOR DETECTION OF STAPHYLOCOCCAL AND STREPTOCOCCAL TOXINS USING TWO-COLOR FLOW CYTOMETRY [3]

Introduction

As discussed in previous chapters, *Staphylococcus aureus* and group A *Streptococcus pyogenes* secrete a family of pyrogenic toxins including staphylococcal enterotoxins A, B, C (SEA, SEB, SEC), toxic shock syndrome toxin-1 (TSST-1) and streptococcal pyrogenic exotoxins (SpeA, SpeC) which act as superantigens (SAg), hence resulting in overstimulation of the immune system. These T-cell mediated reactions are associated with hyperinflammation and in some cases, organ failure or death. Accordingly, these toxins have been incriminated in sepsis, toxic shock syndrome (TSS), infective endocarditis, and skin conditions like atopic dermatitis etc. [2, 5, 114].

Some of the staphylococcal toxins are also associated with food poisoning. Although SEA has often been linked to food poisoning outbreaks [83-88], staphylococcal enterotoxin B, C, D, E and H have also been shown to be present in some cases [86, 115-118]. In the United States, it has been estimated that *Staphylococcus aureus* mediates approximately 240,000 food-borne illnesses per year [79]. Even if the organisms can be destroyed through a sterilization program, staphylococcal enterotoxins are heat stable and potent at consumption levels as low as a few hundred nanograms [84, 89]. As 20 to 30% of humans carry *S. aureus* as a commensal in their skin, its dissemination into foods because of improper handling is a risk factor for food-borne illnesses, compounded by issues associated with improper storage which allows that can allow

[3] Sections of this chapter were submitted to PLOS ONE journal as a research article: Sharma P., Wang N., Chervin, A.S., Quinn C.L., Stone J.D., Kranz D.M. (2015) "A Multiplex Assay for Detection of Staphylococcal and Streptococcal Exotoxins".

growth of bacteria and subsequent production of enterotoxins [119]. Like *Staphylococcus aureus, Streptococcus pyogenes* colonizes human beings and also produces superantigenic toxins including SpeA, SpeC, SMEZ and SSA have also been linked with conditions like sepsis, streptococcal TSS, scarlet fever and guttate psoriasis [2, 120-122].

Given the involvement of the superantigen toxins secreted by *Staphylococcus aureus* and *Streptococcus pyogenes* in human illnesses, there has been considerable interest in the development of assays to detect either the toxin genes or proteins. An assay that could detect the presence of multiple superantigens in clinical samples or in the food supply would allow for improved diagnosis in patients with clinical signs of disease or for improved safety of food sources. Here I report the development of a method for multiplex detection of three staphylococcal (SEA, SEB, TSST-1) and two streptococcal toxins (SpeA and SpeC), which could be used for detecting toxins in food, in supernatants derived from blood cultures of *Staphylococcus aureus* and/or *Streptococcus pyogenes*, or directly in clinical samples.

Traditionally, PCR [123-125] and ELISAs using monoclonal and/or polyclonal anti-toxin antibodies [126, 127] have been the method of choice for toxin detection and identification. Anti-toxin antibodies were also used for toxin detection by double immunodiffusion, enzyme linked fluorescence assay (ELFA) [128] and flow cytometry [129]. Although PCR serves as a potential diagnostic method with high sensitivity, it does not provide information about the level of the toxins. For example, it is well known that different SAgs can vary in levels by orders of magnitude depending on post-transcriptional control [18]. In this regard, SEB and TSST-1 have been shown to be highly upregulated at the protein level compared to many other SAgs. Hence, methods that detect and quantitate the level of the pathogenic agent (i.e. the protein) provide a direct correlate of disease caused by that agent. In addition, whereas the bacterial organism can be at low levels or even absent, (e.g. due to clearance by the immune system), the toxins are extremely stable and can persist in tissues.

Several investigators have demonstrated that ELISAs can detect staphylococcal toxins with good sensitivity [130-132], although concerns have been raised due to non-specific proteins in bacterial culture supernatants (e.g. such as Protein A that binds to IgG or naturally occurring peroxidases in food) [128, 130]. Commercial kits based on ELISA and ELFA using anti-enterotoxin antibody or antibody fragments (Fab, “Fragment antigen binding”) are available with reported sensitivities for staphylococcal enterotoxins A-E of 0.25 to 1 ng/ml. To date, such assays are limited to analysis of individual toxins [116, 133].

In the present study, I took advantage of ultra-high-affinity detecting agents that have been individually engineered in our laboratory for high-affinity binding to SEA, SEB, TSST-1, SpeA and SpeC [33-35, 134]; [Wang & Kranz, Unpublished]. The detecting agents represented the extracellular domain (12kDa) of the normal receptor for the SAgs, the variable domain of the beta chain of the T-cell receptor (Vβ). The collection of five Vβ domains had been engineered, using yeast display and directed evolution, to have ~1,000- to 3 million-fold increases in affinity for the cognate toxins [100, 135]. In this chapter, these five high-affinity Vβ proteins (FL, G5-8, D10V, KKR and HGSM) were further engineered to contain a C-terminal peptide sequence that allowed site-specific biotinylation. The five biotinylated proteins were immobilized on streptavidin coated, fluorescent-labeled beads to enable high-affinity, specific binding to their respective SAgs. Bound SAgs were detected with commercially available polyclonal reagents, followed by fluorescent-labeled detecting agents. Individual assays for each toxin were developed (referred to as singleplex assays, hereafter), which allowed specific and sensitive detection (SD_{50}) at 400 pg/ml SEA, 3 pg/ml SEB, 25 pg/ml TSST-1, 6300 pg/ml SpeA and 100 pg/ml SpeC. These sensitivities were on the order of 4 to 80 fold higher than observed with standard ELISAs using the same reagents.

For comparison, direct coupling of the G5-8 protein to paramagnetic beads yielded a detection sensitivity of 125 pg/ml SEB in different food matrices [133]. I hypothesized that site-

specific biotinylation of high-affinity Vβ proteins would allow their immobilization on streptavidin pre-coated beads in an optimal orientation, thus improving the sensitivity. Indeed, the biotin approach yielded a 40-fold improvement to 3 pg/ml.

In order to detect and quantitate multiple toxins in the same sample, I also developed a multiplex format of the assay. Although this format showed reduced sensitivity due to higher noise associated with the use of multiple polyclonal agents, the sensitivities were still well within the range necessary for detection in food sources or for rapid detection of toxins in bacterial cultures. For example, the assay allowed specific detection and also quantitative determination of staphylococcal SAgs SEA, SEB and TSST-1 in supernatants derived from cultures of 18 strains of *Staphylococcus aureus*. Thus, these reagents and the flow cytometry-based platform can be used for simultaneous detection of these toxins in food sources, or culture supernatants of potential pathogenic strains of *Staphylococcus aureus* and *Streptococcus pyogenes*.

Materials and Methods

Cloning, expression, and purification of high-affinity Vβ proteins in E. coli

The genes encoding high-affinity Vβ proteins (FL, G5-8, D10V, KKR and HGSM) were cloned with a N-terminal 6X-His tag and a C-terminal Avitag (Avidity, LLC) in pET28a expression vector (Novagen), either including or excluding thrombin cleavage site between 6X His-tag and the Vβ sequence. For protein expression, Vβ containing pET28a constructs were transformed into *E.coli* BL21 (DE3) cells by heat shock method. Small scale cultures were induced for 4 hours at 37^0C with 1mM IPTG. Protein expression in the lysates of uninduced and induced cultures was analyzed on Coomassie brilliant blue stained, 4-20% SDS-PAGE gels. Inclusion bodies were harvested from induced BL21 cells lysed by microfluidizer, washed using cold buffer (20 mM Tris, pH 8.0; 2.5 mM EDTA) and stored at -80^0C.

For refolding, frozen aliquots of inclusion bodies were thawed to room temperature and solubilized with guanidine-HCl and β-mercaptoethanol. Solubilized inclusion bodies were analyzed on 4-20% SDS-PAGE gel and refolded by slow dilution. Refolded Vβ were purified using Ni-NTA agarose resin (Qiagen) followed by HPLC (Biocad Sprint), using a Superdex 200, size exclusion column (GE Healthcare), as described previously [33]. A gel filtration standard (Biorad) was used to track the purification of monomeric fractions of refolded, high-affinity Vβ proteins.

In vitro biotinylation of purified Vβ proteins

Monomeric fractions of refolded proteins were biotinylated at the specific lysine residue in the C-terminal Avitag sequence (GGGLNDIFEAQKIEWHE), using BirA enzyme (Avidity, LLC) overnight at 4°C. Excess biotin was removed and biotinylation buffer was exchanged to 1X PBS, pH=7.4 using Zeba spin columns (Thermo Fisher Scientific Inc). Biotinylation was assessed by incubating the proteins with streptavidin and analyzing their change in mobility ("gel-shift") on 4-20% polyacrylamide gels. Biotinylated and unbiotinylated proteins were quantified by BCA Protein Assay kit (Thermo Fisher Scientific Inc).

Pilot, singleplex assays for toxin binding by Vβ coated beads

Biotinylated, high-affinity Vβ proteins (KKR, D10V, HGSM, G5-8 and FL) were immobilized on fluorescent, yellow, polystyrene beads (P2, P6, P8, P10 and P12 respectively, $\lambda_{emission}$ = 525 nm) that contained covalent-linked streptavidin (Spherotech, Inc.) overnight at 4^0C. Once biotin-Vβ was immobilized on the beads, unbound protein was washed away and the Vβ immobilized-beads were incubated with 50 µl of 50 nM cognate, recombinant toxin solutions (SpeA, TSST-1, SpeC, SEB and SEA respectively) (Toxin Technology, Inc.) for 1.5-2 hours at 4^0C. After washing, biotin-Vβ beads were incubated with 50 µl of 1:100 or 1:1000 dilution of rabbit anti-toxin polyclonal antibodies from rabbit (anti-SpeA, Abcam; anti-TSST-1, Abcam; anti-SpeC, Abcam; anti-SEB, Pierce and anti-SEA, whole antiserum, Sigma-Aldrich respectively] for 45-60 minutes at 4^0C. After washing, the biotin-Vβ beads were incubated with 1:100 dilution of goat-anti rabbit IgG(H+L)

labelled with Alexa fluor 647 (Life Technologies). After 45-60 minutes, the beads were washed and bound toxins were detected by flow cytometry as an increase in signal in the appropriate fluorescence channel ($\lambda_{emission}$ of Alexa fluor 647= 688 nm) by Accuri C6 flow cytometer (BD Biosciences). The fluorescence emitted by the yellow beads themselves was also recorded ($\lambda_{emission}$ = 525 nm). 1X PBS + 2% BSA was used for diluting all reagents and washing the beads.

Cross-reactivity of Vβ proteins engineered from the same template proteins, towards non-cognate toxin in singleplex assays

For assessing cross-reactivity of KKR and G5-8 (both engineered from mVβ8.2) toward SEB and SpeA respectively, biotinylated KKR and G5-8 coated beads were incubated with either SpeA or SEB solution. After 60 minutes, the biotin Vβ-beads were washed and incubated with 1:100 dilution of rabbit anti-SpeA or anti-SEB. After 60 minutes, the beads were washed with 1:100 dilution of goat-anti rabbit IgG (H+L) labelled with Alexa-647. After washing, bead-bound toxins were detected as an increase in signal in fluorescence in appropriate fluorescence channel ($\lambda_{emission}$ of Alexa fluor 647= 688 nm) by flow cytometry. Since anti-SpeA couldn't detect SpeA bound to KKR coated beads efficiently and anti-SEB was found to contain antibodies that cross-reacted with the structurally similar SpeA, hence anti-SEB was used for SpeA detection in future experiments.

Similarly, for assessing cross-reactivity of D10V and HGSM (engineered from hVβ2.1) toward SpeC and TSST-1 respectively, biotinylated D10V and HGSM coated beads were incubated with various concentrations of either SpeC or TSST-1 solution. After 60 minutes, the biotin Vβ-beads were washed and incubated with 1:100 dilution of rabbit anti-SpeC or anti-TSST-1. After 60 minutes, the beads were washed followed by incubation with 1:100 dilution of goat-anti rabbit IgG (H+L) labelled with Alexa-647. After washing, bead-bound toxins were detected as an increase in signal in fluorescence in appropriate fluorescence channel ($\lambda_{emission}$ of Alexa fluor 647= 688 nm) by flow cytometry.

Comparing the efficiency of using fluorescently labeled, rabbit anti-toxin antibody versus unlabeled rabbit anti-toxin antibody for toxin detection

To prevent the interference that could be caused due to the fluorescent-goat-anti rabbit IgG reagent while detecting toxins in rabbit serum, and also to reduce the number of incubation steps in the assay, I attempted fluorescent-labeling of anti-TSST-1 and using it for TSST-1 detection. APEX™ Alexa Fluor® 647 Antibody Labeling Kit (Life Technologies) was used for covalently labeling anti-TSST-1 antibody with Alexa Fluor® 647 dye at its primary amine residues through succinimidyl ester linkage.

For comparing unlabeled or labeled anti-TSST-1 in detection of TSST-1, biotinylated D10V coated beads were incubated with various concentrations of TSST-1. After 60 minutes, the beads were washed and incubated with 1:100 dilution of rabbit anti-TSST-1 (either unlabeled or labeled with Alexa-647). After 60 minutes, washed beads were incubated with either 1:100 dilution of goat-anti rabbit IgG (H+L) labelled with Alexa-647 or buffer (1X PBS + 2% BSA). After 60 minutes, the beads were washed and bound TSST-1 was detected as an increase in signal in fluorescence in appropriate fluorescence channel ($\lambda_{emission}$ of Alexa fluor 647= 688 nm) by flow cytometry.

Detection of TSST-1 in pooled, human serum by singleplex assay

To assess if this strategy could be used in detecting toxins in serum, biotinylated D10V coated beads were added to various dilutions of TSST-1 prepared in 0, 0.1, 1 and 10% pooled, human serum (Sigma-Aldrich). After 60 minutes, the beads were washed and incubated with 1:100 dilution of rabbit anti-TSST-1. After 60 minutes, washed beads were incubated with 1:100 dilution of goat-anti rabbit IgG (H+L) labelled with Alexa-647 or buffer (1X PBS + 2% BSA). After 60 minutes, the beads were washed and bound TSST-1 was detected as an increase in signal in fluorescence in appropriate fluorescence channel ($\lambda_{emission}$ of Alexa fluor 647= 688 nm) by flow cytometry.

Effect of varying coating density of biotin-Vβ proteins and biotin in the assay

Relative to the binding capacity of streptavidin beads, different amounts of biotin-Vβ (FL, G5-8, D10V, KKR and HGSM) were immobilized on streptavidin beads to determine optimum density of each biotin-Vβ on the bead surface that yielded minimum background and maximum sensitivity. Unbound proteins were washed away, and any unoccupied sites on Vβ coated, streptavidin beads were blocked with 7.5 mM free biotin (Sigma-Aldrich), to assess the effect of blocking on signal: noise in the assay. After washing, the beads were incubated with different concentrations of cognate, recombinant toxin solutions (SEA, SEB, TSST-1, SpeA and SpeC respectively). After 60 minutes, the beads were washed and incubated with 1:100 dilution of rabbit anti-toxin polyclonal antibodies (anti-SEA, anti-SEB, anti-TSST-1, anti-SEB and anti-SpeC respectively). After 60 minutes, the washed beads were incubated with 1:100 dilution of goat-anti rabbit IgG (H+L) labelled with Alexa fluor 647 (Life Technologies). After washing, toxins bound to the beads were detected as an increase in signal in fluorescence in appropriate fluorescence channel ($\lambda_{emission}$ of Alexa fluor 647= 688 nm) by flow cytometry.

Toxin binding titration with Vβ coated b*eads in singleplex format*

Biotinylated, high-affinity Vβ proteins (FL, G5-8, D10V, KKR and HGSM) were immobilized on streptavidin beads at optimum densities determined in preliminary experiments. Once biotin-Vβ was immobilized on the beads, unbound protein was washed away and any unoccupied biotin binding sites were saturated by incubation with 7.5 mM free biotin, which was 1000 times excess than the available biotin binding sites on the streptavidin beads. After blocking with excess biotin, Vβ immobilized-beads were washed and incubated with various concentrations of recombinant toxins (SEA, SEB, TSST-1, SpeA or SpeC). After 60 minutes, the beads were washed and incubated with 1:100 dilution of rabbit anti-toxin polyclonal antibodies (anti-SEA, anti-SEB, anti-TSST-1, anti-SpeC). In preliminary experiments, anti-SEB was found to contain antibodies that cross-reacted with the structurally similar SpeA, hence it was used for SpeA detection. After

washing, the biotin-Vβ beads were incubated with 1:200 dilution of goat-anti rabbit IgG(H+L) labelled with Alexa fluor 647 (Life Technologies). After 45-60 minutes, the beads were washed and bound toxins were detected by flow cytometry as an increase in signal in the appropriate fluorescence channel ($\lambda_{emission}$ of Alexa fluor 647= 688 nm). All assays with the five different Vβ proteins were quantitatively validated in singleplex format prior to use in multiplex format.

Toxin binding titration by high-affinity Vβ in capture ELISA

High-affinity Vβ proteins FL, G5-8, D10V, KKR and HGSM were immobilized on the wells of an ELISA plate at 5 µg/ml, overnight at 4^0C. Unbound proteins were washed away with 1X PBS + 0.1% Tween-20, and any unoccupied sites on the wells were blocked with blocking buffer (1X PBS + 1% milk). Vβ molecules immobilized on the wells were used to "capture" various concentrations of recombinant toxins (SEA, SEB, TSST-1, SpeA and SpeC respectively). After washing, 50 µl of 1:100 dilution of rabbit anti-toxin polyclonal antibodies (anti-SEA, anti-SEB, anti-TSST-1, anti-SEB and anti-SpeC respectively) were added to the wells, followed by washing and incubation with 1:2000 dilution of goat-anti rabbit IgG(H+L) labelled with HRP (Sigma-Aldrich). After washing the wells twice, TMB substrate (KPL, Inc.) was added and the colorimetric reaction catalyzed by HRP was allowed to proceed for ~ 2 minutes, after which it was stopped by addition of 1N H_2SO_4 to yield a yellow colored product whose absorbance was measured at 450 nm using a plate reader (Biorad). Toxin titrations were performed in duplicate, to determine sensitivity of toxin detection by each Vβ in capture ELISA format.

Toxin detection with mixtures of Vβ immobilized-beads in multiplex format

Biotinylated, high-affinity Vβ proteins (FL, G5-8, D10V, KKR and HGSM) were immobilized on individual fluorescent polystyrene beads (P12, P10, P6, P2 and P8 respectively, each having unique fluorescence in the FL-1 channel ($\lambda_{emission}$ of yellow beads= 525 nm) that contained covalently linked streptavidin (Spherotech, Inc.). After blocking with excess biotin, the Vβ immobilized-beads were washed, combined and incubated with various recombinant toxins at

different concentrations or culture supernatants from strains of *Staphylococcus aureus.* After 60 minutes, beads were washed and incubated with a mixture of rabbit anti-toxin polyclonal antibodies (1:100 dilution), followed by washing and incubation with 1:200 dilution of goat-anti rabbit IgG(H+L) labelled with Alexa fluor 647 (Life Technologies). After 45 minutes, the beads were washed and bound toxins were detected as an increase in signal in the appropriate fluorescence channel ($\lambda_{emission}$ of Alexa fluor 647= 688 nm), while the identity of the specific toxin was established by determining the fluorescent bead(s) (in the spectrally distinct, FL-1 channel; $\lambda_{emission}$ = 525 nm).

Culture of various strains of S. aureus

Eighteen strains of *S. aureus* used in this work were purchased from the Network on Antimicrobial Resistance in Staphylococcus aureus (NARSA), now BEI Resources (http://www.beiresources.org/). Strains were grown by Micromyx, LLC (Kalamazoo, MI) in Todd Hewitt Broth (THB) for 16-20 hours with shaking at 200 rpm at 37°C. After incubation, cultures were centrifuged at 5,000 x g for 10 minutes to pellet the cells. The supernatant was passed through a 0.2 µm filter to obtain cell free supernatant. Supernatants were stored at -20°C, prior to using in multiplex assays.

Results

Design of the bead-based two-color flow cytometry assay

The bead-based multiplex assay took advantage of a panel of streptavidin coated polystyrene beads (P2, P6, P8, P10, P12), each with distinct fluorescence intensities in FL-1 channel ($\lambda_{emission}$ = 525 nm) (Fig. 3.1). Each type of bead was used to immobilize a single, purified high-affinity Vβ protein with covalently linked biotin. The high-affinity Vβ proteins (FL, G5-8, D10V, KKR and HGSM) served to “capture” the specific toxin (SEA, SEB, TSST-1, SpeA and SpeC) against which they were engineered. KKR and D10V also have low affinities for the structurally

related SAgs SEB and SpeC, respectively [33-35, 134]; [Wang & Kranz, Unpublished]. The "captured", bead-bound toxins were detected by use of rabbit polyclonal anti-toxin antibodies followed by a fluorescent-labeled (Alexa fluor 647) goat-anti rabbit IgG.

The use of both the single Vβ agents and the polyclonal reagents each provided an opportunity for specificity in the assays. Two-color flow cytometry allowed the fluorescence emitted by the fluorophore within each class of beads ($\lambda_{emission}$ = 525 nm, FL-1 channel) to be distinguished from the fluorescence due to the bound toxin ($\lambda_{emission}$ = 688 nm, FL-4 channel). This design allowed identification of the toxin by association with the specific Vβ-immobilized bead, and quantification of the amount of toxin by the level of fluorescence from the Alexa fluor 647 reagent (Fig. 3.1, lower panel).

Cloning, expression, and purification of high-affinity Vβ proteins from E. coli

In order to generate bead-based arrays of high-affinity capture agents, the genes encoding six high-affinity Vβ proteins (FL, G5-8, L3, TSST-1, KKR and HGSM) (Fig. 3.2) were cloned with an N-terminal 6X-His tag for purification and a C-terminal 'Avitag' sequence (GGGLNDIFEAQKIEWHE) for enzymatic linkage of biotin to lysine. Initial cloning efforts involved cloning sequences encoding D10V and FL in pET28a as an NcoI and XhoI fragment, hence including a thrombin cleavage site between N- terminal 6X-His tag and Vβ sequence. In order to avoid removal of His tag from the proteins during storage, all Vβ sequences were later cloned excluding thrombin cleavage site. However, it was noted during test inductions as well as large scale expression in *E.coli* that the yield of G5-8 and L3 was reduced when thrombin cleavage site was absent, compared to when it was present between the 6X His-tag and the Vβ sequence (Fig. 3.3. 3.4, Table 3.1). The sequences encoding G5-8 and L3 were later cloned in pET28a including thrombin cleavage site between 6X His-tag and the Vβ sequence, which resulted in increases in the yield of inclusion bodies (Fig. 3.4, Table 3.1). Although the exact reason behind the differences in protein expression of G5-8 and L3 proteins in the presence or absence of thrombin cleavage

site was not explored, it could be because of instability of corresponding mRNA or protein sequence or ineffective transcription/translation processes.

High-affinity Vβ proteins purified as inclusion bodies from *E.coli* (Fig. 3.4) were subjected to refolding *in vitro*. Ni-affinity purified proteins were subjected to S200 gel filtration chromatography monomeric fractions of refolded Vβ (~15 to 18 kDa apparent mobility) were purified (Fig. 3.5). As evidenced in the chromatogram, D10V eluted as a mixture of primarily monomeric, but also dimeric species that presumably arose due to interactions between hydrophobic side chains of the two D10V molecules, which were noted to be 5Å apart in the crystal structure.

In vitro biotinylation of purified Vβ proteins

Monomeric fractions of purified Vβ proteins were concentrated and subjected to biotinylation by incubating with BirA ligase and 100 μM biotin. To estimate the fraction of Vβ protein that was biotinylated, a gel-shift assay was used. The assay took advantage of the observation that biotin remains bound to streptavidin (SAv) even under SDS-PAGE conditions. Over 80% biotinylation of each of the Vβ proteins was evidenced by the disappearance of the majority of the Vβ-biotin species (~15 kDa band) in the presence of SAv (Fig. 3.6). The emergence of a molecular weight species of approximately 70 kDa was presumably due to the migration of the Vβ-biotin (~ 15 kDa) complexed with tetrameric streptavidin (~ 55 kDa), which is structurally more compact (and hence migrates faster on SDS-PAGE) than the higher molecular weight bands (100-130 kDa) which could correspond to unbound streptavidin tetramers, or aggregates of streptavidin tetramers [136, 137].

To test that the biotinylated Vβ proteins could be immobilized on streptavidin beads, the proteins were incubated with streptavidin-coated beads at 4 ^{0}C, overnight. On the next day, the beads were centrifuged and the protein left in supernatant was analyzed on a 4-20% SDS-PAGE gel (Fig. 3.7). The decrease in amount of protein in the supernatant, compared with the initial

amount that was added to beads, indicated that the biotin-Vβ was indeed immobilized on streptavidin coated beads.

Pilot, singleplex assays for toxin binding by Vβ coated beads

In a pilot flow cytometry assay, Vβ-immobilized fluorescent beads (P2-KKR, P6-D10V, P8-HGSM, P10-G5-8 and P12-FL; $\lambda_{emission}$ of yellow beads = 525 nm; fluorescence measured in FL-1 channel) were incubated with 50 nM cognate toxin (SpeA, TSST-1, SpeC, SEB and SEA respectively), followed by washing and incubation with 1:100 or 1:1000 dilutions of rabbit anti-toxin polyclonal antibodies (anti-SEA, anti-SEB, anti-TSST-1, anti-SpeA and anti-SpeC respectively). After washing, the beads were incubated with 1:100 dilution of goat-anti rabbit IgG(H+L) labelled with Alexa fluor 647 ($\lambda_{emission}$ of Alexa fluor 647= 688 nm; measured in FL-4 channel). After washing, fluorescence emitted by the beads was measured in both FL-1 and FL-4 channels and analyzed on one-dimensional histograms as well as two-dimensional scatter plots (Fig. 3.8 and 3.9). Toxin binding by biotin-Vβ coated beads was detected as an increase in fluorescence in the FL-4 channel, compared to when no toxin was added to the beads (Fig. 3.8 and 3.9, right panel). As expected, the fluorescence in FL-1 channel (emitted by the beads themselves) was not affected by the presence or absence of toxin (Fig. 3.8 and 3.9, left panel). Since, fluorescent signal in FL-4 channel due to toxin binding was higher when 1: 100 dilution of anti-toxin antibodies was used, this dilution was used in future experiments in anticipation that it will lead to higher sensitivity.

It was also noted that the fluorescence signal arising due to SpeA binding by KKR coated beads was very weak compared to other Vβ coated beads binding to their cognate toxins (Fig. 3.8, top panel and Fig. 3.10, panel A). This probably was due to poor affinity of anti-SpeA preparation to SpeA. Owing to the structural similarity between SpeA and SEB, I predicted that polyclonal anti-SEB might contain antibodies that could cross-react with SpeA. Upon testing, flow cytometry experiments indicated that anti-SEB indeed contained antibodies that in fact bound

SpeA better than the anti-SpeA preparation (Fig. 3.10). Hence, polyclonal anti-SEB was used for SpeA detection in future experiments.

While testing for the presence of antibodies in polyclonal anti-SEB that could cross-react with SpeA, it was found that the anti-SEB also contained antibodies that could bind to the structurally related superantigen SEC3, although the binding to SEC3 was several fold lower than binding to SpeA (Fig. 3.11). Accordingly, SEC3 detection by L3 coated on P4 beads, was excluded from multiplex assays since a rabbit anti-SEC polyclonal antibody was not available. In addition, it was found that the fluorescence emitted by P4 beads overlapped with fluorescence emitted by P2 and P6 beads that would have further resulted in difficulties in establishing toxin identity.

Cross-reactivity of Vβ proteins engineered from the same template proteins, towards non-cognate toxin in singleplex assays

It has been previously demonstrated that G5-8 and KKR (both engineered from mVβ8.2 for binding with high affinity to SEB and SpeA respectively) cross-react at lower levels with SpeA and SEB, respectively (K_D ~ 5 nM and 68 nM respectively) [35]. This cross-reactivity was also observed in the assays when anti-SEB was used for detection of bound toxins, but not with anti-SpeA probably because the polyclonal anti-SpeA reagent used did not contain sufficient antibodies that bound to SEB (Fig. 3.10). Similarly, I also noted that D10V and HGSM (engineered for binding with high affinity to TSST-1 and SpeC respectively) exhibited cross-reactivity toward SpeC and TSST-1, respectively (Fig. 3.12), probably because TSST-1 and SpeC both bind to the same human Vβ region, Vβ2.1, and the fact that D10V and HGSM were both engineered from the human Vβ2.1 mutant EP-8 that binds to both SAgs [34]. However, as indicated in the histograms, TSST-1 binding by bead-bound D10V was at least 2000-fold higher than bead-bound HGSM. Similarly, SpeC binding by bead-bound HGSM was at least 200-fold higher than bead-

bound D10V (Fig. 3.12). Thus, a high degree of specificity could be realized at the expected physiological concentrations of these toxins.

Comparing the efficiency of using fluorescently labeled, rabbit anti-toxin antibody versus unlabeled rabbit anti-toxin antibody for toxin detection

During assay development, I attempted to directly label the rabbit anti-toxin antibody (here, anti-TSST-1) with a fluorophore (Alexa Fluor® 647 dye) to use it for toxin detection, (rather than the goat-anti rabbit IgG (H+L) labelled with Alexa-647). This modification in the assay would have not only reduced the time required for the assay, but would have allowed toxin detection in rabbit serum samples, since rabbits are often used in models of *S. aureus*. However, it was noted that the fluorescence signal arising due to TSST-1 binding by D10V coated beads was substantially reduced when fluorescent-labeled anti-TSST-1 was used compared to unlabeled anti-TSST-1, probably because of inefficient labeling and/or inactivation of the protein during the labeling reaction (Fig. 3.13). Because of this reduced sensitivity, direct fluorescent-labeled anti-toxin antibodies were not used further for toxin detection.

Detection of TSST-1 in pooled, human serum by singleplex assay

To assess if the assay could also be used for toxin detection in blood or serum samples, a singleplex assay was set up with biotin-D10V beads and anti-TSST-1 for detecting TSST-1 in various dilutions of TSST-1 prepared in 0, 0.1, 1 and 10% commercially available, pooled, human serum. It was noted that the sensitivity of TSST-1 detection was reduced by about 100 fold in 10% serum, compared to when TSST-1 dilutions were made in buffer (Fig. 3.14). The reduction in sensitivity was presumably due to pre-existing anti-TSST-1 antibodies in the serum [138, 139], which competed with bead-bound D10V for binding to TSST-1. With this method, ~10 ng/ml TSST-1 could be detected in undiluted pooled human serum indicating that the sensitivity of this assay would vary in human serum samples depending on the prior exposure of individuals to these toxins.

Effect of varying coating density of biotin-Vβ proteins and blocking with biotin

To study how the density of biotin-Vβ molecules on streptavidin bead surface would affect sensitivity of toxin detection, different amounts of biotin-Vβ molecules were immobilized on the bead surfaces. Such beads with different Vβ coating densities (1X, 2X or 5X, relative to the binding capacity of the beads) were then tested for binding to different concentrations of cognate toxins in singleplex assays. As indicated in figure 3.15, the signal arising due to toxin binding was often reduced when excess biotin-Vβ was added to the beads. It is possible that once the streptavidin binding sites on beads were saturated, excess Vβ molecules adsorbed non-specifically, or were present at low levels after washing. These weakly bound or free biotin-Vβ molecules could possibly compete for toxin binding with the bead-bound biotin-Vβ molecules, hence resulting in decreased signal.

To ensure that the polyclonal reagents used in the assays did not bind non-specifically to the bead surface, the bead surface was saturated with excess biotin (~1000 fold, compared to the binding capacity of the beads) after immobilizing biotin-Vβ molecules. Blocking of the unbound sites on bead surface with excess biotin resulted in a reduction in the background and an improvement in fluorescent signal due to toxin binding. Based on these experiments, optimum coating density of each biotin-Vβ was determined, and this along with blocking with excess biotin was used to obtain Vβ-coated beads with minimum background and maximum sensitivity of toxin detection.

Sensitivity of toxin detection in singleplex assays

After optimizing various parameters of the assays (e.g. concentrations of polyclonal reagents, biotin-Vβ coating densities on streptavidin bead surface, blocking with biotin etc.), each high-affinity Vβ was subjected to toxin binding titrations in singleplex, flow cytometry based assays for determining detection sensitivity for each toxin (Fig. 3.16 and 3.17). Each assay showed a dynamic range of over three orders of magnitude for determining concentrations of the specific

toxin. The range spanned the picogram to hundreds of nanograms per ml concentrations. Thus, each toxin detection assay exhibited linearity over a range of concentrations, which could be used to calculate concentrations of toxins in unknown samples (Fig. 3.18). As determined from the low end of the flow cytometry histograms (Fig. 3.16), the assay detection limits were approximately 400 pg/ml SEA, 3 pg/ml SEB, 25 pg/ml TSST-1, 6000 pg/ml SpeA and 100 pg/ml SpeC.

I compared the sensitivities of toxin detection in the flow-cytometry singleplex assays with a standard capture ELISA (where the Vβ proteins were adsorbed to 96-well plates, and detection was with the same polyclonal reagents as in the flow cytometry assay) (Fig. 3.19). Sensitivities of toxin detection by bead-based, singleplex/multiplex flow cytometry assays or by ELISAs, were calculated as the lowest toxin concentration at which the median fluorescence intensity or optical density was at least 3 standard deviations above the negative control. The detection limits in the capture ELISAs were 4 to 80 fold higher than in the flow cytometry assay (Table 3.2). I believe that the enhanced sensitivity is in part due to the greater surface density of properly arrayed Vβ domains on the beads compared to the adsorption of Vβ proteins, some in a non-binding configuration, to the wells of a 96-well microtitre plate. It is worth noting the lower sensitivity of SpeA detection in both the bead-based approach and in ELISAs, compared to all of the other toxins. I believe that this could have to do with the fact that I was unable to identify an optimal anti-SpeA polyclonal preparation and thus used a cross-reacting anti-SEB antibody preparation.

Sensitivity of toxin detection and cross-reactivity in multiplex assays

Given the remarkable sensitivity of toxin detection in singleplex assays, I examined the sensitivities when the five singleplex assays were combined to generate a multiplex assay. For assessing sensitivity of detecting each toxin in a multiplex assay, a mixture of biotin-Vβ coated beads were incubated with different concentrations of single toxin. After washing, bead-bound toxin molecules were detected with a mixture of polyclonal anti-toxin antibodies (Fig. 3.20). I noted that the sensitivity of toxin detection in multiplex assay reduced by 1 to 2 orders of magnitude

compared to the singleplex format, presumably due to the higher background "noise" associated with non-specific binding of Vβ-coated beads by the mixture of polyclonal antibodies (Table 3.3). The sensitivities of toxin detection by multiplex assay were approximately 10 ng/ml SEA, 0.1 ng/ml SEB, 0.1 ng/ml TSST-1, 10 ng/ml SpeA and 1 ng/ml SpeC, which were still within range for toxin detection in culture supernatants of *Staphylococcus aureus* strains (as described below).

SEA and SpeA multiplex detection assays exhibited linearity up to 100 ng/ml, while SEB, TSST-1 and SpeC detection assays exhibited linearity up to 10 ng/ml, which could be used for estimating concentrations (Fig. 3.21). As seen in singleplex assays, bead-bound KKR (P2-KKR) cross-reacted with SEB (Fig. 3.20). Similarly, P8-HGSM cross-reacted with TSST-1 and P6-D10V cross-reacted with SpeC. SEA detection in multiplex format was most specific, since no cross-reactivity of bead-bound FL protein with other toxins was detected in the assay.

Detection and quantitation of multiple toxins in a multiplex assay

In order to detect and quantitate multiple toxins in the same sample, multiplex assays with mixture of biotin-Vβ coated beads were performed. Solutions containing one toxin or combinations of two or more toxins were assayed in the multiplex format (Fig. 3.22 and 3.23). Although the maximum fluorescence intensity observed with individual detection system varied, the assay showed that in all cases the expected toxin was detected in the appropriate channel for that Vβ-immobilized bead.

Multiplex assay for detection of toxins in Staphylococcus aureus culture supernatants

To validate the use of this assay for detection of toxins in potential clinical isolates or other unknown sources (Table 3.4), 18 strains of *Staphylococcus aureus* from the NARSA repository were cultured. The strains were chosen based on the known SAg gene expression profiles of at least some of them. The multiplex assay was performed with diluted culture supernatants (diluted 1:4) from the 18 strains and the fluorescence intensity for each of the five Vβ systems was determined (Fig.3.24). Upon comparing the fluorescence intensity arising due to binding of

toxin(s) in supernatants with FL, G5-8 or D10V coated beads, approximate concentrations could be estimated based on linear regression using correlation curves shown in Fig. 3.21 (Table 3.5). In situations where fluorescence intensity was outside the linear range, estimation of toxin concentrations was performed using non-linear regression methods.

The results showed that 12 of the 18 strains expressed SEA, SEB and/or TSST-1 (note that some signal from KKR (Vβ-SpeA) was present when SEB was detected due to its cross-reactivity with SEB). SEB was expressed in four of the *S. aureus* strains (NRS100, NRS113, NRS114 and NRS387). TSST-1 was expressed in seven strains (NRS1, NRS2, NRS70, NRS111, NRS112, NRS651, and NRS701). Interestingly, five of the seven TSST-1 positive strains (NRS1, NRS2, NRS111, NRS112 and NRS651) also expressed significant levels of SEA. Estimated concentrations of toxins expressed in the supernatants of different strains ranged from 10 – 500 ng/ml, depending on the toxin (Table 3.5).

Discussion

The varied clinical effects of the superantigens produced by *Staphylococcus aureus* and *Streptococcus pyogenes* has prompted considerable effort in the development of assays for their detection in food sources or in clinical samples. The approaches have included DNA-based systems such as PCR for gene detection and use of antibodies as probes for detections of the toxins themselves [123-127]. While PCR can provide a rapid and sensitive method for confirming the presence of genes encoding the toxin gene, this approach requires an adequate number of bacterial cells and it does not provide information about the level of the toxins that are in a sample. For example, tissue-localized organisms could serve as a reservoir for the toxins that are released into the blood stream. Alternatively, cultures derived from a sterilized food source may be negative but the sample could contain preformed, heat stable enterotoxins. Hence, I propose methods that detect the clinically relevant agent, the toxins, are a preferred approach.

In this study, highly sensitive, singleplex assays were developed for detection of five staphylococcal and streptococcal toxins that have been associated with human disease. The assays made use of high-affinity, *in vitro* engineered probes (a variable domain of the TCR β chain) for each of the toxins. The singleplex assays were combined to yield a multiplex assay that allowed reliable detection of the toxins in a single sample, including from culture supernatants of various *S. aureus* strains.

The design of the singleplex assays involved the arraying of high-affinity Vβ proteins, using site-directed biotinylation. The streptavidin-bound Vβ domains served as a capturing agent for the toxin against which they were engineered [33-35, 135]; [Wang & Kranz, Unpublished]. Commercially available, polyclonal antibodies against the toxins served as the detecting agents.

By way of comparison, the assay used in the present study with biotinylated G5-8 coated streptavidin beads enabled detection of SEB at concentrations as low as 3 pg/ml in singleplex assay. This was 40 fold better than previous effort from our lab of detecting SEB where G5-8 was coated on paramagnetic beads by means of amine coupling [32] (0.125 ng/ml SEB in Tallent et al. 2013). I believe that the site-specific biotinylation of Vβ protein allowed its immobilization on streptavidin coated in an optimal orientation hence leading to improved sensitivity of toxin detection, than immobilizing Vβ via amine coupling methods which may have yielded heterogeneous orientations.

Another factor that I believe contributed to the high sensitivity of SEB detection in singleplex assay was the remarkably high affinity of the engineered G5-8 protein for SEB (K_D = 50 pM) [34]. In fact, the detection sensitivities for the other toxins in the singleplex assays, i.e. TSST-1 (25 pg/ml), SpeC (100 pg/ml), SpeA (6300 pg/ml) and SEA (400 pg/ml) also appeared to correlate to some extent with the affinities of the Vβ domains for their respective toxins: D10V (K_D = 50 pM), HGSM (K_D = 500 pM), KKR (K_D = 270 pM), and FL (K_D = 4 nM) (Table 3.6) [33,35,36]. I suggest that the exception, lower sensitivity of SpeA detection despite the relatively high affinity

of the KKR, was due to lack of a good, anti-SpeA polyclonal antibody, requiring us to use a cross-reacting anti-SEB polyclonal antibody for SpeA detection.

In addition to the contribution to the sensitivity of the singleplex assays, the use of two distinct toxin binding proteins (i.e., high-affinity Vβ proteins to capture the toxin and anti-toxin antibody to detect the "captured" toxin) provided additional specificity to the toxin detection. In multiplex assay, some expected cross-reactivities identified in the singleplex format, were noted for high-affinity Vβ proteins which were engineered from same template Vβ (KKR and G5-8 engineered from mVβ8 cross-reacted with SEB and SpeA respectively; HGSM and D10V engineered from hVβ2.1, cross-reacted with TSST-1 and SpeC respectively) (Fig. 3.20) [34, 35]

The flow cytometry-based assays described here can be used to detect toxins in food sources or in culture supernatants of *Staphylococcus aureus* and/or *Streptococcus pyogenes*, or in clinical samples. Enterotoxins like SEA in contaminated food sources have been shown to be present in the range from 0.05 to 20 ng/g of food [131, 140]. In foods isolated from food poisoning outbreaks, staphylococcal enterotoxins (particularly, SEA, SEE and SEH) were reported in the range of 0.08 to 0.5 ng/ml [83, 84] and 0.36-20 ng/g [83, 86, 87, 117] . Importantly, these studies required concentration steps for the food sample in order to detect and quantitate the levels of the toxins that were recovered. These assays reported assay sensitivities from ~ 0.1 - 0.5 ng/ml, similar to our singleplex assay for SEA (0.4 ng/ml SEA). However, our SEB and TSST-1 assays had sensitivities that were two orders of magnitude higher than these and other commercial assays [116, 128, 141, 142]. The possible linkage between SEA and TSST-1 expression among strains suggests that TSST-1 detection could be a biomarker for SEA, if the latter falls below the levels of detection.

More recently, highly automated, DNA based tests have been developed for rapid identification of microorganisms from blood cultures of patients [143, 144]. Since these tests also provide information about antibiotic resistance of the microorganism present, they could guide

appropriate antibiotic treatment for patients. However in situations where a patient's blood culture is negative for microorganisms, for example, in a case of deep tissue infection by *Staphylococcus aureus* or *Streptococcus pyogenes*, the patient could still develop shock-like or inflammatory symptoms that might arise due to the secretion of superantigenic toxins by the bacteria [145-147]. In such situations, or in cases when bacterial burden in blood is minimal, methods that detect the toxin directly could be useful.

In this study, 18 strains of *Staphylococcus aureus* obtained from the NARSA repository were also examined for toxin secretion. The collection included several strains that were isolated from clinical samples. The supernatants from these cultures were analyzed by multiplex assay for simultaneous detection of SEA, SEB and TSST-1. The expression of the toxins was consistent with the presence of genes in strains for which genomic data was available, as in the case of NRS1 (*entA* (SEA) and *tst* (TSST-1)), NRS70 (*tst* (TSST-1)) and NRS100 (*entB* (SEB)). NRS22 served as a negative control since it has been reported to lack the genes that encode SEA, SEB, and TSST-1. Complete absence of signal in five other strains (NRS382, NRS384, NRS667, NRS725, NRS741) supported the view that the assay was specific for the target toxins and did not yield false positives for unrelated proteins, such as Protein A expressed by *S. aureus* [128, 130].

I also noted that five of the seven strains that expressed TSST-1 also expressed SEA. This toxin expression profile was particularly interesting because previous reports have linked SEA co-expression with TSST-1 in menstrual TSS, more often than in non-menstrual TSS [148, 149]. In the collection of strains tested here, NRS112 (MN8) was isolated from a menstrual TSS patient and I detected both SEA and TSST-1 in the culture supernatant of this strain. Interestingly, other investigators detected the gene corresponding to SEA in this strain by PCR, but they could not detect the protein probably because the concentration of SEA secreted was very low [150].

The *S. aureus* strain NRS111 (FRI913) was obtained from a food poisoning outbreak, and it was thus not surprising that SEA was detected in the culture supernatant of this strain, since SEA has been incriminated in most *S. aureus* food poisoning outbreaks around the world [83, 84, 86-88]. I also detected TSST-1, which is not enterotoxic, although it could serve as a biomarker for the presence of *S. aureus* or possibly even SEA [4]. Investigators have confirmed the presence of *sea* and *tst* genes in this strain by PCR [151]. Our detection of SEB in NRS114 was also consistent with the presence of the *seb* gene by PCR [151].

In summary, I present here a sensitive flow cytometry-based assay for the detection of three staphylococcal and two streptococcal toxins using ultra-high-affinity Vβ proteins and polyclonal antibody reagents. Similar approaches can be used for the detection of other SAgs. Multiplex formatting of the assays, using beads with a range of fluorescent dyes, enabled simultaneous detection of SEA, SEB and TSST-1, in culture supernatants of several strains of *S. aureus.* I also reported that the multiplex assay could be used for detection of SpeA and SpeC toxins, for which no commercial assays are available yet.

FIGURES

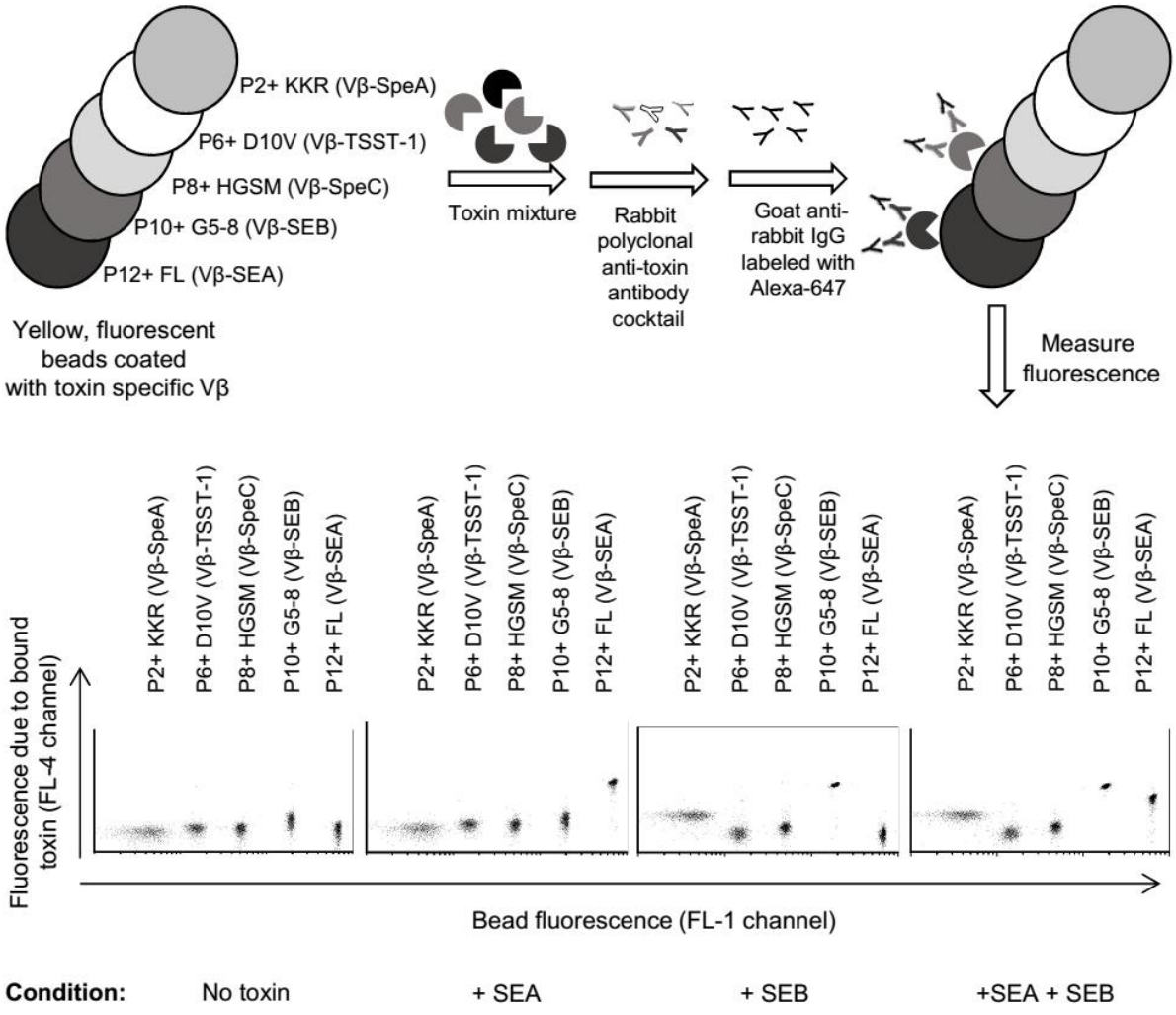

Fig. 3.1. Schematic representing the multiplex assay
Yellow, streptavidin beads (P2, P6, P8, P10, and P12 --- with distinct fluorescence intensities in FL-1 channel, $\lambda_{emission}$ = 525 nm) coated with biotinylated, high-affinity Vβ are added to an unknown solution, to determine the presence of SEA, SEB, TSST-1, SpeA and/or SpeC toxin. Polyclonal, rabbit anti-toxin antibodies bind to the toxins bound to the Vβ-coated beads; which are detected by goat-anti rabbit IgG labelled with Alexa fluor 647 (FL-4 channel, $\lambda_{emission}$ = 688 nm). Scatter plots in the presence or absence of toxin(s) are shown in the lower panel. An increase in fluorescence emitted by the beads in the FL-4 channel (Y-axis) indicates the presence of toxin(s) in the unknown sample. Since each class of beads emits distinct fluorescence in FL-1 channel (X-axis), identity of the toxin present is established by identifying the specific, Vβ-immobilized bead(s) undergoing an increase in fluorescence in the FL-4 channel (Y-axis).

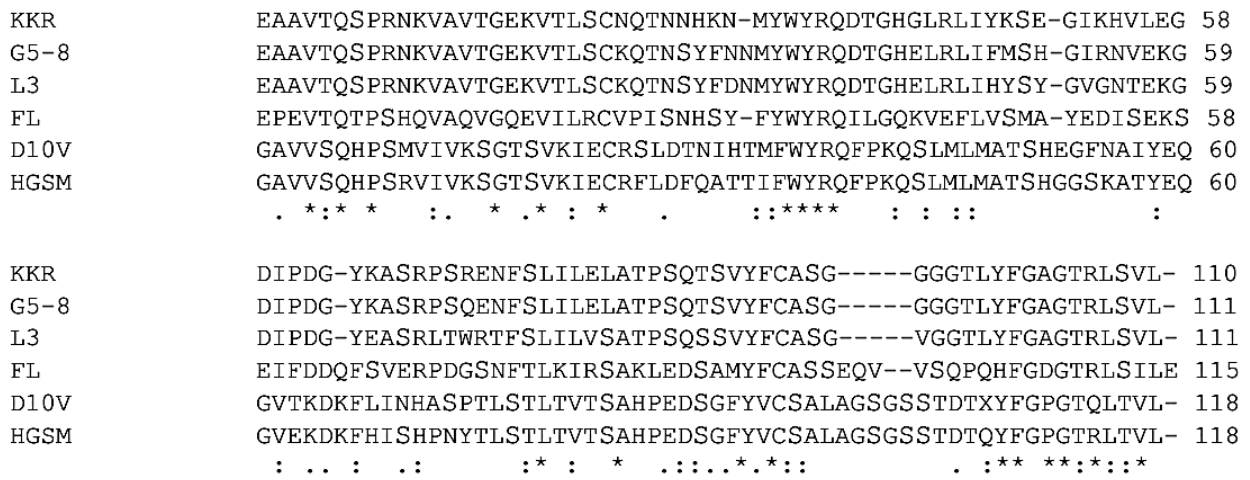

Fig. 3.2 Sequences of Vβ proteins engineered for high affinity towards staphylococcal and streptococcal toxins

Multiple sequence alignment between sequences of high-affinity Vβ proteins by Clustal 2.1 is shown. Genes encoding each high affinity Vβ proteins were cloned in pET28a vector with a N-terminal 6X His tag (which aided in affinity purification) and a C-terminal Avitag (which allowed site-specific biotinylation).

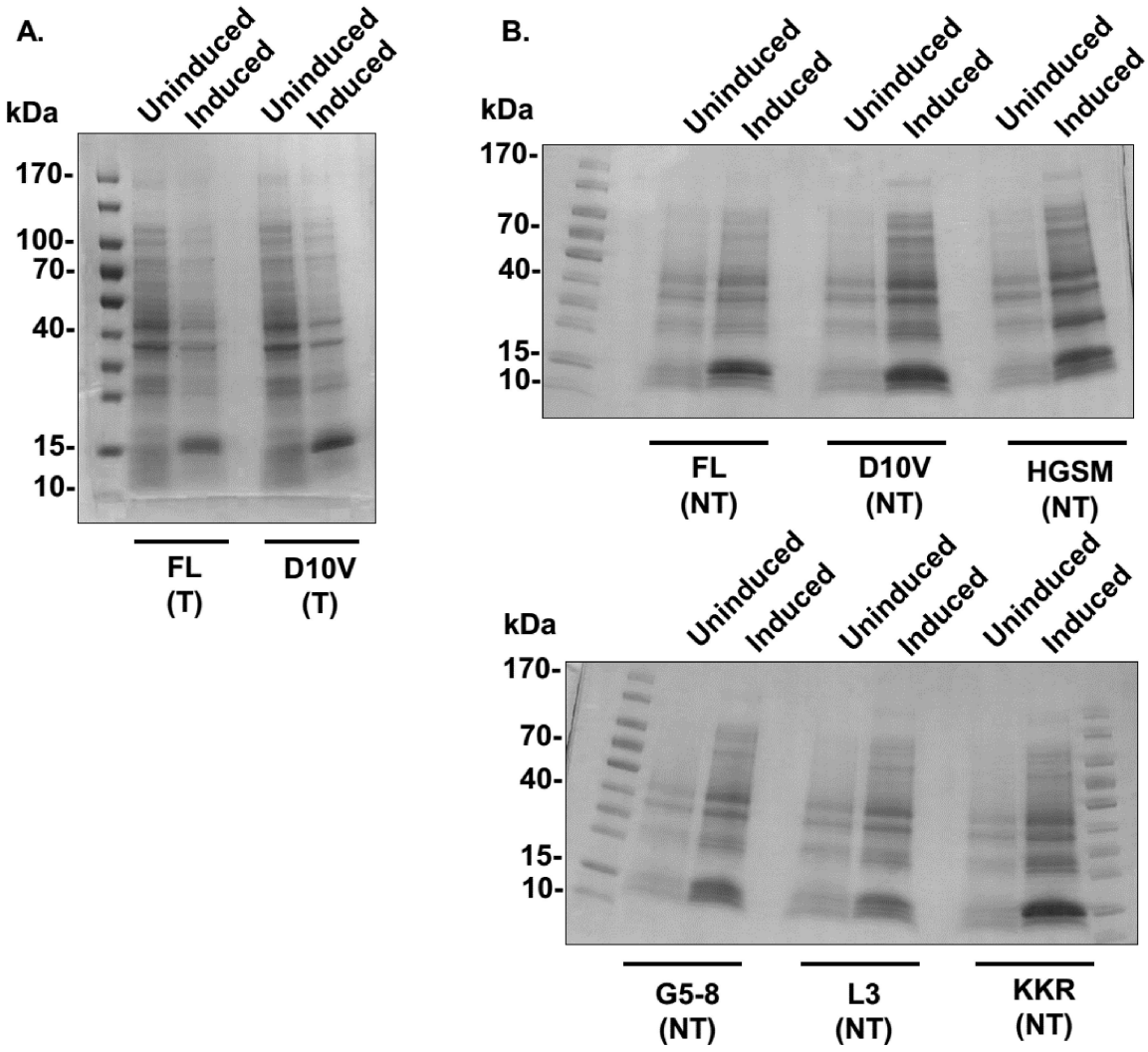

Fig. 3.3. Test inductions indicating expression of high-affinity Vβ proteins from pET28a constructs

Genes encoding high-affinity Vβ proteins were cloned in pET28a in two formats: (A) with thrombin cleavage site (T) between 6X His-tag and the Vβ sequence; (B) without thrombin cleavage site (NT) between 6X His-tag and the Vβ sequence. Transformed *E.coli* BL21 (DE3) cells were cultured for 4 hours, followed by induction for 4 hours with IPTG. Lysates of induced and uninduced cultures were analyzed on 4-20% SDS-PAGE gels for assessing protein expression.

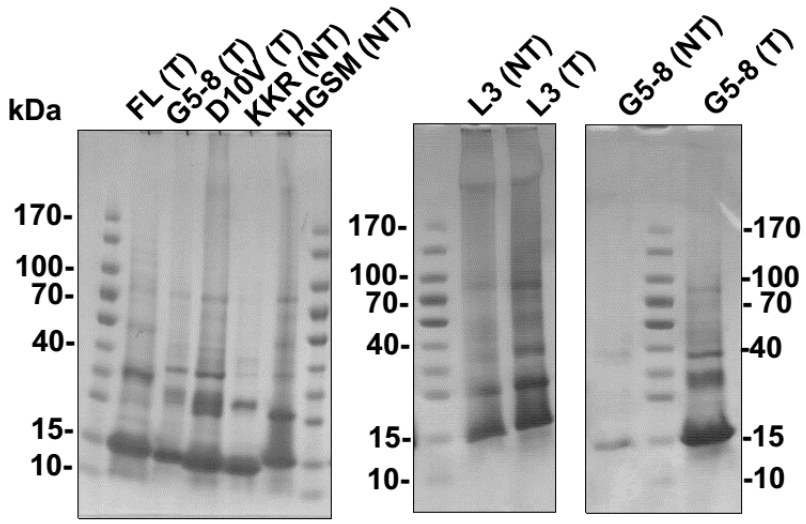

Fig. 3.4. Large scale expression of high-affinity Vβ proteins as inclusion bodies, from *E.coli*
High-affinity Vβ proteins were expressed as inclusion bodies in *E.coli* transformed with pET28a containing either thrombin cleavage site (T) between 6X His-tag and the Vβ sequence; or without thrombin cleavage site (NT) between 6X His-tag and the Vβ sequence. Solubilized inclusion bodies were analyzed on a 4-20% SDS-PAGE gel.

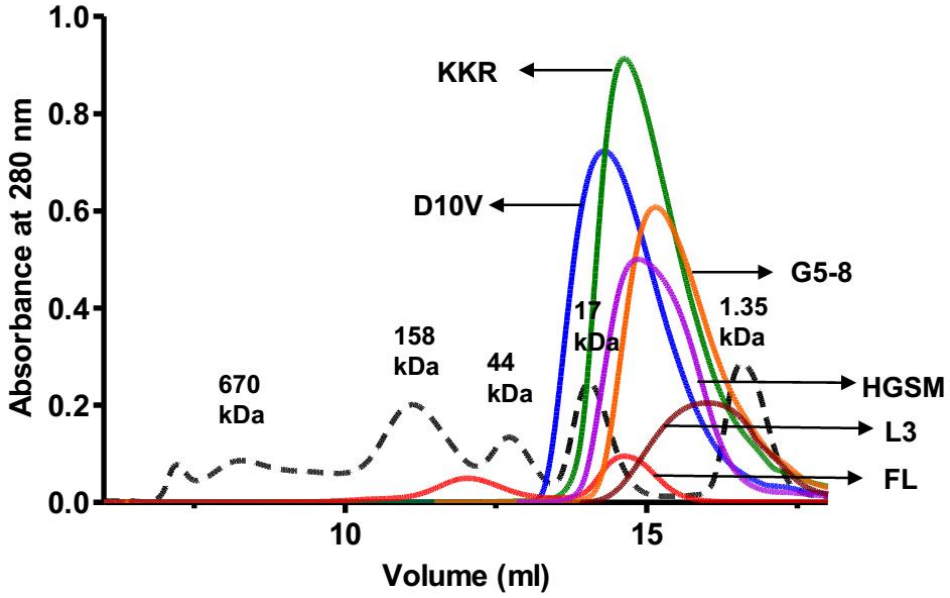

Fig. 3.5. Size exclusion chromatograms of refolded, high-affinity Vβ proteins
In vitro refolded, high-affinity Vβ proteins were purified by affinity chromatography with Ni agarose; followed by size exclusion chromatography using a S200 column. Molecular weight standards (dashed line) was used to track the purification of monomeric fractions of refolded, high-affinity Vβ proteins.

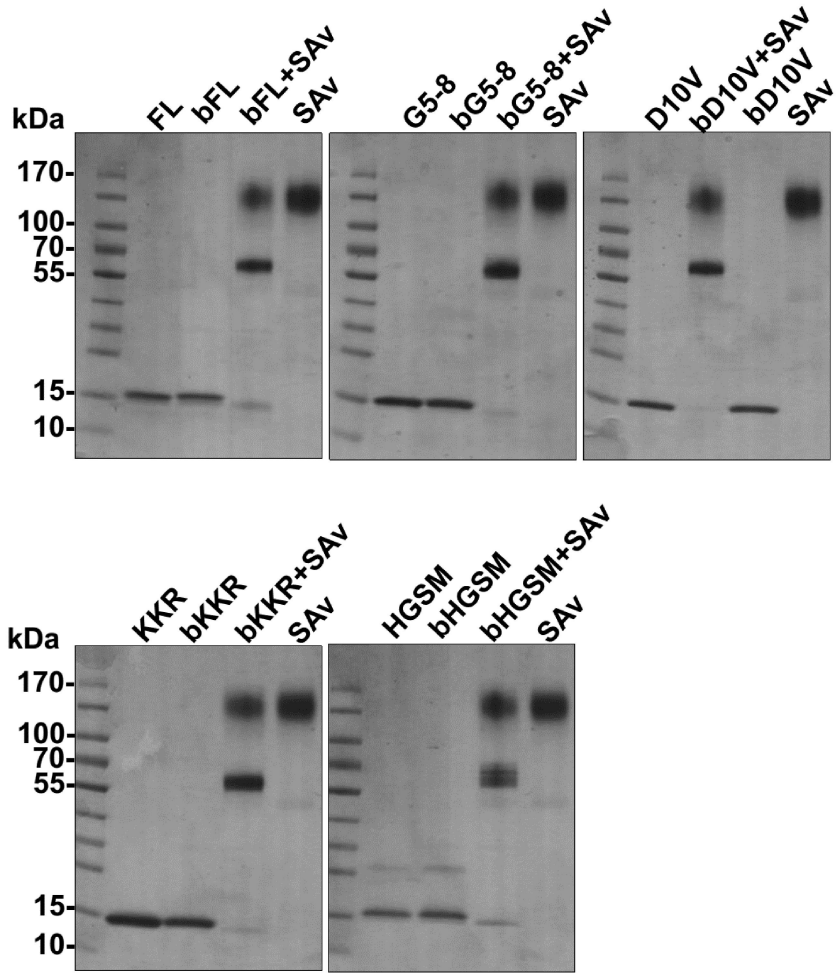

Fig. 3.6. Gel-shift assay for assessing biotinylation of high-affinity Vβ proteins on SDS-PAGE

Monomeric fractions of high-affinity Vβ proteins were biotinylated at a specific lysine residue in Avitag sequence *in vitro*, by BirA enzyme. Biotinylation was assessed by analyzing change in mobility of biotinylated-Vβ (~15 kDa band), in the presence or absence of streptavidin (SAv) on 4-20% SDS-PAGE gels.

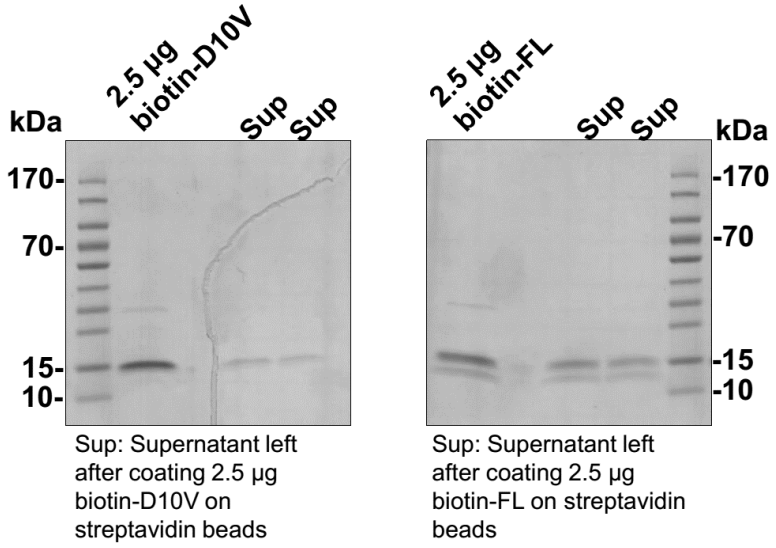

Fig. 3.7. SDS-PAGE gels for assessing immobilization of high-affinity Vβ proteins on streptavidin beads

2.5 µg of biotinylated D10V or FL protein was added to streptavidin beads and incubated overnight. Next day, supernatants (Sup) left from the reaction were loaded on a 4-20% SDS-PAGE gels and compared with an equivalent amount of biotinylated protein. Reduction in intensity of biotin-Vβ band in “Sup” lanes indicated biotin-Vβ was immobilized on streptavidin beads.

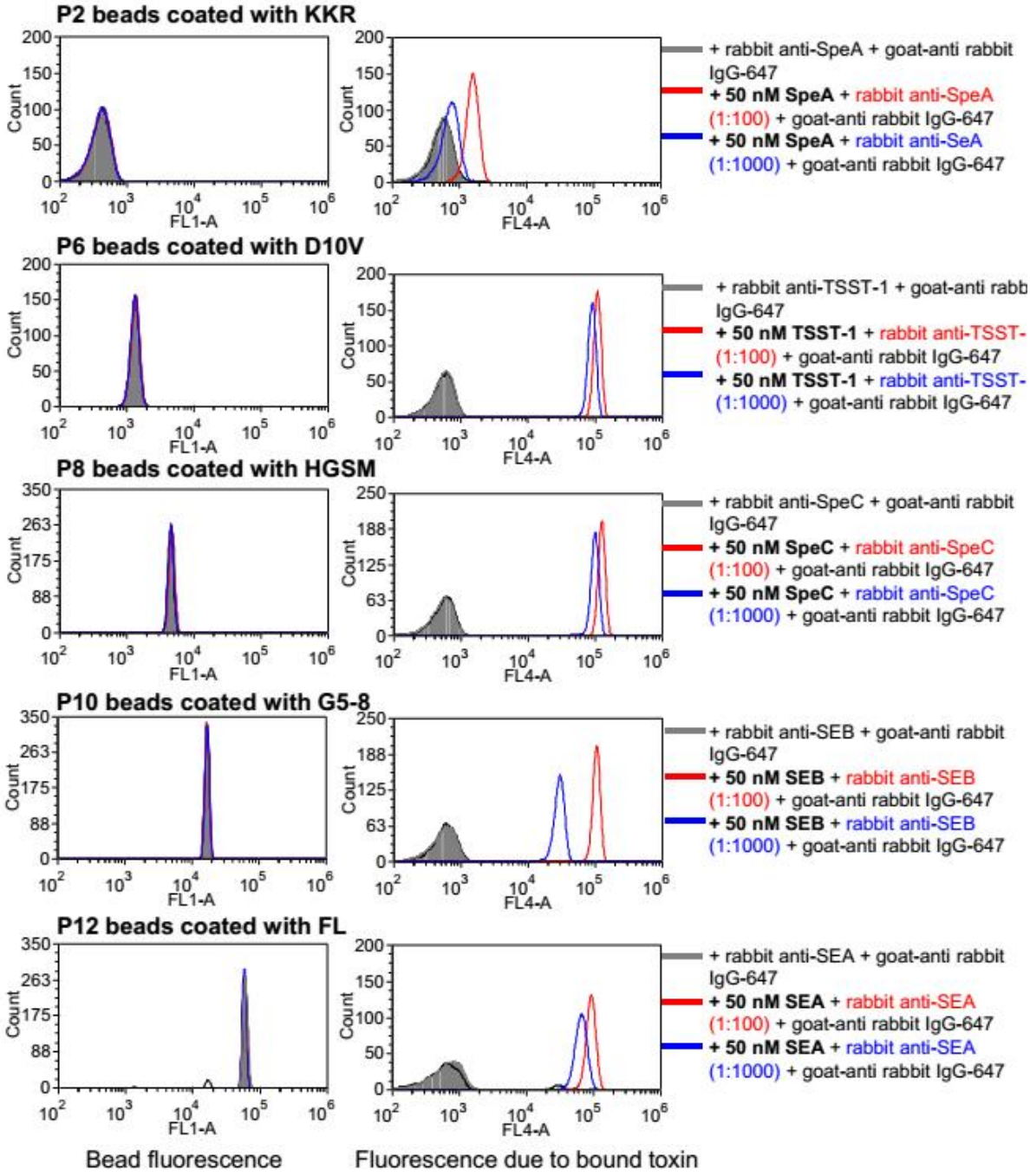

Fig. 3.8. Pilot singleplex assays for detecting binding of high-affinity Vβ proteins to the toxins against which they were engineered

Biotinylated, high-affinity Vβ proteins coated fluorescent streptavidin beads, were incubated with 50 nM toxin against which they were engineered. Bound toxin was detected by rabbit anti-toxin polyclonal antibodies, followed by goat-anti rabbit IgG(H+L) labelled with Alexa fluor 647. Fluorescence in the absence of toxin, is represented by gray (filled) trace on each histogram.

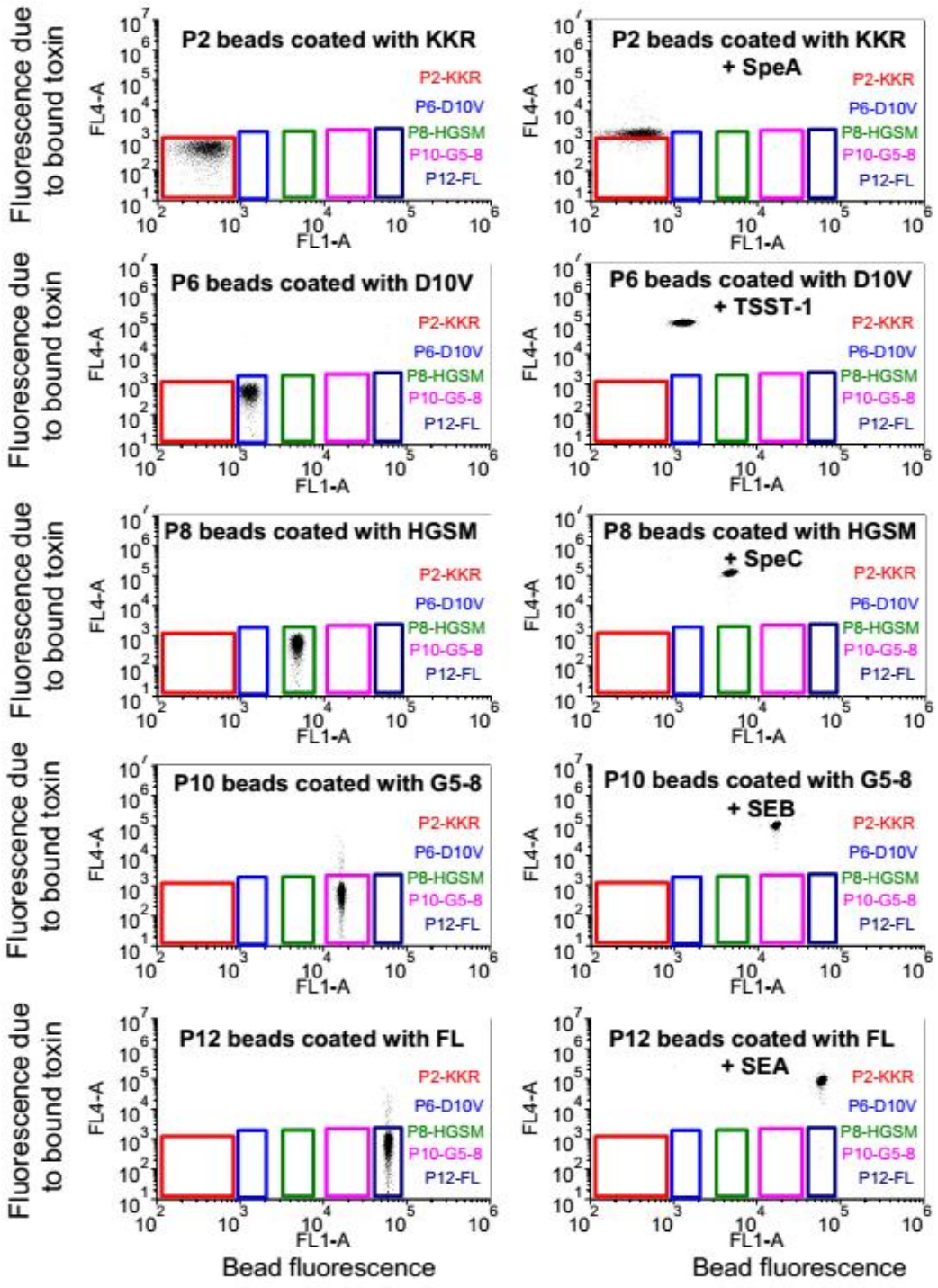

Fig. 3.9. Pilot singleplex assays for detecting binding of high-affinity Vβ proteins to the toxins against which they were engineered

Biotinylated, high-affinity Vβ proteins coated fluorescent streptavidin beads, were incubated with 50 nM toxin against which they were engineered. Bound toxin was detected by rabbit anti-toxin polyclonal antibodies, followed by goat-anti rabbit IgG(H+L) labelled with Alexa fluor 647. Two-dimensional scatter plots are shown, with fluorescence arising from beads on X-axis, and fluorescence arising due to toxin binding on Y-axis.

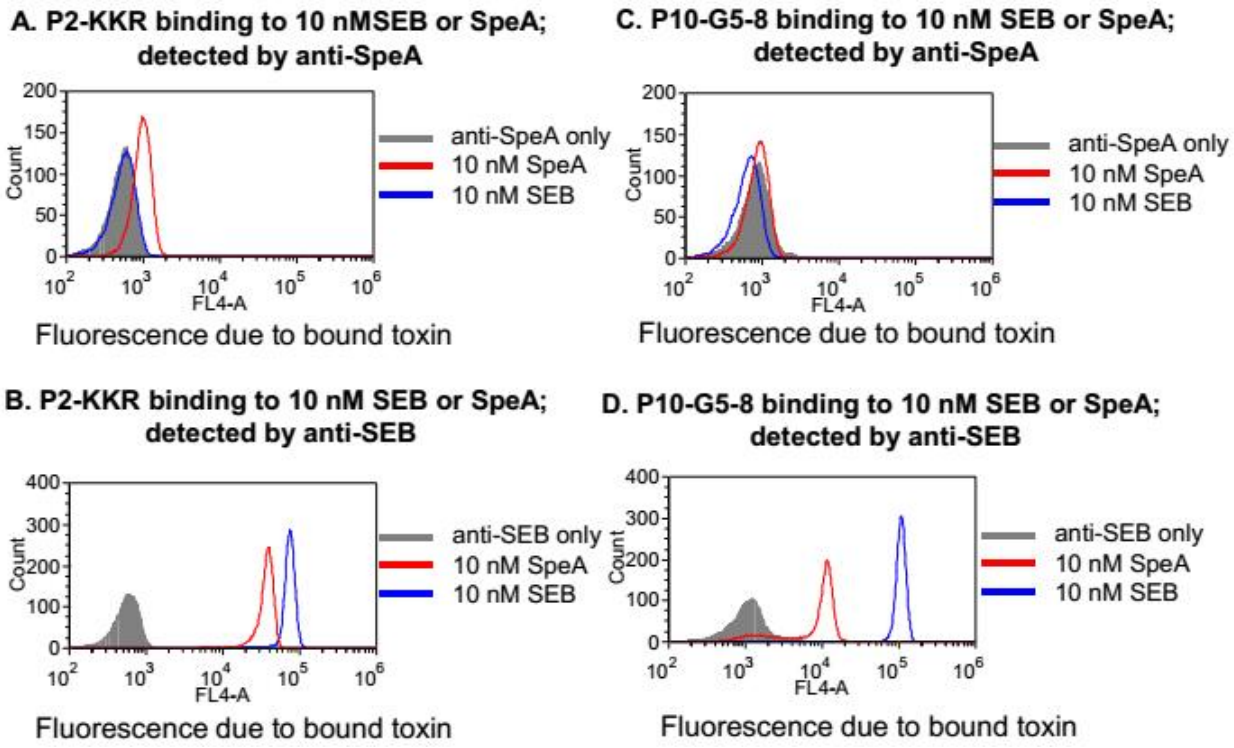

Fig. 3.10. Cross-reactivity of high-affinity Vβ proteins engineered from mVβ8.2, KKR and G5-8, to SEB and SpeA respectively

Cross-reactivity of KKR to SEB, and G5-8 to SpeA was detected when anti-SEB was used to detect toxin binding (panels B & D), but not with anti-SpeA (panels A & C). Flow cytometry histograms for binding are shown. Fluorescence in the absence of toxin, is represented by gray (filled) trace on each histogram.

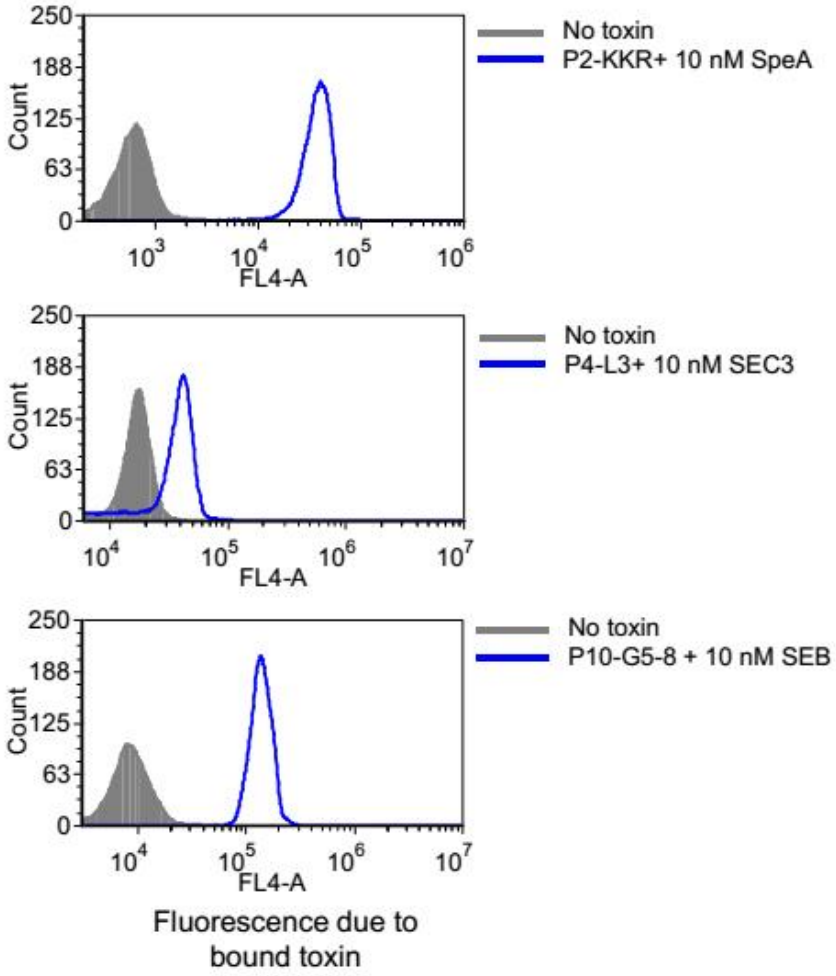

Fig. 3.11. Binding of mVβ8.2 derived, high-affinity proteins (KKR, L3, G5-8) to cognate toxins (SpeA, SEC3, SEB) can be detected using anti-SEB

KKR, L3 and G5-8 were coated on individual, fluorescent streptavidin beads, followed by incubation with 10 nM SpeA, SEC3 and SEB respectively. Bound toxin in each case was detected as an increase in fluorescence, upon incubation with rabbit anti-SEB antibody, followed by washing and incubation with goat-anti rabbit IgG labelled with Alexa-647. Fluorescence in the absence of toxin, is represented by gray (filled) trace on each histogram. *** Note that the fluorescence in the absence of toxin is different for each Vβ, indicating that anti-SEB antibody (polyclonal) exhibited different degree of non-specificity towards each Vβ.

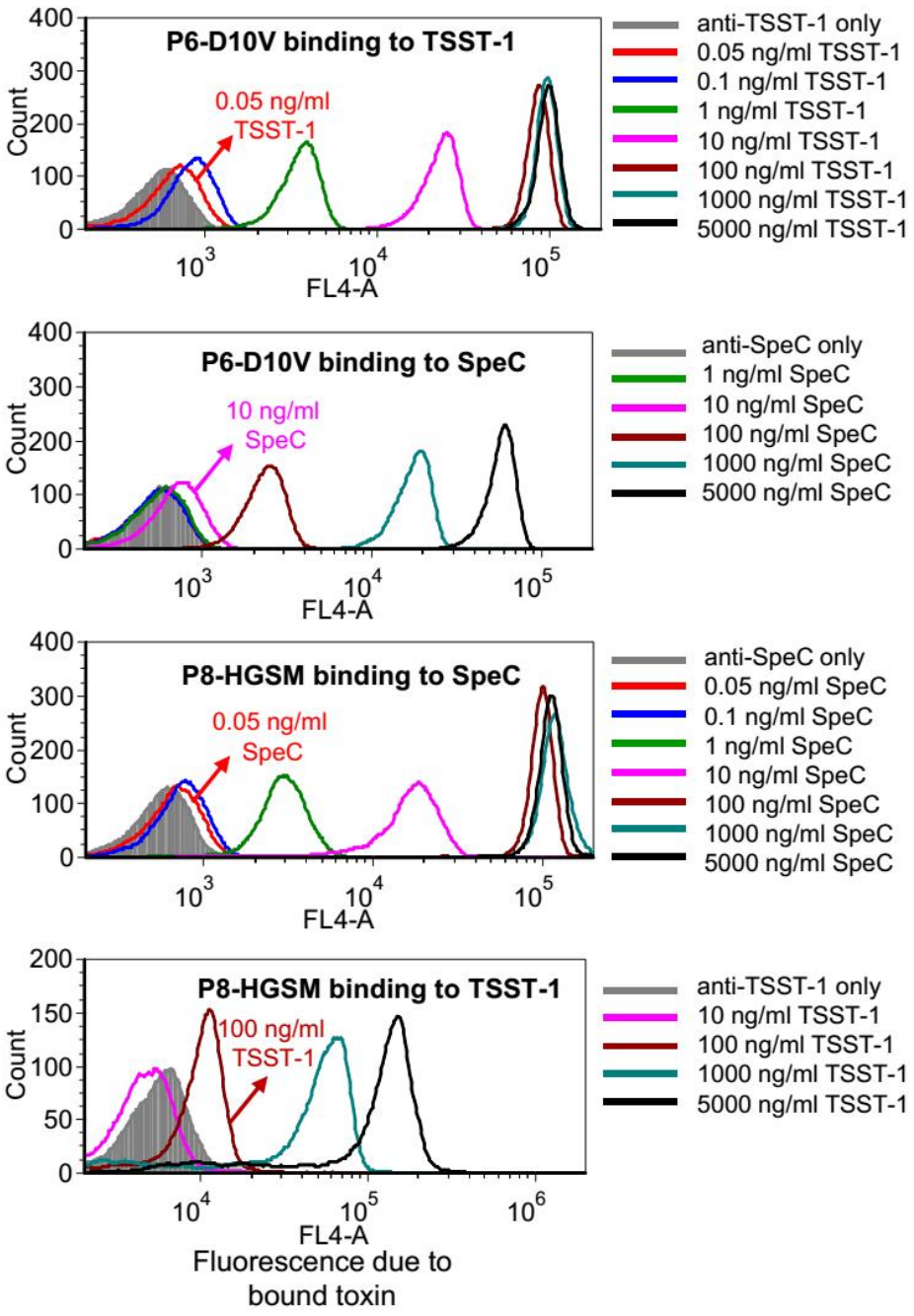

Fig. 3.12. Cross-reactivity of high-affinity Vβ proteins engineered from hVβ2.1, D10V and HGSM, toward SpeC and TSST-1 respectively

D10V and HGSM were coated on individual, fluorescent streptavidin beads, followed by incubation with various concentrations of TSST-1 or SpeC. Bound toxin was detected as an increase in fluorescence, upon incubation with rabbit anti-TSST-1 or anti-SpeC antibody, followed by goat-anti rabbit IgG labelled with Alexa-647. Fluorescence in the absence of toxin, is represented by gray (filled) trace on each histogram.

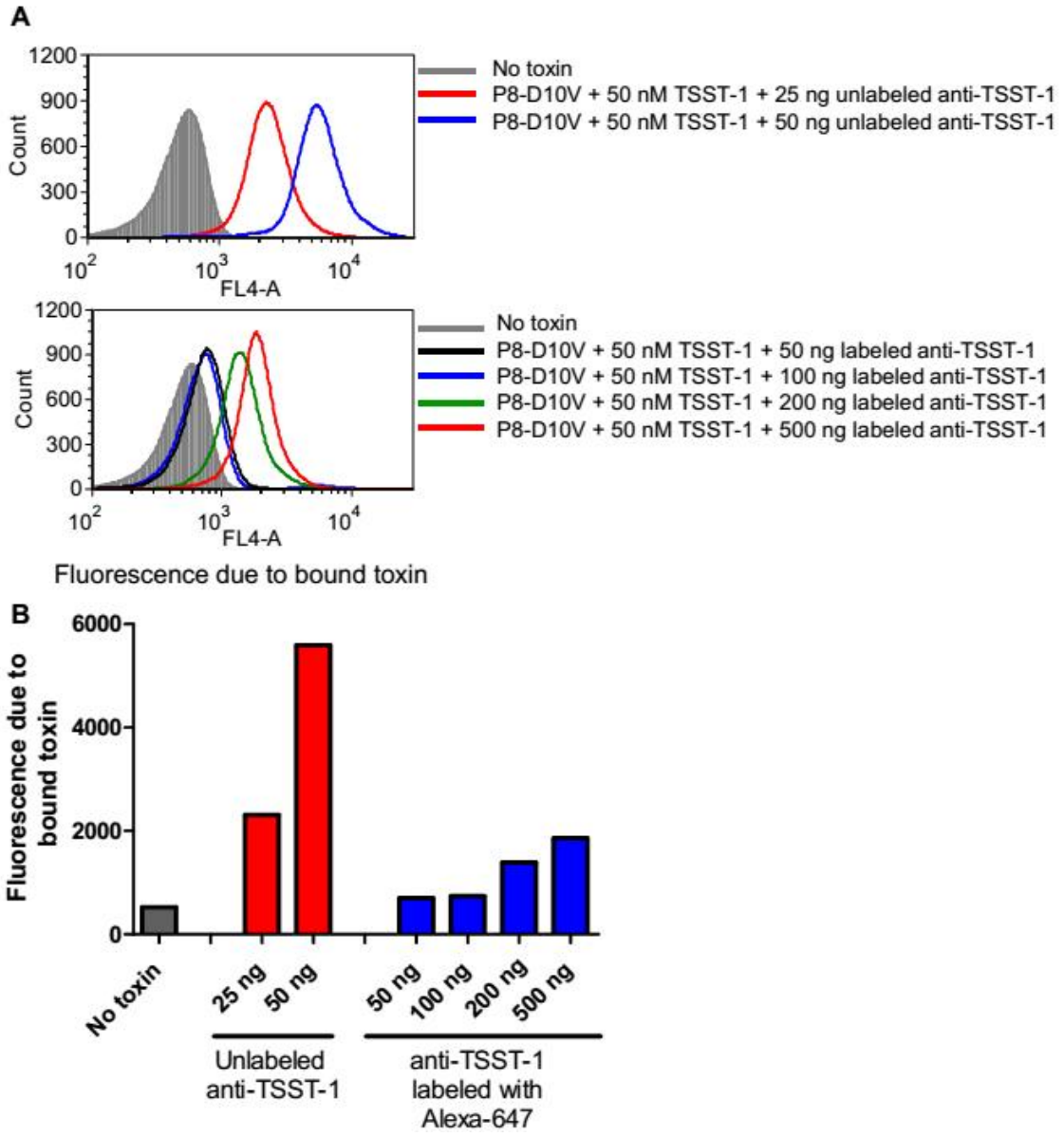

Fig. 3.13. Comparing the efficiency of using fluorescently labeled, rabbit anti-toxin antibody (anti-TSST-1 here), versus unlabeled, rabbit anti-toxin antibody for toxin detection in singleplex assay

(A) D10V coated P8 beads were added to different concentrations of TSST-1. Bound toxin was detected as an increase in fluorescence, upon incubation with unlabeled anti-TSST-1 antibody (rabbit), followed by goat-anti rabbit IgG labelled with Alexa-647; or with anti-TSST-1 antibody labeled with Alexa-647. Flow cytometry histograms for TSST-1 binding are shown. Fluorescence in the absence of toxin, is represented by gray (filled) trace on each histogram. (B) Comparison of efficiency of TSST-1 detection by fluorescently labeled anti-TSST-1 versus unlabeled anti-TSST-1 antibody. Median fluorescence units from the histograms above, were used to generate the bar graph.

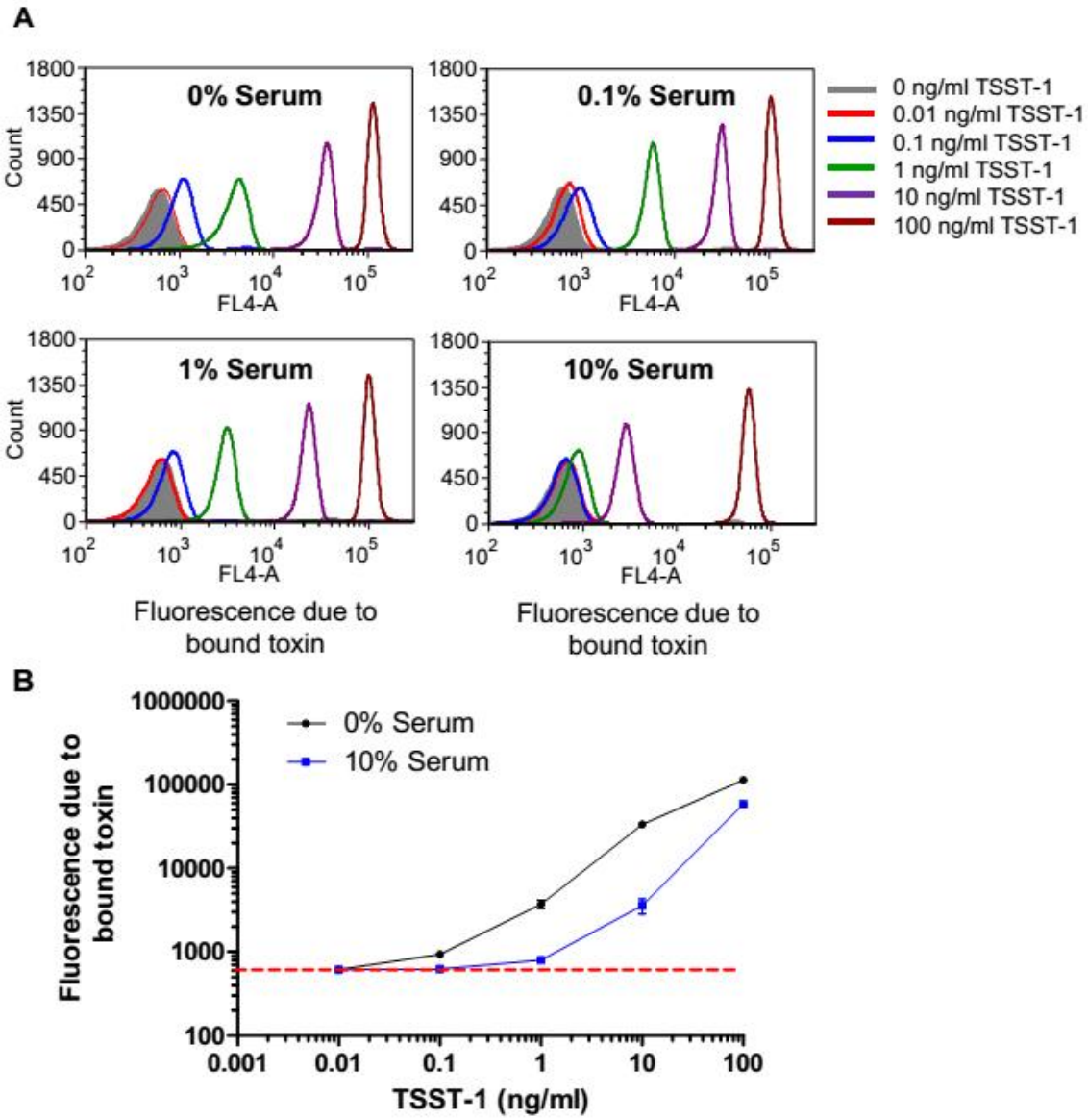

Fig. 3.14. Detection of TSST-1 in pooled, human serum by singleplex assay
(A) D10V coated P4 beads were added to different dilutions of TSST-1 prepared in 0, 0.1, 1 and 10% serum. Bound toxin was detected as an increase in fluorescence, upon incubation with rabbit anti-TSST-1 antibody, followed goat-anti rabbit IgG labelled with Alexa-647. Flow cytometry histograms for binding are shown. Fluorescence in the absence of toxin, is represented by gray (filled) trace on each histogram. (B) Median fluorescence units due to bound toxin were used to generate binding curves.

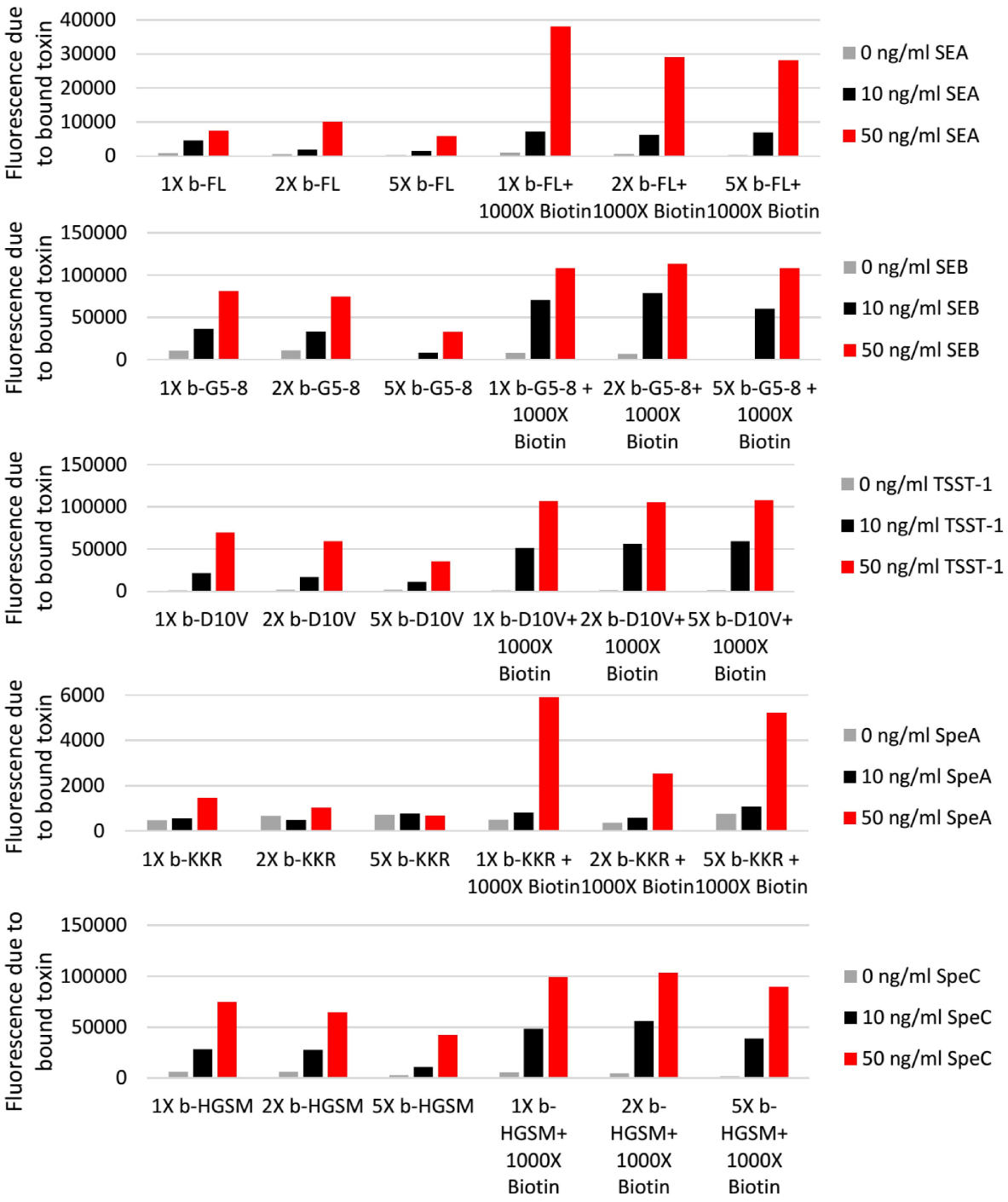

Fig. 3.15. Effect of varying coating density of biotin-Vβ on streptavidin bead surface, and blocking unoccupied sites with biotin

Streptavidin beads were coated with different amounts of biotin-Vβ to yield different coating densities. Washed beads were incubated either with buffer, or with excess biotin to saturate any unbound sites. Such beads with different Vβ coating density (either blocked with biotin or not) were used to detect different concentrations of cognate toxins. Median fluorescence units from histograms were used to generate bar graphs. Fluorescence in the absence of toxin, is represented by gray bar.

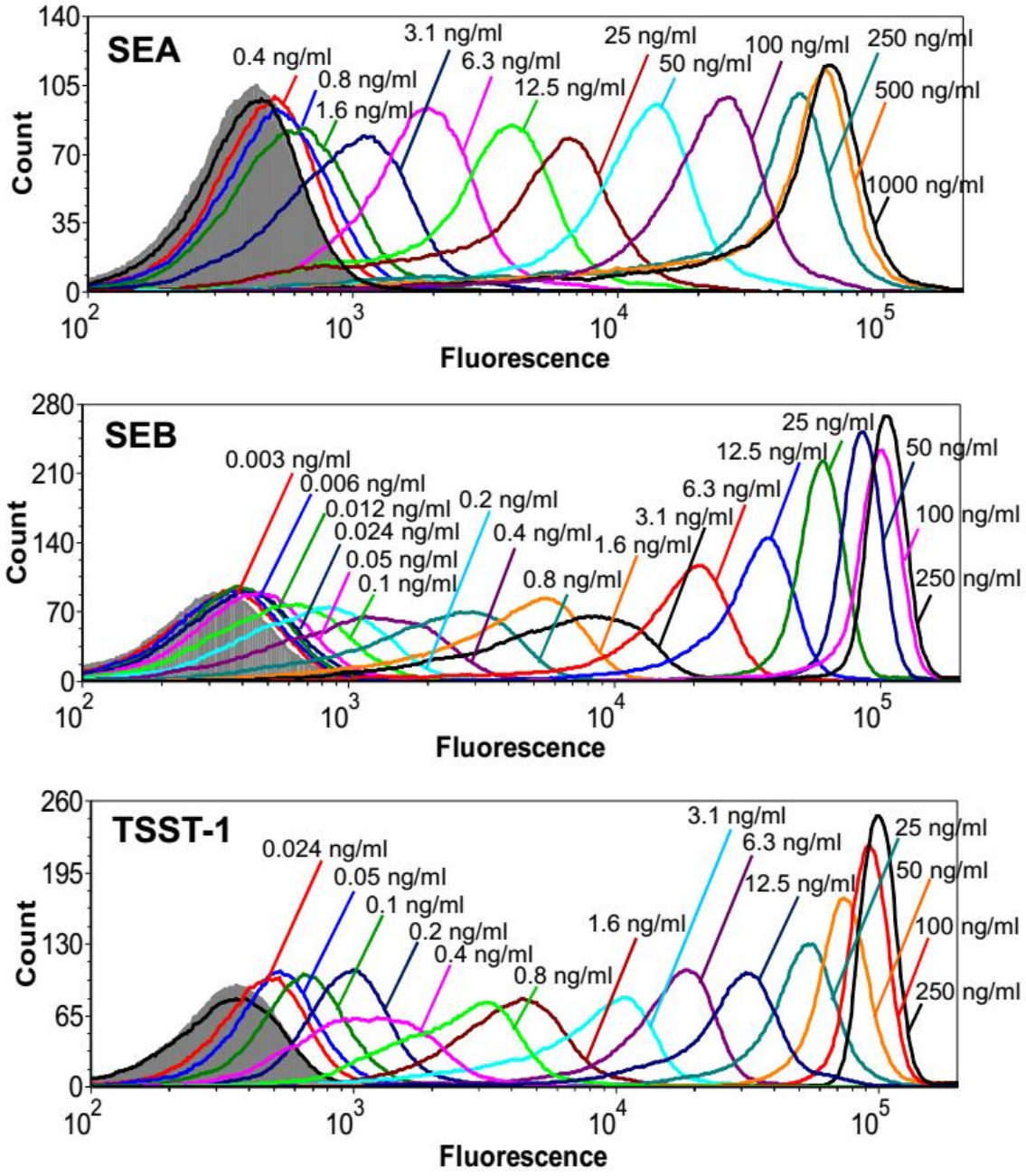

Fig. 3.16. Toxin binding titration by biotinylated, high-affinity Vβ coated on fluorescent beads, in singleplex assays

Each biotinylated, high-affinity Vβ protein, coated on fluorescent yellow, streptavidin beads was used to capture various concentrations of cognate, recombinant toxin. Bound toxins were detected by rabbit polyclonal anti-toxin antibodies, followed by goat-anti rabbit IgG labelled with Alexa fluor 647. Flow cytometry histograms for each binding titration are shown, with fluorescence arising due to toxin-binding on X-axis. Fluorescence in the absence of toxin, is represented by gray (filled) trace on each histogram. Data shown are representative of experiments performed in triplicate.

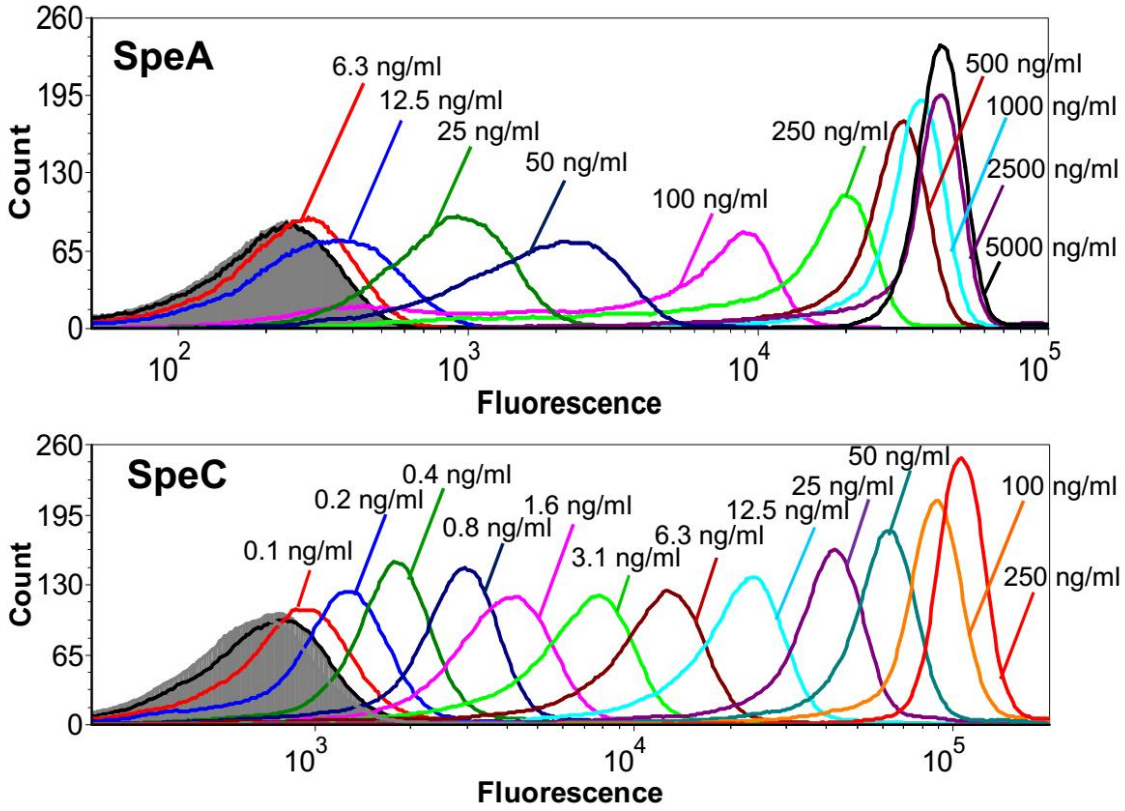

Fig. 3.16 (cont.). Toxin binding titration by biotinylated, high-affinity Vβ coated on fluorescent beads, in singleplex assays

Each biotinylated, high-affinity Vβ protein, coated on fluorescent yellow, streptavidin beads was used to capture various concentrations of cognate, recombinant toxin. Bound toxins were detected by rabbit polyclonal anti-toxin antibodies, followed by goat-anti rabbit IgG labelled with Alexa fluor 647. Flow cytometry histograms for each binding titration are shown, with fluorescence arising due to toxin-binding on X-axis. Fluorescence in the absence of toxin, is represented by gray (filled) trace on each histogram. Data shown are representative of experiments performed in triplicate.

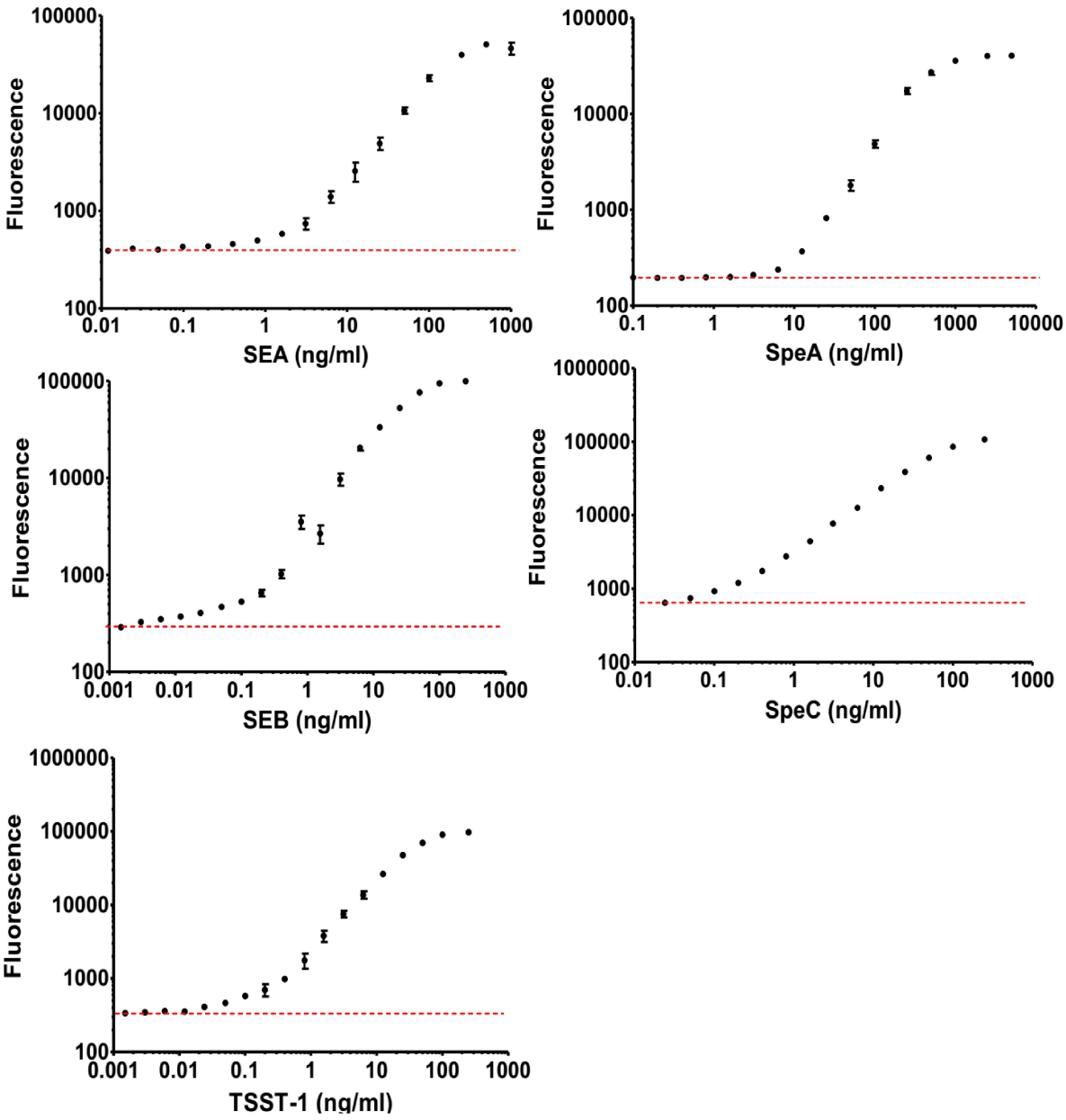

Fig. 3.17. Titration curves for binding of cognate toxins by biotinylated, high-affinity Vβ coated on fluorescent beads, in singleplex assays

Median fluorescence units due to toxin binding (in FL-4 channel) from the histograms (shown in previous figure) were used to generate binding curves. Red, dashed line indicates fluorescence in the absence of toxin, in each case. Data shown are representative of experiments performed in triplicate.

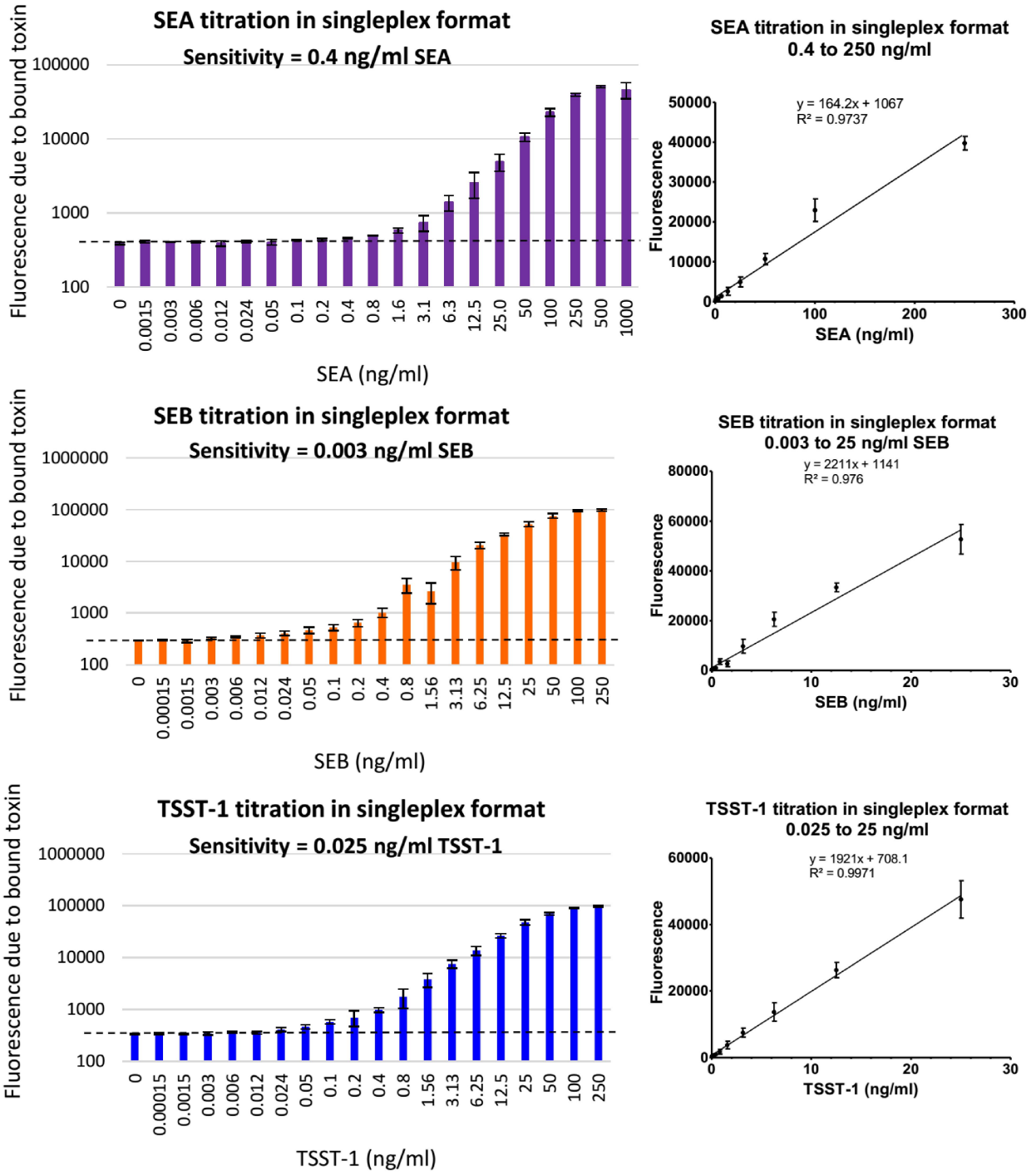

Fig. 3.18. Toxin binding titration by biotinylated, high-affinity Vβ coated on fluorescent beads, in singleplex assays

Median fluorescence units due to toxin binding (in FL-4 channel) from the histograms shown in figure 3.16, were used to generate bar graphs on the left. Black, dashed line indicates fluorescence in the absence of toxin, in each case. Data shown are representative of experiments performed in triplicate. Correlation plots shown on the right indicate the concentration range in which there was a linear correlation (R^2 ~0.9), between fluorescence due to toxin binding (Y-axis) and toxin concentration (X-axis).

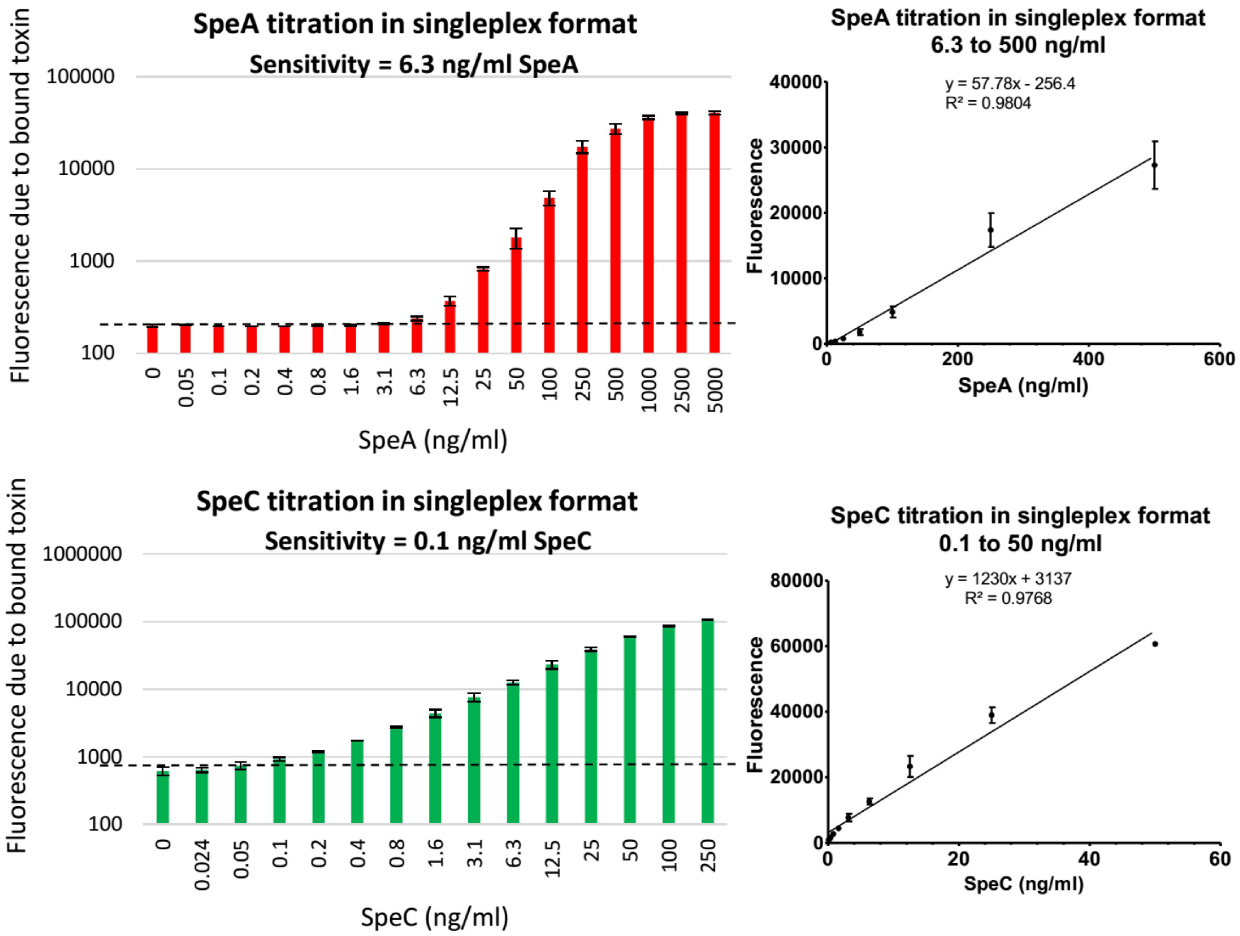

Fig. 3.18 (cont.). Toxin binding titration by biotinylated, high-affinity Vβ coated on fluorescent beads, in singleplex assays

Median fluorescence units due to toxin binding (in FL-4 channel) from the histograms shown in figure 3.16, were used to generate bar graphs on the left. Black, dashed line indicates fluorescence in the absence of toxin, in each case. Data shown are representative of experiments performed in triplicate. Correlation plots shown on the right indicate the concentration range in which there was a linear correlation (R^2 ~0.9), between fluorescence due to toxin binding (Y-axis) and toxin concentration (X-axis).

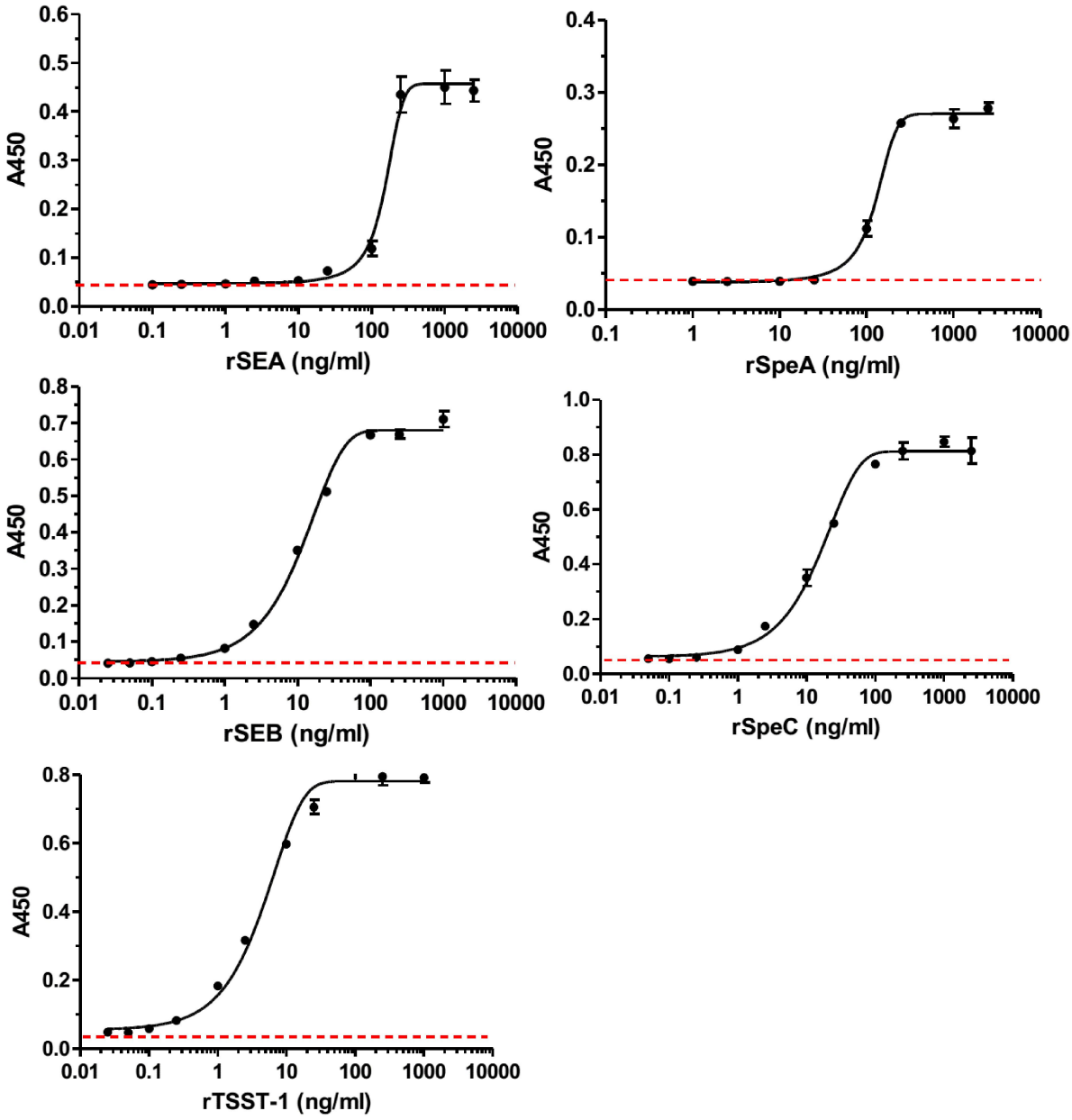

Fig. 3.19. Capture ELISA for staphylococcal or streptococcal toxin detection
High-affinity Vβ proteins were immobilized on wells of an ELISA plate to capture various concentrations of cognate, recombinant toxins. Bound toxins were detected by polyclonal, anti-toxin antibodies from rabbit, followed by goat-anti rabbit IgG-HRP. TMB substrate was added and the reaction was stopped with 1N H_2SO_4 to yield a yellow colored product. Absorbance at 450 nm (A450) was recorded and used to generate binding curves. Red, dashed line indicates absorbance in the absence of toxin. The error-bars represent standard deviations from two independent experiments.

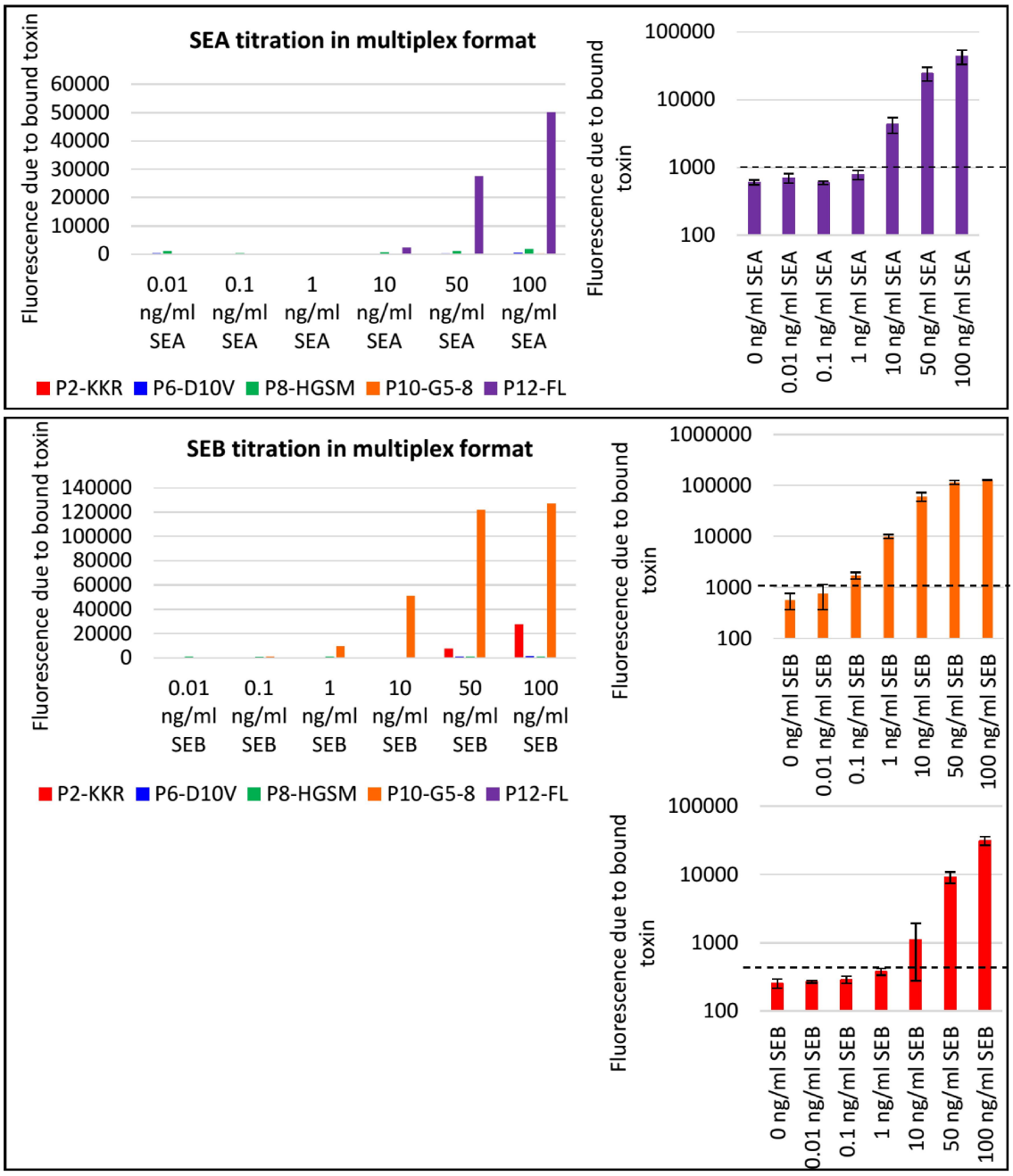

Fig. 3.20. Toxin binding titration by biotinylated, high-affinity Vβ coated on fluorescent beads in multiplex format, indicating sensitivity and cross-reactivity

Solutions containing different concentrations of toxins were added to a mixture of five fluorescent beads coated with five, high-affinity Vβ proteins. Bound toxins were detected upon incubation with a mixture of rabbit polyclonal, anti-toxin antibodies, followed by goat-anti rabbit IgG(H+L) labelled with Alexa fluor 647. Median fluorescence units (in FL-1 and FL-4 channels) from the beads were analyzed on a scatter plot. Bar graphs indicating fluorescence in FL-4 channel (due to toxin binding) exhibited by each Vβ coated bead are shown. Fluorescence emitted by KKR (Vβ-SpeA), D10V (Vβ-TSST-1), HGSM (Vβ-SpeC), G5-8 (Vβ-SEB) and FL (Vβ-SEA) coated beads, is shown by red, blue, green, orange and purple bars respectively. Black, dashed line indicates fluorescence in the absence of toxin. Data shown are representative of two experiments.

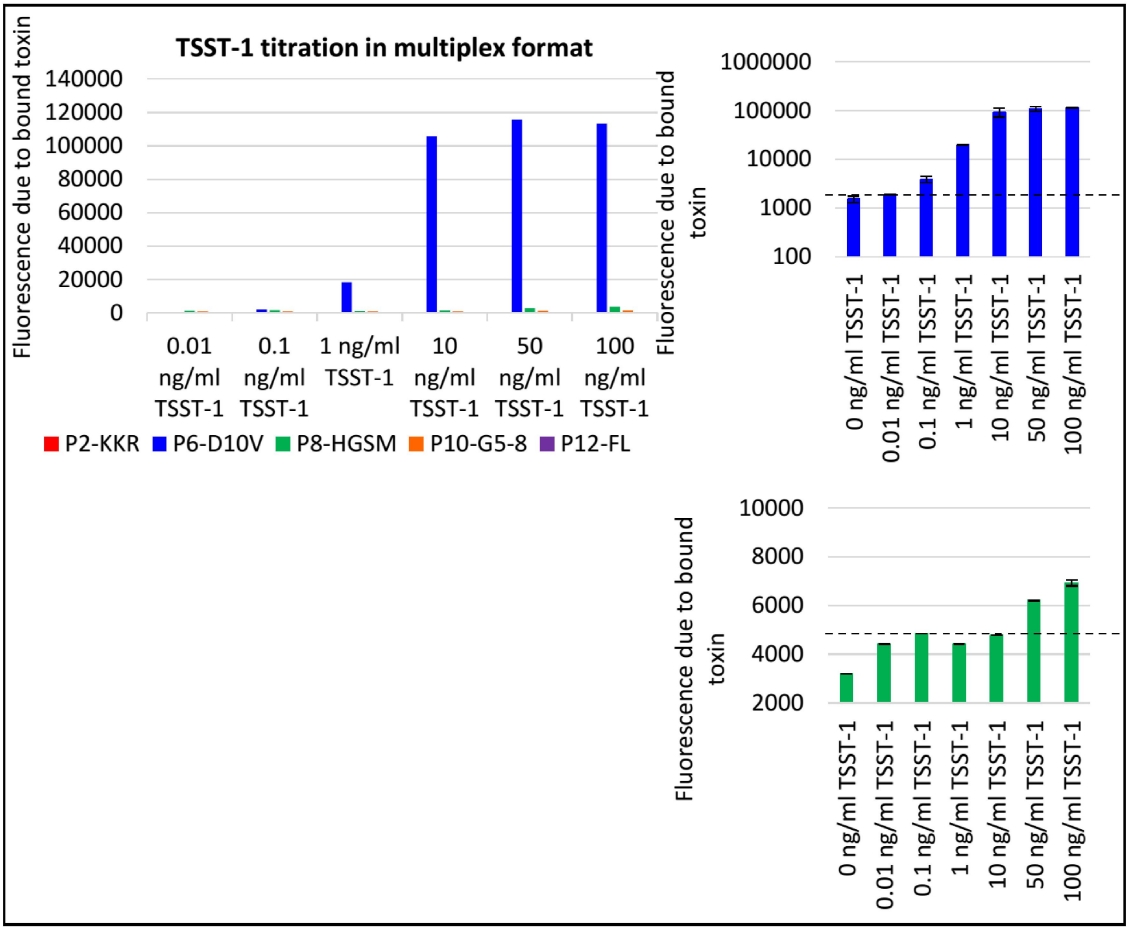

Fig. 3.20 (cont.). Toxin binding titration by biotinylated, high-affinity Vβ coated on fluorescent beads in multiplex format, indicating sensitivity and cross-reactivity
Solutions containing different concentrations of toxins were added to a mixture of five fluorescent beads coated with five, high-affinity Vβ proteins. Bound toxins were detected upon incubation with a mixture of rabbit polyclonal, anti-toxin antibodies, followed by goat-anti rabbit IgG(H+L) labelled with Alexa fluor 647. Median fluorescence units (in FL-1 and FL-4 channels) from the beads were analyzed on a scatter plot. Bar graphs indicating fluorescence in FL-4 channel (due to toxin binding) exhibited by each Vβ coated bead are shown. Fluorescence emitted by KKR (Vβ-SpeA), D10V (Vβ-TSST-1), HGSM (Vβ-SpeC), G5-8 (Vβ-SEB) and FL (Vβ-SEA) coated beads, is shown by red, blue, green, orange and purple bars respectively. Black, dashed line indicates fluorescence in the absence of toxin. Data shown are representative of two experiments.

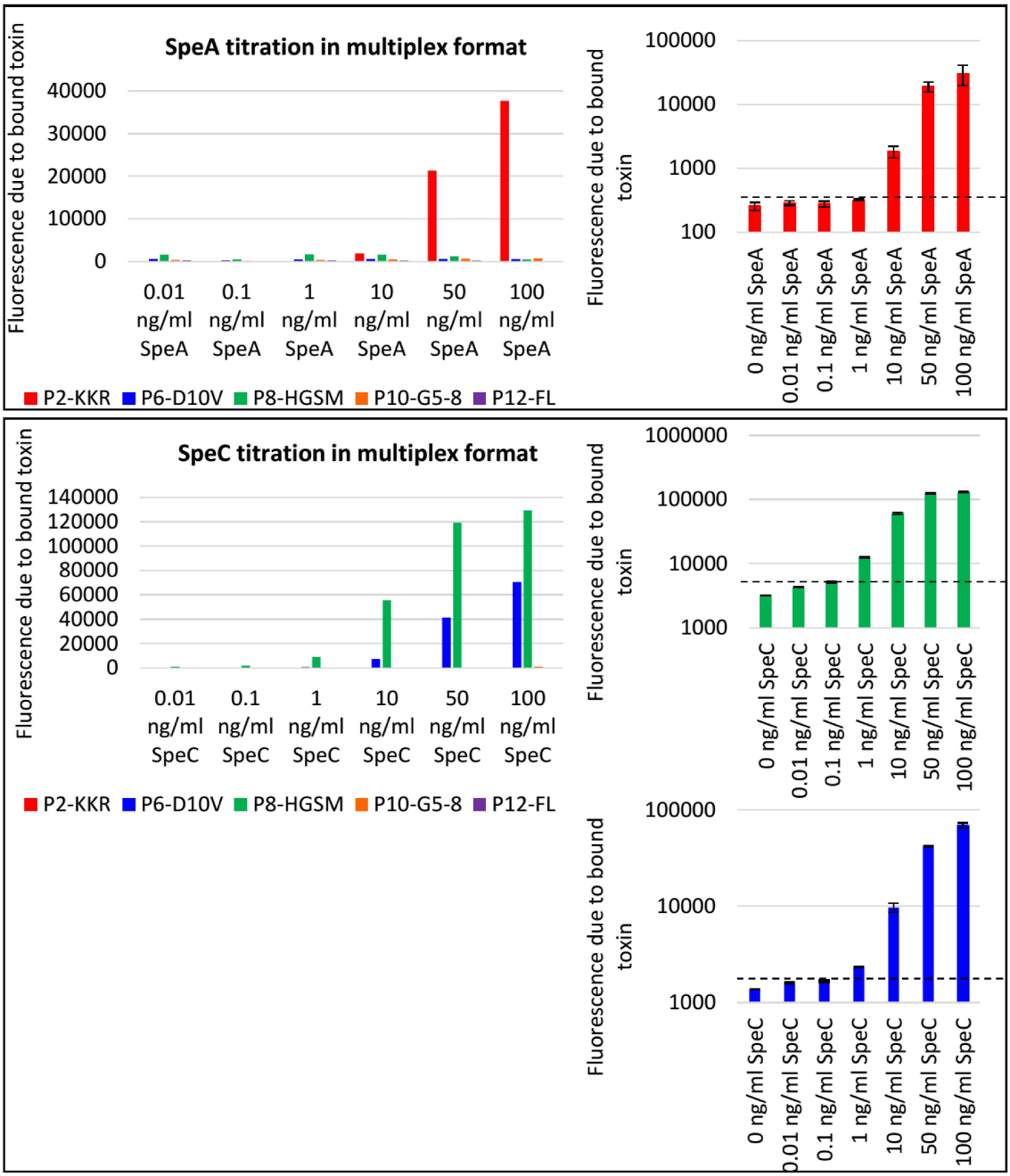

Fig. 3.20. (cont.). Toxin binding titration by biotinylated, high-affinity Vβ coated on fluorescent beads in multiplex format, indicating sensitivity and cross-reactivity

Solutions containing different concentrations of toxins were added to a mixture of five fluorescent beads coated with five, high-affinity Vβ proteins. Bound toxins were detected upon incubation with a mixture of rabbit polyclonal, anti-toxin antibodies, followed by goat-anti rabbit IgG(H+L) labelled with Alexa fluor 647. Median fluorescence units (in FL-1 and FL-4 channels) from the beads were analyzed on a scatter plot. Bar graphs indicating fluorescence in FL-4 channel (due to toxin binding) exhibited by each Vβ coated bead are shown. Fluorescence emitted by KKR (Vβ-SpeA), D10V (Vβ-TSST-1), HGSM (Vβ-SpeC), G5-8 (Vβ-SEB) and FL (Vβ-SEA) coated beads, is shown by red, blue, green, orange and purple bars respectively. Black, dashed line indicates fluorescence in the absence of toxin. Data shown are representative of two experiments.

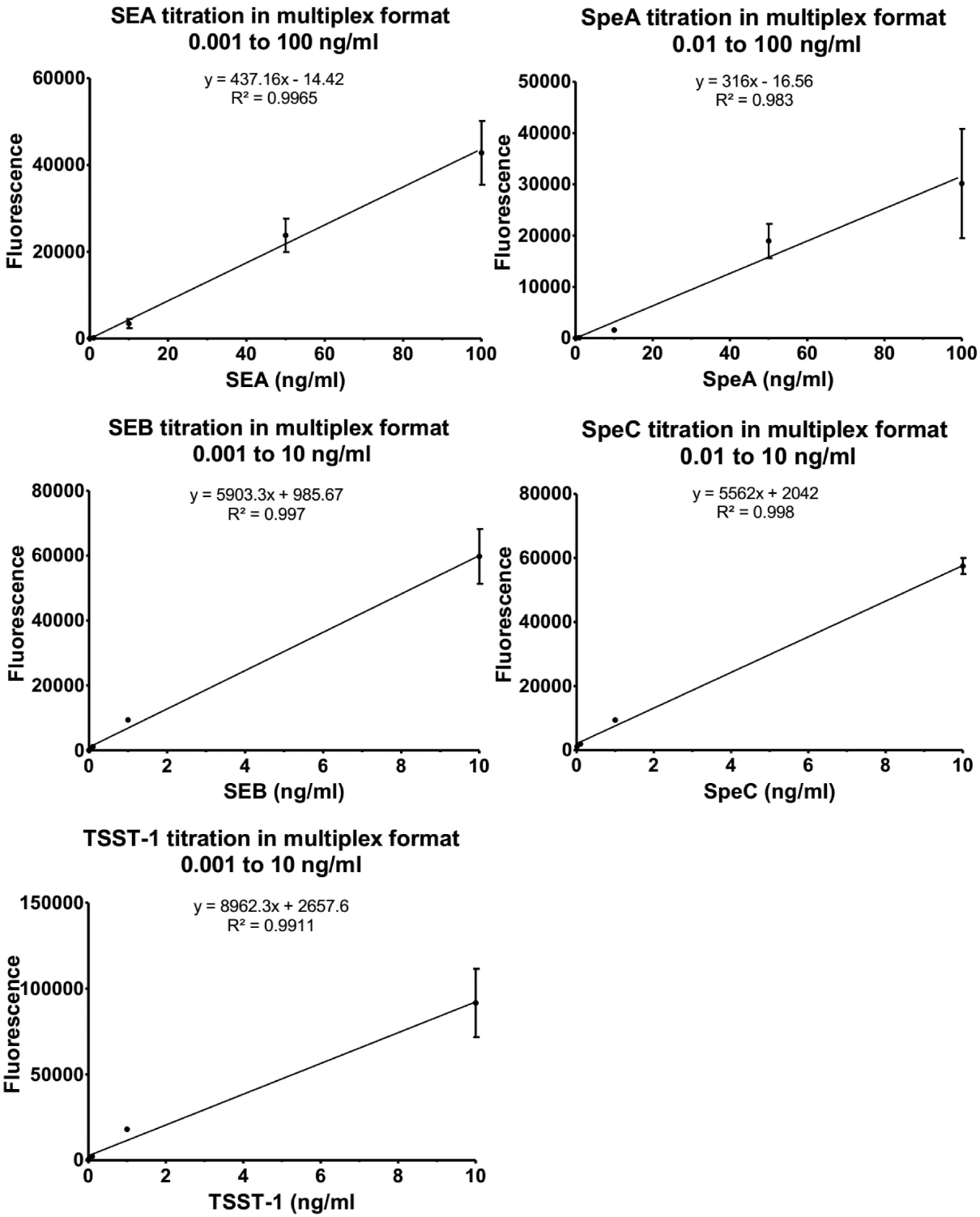

Fig. 3.21. Linear correlation plots for toxin titration in multiplex format

The concentration range in which there was a linear correlation (R^2 ~0.9), between fluorescence due to toxin binding (Y-axis) and toxin concentration (X-axis) was plotted to generate correlation plots, which could be used for estimating concentrations of these toxins present in unknown samples.

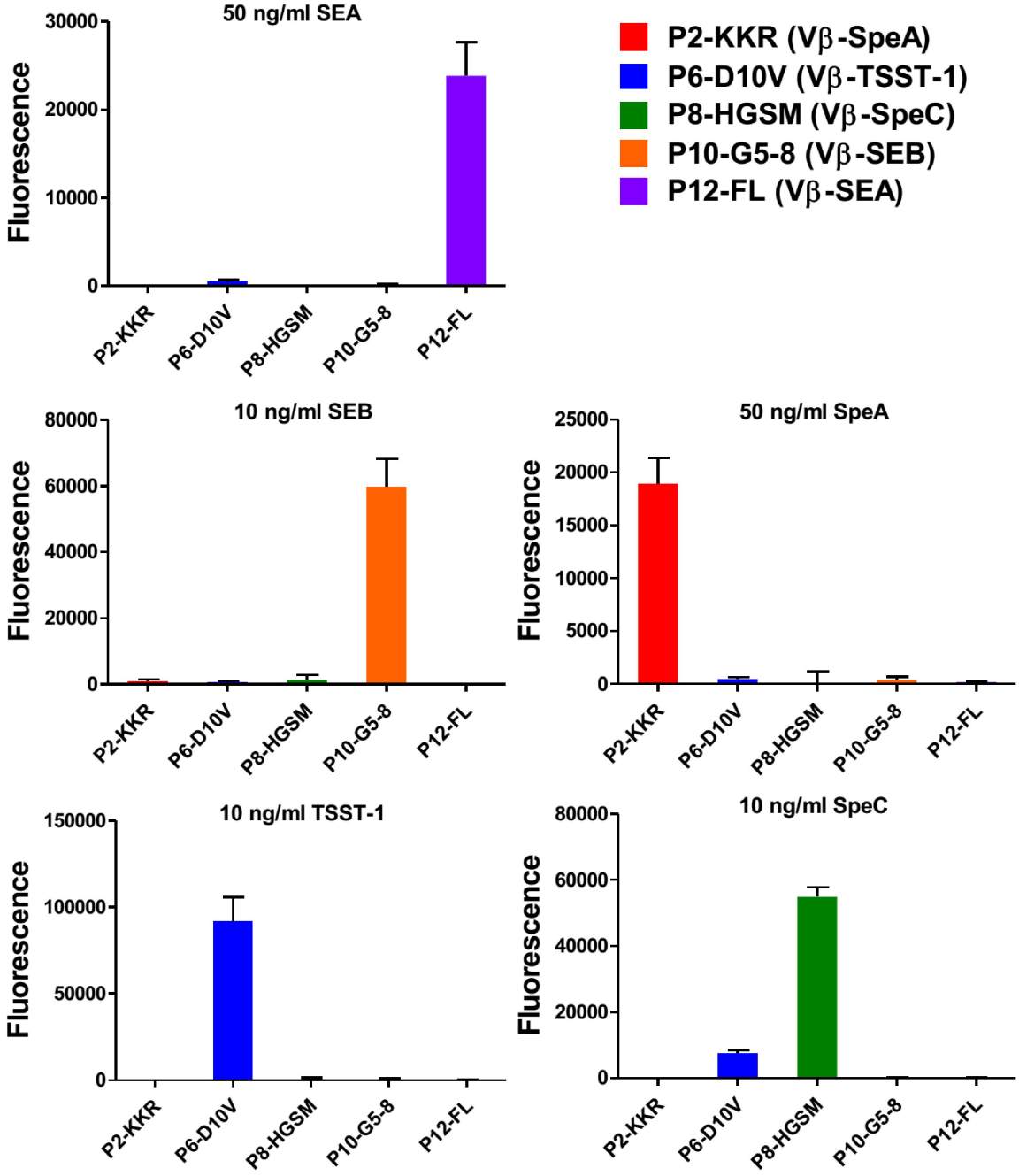

Fig. 3.22. Detection of a single toxin by multiplex assay
Solutions containing 50 ng/ml SEA, 10 ng/ml SEB, 10 ng/ml TSST-1, 50 ng/ml SpeA or 10 ng/ml SpeC were tested in multiplex assays with the five fluorescent beads coated with five, high-affinity Vβ proteins. Fluorescence emitted by each Vβ-coated bead due to toxin binding, was plotted on bar graphs shown. In all cases, the toxins were detected by the beads immobilized with the high-affinity Vβ engineered for that toxin. Fluorescence emitted by KKR (Vβ-SpeA), D10V (Vβ-TSST-1), HGSM (Vβ-SpeC), G5-8 (Vβ-SEB) and FL (Vβ-SEA) coated beads, is shown by red, blue, green, orange and purple bars respectively. The error-bars represent standard deviations from two independent experiments.

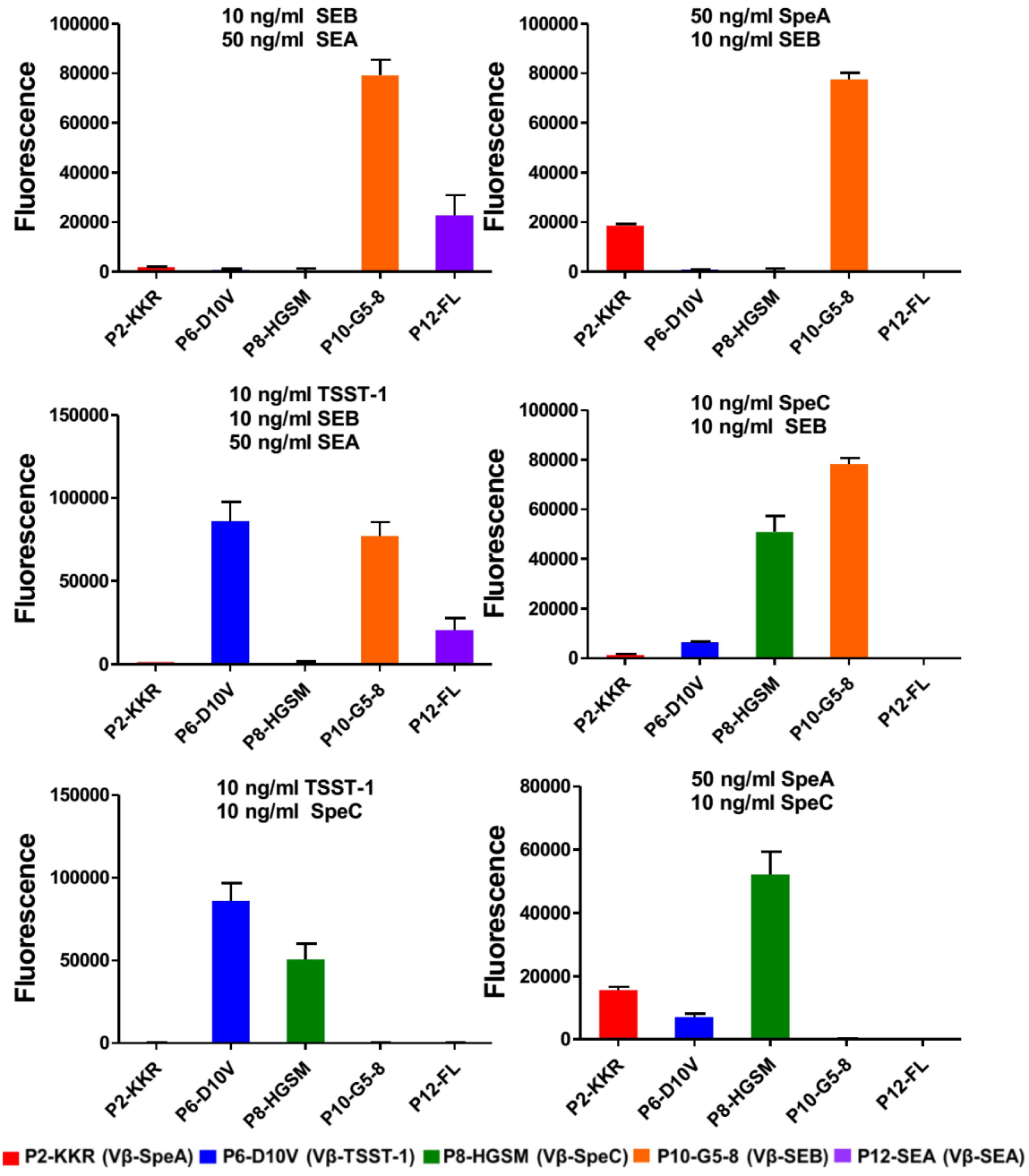

Fig. 3.23. Detection of multiple toxins in a multiplex assay
Solutions containing a mixture of two or more toxins were tested in multiplex assays, at the indicated concentrations. Fluorescence emitted by each Vβ-immobilized bead due to toxin binding, was plotted on bar graphs shown. Fluorescence emitted by KKR (Vβ-SpeA), D10V (Vβ-TSST-1), HGSM (Vβ-SpeC), G5-8 (Vβ-SEB) and FL (Vβ-SEA) coated beads, is shown by red, blue, green, orange and purple bars respectively. The error-bars represent standard deviations from two independent experiments.

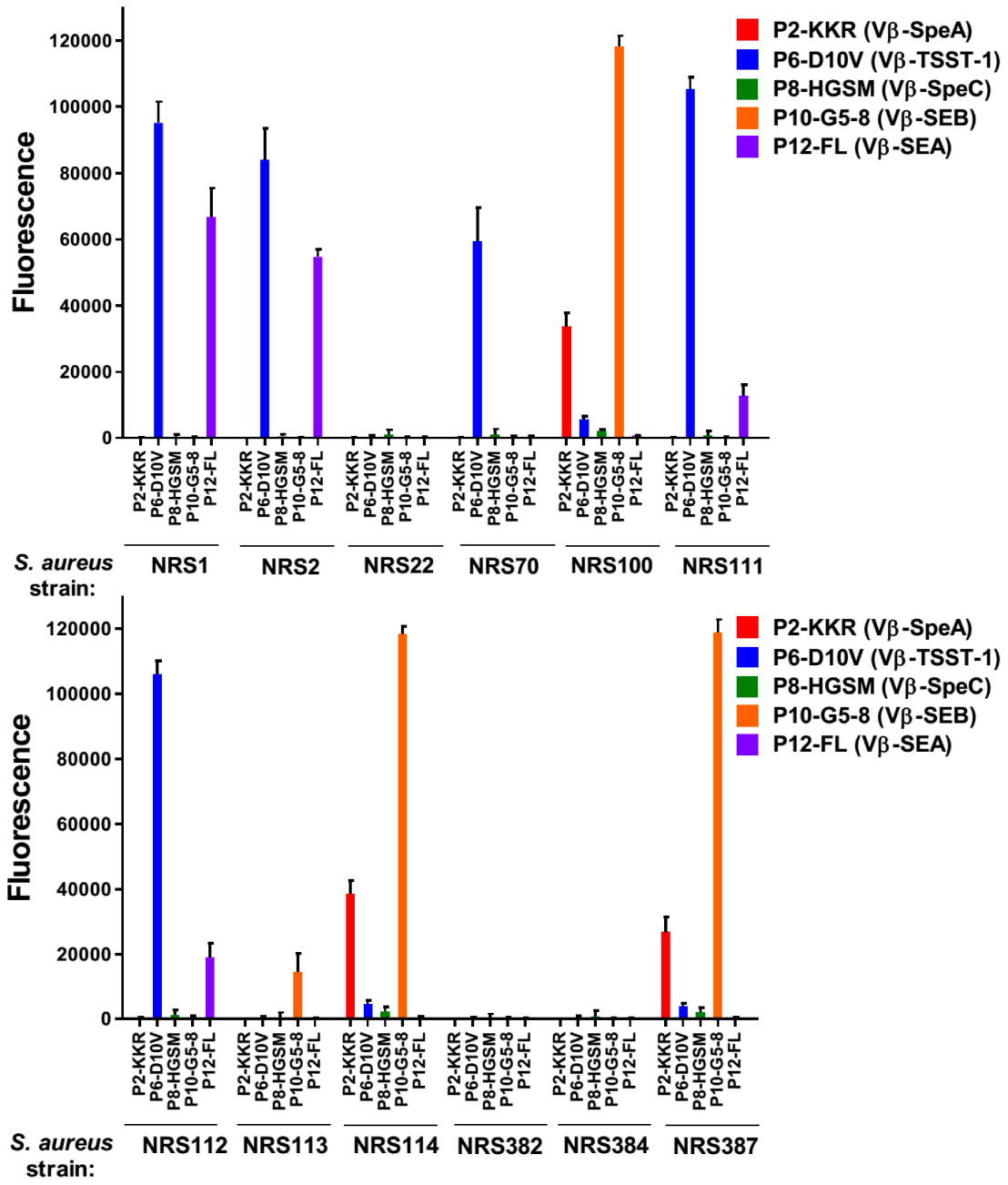

Fig. 3.24. Multiplex assay for toxin detection in culture supernatants of various strains of *Staphylococcus aureus*

Supernatants (diluted 1:4) from cultures of 18 strains of *Staphylococcus aureus* obtained from the NARSA repository, were tested in a multiplex assay to determine their toxin expression profile. Median fluorescence units (in FL-1 and FL-4 channels) emitted by each Vβ-immobilized were analyzed on a scatter plot to determine the presence or absence of toxin(s), and identity of the toxin. Bar graphs indicating fluorescence in FL-4 channel (due to toxin binding) exhibited by each Vβ coated bead are shown. Fluorescence emitted by KKR (Vβ-SpeA), D10V (Vβ-TSST-1), HGSM (Vβ-SpeC), G5-8 (Vβ-SEB) and FL (Vβ-SEA) coated beads, is shown by red, blue, green, orange and purple bars respectively. The error-bars represent standard deviations from two independent experiments.

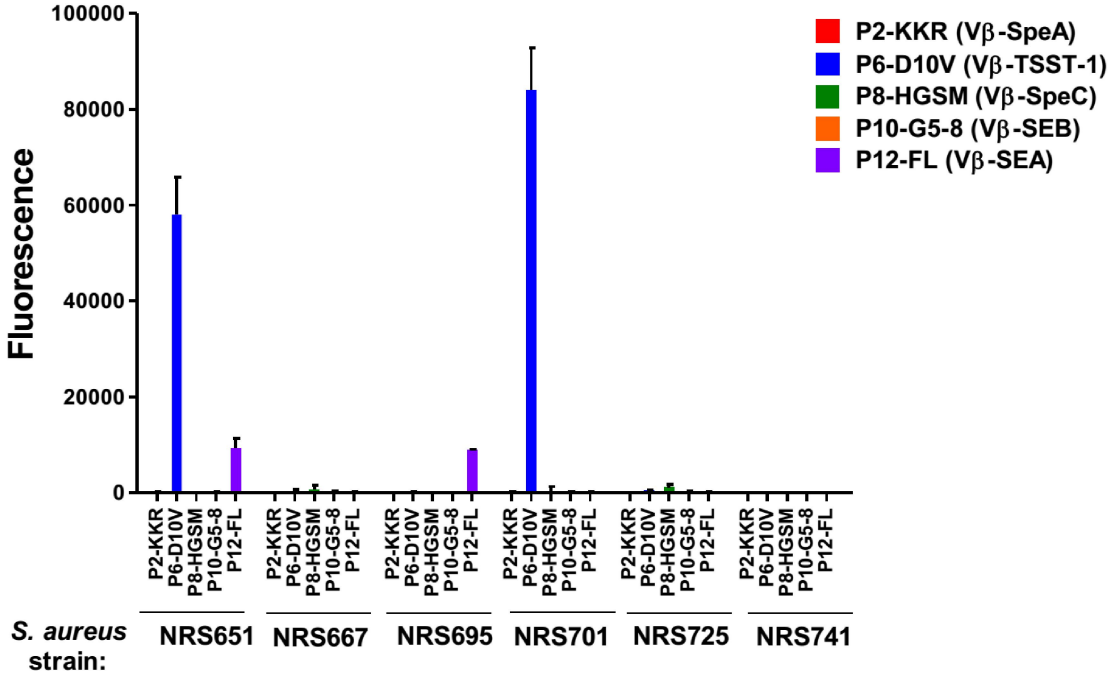

Fig. 3.24 (cont.). Multiplex assay with supernatants from cultures of various strains of *Staphylococcus aureus*

Supernatants (diluted 1:4) from cultures of 18 strains of *Staphylococcus aureus* obtained from the NARSA repository, were tested in a multiplex assay to determine their toxin expression profile. Median fluorescence units (in FL-1 and FL-4 channels) emitted by each Vβ-immobilized were analyzed on a scatter plot to determine the presence or absence of toxin(s), and identity of the toxin. Bar graphs indicating fluorescence in FL-4 channel (due to toxin binding) exhibited by each Vβ coated bead are shown. Fluorescence emitted by KKR (Vβ-SpeA), D10V (Vβ-TSST-1), HGSM (Vβ-SpeC), G5-8 (Vβ-SEB) and FL (Vβ-SEA) coated beads, is shown by red, blue, green, orange and purple bars respectively. The error-bars represent standard deviations from two independent experiments.

TABLES

Table 3.1. Yield of high-affinity Vβ proteins as inclusion bodies, from *E.coli*
High-affinity Vβ proteins were expressed as inclusion bodies in *E.coli* transformed with pET28a containing either thrombin cleavage site (T) between 6X His-tag and the Vβ sequence; or without thrombin cleavage site (NT) between 6X His-tag and the Vβ sequence. Cells were lysed using a microfluidizer and inclusion bodies were harvested. Yields (in g/l) are indicated.

High-affinity Vβ protein	Inclusion bodies prepared (g)	Inclusion bodies harvested from *E.coli* culture (l)	Yield (g/l)
FL (T)	1.43	3	0.48
D10V (T)	1.17	3	0.4
G5-8 (NT)	0.32	1.5	0.21
G5-8 (T)	1	3	0.33
L3 (NT)	0.29	1.5	0.2
L3 (T)	1.03	3	0.34
HGSM (NT)	0.43	1.5	0.29
KKR (NT)	0.74	1.5	0.5

Table 3.2. Comparison of sensitivities of toxin detection in capture ELISA versus a bead-based, singleplex flow cytometry assay

Toxin	Sensitivity of detection		Fold improvement in sensitivity in bead-based, singleplex, flow cytometry assay
	Capture ELISA (ng/ml)	Singleplex assay (Flow cytometry) (ng/ml)	
SEA	2.5-10	0.4	6.25-25
SEB	0.25	0.003	83.33
TSST-1	0.1-0.25	0.025	4-10
SpeA	25-100	6.3	4-16
SpeC	1-2.5	0.1	10-25

Table 3.3. Comparison of sensitivities of toxin detection in bead-based, singleplex versus multiplex flow cytometry assay

Toxin	Sensitivity of detection		Fold decrease in sensitivity in multiplex set up
	Singleplex assay (Flow cytometry) (ng/ml)	Multiplex assay (Flow cytometry) (ng/ml)	
SEA	0.4	10	25
SEB	0.003	0.1	33.33
TSST-1	0.025	0.1	4
SpeA	6.3	10	~ 1.6
SpeC	0.1	1	10

Table 3.4. Summary of sources of *Staphylococcus aureus* strains analyzed
Where available, information about presence or absence of SAg genes, and/or proteins, is shown. Also shown are the SAg expression profiles as determined by multiplex assay in the present work.

Strain (NARSA nomenclature/ aliases)	Source of isolate[a]	Presence or absence of SEA, SEB, or TSST-1 gene(s) or protein(s), GenBank[b]/NARSA[c]/ other investigators[d]	Presence of SAg determined by Multiplex assay		
			SEA	SEB	TSST-1
NRS1/ ATCC700699/ Mu50	Pus and debrided tissue at surgical incision in sternum of 4 month-old infant, Japan	SEA gene$^+$ (GenBank); TSST-1 gene$^+$ (GenBank)	+		+
NRS2/ ATCC700698	Not reported	Not reported	+		+
NRS22/ HIP07930/ USA600/99758	Bloodstream of an adult female ICU patient, US	SEA gene$^-$ (NARSA); SEB gene$^-$ (NARSA); TSST-1 gene$^-$ (NARSA)			
NRS70/ N315/USA100	Pharyngeal smear of a patient, Japan	TSST-1 gene$^+$ (GenBank)			+
NRS100/ COL	Archaic methicillin resistant *S.aureus* (MRSA) strain, UK	SEB gene$^+$ (GenBank)		+	
NRS111/ TKI913/ FRI913	Food associated with a staphylococcal food poisoning outbreak, US	SEA gene$^+$ (NARSA); TSST-1 gene$^+$ (NARSA); SEA gene$^+$ (PCR) [151]; TSST-1 gene$^+$ (PCR) [151];	+		+
NRS112/ MN8	Patient with menstrual TSS, US	SEA gene$^+$ (PCR) [150]; TSST-1$^+$ [150];	+		+
NRS113/ MNDON	Not reported	Not reported		+	
NRS114/ MNHOCH	Not reported	SEB gene$^+$ (PCR) [151];		+	
NRS382/ USA100	Bloodstream sample, US	Not reported			
NRS382/ USA100	Bloodstream sample, US	Not reported			

Table 3.4 (cont.). Summary of sources of *Staphylococcus aureus* strains analyzed
Where available, information about presence or absence of SAg genes, and/or proteins, is shown. Also shown are the SAg expression profiles as determined by multiplex assay in the present work.

Strain (NARSA nomenclature/ aliases)	Source of isolate[a]	Presence or absence of SEA, SEB, or TSST-1 gene(s) or protein(s), GenBank[b]/NARSA[c]/ other investigators[d]	Presence of SAg determined by Multiplex assay		
			SEA	SEB	TSST-1
NRS384/ USA300	Isolated from wound, US	Not reported			
NRS387/ USA800	Isolated from wound, US	SEB gene$^+$ (NARSA)		+	
NRS651/ CA-409	Isolated from peritoneal fluid, US	TSST-1 gene$^+$ (NARSA)	+		+
NRS667/ CO-71	Not reported	Not reported			
NRS695	Not reported	Not reported	+		
NRS701/ MN-082	Not reported	Not reported			+
NRS725/ OR-25	Not reported	Not reported			
NRS741/ TN90	Not reported	Not reported			

[a]Sources of the isolates were described by NARSA or ATCC (American Type Culture Collection).
[b]Information about presence or absence of SAg genes was obtained by performing BLAST analysis on genome sequences available in GenBank (NIH genetic sequence database).
[c]Information about presence or absence of SAg genes was obtained as annotations from NARSA website.
[d]Information about presence or absence of SAg genes was established by other investigators (references indicated).

Table 3.5. Estimated concentrations of SEA, SEB and TSST-1 in the supernatants of various *Staphylococcus aureus* strains, by linear or nonlinear regression methods

Staphylococcus aureus strain	Concentration of toxins estimated by multiplex assay		
	SEA (ng/ml)	SEB (ng/ml)	TSST-1 (ng/ml)
NRS1	611 ± 111 (>400 ng/ml**)		41 ± 4
NRS2	500 ± 30 (>400 ng/ml**)		36 ± 6
NRS22			
NRS70			25 ± 6
NRS100		271 ± 78**	
NRS111	116 ± 44		115 ± 24**
NRS112	175 ± 54		119 ± 27**
NRS113		9.2 ± 3	
NRS114		270 ± 65**	
NRS382			
NRS384			
NRS387		286 ±103**	
NRS651	85 ± 26		25 ± 5
NRS667			
NRS695	82 ± 1		
NRS701			36 ± 6
NRS725			
NRS741			
Sensitivity of toxin detection (ng/ml)	10	0.1	0.1
** MFU values for these strains were outside the linear range, hence concentrations were approximated by non-linear regression.			

Table 3.6. Comparison of sensitivities of toxin detection by different assays and the K_D of Vβ: toxin interaction.

Toxin	Sensitivity of detection			K_D (Vβ:toxin) (nM)
	Capture ELISA (ng/ml)	Singleplex assay (Flow cytometry) (ng/ml)	Multiplex assay (Flow cytometry) (ng/ml)	
SEA	2.5-10	0.4	10	4
SEB	0.25	0.003	0.1	0.05
TSST-1	0.1-0.25	0.025	0.1	0.05
SpeA	25-100	6.3	10	0.27
SpeC	1-2.5	0.1	1	0.5

REFERENCES

1. Marrack, P. and Kappler, J., *The staphylococcal entertoxins and their relatives.* Science, 1990. 248: p. 705-711.

2. Spaulding, A.R., Salgado-Pabon, W., Kohler, P.L., Horswill, A.R., Leung, D.Y., and Schlievert, P.M., *Staphylococcal and streptococcal superantigen exotoxins.* Clinical Microbioliology Reviews, 2013. 26(3): p. 422-47.

3. Krakauer, T. and Stiles, B.G., *The staphylococcal enterotoxin (SE) family: SEB and siblings.* Virulence, 2013. 4(8): p. 759-73.

4. Dinges, M.M., Orwin, P.M., and Schlievert, P.M., *Exotoxins of Staphylococcus aureus.* Clinical Microbioliology Reviews, 2000. 13(1): p. 16-34.

5. McCormick, J.K., Yarwood, J.M., and Schlievert, P.M., *Toxic shock syndrome and bacterial superantigens: an update.* Annual Review of Microbiology, 2001. 55: p. 77-104.

6. Li, H., Llera, A., Malchiodi, E.L., and Mariuzza, R.A., *The structural basis of T cell activation by superantigens.* Annual Review of Immunology, 1999. 17: p. 435-66.

7. Baker, M.D. and Acharya, K.R., *Superantigens: structure-function relationships.* International Journal of Medical Microbiology, 2004. 293(7-8): p. 529-37.

8. Papageorgiou, A.C. and Acharya, K.R., *Microbial superantigens: from structure to function.* Trends in Microbiology, 2000. 8(8): p. 369-75.

9. Fraser, J.D. and Proft, T., *The bacterial superantigen and superantigen-like proteins.* Immunological Reviews, 2008. 225: p. 226-43.

10. Pless, D.D., Ruthel, G., Reinke, E.K., Ulrich, R.G., and Bavari, S., *Persistence of zinc-binding bacterial superantigens at the surface of antigen-presenting cells contributes to the extreme potency of these superantigens as T-cell activators.* Infection and Immunity, 2005. 73(9): p. 5358-5366.

11. Bavari, S., Ulrich, R.G., and LeClaire, R.D., *Cross-reactive antibodies prevent the lethal effects of Staphylococcus aureus superantigens.* Journal of Infectious Diseases, 1999. 180(4): p. 1365-9.

12. Varshney, A.K., Mediavilla, J.R., Robiou, N., Guh, A., Wang, X., Gialanella, P., Levi, M.H., Kreiswirth, B.N., and Fries, B.C., *Diverse enterotoxin gene profiles among clonal complexes of Staphylococcus aureus isolates from the Bronx, New York.* Applied and Environmental Microbiology, 2009. 75(21): p. 6839-6849.

13. Hu, D.L., Omoe, K., Inoue, F., Kasai, T., Yasujima, M., Shinagawa, K., and Nakane, A., *Comparative prevalence of superantigenic toxin genes in meticillin-resistant and meticillin-susceptible Staphylococcus aureus isolates.* Journal of Medical Microbiology, 2008. 57(Pt 9): p. 1106-12.

14. Lindsay, J.A., Ruzin, A., Ross, H.F., Kurepina, N., and Novick, R.P., *The gene for toxic shock toxin is carried by a family of mobile pathogenicity islands in Staphylococcus aureus.* Molecular Microbiology, 1998 29(2): p. 527-543.

15. Novick, R.P., Schlievert, P., and Ruzin, A., *Pathogenicity and resistance islands of staphylococci.* Microbes and Infection, 2001. 3(7): p. 585-94.

16. Fitzgerald, J.R., Monday, S.R., Foster, T.J., Bohach, G.A., Hartigan, P.J., Meaney, W.J., and Smyth, C.J., *Characterization of a putative pathogenicity island from bovine Staphylococcus aureus encoding multiple superantigens.* Journal of Bacteriology, 2001. 183(1): p. 63-70.

17. Betley, M.J. and Mekalanos, J.J., *Staphylococcal Enterotoxin-a Is Encoded by Phage.* Science, 1985. 229(4709): p. 185-187.

18. Derzelle, S., Dilasser, F., Duquenne, M., and Deperrois, V., *Differential temporal expression of the staphylococcal enterotoxins genes during cell growth.* Food Microbiology, 2009. 26(8): p. 896-904.

19. Bachert, C., Gevaert, P., Zhang, N., van Zele, T., and Perez-Novo, C., *Role of staphylococcal superantigens in airway disease.* Chem Immunology and Allergy, 2007. 93: p. 214-36.

20. Strandberg, K.L., Rotschafer, J.H., Vetter, S.M., Buonpane, R.A., Kranz, D.M., and Schlievert, P.M., *Staphylococcal superantigens cause lethal pulmonary disease in rabbits.* Journal of Infectious Diseases, 2010. 202(11): p. 1690-7.

21. Schlievert, P.M., Case, L.C., Strandberg, K.L., Abrams, B.B., and Leung, D.Y., *Superantigen profile of Staphylococcus aureus isolates from patients with steroid-resistant atopic dermatitis.* Clinical Infectious Diseases, 2008. 46(10): p. 1562-7.

22. Macias, E.S., Pereira, F.A., Rietkerk, W., and Safai, B., *Superantigens in dermatology.* Journal of the American Academy of Dermatology, 2011. 64(3): p. 455-72; quiz 473-4.

23. Bohach, G.A., Fast, D.J., Nelson, R.D., and Schlievert, P.M., *Staphylococcal and streptococcal pyrogenic toxins involved in toxic shock syndrome and related illnesses.* Critical Reviews in Microbiology, 1990. 17(4): p. 251-72.

24. Lappin, E. and Ferguson, A.J., *Gram-positive toxic shock syndromes.* Lancet Infectious Diseases, 2009. 9(5): p. 281-90.

25. Dhodapkar, K., Corbacioglu, S., Chang, M.W., Karpatkin, M., and DiMichele, D., *Purpura fulminans caused by group A beta-hemolytic Streptococcus sepsis.* Journal of Pediatrics, 2000. 137(4): p. 562-7.

26. Tilahun, A.Y., Holz, M., Wu, T.T., David, C.S., and Rajagopalan, G., *Interferon gamma-dependent intestinal pathology contributes to the lethality in bacterial superantigen-induced toxic shock syndrome.* PLoS One, 2011. 6(2): p. e16764.

27. Tilahun, A.Y., Karau, M.J., Clark, C.R., Patel, R., and Rajagopalan, G., *The impact of tacrolimus on the immunopathogenesis of staphylococcal enterotoxin-induced systemic*

inflammatory response syndrome and pneumonia. Microbes and Infection, 2012. 14(6): p. 528-36.

28. Kieke, M.C., Sundberg, E., Shusta, E.V., Mariuzza, R.A., Wittrup, K.D., and Kranz, D.M., *High affinity T cell receptors from yeast display libraries block T cell activation by superantigens.* Journal of Molecular Biology, 2001. 307(5): p. 1305-15.

29. *Etanercept. Soluble tumour necrosis factor receptor, TNF receptor fusion protein, TNFR-Fc, TNR 001, Enbrel.* Drugs R D, 1999. 1(1): p. 75-7.

30. Neregard, P., Krishnamurthy, A., Revu, S., Engstrom, M., af Klint, E., and Catrina, A.I., *Etanercept decreases synovial expression of tumour necrosis factor-alpha and lymphotoxin-alpha in rheumatoid arthritis.* Scandinavian Journal of Rheumatology, 2014. 43(2): p. 85-90.

31. Boder, E.T. and Wittrup, K.D., *Yeast surface display for directed evolution of protein expression, affinity, and stability.* Methods in Enzymology, 2000. 328: p. 430-44.

32. Boder, E.T. and Wittrup, K.D., *Yeast surface display for screening combinatorial polypeptide libraries.* Nature Biotechnology, 1997. 15(6): p. 553-7.

33. Buonpane, R.A., Churchill, H.R., Moza, B., Sundberg, E.J., Peterson, M.L., Schlievert, P.M., and Kranz, D.M., *Neutralization of staphylococcal enterotoxin B by soluble, high-affinity receptor antagonists.* Nature Medicine, 2007. 13(6): p. 725-9.

34. Buonpane, R.A., Moza, B., Sundberg, E.J., and Kranz, D.M., *Characterization of T cell receptors engineered for high affinity against toxic shock syndrome toxin-1.* Journal of Molecular Biology, 2005. 353(2): p. 308-21.

35. Wang, N., Mattis, D.M., Sundberg, E.J., Schlievert, P.M., and Kranz, D.M., *A single, engineered protein therapeutic agent neutralizes exotoxins from both Staphylococcus aureus and Streptococcus pyogenes.* Clinical and Vaccine Immunology, 2010. 17(11): p. 1781-9.

36. Mattis, D.M., Spaulding, A.R., Chuang-Smith, O.N., Sundberg, E.J., Schlievert, P.M., and Kranz, D.M., *Engineering a soluble high-affinity receptor domain that neutralizes staphylococcal enterotoxin C in rabbit models of disease.* Protein Engineering, Design and Selection, 2013. 26(2): p. 133-42.

37. Sharma, P., Postel, S., Sundberg, E.J., and Kranz, D.M., *Characterization of the Staphylococcal enterotoxin A: Vβ receptor interaction using human receptor fragments engineered for high affinity.* Protein Engineering, Design and Selection, 2013. 26(12): p. 781-789.

38. John, C.C., Niermann, M., Sharon, B., Peterson, M.L., Kranz, D.M., and Schlievert, P.M., *Staphylococcal toxic shock syndrome erythroderma is associated with superantigenicity and hypersensitivity.* Clin Infectious Diseases, 2009. 49(12): p. 1893-6.

39. Li, H., Llera, A., Tsuchiya, D., Leder, L., Ysern, X., Schlievert, P.M., Karjalainen, K., and Mariuzza, R.A., *Three-dimensional structure of the complex between a T cell receptor*

beta chain and the superantigen staphylococcal enterotoxin B. Immunity, 1998. 9(6): p. 807-16.

40. Fields, B.A., Malchiodi, E.L., Li, H., Ysern, X., Stauffacher, C.V., Schlievert, P.M., Karjalainen, K., and Mariuzza, R.A., *Crystal structure of a T-cell receptor β-chain complexed with a superantigen.* Nature, 1996. 384: p. 188-192.

41. Sundberg, E.J., Li, H., Llera, A.S., McCormick, J.K., Tormo, J., Schlievert, P.M., Karjalainen, K., and Mariuzza, R.A., *Structures of two streptococcal superantigens bound to TCR beta chains reveal diversity in the architecture of T cell signaling complexes.* Structure, 2002. 10(5): p. 687-99.

42. Moza, B., Varma, A.K., Buonpane, R.A., Zhu, P., Herfst, C.A., Nicholson, M.J., Wilbuer, A.K., Seth, N.P., Wucherpfennig, K.W., McCormick, J.K., Kranz, D.M., and Sundberg, E.J., *Structural basis of T-cell specificity and activation by the bacterial superantigen TSST-1.* EMBO Journal, 2007. 26(4): p. 1187-97.

43. Petersson, K., Thunnissen, M., Forsberg, G., and Walse, B., *Crystal structure of a SEA variant in complex with MHC class II reveals the ability of SEA to crosslink MHC molecules.* Structure, 2002. 10(12): p. 1619-26.

44. Jardetzky, T.S., Brown, J.H., Gorga, J.C., Stern, L.J., Urban, R.G., Chi, Y.I., Stauffacher, C., Strominger, J.L., and Wiley, D.C., *Three-dimensional structure of a human class II histocompatibility molecule complexed with superantigen.* Nature, 1994. 368(6473): p. 711-8.

45. Sundberg, E.J., Andersen, P.S., Schlievert, P.M., Karjalainen, K., and Mariuzza, R.A., *Structural, energetic, and functional analysis of a protein-protein interface at distinct stages of affinity maturation.* Structure, 2003. 11(9): p. 1151-61.

46. Papageorgiou, A.C., Collins, C.M., Gutman, D.M., Kline, J.B., O'Brien, S.M., Tranter, H.S., and Acharya, K.R., *Structural basis for the recognition of superantigen streptococcal pyrogenic exotoxin A (SpeA1) by MHC class II molecules and T-cell receptors.* EMBO Journal, 1999. 18(1): p. 9-21.

47. Li, Y., Li, H., Dimasi, N., McCormick, J.K., Martin, R., Schuck, P., Schlievert, P.M., and Mariuzza, R.A., *Crystal structure of a superantigen bound to the high-affinity, zinc-dependent site on MHC class II.* Immunity, 2001. 14(1): p. 93-104.

48. Wang, X., Xu, M., Cai, Y., Yang, H., Zhang, H., and Zhang, C., *Functional analysis of the disulphide loop mutant of staphylococcal enterotoxin C2.* Applied Microbiology and Biotechnology, 2009. 82(5): p. 861-71.

49. Hovde, C.J., Marr, J.C., Hoffmann, M.L., Hackett, S.P., Chi, Y.I., Crum, K.K., Stevens, D.L., Stauffacher, C.V., and Bohach, G.A., *Investigation of the role of the disulphide bond in the activity and structure of staphylococcal enterotoxin C1.* Molecular Microbiology, 1994. 13(5): p. 897-909.

50. Schlievert, P.M., Jablonski, L.M., Roggiani, M., Sadler, I., Callantine, S., Mitchell, D.T., Ohlendorf, D.H., and Bohach, G.A., *Pyrogenic toxin superantigen site specificity in toxic*

shock syndrome and food poisoning in animals. Infection and Immunity, 2000. 68(6): p. 3630-4.

51. Kim, J., Urban, R.G., Strominger, J.L., and Wiley, D.C., *Toxic shock syndrome toxin-1 complexed with a class II major histocompatibility molecule HLA-DR1.* Science, 1994. 266(5192): p. 1870-4.

52. Tiedemann, R.E., Urban, R.J., Strominger, J.L., and Fraser, J.D., *Isolation of HLA-DR1.(staphylococcal enterotoxin A)2 trimers in solution.* Proceedings of the National Academy of Sciences of the United States of America, 1995. 92(26): p. 12156-9.

53. Saline, M., Rodstrom, K.E.J., Fischer, G., Orekhov, V.Y., Karlsson, B.G., and Lindkvist-Petersson, K., *The structure of superantigen complexed with TCR and MHC reveals novel insights into superantigenic T cell activation.* Nature Communications, 2010. 1(19).

54. Petersson, K., Pettersson, H., Skartved, N.J., Walse, B., and Forsberg, G., *Staphylococcal enterotoxin H induces V alpha-specific expansion of T cells.* Journal of Immunology, 2003. 170(8): p. 4148-54.

55. Kappler, J., Kotzin, B., Herron, L., Gelfand, E.W., Bigler, R.D., Boylston, A., Carrel, S., Posnett, D.N., Choi, Y., and Marrack, P., *V beta-specific stimulation of human T cells by staphylococcal toxins.* Science, 1989. 244(4906): p. 811-3.

56. Thomas, D., Dauwalder, O., Brun, V., Badiou, C., Ferry, T., Etienne, J., Vandenesch, F., and Lina, G., *Staphylococcus aureus superantigens elicit redundant and extensive human Vbeta patterns.* Infection and Immunity, 2009. 77(5): p. 2043-50.

57. Malchiodi, E.L., Eisenstein, E., Fields, B.A., Ohlendorf, D.H., Schlievert, P.M., Karjalainen, K., and Mariuzza, R.A., *Superantigen binding to a T cell receptor beta chain of known three-dimensional structure.* Journal of Experimental Medicine, 1995. 182(6): p. 1833-45.

58. Khandekar, S.S., Bettencourt, B.M., Wyss, D.F., Naylor, J.W., Brauer, P.P., Huestis, K., Dwyer, D.S., Profy, A.T., Osburne, M.S., Banerji, J., and Jones, B., *Conformational integrity and ligand binding properties of a single chain T-cell receptor expressed in Escherichia coli.* Journal of Biological Chemistry, 1997. 272(51): p. 32190-7.

59. Andersen, P.S., Geisler, C., Buus, S., Mariuzza, R.A., and Karjalainen, K., *Role of TCR-ligand affinity in T cell activation by bacterial superantigens.* Journal of Biological Chemistry, 2001. 276: p. 33452-33457.

60. Kieke, M.C., Shusta, E.V., Boder, E.T., Teyton, L., Wittrup, K.D., and Kranz, D.M., *Selection of functional T cell receptor mutants from a yeast surface- display library.* Proceedings of the National Academy of Sciences of the United States of America, 1999. 96(10): p. 5651-6.

61. Richman, S.A., Aggen, D.H., Dossett, M.L., Donermeyer, D.L., Allen, P.M., Greenberg, P.D., and Kranz, D.M., *Structural features of T cell receptor variable regions that enhance domain stability and enable expression as single-chain ValphaVbeta fragments.* Molecular Immunology, 2009. 46(5): p. 902-16.

62. Shusta, E.V., Kieke, M.C., Parke, E., Kranz, D.M., and Wittrup, K.D., *Yeast polypeptide fusion surface display levels predict thermal stability and soluble secretion efficiency.* Journal of Molecular Biology, 1999. 292(5): p. 949-56.

63. Sundberg, E.J., Deng, L., and Mariuzza, R.A., *TCR recognition of peptide/MHC class II complexes and superantigens.* Seminars in Immunology, 2007. 19(4): p. 262-71.

64. Nur-ur Rahman, A.K., Bonsor, D.A., Herfst, C.A., Pollard, F., Peirce, M., Wyatt, A.W., Kasper, K.J., Madrenas, J., Sundberg, E.J., and McCormick, J.K., *The T cell receptor beta-chain second complementarity determining region loop (CDR2beta governs T cell activation and Vbeta specificity by bacterial superantigens.* Journal of Biological Chemistry, 2011. 286(6): p. 4871-81.

65. Moza, B., Buonpane, R.A., Zhu, P., Herfst, C.A., Rahman, A.K., McCormick, J.K., Kranz, D.M., and Sundberg, E.J., *Long-range cooperative binding effects in a T cell receptor variable domain.* Proceedings of the National Academy of Sciences of the United States of America, 2006. 103(26): p. 9867-72.

66. Cho, S., Swaminathan, C.P., Yang, J., Kerzic, M.C., Guan, R., Kieke, M.C., Kranz, D.M., Mariuzza, R.A., and Sundberg, E.J., *Structural basis of affinity maturation and intramolecular cooperativity in a protein-protein interaction.* Structure, 2005. 13(12): p. 1775-87.

67. Bonsor, D.A., Postel, S., Pierce, B.G., Wang, N., Zhu, P., Buonpane, R.A., Weng, Z., Kranz, D.M., and Sundberg, E.J., *Molecular basis of a million-fold affinity maturation process in a protein-protein interaction.* Journal of Molecular Biology, 2011. 411(2): p. 321-8.

68. Churchill, H.R.O., Andersen, P.S., Parke, E.A., Mariuzza, R.A., and Kranz, D.M., *Mapping the energy of superantigen Staphylococcus enterotoxin C3 recognition of an alpha/beta T cell receptor using alanine scanning mutagenesis.* Journal of Experimental Medicine, 2000. 191(5): p. 835-846.

69. Yang, J., Swaminathan, C.P., Huang, Y., Guan, R., Cho, S., Kieke, M.C., Kranz, D.M., Mariuzza, R.A., and Sundberg, E.J., *Dissecting cooperative and additive binding energetics in the affinity maturation pathway of a protein-protein interface.* Journal of Biological Chemistry, 2003. 278: p. 50412-50421.

70. Hong-Geller, E., Mollhoff, M., Shiflett, P.R., and Gupta, G., *Design of chimeric receptor mimics with different TcRVbeta isoforms. Type-specific inhibition of superantigen pathogenesis.* Journal of Biological Chemistry, 2004. 279(7): p. 5676-84.

71. Yang, X., Buonpane, R.A., Moza, B., Rahman, A.K., Wang, N., Schlievert, P.M., McCormick, J.K., Sundberg, E.J., and Kranz, D.M., *Neutralization of multiple staphylococcal superantigens by a single-chain protein consisting of affinity-matured, variable domain repeats.* Journal of Infectious Diseases, 2008. 198(3): p. 344-8.

72. Schad, E.M., Zaitseva, I., Zaitsev, V.N., Dohlsten, M., Kalland, T., Schlievert, P.M., Ohlendorf, D.H., and Svensson, L.A., *Crystal structure of the superantigen staphylococcal enterotoxin type A.* EMBO Journal, 1995. 14(14): p. 3292-301.

73. Sundstrom, M., Hallen, D., Svensson, A., Schad, E., Dohlsten, M., and Abrahmsen, L., *The Co-crystal structure of staphylococcal enterotoxin type A with Zn2+ at 2.7 A resolution. Implications for major histocompatibility complex class II binding.* Journal of Biological Chemistry, 1996. 271(50): p. 32212-6.

74. Papageorgiou, A.C., Tranter, H.S., and Acharya, K.R., *Crystal structure of microbial superantigen staphylococcal enterotoxin B at 1.5 A resolution: implications for superantigen recognition by MHC class II molecules and T-cell receptors.* Journal of Molecular Biology, 1998. 277(1): p. 61-79.

75. Chi, Y.I., Sadler, I., Jablonski, L.M., Callantine, S.D., Deobald, C.F., Stauffacher, C.V., and Bohach, G.A., *Zinc-mediated dimerization and its effect on activity and conformation of staphylococcal enterotoxin type C.* Journal of Biological Chemistry, 2002. 277(25): p. 22839-46.

76. Papageorgiou, A.C., Brehm, R.D., Leonidas, D.D., Tranter, H.S., and Acharya, K.R., *The refined crystal structure of toxic shock syndrome toxin-1 at 2.07 A resolution.* Journal of Molecular Biology, 1996. 260(4): p. 553-569.

77. Earhart, C.A., Vath, G.M., Roggiani, M., Schlievert, P.M., and Ohlendorf, D.H., *Structure of streptococcal pyrogenic exotoxin A reveals a novel metal cluster.* Protein Science, 2000. 9(9): p. 1847-51.

78. Roussel, A., Anderson, B.F., Baker, H.M., Fraser, J.D., and Baker, E.N., *Crystal structure of the streptococcal superantigen SPE-C: dimerization and zinc binding suggest a novel mode of interaction with MHC class II molecules.* Nature Structural Biology, 1997. 4(8): p. 635-43.

79. Scallan, E., Hoekstra, R.M., Angulo, F.J., Tauxe, R.V., Widdowson, M.-A., Roy, S.L., Jones, J.L., and Griffin, P.M., *Foodborne Illness Acquired in the United States—Major Pathogens.* Emerging Infectious Diseases, 2011. 17(1): p. 7-15.

80. Marrack, P. and Kappler, J., *The staphylococcal enterotoxins and their relatives.* Science, 1990. 248(4956): p. 705-11.

81. Hennekinne, J.A., De Buyser, M.L., and Dragacci, S., *Staphylococcus aureus and its food poisoning toxins: characterization and outbreak investigation.* FEMS Microbiology Reviews, 2012. 36(4): p. 815-36.

82. Sundstrom, M., Abrahmsen, L., Antonsson, P., Mehindate, K., Mourad, W., and Dohlsten, M., *The crystal structure of staphylococcal enterotoxin type D reveals Zn2+-mediated homodimerization.* EMBO Journal, 1996. 15(24): p. 6832-40.

83. Asao, T., Kumeda, Y., Kawai, T., Shibata, T., Oda, H., Haruki, K., Nakazawa, H., and Kozaki, S., *An extensive outbreak of staphylococcal food poisoning due to low-fat milk in Japan: estimation of enterotoxin A in the incriminated milk and powdered skim milk.* Epidemiology and Infection, 2003. 130(1): p. 33-40.

84. Evenson, M.L., Hinds, M.W., Bernstein, R.S., and Bergdoll, M.S., *Estimation of human dose of staphylococcal enterotoxin A from a large outbreak of staphylococcal food*

poisoning involving chocolate milk. International Journal of Food Microbiology, 1988. 7(4): p. 311-6.

85. Fetsch, A., Contzen, M., Hartelt, K., Kleiser, A., Maassen, S., Rau, J., Kraushaar, B., Layer, F., and Strommenger, B., *Staphylococcus aureus food-poisoning outbreak associated with the consumption of ice-cream.* International Journal of Food Microbiology, 2014. 187: p. 1-6.

86. Ikeda, T., Tamate, N., Yamaguchi, K., and Makino, S., *Mass outbreak of food poisoning disease caused by small amounts of staphylococcal enterotoxins A and H.* Applied and Environmental Microbiology, 2005. 71(5): p. 2793-5.

87. Levine, W.C., Bennett, R.W., Choi, Y., Henning, K.J., Rager, J.R., Hendricks, K.A., Hopkins, D.P., Gunn, R.A., and Griffin, P.M., *Staphylococcal food poisoning caused by imported canned mushrooms.* Journal of Infectious Diseases, 1996. 173(5): p. 1263-7.

88. Miwa, N., Kawamura, A., Masuda, T., and Akiyama, M., *An outbreak of food poisoning due to egg yolk reaction-negative Staphylococcus aureus.* International Journal of Food Microbiology, 2001. 64(3): p. 361-6.

89. Balaban, N. and Rasooly, A., *Staphylococcal enterotoxins.* International Journal of Food Microbiology, 2000. 61(1): p. 1-10.

90. Ellis, M., Serreli, A., Colque-Navarro, P., Hedstrom, U., Chacko, A., Siemkowicz, E., and Mollby, R., *Role of staphylococcal enterotoxin A in a fatal case of endocarditis.* Journal of Medical Microbiology, 2003. 52(Pt 2): p. 109-12.

91. McCollister, B.D., Kreiswirth, B.N., Novick, R.P., and Schlievert, P.M., *Production of toxic shock syndrome-like illness in rabbits by Staphylococcus aureus D4508: association with enterotoxin A.* Infection and Immunity, 1990. 58(7): p. 2067-70.

92. Fernandez, M.M., Cho, S., De Marzi, M.C., Kerzic, M.C., Robinson, H., Mariuzza, R.A., and Malchiodi, E.L., *Crystal structure of staphylococcal enterotoxin G (SEG) in complex with a mouse T-cell receptor {beta} chain.* Journal of Biological Chemistry, 2011. 286(2): p. 1189-95.

93. Fraser, J., Arcus, V., Kong, P., Baker, E., and Proft, T., *Superantigens - powerful modifiers of the immune system.* Molecular Medicine Today, 2000. 6(3): p. 125-32.

94. Fraser, J.D., *Clarifying the mechanism of superantigen toxicity.* PLoS Biology, 2011. 9(9): p. e1001145.

95. Bergdoll, M.S., Sugiyama, H., and Dack, G.M., *Staphylococcal enterotoxin. I. Purification.* Archives of Biochemistry and Biophysics, 1959. 85: p. 62-9.

96. Chu, F.S., Thadhani, K., Schantz, E.J., and Bergdoll, M.S., *Purification and characterization of staphylococcal enterotoxin A.* Biochemistry, 1966. 5(10): p. 3281-9.

97. Hudson, K.R., Tiedemann, R.E., Urban, R.G., Lowe, S.C., Strominger, J.L., and Fraser, J.D., *Staphylococcal enterotoxin A has two cooperative binding sites on major*

histocompatibility complex class II. Journal of Experimental Medicine, 1995. 182(3): p. 711-20.

98. Llewelyn, M., Sriskandan, S., Terrazzini, N., Cohen, J., and Altmann, D.M., *The TCR Vbeta signature of bacterial superantigens spreads with stimulus strength.* International Immunology, 2006. 18(10): p. 1433-41.

99. Fromant, M., Blanquet, S., and Plateau, P., *Direct random mutagenesis of gene-sized DNA fragments using polymerase chain reaction.* Analytical Biochemistry, 1995. 224(1): p. 347-53.

100. Richman, S.A., Kranz, D.M., and Stone, J.D., *Biosensor detection systems: engineering stable, high-affinity bioreceptors by yeast surface display.* Methods in Molecular Biology, 2009. 504: p. 323-50.

101. Kieke, M.C., Shusta, E.V., Boder, E.T., Teyton, L., Wittrup, K.D., and Kranz, D.M., *Selection of functional T cell receptor mutants from a yeast surface-display library.* Proceedings of the National Academy of Sciences of the United States of America, 1999. 96(10): p. 5651-6.

102. Weber, K.S., Donermeyer, D.L., Allen, P.M., and Kranz, D.M., *Class II-restricted T cell receptor engineered in vitro for higher affinity retains peptide specificity and function.* Proceedings of the National Academy of Sciences of the United States of America, 2005. 102(52): p. 19033-8.

103. Orr, B.A., Carr, L.M., Wittrup, K.D., Roy, E.J., and Kranz, D.M., *Rapid method for measuring ScFv thermal stability by yeast surface display.* Biotechnology Progress, 2003. 19(2): p. 631-8.

104. Andersen, P.S., Geisler, C., Buus, S., Mariuzza, R.A., and Karjalainen, K., *Role of the T cell receptor ligand affinity in T cell activation by bacterial superantigens.* Journal of Biological Chemistry, 2001. 276(36): p. 33452-7.

105. Fields, B.A., Malchiodi, E.L., Li, H., Ysern, X., Stauffacher, C.V., Schlievert, P.M., Karjalainen, K., and Mariuzza, R.A., *Crystal structure of a T-cell receptor beta-chain complexed with a superantigen.* Nature, 1996. 384(6605): p. 188-92.

106. Holtfreter, S., Bauer, K., Thomas, D., Feig, C., Lorenz, V., Roschack, K., Friebe, E., Selleng, K., Lovenich, S., Greve, T., Greinacher, A., Panzig, B., Engelmann, S., Lina, G., and Broker, B.M., *egc-Encoded superantigens from Staphylococcus aureus are neutralized by human sera much less efficiently than are classical staphylococcal enterotoxins or toxic shock syndrome toxin.* Infection and Immunity, 2004. 72(7): p. 4061-71.

107. Jones, L.L., Brophy, S.E., Bankovich, A.J., Colf, L.A., Hanick, N.A., Garcia, K.C., and Kranz, D.M., *Engineering and characterization of a stabilized alpha1/alpha2 module of the class I major histocompatibility complex product Ld.* Journal of Biological Chemistry, 2006. 281(35): p. 25734-44.

108. Schodin, B.A., Tsomides, T.J., and Kranz, D.M., *Correlation between the number of T cell receptors required for T cell activation and TCR-ligand affinity.* Immunity, 1996. 5(2): p. 137-46.

109. Andersen, P.S., Lavoie, P.M., Sekaly, R.P., Churchill, H., Kranz, D.M., Schlievert, P.M., Karjalainen, K., and Mariuzza, R.A., *Role of the T cell receptor alpha chain in stabilizing TCR-superantigen-MHC class II complexes.* Immunity, 1999. 10(4): p. 473-83.

110. Antonsson, P., Wingren, A.G., Hansson, J., Kalland, T., Varga, M., and Dohlsten, M., *Functional characterization of the interaction between the superantigen staphylococcal enterotoxin A and the TCR.* Journal of Immunology, 1997. 158(9): p. 4245-51.

111. Hudson, K.R., Robinson, H., and Fraser, J.D., *Two adjacent residues in staphylococcal enterotoxins A and E determine T cell receptor V beta specificity.* Journal of Experimental Medicine, 1993. 177(1): p. 175-84.

112. Mollick, J.A., Mcmasters, R.L., Grossman, D., and Rich, R.R., *Localization of a Site on Bacterial Superantigens That Determines T-Cell Receptor Beta-Chain Specificity.* Journal of Experimental Medicine, 1993. 177(2): p. 283-293.

113. Swaminathan, S., Furey, W., Pletcher, J., and Sax, M., *Residues defining V beta specificity in staphylococcal enterotoxins.* Nature Structural Biology, 1995. 2(8): p. 680-6.

114. Salgado-Pabon, W., Breshears, L., Spaulding, A.R., Merriman, J.A., Stach, C.S., Horswill, A.R., Peterson, M.L., and Schlievert, P.M., *Superantigens are critical for Staphylococcus aureus Infective endocarditis, sepsis, and acute kidney injury.* MBio, 2013. 4(4).

115. Kerouanton, A., Hennekinne, J.A., Letertre, C., Petit, L., Chesneau, O., Brisabois, A., and De Buyser, M.L., *Characterization of Staphylococcus aureus strains associated with food poisoning outbreaks in France.* International Journal of Food Microbiology, 2007. 115(3): p. 369-75.

116. Hait, J., Tallent, S., Melka, D., Keys, C., and Bennett, R., *Prevalence of enterotoxins and toxin gene profiles of Staphylococcus aureus isolates recovered from a bakery involved in a second staphylococcal food poisoning occurrence.* Journal of Applied Microbiology, 2014. 117(3): p. 866-75.

117. Ostyn, A., De Buyser, M.L., Guillier, F., Groult, J., Felix, B., Salah, S., Delmas, G., and Hennekinne, J.A., *First evidence of a food poisoning outbreak due to staphylococcal enterotoxin type E, France, 2009.* Euro Surveillance, 2010. 15(13).

118. Veras, J.F., do Carmo, L.S., Tong, L.C., Shupp, J.W., Cummings, C., Dos Santos, D.A., Cerqueira, M.M., Cantini, A., Nicoli, J.R., and Jett, M., *A study of the enterotoxigenicity of coagulase-negative and coagulase-positive staphylococcal isolates from food poisoning outbreaks in Minas Gerais, Brazil.* International Journal of Infectious Diseases, 2008. 12(4): p. 410-5.

119. Argudin, M.A., Mendoza, M.C., and Rodicio, M.R., *Food poisoning and Staphylococcus aureus enterotoxins.* Toxins (Basel), 2010. 2(7): p. 1751-73.

120. Hauser, A.R., Stevens, D.L., Kaplan, E.L., and Schlievert, P.M., *Molecular analysis of pyrogenic exotoxins from Streptococcus pyogenes isolates associated with toxic shock-like syndrome.* Journal of Clinical Microbiology, 1991. 29(8): p. 1562-7.

121. Leung, D.Y., Travers, J.B., Giorno, R., Norris, D.A., Skinner, R., Aelion, J., Kazemi, L.V., Kim, M.H., Trumble, A.E., Kotb, M., and et al., *Evidence for a streptococcal superantigen-driven process in acute guttate psoriasis.* Journal of Clinical Investigation, 1995. 96(5): p. 2106-12.

122. Commons, R.J., Smeesters, P.R., Proft, T., Fraser, J.D., Robins-Browne, R., and Curtis, N., *Streptococcal superantigens: categorization and clinical associations.* Trends in molecular medicine, 2014. 20(1): p. 48-62.

123. Chung, J.W., Karau, M.J., Greenwood-Quaintance, K.E., Ballard, A.D., Tilahun, A., Khaleghi, S.R., David, C.S., Patel, R., and Rajagopalan, G., *Superantigen profiling of Staphylococcus aureus infective endocarditis isolates.* Diagnostic Microbiology and Infectious Disease, 2014. 79(2): p. 119-24.

124. Fosheim, G.E., Nicholson, A.C., Albrecht, V.S., and Limbago, B.M., *Multiplex real-time PCR assay for detection of methicillin-resistant Staphylococcus aureus and associated toxin genes.* Journal of Clinical Microbiology, 2011. 49(8): p. 3071-3.

125. Berman, H.F., Tartof, S.Y., Reis, J.N., Reis, M.G., and Riley, L.W., *Distribution of superantigens in group A streptococcal isolates from Salvador, Brazil.* BMC Infectious Diseases, 2014. 14: p. 294.

126. Cook, E., Wang, X., Robiou, N., and Fries, B.C., *Measurement of staphylococcal enterotoxin B in serum and culture supernatant with a capture enzyme-linked immunosorbent assay.* Clinical and Vaccine Immunology, 2007. 14(9): p. 1094-101.

127. Garber, E.A., Venkateswaran, K.V., and O'Brien, T.W., *Simultaneous multiplex detection and confirmation of the proteinaceous toxins abrin, ricin, botulinum toxins, and Staphylococcus enterotoxins a, B, and C in food.* Journal of Agricultural and Food Chemistry, 2010. 58(11): p. 6600-7.

128. Vernozy-Rozand, C., Mazuy-Cruchaudet, C., Bavai, C., and Richard, Y., *Comparison of three immunological methods for detecting staphylococcal enterotoxins from food.* Letters in Applied Microbiology, 2004. 39(6): p. 490-4.

129. Miyamoto, T., Kamikado, H., Kobayashi, H., Honjoh, K., and Iio, M., *Immunomagnetic flow cytometric detection of staphylococcal enterotoxin B in raw and dry milk.* Journal of Food Protection, 2003. 66(7): p. 1222-6.

130. Edwin, C., *Quantitative determination of staphylococcal enterotoxin A by an enzyme-linked immunosorbent assay using a combination of polyclonal and monoclonal antibodies and biotin-streptavidin interaction.* Journal of Clinical Microbiology, 1989. 27(7): p. 1496-501.

131. Clarisse, T., Michele, S., Olivier, T., Valerie, E., Vincent, L., Jacques-Antoine, H., Michel, G., and Florence, V., *Detection and quantification of staphylococcal enterotoxin A in*

foods with specific and sensitive polyclonal antibodies. Food Control, 2013. 32(1): p. 255-261.

132. Kuang, H., Wang, W., Xu, L., Ma, W., Liu, L., Wang, L., and Xu, C., *Monoclonal antibody-based sandwich ELISA for the detection of staphylococcal enterotoxin A.* International Journal of Environmental Research and Public Health, 2013. 10(4): p. 1598-608.

133. Tallent, S.M., Degrasse, J.A., Wang, N., Mattis, D.M., and Kranz, D.M., *Novel platform for the detection of Staphylococcus aureus enterotoxin B in foods.* Applied and Environmental Microbiology, 2013. 79(5): p. 1422-7.

134. Sharma, P., Postel, S., Sundberg, E.J., and Kranz, D.M., *Characterization of the Staphylococcal enterotoxin A: Vbeta receptor interaction using human receptor fragments engineered for high affinity.* Protein Engineering, Design and Selection, 2013. 26(12): p. 781-9.

135. Sharma, P., Wang, N., and Kranz, D.M., *Soluble T cell receptor Vbeta domains engineered for high-affinity binding to staphylococcal or streptococcal superantigens.* Toxins (Basel), 2014. 6(2): p. 556-74.

136. Sano, T. and Cantor, C.R., *Cooperative biotin binding by streptavidin. Electrophoretic behavior and subunit association of streptavidin in the presence of 6 M urea.* Journal of Biological Chemistry, 1990. 265(6): p. 3369-73.

137. Weber, P.C., Ohlendorf, D.H., Wendoloski, J.J., and Salemme, F.R., *Structural origins of high-affinity biotin binding to streptavidin.* Science, 1989. 243(4887): p. 85-8.

138. LeClaire, R.D. and Bavari, S., *Human antibodies to bacterial superantigens and their ability to inhibit T-cell activation and lethality.* Antimicrobial Agents and Chemotherapy, 2001. 45(2): p. 460-3.

139. Kimber, I., Nookala, S., Davis, C.C., Gerberick, G.F., Tucker, H., Foertsch, L.M., Dearman, R.J., Parsonnet, J., Goering, R.V., Modern, P., Donnellen, M., Morel, J., and Kotb, M., *Toxic shock syndrome: characterization of human immune responses to TSST-1 and evidence for sensitivity thresholds.* Toxicological Sciences, 2013. 134(1): p. 49-63.

140. Reddy, P., Ramlal, S., Sripathy, M.H., and Batra, H.V., *Development and evaluation of IgY ImmunoCapture PCR ELISA for detection of Staphylococcus aureus enterotoxin A devoid of protein A interference.* Journal of Immunological Methods, 2014. 408: p. 114-22.

141. Park, C.E., Akhtar, M., and Rayman, M.K., *Evaluation of a commercial enzyme immunoassay kit (RIDASCREEN) for detection of staphylococcal enterotoxins A, B, C, D, and E in foods.* Applied and Environmental Microbiology, 1994. 60(2): p. 677-81.

142. Park, C.E., Akhtar, M., and Rayman, M.K., *Nonspecific reactions of a commercial enzyme-linked immunosorbent assay kit (TECRA) for detection of staphylococcal enterotoxins in foods.* Applied and Environmental Microbiology, 1992. 58(8): p. 2509-12.

143. Buchan, B.W., Ginocchio, C.C., Manii, R., Cavagnolo, R., Pancholi, P., Swyers, L., Thomson, R.B., Jr., Anderson, C., Kaul, K., and Ledeboer, N.A., *Multiplex identification of gram-positive bacteria and resistance determinants directly from positive blood culture broths: evaluation of an automated microarray-based nucleic acid test.* PLoS Medicine, 2013. 10(7): p. e1001478.

144. Wojewoda, C.M., Sercia, L., Navas, M., Tuohy, M., Wilson, D., Hall, G.S., Procop, G.W., and Richter, S.S., *Evaluation of the Verigene Gram-positive blood culture nucleic acid test for rapid detection of bacteria and resistance determinants.* Journal of Clinical Microbiology, 2013. 51(7): p. 2072-6.

145. Peters, T.R., Hammon, D.E., Jarrah, R.J., Palavecino, E.L., Blakeney, E.S., and Poehling, K.A., *Staphylococcal Toxic Shock Syndrome Complicating Influenza A Infection in a Young Child.* ISRN Pulmonology, 2011. 2011: p. 1-3.

146. Stevens, D.L., *Invasive group A streptococcus infections.* Clinical Infectious Diseases, 1992. 14(1): p. 2-11.

147. Shalaby, T., Anandappa, S., Pocock, N.J., Keough, A., and Turner, A., *Lesson of the month 2: toxic shock syndrome.* Clinical Medicine, 2014. 14(3): p. 316-8.

148. Kain, K.C., Schulzer, M., and Chow, A.W., *Clinical spectrum of nonmenstrual toxic shock syndrome (TSS): comparison with menstrual TSS by multivariate discriminant analyses.* Clinical Infectious Diseases, 1993. 16(1): p. 100-6.

149. Descloux E., Perpoint T., Ferry T., Lina G., Bes M., Vandenesch F., Mohammedi I., and J., E., *One in five mortality in non-menstrual toxic shock syndrome versus no mortality in menstrual cases in a balanced French series of 55 cases.* European Journal of Clinical Microbiology & Infectious Diseases, 2008 27(1): p. 37-43.

150. Peterson, M.L., Ault, K., Kremer, M.J., Klingelhutz, A.J., Davis, C.C., Squier, C.A., and Schlievert, P.M., *The innate immune system is activated by stimulation of vaginal epithelial cells with Staphylococcus aureus and toxic shock syndrome toxin 1.* Infection and Immunity, 2005. 73(4): p. 2164-74.

151. Kwon, K.H., Hwang, S.Y., Park, Y.K., Yoon, J.W., Kim, S., and Hong, J., *A Quantitative Real-Time Immuno-PCR Assay for Detection ofStaphylococcus AureusEnterotoxin H.* Journal of Food Safety, 2014. 34(3): p. 249-256.